

RADIOLOGY AND ONCOLOGY

**Including papers from the
7th Conference of Experimental
and Translational Oncology**

**April, 20-24, 2013
Portorož, Slovenia**

vol.47 no.4

december 2013



NOVA SMER DO PODALJŠANJA CELOKUPNEGA PREŽIVETJA



Prva in edina samostojna kemoterapija, ki v primerjavi z ostalimi možnostmi zdravljenja z enim zdravilom, pri bolnicah s predhodno že večkratno zdravljenim metastatskim rakom dojke, dokazano značilno podaljša celokupno preživetje.^{1,2}



- **Halaven** (eribulin): ne-taksanski zaviralec dinamike mikrotubulov, prvo zdravilo iz nove skupine kemoterapevtikov, imenovanih *halihondrini*.
- Monoterapija z zdravilom HALAVEN je indicirana za zdravljenje bolnic z lokalno napredovalim ali metastatskim rakom dojke, ki je napredoval po vsaj dveh režimih kemoterapije za napredovalo bolezen. Predhodna zdravljenja morajo vključevati antraciklin in taksan, razen če to zdravljenje za bolnice ni bilo primerno.¹
- Priporočeni odmerek 1,23 mg/m², intravensko, v obliki 2- do 5-minutne infuzije, 1. in 8. dan vsakega 21-dnevnega cikla.
- Ena 2 ml viala vsebuje 0,88 mg eribulina.
- Raztopina, pripravljena za uporabo, redčenje ni potrebno.

SKRAJŠAN POVZETEK GLAVNIH ZNAČILNOSTI ZDRAVILA

HALAVEN 0,44 mg/ml raztopina za injiciranje (eribulin)
TERAPEVTSKE INDIKACIJE: Zdravljenje lokalno napredovalega ali metastatskega raka dojke, ki je napredoval po vsaj dveh režimih kemoterapije za napredovalo bolezen vključno z antraciklinom in taksanom, razen če to ni bilo primerno. **ODMERJANJE IN NAČIN UPORABE:** Halaven se daje v enotah, specializiranih za dajanje citotoksične kemoterapije, in le pod nadzorom usposobljenega zdravnika z izkušnjami v uporabi citotoksičnih zdravil. **ODMERJANJE:** Priporočeni odmerek eribulina v obliki raztopine je 1,23 mg/m² i. v. obliki 2- do 5- minutne infuzije 1. in 8. dan vsakega 21-dnevnega cikla. Bolnikom je lahko slabo ali bruhanje. Treba je razmisliti o antiemetični profilaksi, vključno s kortikosteroidi. **Preložitev odmerka med zdravljenjem:** Dajanje Halavena je treba preložiti, če se pojavi kaj od naslednjega: absolutno število nevtrofilcev (ANC) < 1 x 10⁹/l, trombociti < 75 x 10⁹/l ali nehematološki neželeni učinki 3. ali 4. stopnje. **Zmanjšanje odmerka med zdravljenjem:** Za priporočila za zmanjšanje odmerka ob pojavu hematoloških ali nehematoloških neželenih učinkov glejte celoten povzetek glavnih značilnosti zdravila. **Okvara jeter zaradi zasevkov:** Priporočeni odmerek pri blagi okvari jeter (stopnje A po Child-Pughu) je 0,97 mg/m² v obliki 2- do 5- minutne i. v. infuzije 1. in 8. dan 21-dnevnega cikla. Priporočeni odmerek pri zmerni okvari jeter (stopnje B po Child-Pughu) je 0,62 mg/m² v obliki 2- do 5- minutne i. v. infuzije 1. in 8. dan 21-dnevnega cikla. Pri hudi okvari jeter (stopnje C) se pričakuje, da je treba dati še manjši odmerek eribulina. **Okvara jeter zaradi ciroze:** Zgornje odmerke se lahko uporabi za blago do zmerno okvaro, vendar se priporoča skrbno nadziranje, saj bo odmerek morda treba ponovno prilagoditi. **Okvara ledvic:** Pri hudi okvari ledvic (očistek kreatinina <40 ml/min) bo morda treba odmerek zmanjšati. Priporočila se skrbno nadzirajo varnosti. **NAČIN UPORABE:** Odmerek se lahko razredči z do 100 ml 0,9 % natrijevega klorida (9 mg/ml) za injiciranje. Ne sme se ga redčiti v 5 % infuzijski raztopini glukoze. Pred dajanjem glejte navodila glede redčenja zdravila v celotnem povzetku glavnih značilnosti zdravila ter se prepričajte, da obstaja dober periferni venski dostop ali prehodna centralna linija. Ni znakov, da bi eribulin povzročal mehurje ali dražlj. V primeru ekstravazacije mora biti zdravljenje simptomatsko. **KONTRAINDIKACIJE:** Preobčutljivost na zdravilno učinkovino ali katerokoli pomožno snov. Dojenje. **POSEBNA OPOZORILA IN PREVIDNOSTNI UKREPI:** Mielosupresija je odvisna od odmerka in se kaže kot nevtropenija. Pred vsakim odmerkom eribulina je treba opraviti pregled celotne krvne slike. Zdravljenje z eribulinom se lahko uvede le pri bolnikih z vrednostmi ANC $\geq 1,5 \times 10^9/l$ in s trombociti > 100 x 10⁹/l. Bolnike, pri katerih se pojavijo febrilna

nevtropenija, huda nevtropenija ali trombocitopenija, je treba zdraviti v skladu s priporočili v celotnem povzetku glavnih značilnosti zdravila. Hudo nevtropenijo se lahko zdravi z uporabo G-CSF ali enakovrednim zdravilom v skladu s smernicami. Bolnike je treba skrbno nadzirati za znake periferne motorične in senzorične nevtropenije. Pri razvoju hude periferne nevtropenije je treba odmerek prestaviti ali zmanjšati. Če začnemo zdravljenje pri bolnikih s kongestivnim srčnim popuščanjem, z bradikardijami, z zdravili, za katera je znano, da podaljšujejo interval QT, vključno z antiaritmiki razreda Ia in III, in z elektrolitskimi motnjami, je priporočljivo spremljanje EKG. Pred začetkom zdravljenja s Halavenom je treba popraviti hipokaliemijo in hipomagnezijo in te elektrolite je treba občasno kontrolirati med zdravljenjem. Halavena ne smemo dajati bolnikom s prirojenim sindromom dolgega intervala QT. To zdravilo vsebuje majhne količine etanola (alkohola), manj kot 100 mg na odmerek. Eribulin je pri podganah embriotoksičen, fetotoksičen in teratogen. Halavena se ne sme uporabljati med nosečnostjo, razen kadar je to nujno potrebno. Ženske v rodni dobi naj ne zanosijo v času, ko same ali njihov moški partner dobivajo Halaven, in naj med zdravljenjem in še do 3 mesece po njem uporabljajo učinkovito kontracepcijo. Moški naj se pred zdravljenjem posvetujejo o shranjevanju sperme zaradi možnosti nepopravljive neplodnosti. **INTERAKCIJE:** Eribulin se izloča do 70 % prek žolča. Sočasna uporaba učinkovine, ki zavirajo jetrne transportne beljakovine, kot so beljakovine za prenos organskih anionov, P-glikoprotein, beljakovine, odporne na številna zdravila, z eribulinom se ne priporoča (npr. ciklosporin, ritonavir, sakvinavir, lopinavir in nekateri drugi zaviralci proteaze, efavirenz, emtricitabin, verapamil, klaritromicin, kinin, kinidin, dizopiramid itd). Sočasno zdravljenje z indukcijskimi učinkovinami, kot so rifamicin, karbamazepin, fenitoin, šentjanževka lahko povzroči znižanje koncentracij eribulina v plazmi, zato je ob sočasni uporabi induktorjev potrebna previdnost. Eribulin lahko zavira encim CYP3A4. Pri sočasni uporabi z učinkovinami, ki jih v glavnem presnavlja encim CYP3A4, se priporoča skrbno spremljanje zaradi povečanih koncentracij sočasno uporabljene učinkovine v plazmi. Če ima učinkovina ozek terapevtski razpon, je ne uporabljajte sočasno. **NEZELENI UČINKI:** *Zelo pogosti* ($\geq 1/10$): nevtropenija (54,5 %), (3./4. stopnje: 48,3 %), levkopenija (22,1 %), (3./4. stopnje: 14 %), anemija (20,3 %), (3./4. stopnje: 1,4 %), zmanjšan apetit, periferna nevtropenija (32,0 %), (3./4. stopnje: 6,9 %), glavobol, slabost (35,1 %), (3./4. stopnje: 1,1 %), zaprtost, driska, bruhanje, alopecija, artralgija in mialgija, utrujenost/astenija (52,8 %), (3./4. stopnje: 8,4 %), pireksija. *Pogosti* ($\geq 1/100$ do <1/10): okužba sečil, ustna kandidaza, okužba zgornjih

dihal, nazofaringitis, rinitis, febrilna nevtropenija (4,7 %), (3./4. stopnje: 4,6 %), trombocitopenija, limfopenija, hipokaliemija, hipomagnezija, dehidracija, hiperglikemija, hipofosfatemija, nespečnost, depresija, disgevgija, omotičnost, hipoestezija, letargija, nevtrotoksičnost, obilnejše solzenje, konjunktivitis, vrtoglavica, tahikardija, vročinski valovi, dispneja, kašelj, orofaringealna bolečina, epistaksa, rinoreja, bolečina v trebuhu, stomatitis, suha usta, dispnejska, gastroezofagealna refluksna bolezen, razjede v ustih, napihnjenost želodca, zvišanje alanin aminotransferaze (3,0 %), (3./4. stopnje: 1,1 %) in aspartat aminotransferaze, izpuščaj, pruritus, boleznino nohtov, nočno potenje, palmarno-plantarna eritrodisezija, suha koža, eritem, hiperhidroza, bolečina v okončinah, mišični spazmi, mišično-skeletna bolečina in mišično-skeletna bolečina v prsih, mišična oslabelost, bolečina v kosteh, bolečina v hrbtu, vnetje sluznice (9,8 %), (3./4. stopnje: 1,3 %), periferni edem, bolečina, mrzlica, gripi podobna bolezen, bolečina v prsih, zmanjšanje telesne mase. *Občasni* ($\geq 1/1.000$ do <1/100): pljučnica, nevtropenična sepsa, ustni herpes, herpes zoster, tinitus, globoka venska tromboza, pljučna embolija, intersticijska pljučna bolezen, hiperbilirubinemija, angioedem, disurija, hematurija, proteinurija, odpoved ledvic. *Redki* ($\geq 1/10.000$ do <1/1.000): pankreatitis. Za popoln opis neželenih učinkov glejte celoten povzetek glavnih značilnosti zdravila. **Vrsta ovojinine in vsebina:** viala z 2 ml raztopine. **Režim izdaje:** H. Imetnik dovoljenja za promet: Eisai Europe Ltd, Mosquito Way, Hatfield, Hertfordshire, AL10 9SN, Velika Britanija. HAL-161112

Pred predpisovanjem in uporabo zdravila prosimo preberite celoten povzetek glavnih značilnosti zdravila!

Viri: (1) Povzetek glavnih značilnosti zdravila Halaven, november 2012; (2) Cortes J et al. *Lancet* 2011; 377: 914-23

 **PharmaSwiss**
Choose More Life

Odgovoren za trženje v Sloveniji:
PharmaSwiss d.o.o., Dolenjska cesta 242c, 1000 Ljubljana
telefon: +386 1 236 47 00, faks: +386 1 283 38 10

HAL 0113-01, januar 2013



Publisher

Association of Radiology and Oncology

Affiliated with

Slovenian Medical Association – Slovenian Association of Radiology, Nuclear Medicine Society,
Slovenian Society for Radiotherapy and Oncology, and Slovenian Cancer Society
Croatian Medical Association – Croatian Society of Radiology
Societas Radiologorum Hungarorum
Friuli-Venezia Giulia regional groups of S.I.R.M.
Italian Society of Medical Radiology

Aims and scope

Radiology and Oncology is a journal devoted to publication of original contributions in diagnostic and interventional radiology, computerized tomography, ultrasound, magnetic resonance, nuclear medicine, radiotherapy, clinical and experimental oncology, radiobiology, radiophysics and radiation protection.

Editor-in-Chief

Gregor Serša Ljubljana, Slovenia

Executive Editor

Viljem Kovač Ljubljana, Slovenia

Deputy Editors

Andrej Čör Izola, Slovenia

Maja Čemažar Ljubljana, Slovenia

Igor Kocijančič Ljubljana, Slovenia

Karmen Stanič Ljubljana, Slovenia

Primož Strojjan Ljubljana, Slovenia

Editorial Board

Karl H. Bohuslavizki Hamburg, Germany

Christian Dittrich Vienna, Austria

Metka Filipič Ljubljana, Slovenia

Tullio Giraldi Trieste, Italy

Maria Gódey Budapest, Hungary

Vassil Hadjidekov Sofia, Bulgaria

Håkan Nyström Uppsala, Sweden

Marko Hočevar Ljubljana, Slovenia

Miklós Kásler Budapest, Hungary

Michael Kirschfink Heidelberg, Germany

Janko Kos Ljubljana, Slovenia

Tamara Lah Turnšek Ljubljana, Slovenia

Damijan Miklavčič Ljubljana, Slovenia

Luka Milas Houston, USA

Damir Miletić Rijeka, Croatia

Maja Osmak Zagreb, Croatia

Branko Palčič Vancouver, Canada

Dušan Pavčnik Portland, USA

Geoffrey J. Pilkington Portsmouth, UK

Ervin B. Podgoršak Montreal, Canada

Mirjana Rajer Ljubljana, Slovenia

Borut Štabuc Ljubljana, Slovenia

Ranka Štern-Padovan Zagreb, Croatia

Justin Teissié Toulouse, France

Gillian M. Tozer Sheffield, UK

Andrea Veronesi Aviano, Italy

Branko Zakotnik Ljubljana, Slovenia

Advisory Committee

Marija Auersperg Ljubljana, Slovenia

Tomaž Benulič Ljubljana, Slovenia

Božo Casar Ljubljana, Slovenia

Jure Fettich Ljubljana, Slovenia

Valentin Fidler Ljubljana, Slovenia

Berta Jereb Ljubljana, Slovenia

Vladimir Jevtič Ljubljana, Slovenia

Maksimilijan Kadivec Ljubljana, Slovenia

Stojan Plesničar Ljubljana, Slovenia

Uroš Smrdel Ljubljana, Slovenia

Živa Zupančič Ljubljana, Slovenia

Editorial office

Radiology and Oncology

Zaloška cesta 2

P. O. Box 2217

SI-1000 Ljubljana

Slovenia

Phone: +386 1 5879 369

Phone/Fax: +386 1 5879 434

E-mail: gsertsa@onko-i.si

Copyright © Radiology and Oncology. All rights reserved.

Reader for English

Vida Kološa

Secretary

Mira Klemenčič

Zvezdana Vukmirović

Design

Monika Fink-Serša, Samo Rován, Ivana Ljubanović

Layout

Matjaž Lužar

Printed by

Tiskarna Ozimek, Slovenia

Published quarterly in 600 copies

Beneficiary name: DRUŠTVO RADIOLOGIJE IN ONKOLOGIJE

Zaloška cesta 2

1000 Ljubljana

Slovenia

Beneficiary bank account number: SI56 02010-0090006751

IBAN: SI56 0201 0009 0006 751

Our bank name: Nova Ljubljanska banka, d.d.,

Ljubljana, Trg republike 2,

1520 Ljubljana; Slovenia

SWIFT: LJBAS12X

Subscription fee for institutions EUR 100, individuals EUR 50

The publication of this journal is subsidized by the Slovenian Research Agency.

Indexed and abstracted by:

Science Citation Index Expanded (SciSearch®)

Journal Citation Reports/Science Edition

Scopus

PubMed

PubMed Central

EMBASE/Excerpta Medica

DOAJ

Open J-gate

Chemical Abstracts

Biomedicina Slovenica

Summon by Serial Solutions (ProQuest)

This journal is printed on acid-free paper

On the web: ISSN 1581-3207

<http://www.degruyter.com/view/j/raon>

<http://www.radioloncol.com>



COST - European Cooperation in Science and Technology is an intergovernmental framework aimed at facilitating the collaboration and networking of scientists and researchers at European level. It was established in 1971 by 19 member countries and currently includes 35 member countries across Europe, and Israel as a cooperating state.

COST funds pan-European, bottom-up networks of scientists and researchers across all science and technology fields. These networks, called 'COST Actions', promote international coordination of nationally-funded research. By fostering the networking of researchers at an international level, COST enables break-through scientific developments leading to new concepts and products, thereby contributing to strengthening Europe's research and innovation capacities.

COST's mission focuses in particular on:

- *Building capacity by connecting high quality scientific communities throughout Europe and worldwide;*
- *Providing networking opportunities for early career investigators;*
- *Increasing the impact of research on policy makers, regulatory bodies and national decision makers as well as the private sector.*

Through its inclusiveness, COST supports the integration of research communities, leverages national research investments and addresses issues of global relevance.

Every year thousands of European scientists benefit from being involved in COST Actions, allowing the pooling of national research funding to achieve common goals.

As a precursor of advanced multidisciplinary research, COST anticipates and complements the activities of EU Framework Programmes, constituting a "bridge" towards the scientific communities of emerging countries. In particular, COST Actions are also open to participation by non-European scientists coming from neighbour countries (for example Albania, Algeria, Armenia, Azerbaijan, Belarus, Egypt, Georgia, Jordan, Lebanon, Libya, Moldova, Montenegro, Morocco, the Palestinian Authority, Russia, Syria, Tunisia and Ukraine) and from a number of international partner countries. COST's budget for networking activities has traditionally been provided by successive EU RTD Framework Programmes. COST is currently executed by the European Science Foundation (ESF) through the COST Office on a mandate by the European Commission, and the framework is governed by a Committee of Senior Officials (CSO) representing all its 35 member countries. More information about COST is available at www.cost.eu.

CLINIPORATOR

LEADING CLINICAL ELECTROPORATION



Electrochemotherapy

Effective, safe, simple.

For local tumours control

CLINICAL INDICATIONS

Melanoma and other skin tumors

Local recurrences and cutaneous metastases from breast cancer

Head and neck cancers

High response rate

Preservation of normal tissue and organ function

Efficacy in areas previously treated with radiation therapy

Palliation of painful, ulcerated or bleeding lesions

Improved quality of life and cosmetic results

Before electrochemotherapy

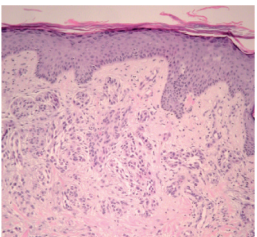


Gehl J, EJC Supplements, Volume 4, N° 11:35-37, 2006

10 weeks after electrochemotherapy

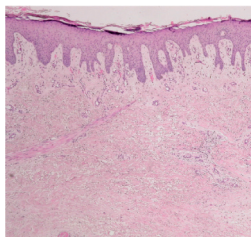


Before electrochemotherapy



Quaglino P, Annals Of Surgical Oncology, 15 (8):2215-2222. 2008

60 days after electrochemotherapy



Special issue of Radiology and Oncology on experimental and translational oncology

Substantial progress in research of cellular and molecular mechanisms of development and progression of cancer provides new insight to malignant diseases, enables the application of new tools in diagnosis and treatment of human cancers and ultimately improves the clinical care of oncology patients. To foster the transfer of knowledge from basic laboratories to clinical practice, Association of Radiology&Oncology organises international conferences on experimental and translational oncology, gathering young and senior scientists to present basic and clinical achievements in oncology and related sciences. The 7th Conference on Experimental and Translational Oncology, held in Portorož, Slovenia, from April 20-24, 2013, was attended by 170 participants from 28 countries. Besides topics, being discussed already at previous conferences, such as Mechanisms of tumour progression, Biomarkers and New drugs and therapeutic targets, this conference additionally addressed Biomedical applications of electroporation and Cellular therapy. The event was co-organized by COST TD 1104 Action. Selected papers covering some of the topics of the conference are published in this issue.

The important role of proteases and other enzymes in tumour progression has been stressed by several speakers. Proteolytic function is crucial in tumour invasion and migration, proteases regulate the apoptosis of tumour cells and mediate tumour directed cytotoxicity of T cells and NK cells. Additionally, the components of tumour proteolytic system can be used as biomarkers to allow molecular classification, early diagnosis and prognosis of human malignancies and to predict the response to anticancer drugs. In the current issue Schmitt et al. presents kallikrein related peptidases as promising biomarkers in female and male reproductive organ malignancies. Besides proteases, growth factors, hormones and cytokines have also been presented as factors involved in regulation of tumour development and growth. Moreover, uroplakins, glycosylated membrane proteins also consist a group of potential tumour biomarkers and, as shown in a paper of Zupančič and Romih, their localisation in urothelium may provide diagnostic information in bladder cancer. MicroRNAs are another group of molecules which underwent extensive investigation during last decade regarding their role in cancer biology. As presented by several speakers they can modulate mRNA expression and translation of various tumour associated genes and some of microRNAs have already been identified as prognostic and diagnostic markers. The paper of Hauptman and Glavač provides the prospects of micro RNA and long non-coding RNA in diagnostics and therapy of cancer.

The section New drugs and therapeutic targets was focused on the development and application of new protease inhibitors in anticancer therapy as well as on improved use of the existing chemo- and radio-therapeutics. The latter is evident from the paper of Filipović et al., where new analogues of cisplatin with improved pharmacological characteristics are presented, and from the paper of Jurdana et al., describing the effect of ionizing radiation on human skeletal muscle precursor cells. Similarly, Trošt et al., describe the altered gene expression and molecular mechanisms involved in the modulation of cisplatin cytotoxicity by biological drug erythropoietin.

Cellular therapy is another rapidly growing area in oncology which can provide exciting new approaches in cancer treatment. Besides the stimulation of the cytotoxicity of T cell and NK cells the speakers emphasized the potential of mesenchymal stem cells in cancer therapy. Encouraging results, being obtained in brain cancer are partially addressed in a paper of Podergajs et al. describing a role of growth factors bFGF and EGF in growth of glioblastoma stem-like cells.

At last, an important part of the conference was dedicated to biomedical applications of electroporation. Electrochemotherapy is a good example of successful translational research of joined contribution of basic and clinical scientists. The advantage of electrotransfer of genes and chemotherapeutics have been

demonstrated by several groups, a part of these studies is published in this issue including a paper of Wichmann Mathiessen et al. on application of electrochemotherapy in patients with breast cancer, the case study of Scelsi et al. on patients with advanced Merkel cell carcinoma of head and neck and the case study of Campana et al. on patients with gastric cancer.

The conference deserved very positive response in broad scientific community what confirms the concept of Association of Radiology and Oncology to promote translational research and to foster cooperation between basic and clinical scientists.

Janko Kos
Gregor Serša
Tamara Lah Turnšek

contents

Articles from 7th Conference of Experimental and Translational Oncology

- 311 **Micro RNAs and long non-coding RNAs: prospects in diagnostics and therapy of cancer**
Nina Hauptman and Damjan Glavac
- 319 **Emerging clinical importance of the cancer biomarkers kallikrein-related peptidases (KLK) in female and male reproductive organ malignancies**
Manfred Schmitt, Viktor Magdolen, Feng Yang, Marion Kiechle, Jane Bayani, George M. Yousef, Andreas Scorilas, Eleftherios P. Diamandis, Julia Dorn
- 330 **Expansive growth of two glioblastoma stem-like cell lines is mediated by bFGF and not by EGF**
Neza Podergajs, Narve Brekka, Bernhard Radlwimmer, Christel Herold-Mende, Krishna M. Talasila, Katja Tiemann, Uros Rajcevic, Tamara T. Lah, Rolf Bjerkvig, Hrvoje Miletic
- 338 **Heterogeneity of uroplakin localization in human normal urothelium, papilloma and papillary carcinoma**
Daša Zupancic and Rok Romih
- 346 **Biological evaluation of trans-dichloridoplatinum(II) complexes with 3- and 4-acetylpyridine in comparison to cisplatin**
Lana Filipovic, Sandra Arandelovic, Nevenka Gligorijevic, Ana Krivokuca, Radmila Jankovic, Tatjana Srdic-Rajic, Gordana Rakic, Zivoslav Tesic, Sinisa Radulovic
- 358 **Dual time point imaging fluorine-18 flourodeoxyglucose positron emission tomography for evaluation of large loco-regional recurrences of breast cancer treated with electrochemotherapy**
Louise Wichmann Matthiessen, Helle Hjorth Johannesen, Kristin Skougaard, Julie Gehl, Helle Westergren Hendel
- 366 **Electrochemotherapy as a new therapeutic strategy in advanced Merkel cell carcinoma of head and neck region**
Daniele Scelsi, Niccolò Mevio, Giulia Bertino, Antonio Occhini, Valeria Brazzelli, Patrizia Morbini, Marco Benazzo
- 370 **Minimally invasive treatment of peristomal metastases from gastric cancer at an ileostomy site by electrochemotherapy**
Luca G. Campana, Marco Scarpa, Antonio Sommariva, Elena Bonandini, Sara Valpione, Leonardo Sartore, Carlo R. Rossi

- 376 **Effect of ionizing radiation on human skeletal muscle precursor cells**
Mihaela Jurdana, Maja Cemazar, Katarina Pegan, Tomaz Mars
- 382 **Recombinant human erythropoietin alters gene expression and stimulates proliferation of MCF-7 breast cancer cells**
Nina Trost, Tina Stepisnik, Sabina Berne, Anja Pucer, Toni Petan, Radovan Komel, Natasa Debeljak

Other articles

nuclear medicine

- 390 **The usefulness of F-18 FDG PET/CT-mammography for preoperative staging of breast cancer: comparison with conventional PET/CT and MR-mammography**
Eun-Ha Moon, Seok Tae Lim, Yeon-Hee Han, Young Jin Jeong, Yun-Hee Kang, Hwan-Jeong Jeong, Myung-Hee Sohn

radiology

- 398 **Role of contrast-enhanced ultrasound in evaluating the efficiency of ultrasound guided percutaneous microwave ablation in patients with renal cell carcinoma**
Xin Li, Ping Liang, Jie Yu, Xiao-Ling Yu, Fang-Yi Liu, Zhi-Gang Cheng, Zhi-Yu Han

clinical oncology

- 405 **Impact of CD133 positive stem cell proportion on survival in patients with glioblastoma multiforme**
Marju Kase, Ave Minajeva, Kristi Niinepuu, Sandra Kase, Markus Vardja, Toomas Asser, Jana Jaal

radiophysic

- 411 **Dosimetric evaluation of an ipsilateral intensity modulated radiotherapy beam arrangement for parotid malignancies**
Eda Yirmibesoglu, David V. Fried, Mark Kostich, Julian Rosenman, William Shockley, Mark Weissler, Adam Zanation, Bishamjit Chera

MicroRNAs and long non-coding RNAs: prospects in diagnostics and therapy of cancer

Nina Hauptman and Damjan Glavac

Department of Molecular Genetics, Institute of Pathology, Medical Faculty, University of Ljubljana, Slovenia

Radiol Oncol 2013; 47(4): 311-318.

Received 15 June 2013
Accepted 20 August 2013

Correspondence to: Prof. Damjan Glavac, Ph.D., Department of Molecular Genetics, Institute of Pathology, Medical Faculty, University of Ljubljana, Korytkova 2, SI-1000 Ljubljana, Slovenia. E-mail: damjan.glavac@mf.uni-lj.si

Disclosure: No potential conflicts of interest were disclosed.

The paper was presented at the 7th Conference of Experimental and Translational Oncology, 20-24th April 2013, Portoroz, Slovenia (www.ceto.si) co-organised and supported by COST TD1104 Action (www.electroporation.net).

Background. Non-coding RNAs (ncRNAs) are key regulatory molecules in cellular processes, and are potential biomarkers in many diseases. Currently, microRNAs and long non-coding RNAs are being pursued as diagnostic and prognostic biomarkers, and as therapeutic tools in cancer, since their expression profiling is able to distinguish different cancer types and classify their sub-types.

Conclusions. There are numerous studies confirming involvement of ncRNAs in cancer initiation, development and progression, but have only been recently identified as new diagnostic and prognostic tools. This can be beneficial in future medical cancer treatment options, since ncRNAs are natural antisense interactors included in regulation of many genes connected to survival and proliferation. Research is directed in development of useful markers for diagnosis and prognosis in cancer and in developing new RNA-based cancer therapies, of which some are already in clinical trials.

Key words: microRNAs; long non-coding RNAs; diagnosis; therapy; biomarker

Introduction

Cancer is one of the leading causes of death in the world, following deaths by cardiovascular and infectious disease. Although cancer is widely researched there is still lack of early detection techniques. For detecting early stage tumors and their precise characterization before and after treatment, biomarkers could be used, which consequently could lower the mortality rate.¹ Research for suitable biomarkers for diagnosis and prognosis is wide-spread, and lately directed into detection in body fluids. For this purpose extensive research in the field of non-coding RNAs (ncRNAs) is conducted.

RNA used to be considered the messenger between the gene and the protein encoded by this gene.^{2,3} The minority of the transcripts are protein coding (1.5%), and the rest used to be referred as “dark matter”, now known to be the ncRNA tran-

scripts. Recent transcriptional analyses of genome estimate that ncRNA sequences are the most transcribed ones.^{4,5} The group of ncRNAs is quite diverse and complex. It is divided into ribosomal RNAs (rRNAs), transfer RNAs (tRNAs), microRNAs (miRNAs), long non-coding RNAs (lncRNAs), small nucleolar RNAs (snoRNAs), small interfering RNAs (siRNAs), small nuclear RNAs (snRNAs), and piwi-interacting RNAs (piRNAs) (Figure 1).⁶

MicroRNAs (miRNAs) are ~22 nt long RNA molecules and are involved in post-transcriptional regulation. MiRNAs regulate over 30% of messenger RNAs (mRNAs), mainly through the negative regulation of gene expression, where miRNA bind to regions of mRNA, blocking the translation or completely degrading mRNAs.⁷ It is established that miRNA are included in cellular differentiation, development, proliferation and apoptosis, where they play an important role. In cancer these pro-

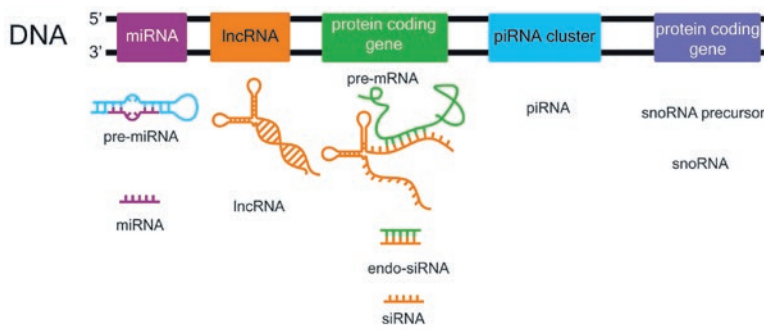


FIGURE 1. Schematic presentation of ncRNAs biogenesis.

cesses are deregulated, meaning that miRNA are involved in carcinogenesis, and could contribute to the initiation and progression of cancer.⁸ Tumor specific miRNA have a potential of becoming cancer biomarkers, since their expression profile can be more specific for determining the classification, diagnosis, and progression in cancer.⁹

LncRNA are classified as over 200 nt long transcripts that lack functionally open reading frame. They are involved in cellular differentiation and proliferation. The mechanisms through which they act are molecular scaffolds, which are involved in transcriptional machinery, as post-transcriptional regulators of splicing or as molecular decoys for miRNA.^{4,10} The lncRNA research is a new field emerging in molecular genetics, therefore only a small number of lncRNA were characterized. Comparing to miRNA, lncRNA studies are scarcer, nonetheless some promising evidence of using lncRNA as biomarkers for diagnosis and prognosis exist.

PiRNA are a class of regulatory small non-coding RNAs, 23-29 nt in length, which form the piRNA-induced silencing complex in the germ line of many animal species. PiRNA are specifically associated with PIWI proteins, which are germline-specific members of AGO protein family. The main function of piRNAs is defence against transposable elements in germ cells, and this role is highly conserved across animal species. Transposable elements threaten the genomic integrity of the host. PiRNAs and their interacting proteins have important role in cellular processes, and some of them are potential regulators of cancer cell development.¹¹

SnoRNAs are 60-300 nucleotides in length and are predominantly found in nucleus. Their classical function is connected to post-transcriptional modification of ribosomal RNAs and some spliceosomal RNAs. These modifications are necessary for efficient and accurate production of ribosomes.¹² Modification of ribosome biogenesis has been implicated in cancer development, which indicates

snoRNAs might contribute to cancer, although this area needs further research.^{12,13}

siRNA are usually 19-23 nucleotides in length, which are known to guide silencing of target mRNA by directing the RNA-induced silencing complex to mediate site-specific cleavage, and destruction of targeted mRNA.¹⁴ Genes associated with cancer are a potential target of siRNAs, their potential is in inhibition and therapeutics.¹⁴⁻¹⁷

In this review we will highlight the potential of miRNA and lncRNA for diagnosis and therapy, focusing on specific and sensitive biomarkers and their availability in body fluids. Additionally we will address the therapeutic benefits of miRNA and strategies of delivery to damaged tissues.

Potential in diagnostics

Biomarkers are biological indicators of disease states, used to classify cancer types or subtypes.¹⁸ Effective and clinically relevant biomarkers are important for subsequent patient's treatment.¹⁹ The research on detection of both miRNAs and lncRNAs is orientated toward their detection in body fluids. Comparing to mRNA, the level of expressions of either miRNA or lncRNA may be a better tool for indication of a certain disease. Furthermore, this can be diagnostically applicable when a distinctly specific pattern of expression for a certain disease exists.

One of the reasons of extensive research done on miRNAs connected to cancer is the possibility of conducting research on formalin fixed paraffin embedded (FFPE) samples. Due to their small length, miRNAs are not affected by formalin fixation and degradation over time like longer RNA molecules, such as mRNA and lncRNA, where fresh frozen samples are needed.²⁰⁻²²

MiRNA diagnostic

The most commonly observed miRNA, which is up-regulated in human cancers, is miR-21 (Table 1). Overexpression was observed in breast, lung, prostate and other cancers, where it was shown to increase cell proliferation and invasion, and its suppression led to decrease in the cell proliferation, invasion, and induced apoptosis.²³⁻²⁵

Another miRNA up-regulated in breast, lung, pancreatic and other cancers is miR-155, which overexpression is also associated with tumorigenesis in lymphoma.⁵² Also in blood samples these two miRNAs are the most deregulated. Other

TABLE 1. Potential diagnostic miRNA biomarkers in tissue and blood samples

Cancer	Tissue samples (FFPE) (expression status ↑, ↓)	Reference	Blood samples (expression status ↑, ↓)	Reference
Breast cancer	miR-21↑, miR-155 ↑, miR-191 ↑, miR-196a ↑, miR-125b ↓, miR-221 ↓, let-7a ↓, miR-145 ↓, miR-205 ↓	23, 26	Serum: miR-10b ↑, miR-34a ↑, miR-155 ↑, miR-21 ↑, miR-106a ↑, miR-155 ↑, miR-126 ↓, miR-199a ↓, miR-335 ↓ Whole blood: miR-195 ↑	27-29
Lung cancer	miR-21, miR-205	30	Serum: miR-10b ↑, miR-155 ↑	31
Gastric cancer	miR-106a ↑, miR-31 ↓	32, 33	Serum: miR-10a ↑, miR-22 ↑, miR-100 ↑, miR-148b ↑, miR-223 ↑, miR-133a ↑, miR-127-3p ↑, miR-1 ↑, miR-20a ↑, miR-27a ↑, miR-34 ↑, miR-423-5p ↑	34, 35
Pancreatic cancer	miR-452 ↑, miR-105 ↑, miR-127 ↑, miR-518a-2 ↑, miR-187 ↑, miR-30a-3p ↑, miR-21 ↑, miR-155 ↑, miR-221 ↑, miR-222 ↑, let-7a ↑	36-38	Serum: miR-21 ↑, miR-155 ↑, miR-196a ↑ Plasma: miR-21 ↑, miR-155 ↑, miR-196a ↑, miR-210 ↑	39-41
Prostate cancer	miR-125b ↑, miR-15a ↓, miR-16 ↓, miR-184 ↑, miR-146a ↓, miR-203 ↓, miR-34c ↓, miR-141 ↑	42-46	Serum: miR-141 ↑, miR-21 ↑, miR-141 ↑, miR-221 ↑, miR-375 ↑	47-51

TABLE 2. lncRNA deregulated in cancer

Name	Size (kb)	Cancer Type	Expression	Reference
ANRIL	~3.9	Prostate, leukemia	↑	58
BC200	0.2	Breast, cervix, esophagus, lung, ovary, parotid, tongue	↑	59, 60
PRNCR1	13	Prostate		61
H19	2.3	Bladder, lung, liver, breast, esophagus, choriocarcinoma, colorectal cancer		62-68
HOTAIR	2.2	Breast, hepatocellular	↑	56, 57, 69, 70
HULC	~0.5	Hepatocellular	↑	71, 72
MALAT1	7.5	Breast, prostate, colon, liver, uterus	↑	73-76
MEG3	1.6	Brain	↓	77, 78
PTNEP1	3.9	Prostate		79
Spry4-it1	~0.7	Melanoma	↑	80
SRA	1.965	Breast, uterus, ovary	↓	81, 82
UCA1/CUDR	1.4, 2.2, 2.7	Bladder, colon, cervix, lung, thyroid, liver, breast, esophagus, stomach	↑	83, 84
PCA3	0.6-4	Prostate	↑	85
GAS5	isoforms	Breast	↓	86

miRNAs do not overlap in the cancer type groups either in tissue or blood samples. The overlap between the tissue and blood samples of the same cancer type was observed in prostate cancer, where miRNA-141 is expressed in tissue and patients sera, and could differentiate between patients with cancer and healthy controls.⁵¹ Another example is observed in plasma of patients with colorectal cancer (CRC), where levels of miR-29a and miR-92a are able to distinguish advanced adenomas and negative controls.⁵³ In the research of circulating miR-141 in 102 plasma samples, a significant correlation to colon cancer stage IV was determined.⁵⁴ The accuracy was further improved by combining the levels of miR-141 to carcinoembryonic antigen marker. For more accurate diagnostics, expression levels of several miRNAs should be monitored.

Expression of 47 miRNAs in 101 FFPE samples of primary cancers and metastasis was evaluated, determining the tissue of origin. The identification of tissue was 100% for primary cancers and 78% for metastases. The accuracy remained high for independent sample validation.⁵⁵ miRNA expression arrays can be utilized, when the other established clinical tests are inconclusive.

lncRNA diagnostic

lncRNA is a fast growing field of research and many discovered lncRNA are deregulated in cancer (Table 2).

HOTAIR interacts with polycomb repressor complex PRC2, which causes the transcriptional silencing of several metastasis suppressor genes lo-

cated in *HOXD* locus on chromosome 2.⁵⁶ Elevated expression of HOTAIR was observed in primary and metastatic breast cancer compared to normal tissue. The high expression of HOTAIR is also correlated to metastasis and poor survival rate.⁵⁶ HOTAIR can be a potential biomarker for the existence of lymph node metastasis in hepatocellular carcinoma (HCC).⁵⁷

ANRIL activates two polycomb repressor complexes, PRC1 and PRC2, which results in chromatin reorganization, silencing the *INK4b-ARF-INK4a* locus encoding tumor suppressor genes, involved in cell cycle inhibition, and stress-induced apoptosis. Overexpression of ANRIL in prostate cancer has shown silencing of *INK4b-ARF-INK4a* and *p15/CDKN2B* by heterochromatin reformation.^{58,87}

MALAT1 is widely expressed in normal human tissues and is found to be up-regulated in a variety of human cancers of the breast, prostate, colon, liver and uterus.^{75,76} The MALAT1 locus is located at 11q13.1 and was found to harbour chromosomal translocation break points associated with cancer.⁸⁸ It has been shown that increased expression of MALAT1 can be used as a prognostic marker for HCC patients following liver transplantation.⁸⁹

H19 and the insulin-like growth factor 2 (*IGF2*) are imprinted, and expressed from the maternal allele, and from parental allele, respectively.^{62,68} The loss of imprinting results in misexpression of *H19* and was observed in many tumors including hepatocellular and bladder cancer.⁶⁴ *c-MYC* induces the expression of *H19* in different cell types where *H19* potentiates tumorigenesis.⁶⁸

lncRNA *MEG3* is a transcript of the maternally imprinted gene. In normal pituitary cells *MEG3* is expressed, the loss of expression is observed in pituitary adenomas and the majority of meningiomas and meningioma cell lines. *MEG3* activates regulation of tumor suppressor protein *p53*.^{77,78}

Growth Arrest-Specific 5 (*GAS5*) functions as a starvation or growth arrest-linked riborepressor for the glucocorticoid receptors by binding to their DNA binding domain inhibiting the association of these receptors with their DNA recognition sequence. This suppresses the induction of several responsive genes including the gene encoding cellular inhibitor of apoptosis 2 (*cIAP2*), reducing cell metabolism and synthesizes cells to apoptosis.⁹⁰ *GAS5* can induce apoptosis directly or indirectly in the prostate and breast cancer cell lines, where it was shown that *GAS5* has a significantly lower expression in breast cancers compared to normal breast epithelial tissues.⁸⁶

One of the lncRNA utilized in a clinical test is prostate cancer associated (*PCA3*), which is a prostate cancer specific lncRNA. It can be detected in urine samples obtained after a prostatic massage.^{91,92} Studies, comparing the levels of *PCA3* to current biomarker prostate specific antigen (*PSA*), were conducted, showing that *PCA3* has higher specificity than *PSA*, reducing the number of biopsies. Also *PCA3* levels correlate better to identification of disease, since *PSA* levels can be also elevated due to inflammatory reasons. The accuracy was improved when profiling of both *PCA3* and *PSA* in blood was performed.⁹³

There are two lncRNA connected to HCC, highly up-regulated in liver cancer (*HULC*) and *HOTAIR*. *HULC* is detected in peripheral blood cells and therefore has a potential as a biomarker.⁷² *HOTAIR* has also been correlated to HCC and has potential to become a biomarker for lymph node metastasis and tumor recurrence in HCC patients' undergone a liver transplant.^{57,70}

Clinical trials on biomarkers are mostly performed on specimens that are easily obtainable, such as blood or urine, and present little discomfort to patients, where on the other hand trials are rare on tumor tissue, due to the specimen unavailability. The detection of early stage disease in body fluids is ideal for patients, due to its non-invasive nature. Still many questions persist, like stability of the circulating molecules, and their stability in the progression of disease. There is also evidence of some specific expression in cancers, but with the on-going research on this topic there will be more evidence of involvement of lncRNA in cancer.^{71,93}

Potential of therapy

After proving many miRNA and lncRNA are down-regulated in cancer, the research now focuses on their role as therapeutic targets.⁹⁴

MiRNAs involved and deregulated in cancer are divided into tumor suppressor and oncogenic miRNAs. Oncogenic miRNAs are overexpressed in cancer, downregulating tumor suppressor genes.⁹⁵ To reverse the oncogenic miRNA expression they have to be inhibited to relieve their targets. This can be achieved by introducing mRNAs targeting specific miRNAs or by using antisense single-stranded oligonucleotides complementary to miRNA, acting as miRNA sponges and miRNA antagonists, respectively.⁹⁶⁻⁹⁸ On the other hand tumor suppressor miRNAs are under expressed in the cancer, their role being down-regulation of oncogenes.^{95,99} To

restore the levels of tumor suppressor miRNAs the replacement therapy of mimics miRNA or DNA coding for specific miRNAs is needed.^{96,100} This is schematically presented in Figure 2.

Inhibition of oncogenic miRNAs has been widely researched through siRNA-based therapeutic modalities, and antisense oligonucleotides, which have been a straightforward approach relieving repressed targets of miRNA.^{101,102} Antisense oligonucleotides can be designed to potentially block several steps during the biogenesis and action of miRNA, miRNA processing or miRNA pairing with targeted mRNA. *In vitro* and *in vivo* mice studies used modified antisense oligonucleotides to inhibit tumor proliferation, migration, invasion, and apoptosis.⁹⁶ Antisense oligonucleotide targeting miR-21 in *in vitro* and *in vivo* xenograft model resulted in the inhibition of breast cancer cell growth, inhibited cell proliferation, and increased apoptosis.¹⁰³ Besides antisense oligonucleotide inhibition, miRNA sponges as another technique to effectively lower the levels of miRNA has been used, where targeted sequence is cloned in multiple copies, and upon transfection into a tumor cell should act as a sponge for the miRNA and relieve its natural target.¹⁰⁴ In breast cancer cell lines, a miRNA sponge trapping up-regulated miR-9 connected to cancer metastasis effectively reduced invasiveness of the tumor cells.¹⁰⁵

The replacement therapy for down-regulated tumor suppressor miRNA is administration of synthetic miRNA. Tumor suppressor let-7 miRNA, known to be associated with many tumors, was delivered intratumorally in a mouse model of non-small-cell lung cancer, which led to reduction of tumor burden.¹⁰⁶ Several studies suggest that let-7 acts through direct repression of *KRAS* and *c-MYC* oncogenes.¹⁰⁷ Another deregulated miRNA associated with several cancers is miR-34. Through transfection or lentiviral-mediated delivery of mimic miR-34 to cancer cells, the cell-cycle arrest, apoptosis and reduction in tumor size was observed.¹⁰⁸

It is observed, in both EU and US, a large increase of patents connected to miRNA. Many miRNA based therapeutics is either in preclinical or clinical trial phase. In cancer treatment Mirna Therapeutics has developed miRNA mimic therapeutics for miR-34 (phase I) and let-7 (preclinical).

While many targeting strategies are implied to reverse the levels of miRNA, for lncRNA these strategies are still being developed. In principle the same strategies as for miRNA could be used, like introducing molecules designed to target lncRNA to lower the expression levels or disrupt the lncRNA in structural or functional way.

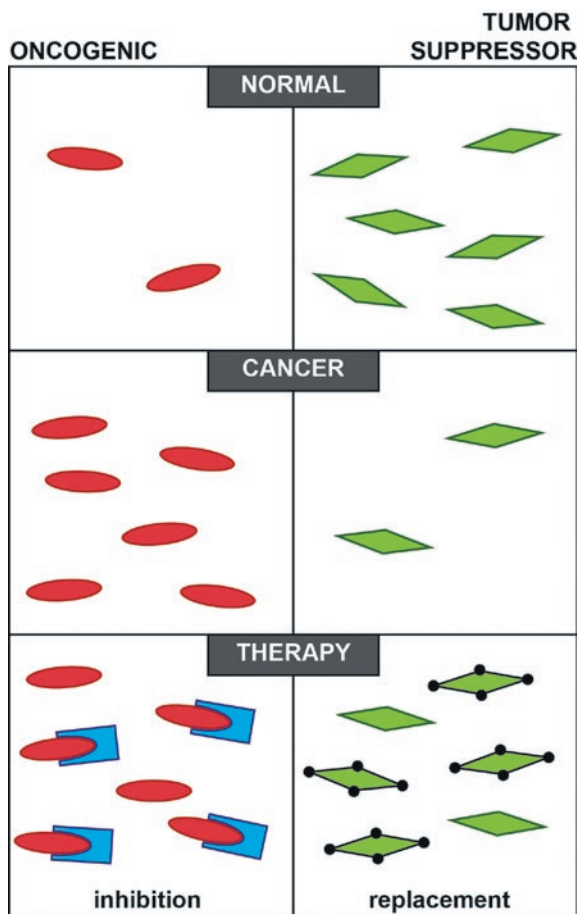


FIGURE 2. Schematic presentation of oncogenic and tumor suppressor miRNAs in normal and cancer cell and the potential of modifying state in cancer cell with therapy.

There is evidence that the expression can be lowered through RNAi technology, degradation by RnaseH or by genomic integration of RNA destabilizing elements.¹⁰⁹ Modifying the expression levels can represent some difficulty due to possible secondary structure of lncRNA. Inactivation of lncRNA is also possible through inhibition of active site via small molecule inhibitors. To be able to do this the molecular function needs to be known, which for most lncRNA is still elusive. It is also possible to disrupt the structure of lncRNA. Due to their length it is presumed some secondary structures exist. With the use of specially designed small molecules this structures would be disrupted leading to lncRNA loss of function. The potential of using specific therapeutics that would enable the mimicking or inhibition of certain non-coding RNA is promising and enormous.¹¹⁰

To reverse the levels of disrupted lncRNA in cancer a replacement therapy is also an option.

Some strategies of delivery are being explored. The use of lncRNA H19 specific expression in tumors has been explored through a plasmid delivery. Intratumoral delivery of plasmid, which carries the gene for the A subunit of diphtheria toxin under the regulation of H19 promoter, induces high expression of diphtheria toxin, which results in reduced tumor size.¹¹¹

Conclusions

Studies of miRNA and lncRNA have highlighted the importance of non-coding part of human genome. Of all lncRNA only few have been well characterized. Research also shows they have important function in cancer initiation, progression and metastasis. Further expression patterns in cancer will improve diagnosis and prognosis of cancer. With more functional and structural studies the potential of lncRNA therapies will be seen.

MiRNA as regulators of multiple genes promise a great potential in therapeutics and a switch from one drug one target to one drug multiple target therapy. Although there were great advances made in replacement and inhibitory strategies there are still challenges that include stability, safety and delivery of the chosen therapeutics. For therapeutics to become a successful application, the drug needs to be delivered in a way that ensures the stability of the molecules' transport to the appropriate cells.

References

- Iorio MV, Croce CM. MicroRNA dysregulation in cancer: diagnostics, monitoring and therapeutics. A comprehensive review. *EMBO Mol Med* 2012; **4**: 143-59.
- Mattick JS. The Genetic Signatures of Noncoding RNAs. *PLoS Genet* 2009; **5**.
- Eddy SR. Non-coding RNA genes and the modern RNA world. *Nat Rev Genet* 2001; **2**: 919-29.
- Mercer TR, Dinger ME, Mattick JS. Long non-coding RNAs: insights into functions. *Nat Rev Genet* 2009; **10**: 155-9.
- Kapranov P, Drenkow J, Cheng J, Long J, Helt G, Dike S, et al. Examples of the complex architecture of the human transcriptome revealed by RACE and high-density tiling arrays. *Genome Res* 2005; **15**: 987-97.
- Sana J, Faltejskova P, Svoboda M, Slaby O. Novel classes of non-coding RNAs and cancer. *J Transl Med* 2012; **10**: 103.
- Zen K, Zhang CY. Circulating MicroRNAs: a novel class of biomarkers to diagnose and monitor human cancers. *Med Res Rev* 2012; **32**: 326-48.
- Taft RJ, Pang KC, Mercer TR, Dinger M, Mattick JS. Non-coding RNAs: regulators of disease. *J Pathol* 2010; **220**: 126-39.
- Cortez MA, Bueso-Ramos C, Ferdin J, Lopez-Berestein G, Sood AK, Calin GA. MicroRNAs in body fluids-the mix of hormones and biomarkers. *Nat Rev Clin Oncol* 2011; **8**: 467-77.
- Rinn JL, Chang HY. Genome regulation by long noncoding RNAs. *Annu Rev Biochem* 2012; **81**: 145-66.
- Siomi MC, Sato K, Pezic D, Aravin AA. PIWI-interacting small RNAs: the vanguard of genome defence. *Nat Rev Mol Cell Bio* 2011; **12**: 246-58.
- Williams GT, Farzaneh F. Are snoRNAs and snoRNA host genes new players in cancer? *Nat Rev Cancer* 2012; **12**: 84-8.
- Montanaro L, Trere D, Derenzini M. Nucleolus, ribosomes, and cancer. *Am J Pathol* 2008; **173**: 301-10.
- Lares MR, Rossi JJ, Ouellet DL. RNAi and small interfering RNAs in human disease therapeutic applications. *Trends Biotechnol* 2010; **28**: 570-9.
- Mesojednik S, Kamensek U, Cemazar M. Evaluation of shRNA-mediated gene silencing by electroporation in LPB fibrosarcoma cells. *Radiol Oncol* 2008; **42**: 82-92.
- Wu XY, Zhong DX, Lin B, Zhai WL, Ding ZQ, Wu J. p38 MAPK regulates the expression of ether a go-go potassium channel in human osteosarcoma cells. *Radiol Oncol* 2013; **47**: 42-9.
- Zhao SH, Zhao F, Zheng JY, Gao LF, Zhao XJ, Cui MH. Knockdown of stat3 expression by RNAi inhibits in vitro growth of human ovarian cancer. *Radiol Oncol* 2011; **45**: 196-203.
- Hui A, How C, Ito E, Liu FF. Micro-RNAs as diagnostic or prognostic markers in human epithelial malignancies. *BMC Cancer* 2011; **11**: 500.
- Bustin SA, Murphy J. RNA biomarkers in colorectal cancer. *Methods* 2013; **59**: 116-25.
- Bresters D, Schipper MEI, Reesink HW, Boesernunnink BDM, Cuyper HTM. The Duration of Fixation Influences the Yield of Hcv Cdna-Pcr Products from Formalin-Fixed, Paraffin-Embedded Liver-Tissue. *J Virol Methods* 1994; **48**: 267-72.
- Cronin M, Pho M, Dutta D, Stephans JC, Shak S, Kiefer MC, et al. Measurement of gene expression in archival paraffin-embedded tissues: development and performance of a 92-gene reverse transcriptase-polymerase chain reaction assay. *Am J Pathol* 2004; **164**: 35-42.
- Nelson PT, Baldwin DA, Searce LM, Oberholtzer JC, Tobias JW, Mourelatos Z. Microarray-based, high-throughput gene expression profiling of microRNAs. *Nature Methods* 2004; **1**: 155-61.
- Hui AB, Shi W, Boutros PC, Miller N, Pintiile M, Fyles T, et al. Robust global micro-RNA profiling with formalin-fixed paraffin-embedded breast cancer tissues. *Lab Invest* 2009; **89**: 597-606.
- Lu Z, Liu M, Stribinskis V, Klinge CM, Ramos KS, Colburn NH, et al. MicroRNA-21 promotes cell transformation by targeting the programmed cell death 4 gene. *Oncogene* 2008; **27**: 4373-9.
- Asangani IA, Rasheed SAK, Nikolova DA, Leupold JH, Colburn NH, Post S, et al. MicroRNA-21 (miR-21) post-transcriptionally downregulates tumor suppressor Pcdcd4 and stimulates invasion, intravasation and metastasis in colorectal cancer. *Oncogene* 2008; **27**: 2128-36.
- Sempere LF, Christensen M, Silahatoglu A, Bak M, Heath CV, Schwartz G, et al. Altered microRNA expression confined to specific epithelial cell Subpopulations in breast cancer. *Cancer Res* 2007; **67**: 11612-20.
- Roth C, Rack B, Muller V, Janni W, Pantel K, Schwarzenbach H. Circulating microRNAs as blood-based markers for patients with primary and metastatic breast cancer. *Breast Cancer Res* 2010; **12**: R90.
- Wang FJ, Zheng ZG, Guo JF, Ding XF. Correlation and quantitation of microRNA aberrant expression in tissues and sera from patients with breast tumor. *Gynecol Oncol* 2010; **119**: 586-93.
- Heneghan HM, Miller N, Kelly R, Newell J, Kerin MJ. Systemic miRNA-195 Differentiates Breast Cancer from Other Malignancies and Is a Potential Biomarker for Detecting Noninvasive and Early Stage Disease. *Oncologist* 2010; **15**: 673-82.
- Lebanony D, Benjamin H, Gilad S, Ezagouri M, Dov A, Ashkenazi K, et al. Diagnostic Assay Based on hsa-miR-205 Expression Distinguishes Squamous From Nonsquamous Non-Small-Cell Lung Carcinoma. *J Clin Oncol* 2009; **27**: 2030-7.
- Roth C, Kasimir-Bauer S, Pantel K, Schwarzenbach H. Screening for circulating nucleic acids and caspase activity in the peripheral blood as potential diagnostic tools in lung cancer. *Mol Oncol* 2011; **5**: 281-91.

32. Xiao BX, Guo JM, Miao Y, Jiang Z, Huan R, Zhang YY, et al. Detection of miR-106a in gastric carcinoma and its clinical significance. *Clin Chim Acta* 2009; **400**: 97-102.
33. Zhang YY, Guo JM, Li D, Xiao BX, Miao Y, Jiang Z, et al. Down-regulation of miR-31 expression in gastric cancer tissues and its clinical significance. *Med Oncol* 2010; **27**: 685-9.
34. Zhang CN, Wang C, Chen X, Yang CH, Li K, Wang JJ, et al. Expression Profile of MicroRNAs in Serum: A Fingerprint for Esophageal Squamous Cell Carcinoma. *Clin Chem* 2010; **56**: 1871-9.
35. Liu R, Zhang CN, Hu ZB, Li G, Wang C, Yang CH, et al. A five-microRNA signature identified from genome-wide serum microRNA expression profiling serves as a fingerprint for gastric cancer diagnosis. *Eur J Cancer* 2011; **47**: 784-91.
36. Bloomston M, Frankel WL, Petrocca F, Volinia S, Alder H, Hagan JP, et al. MicroRNA expression patterns to differentiate pancreatic adenocarcinoma from normal pancreas and chronic pancreatitis. *Jama-J Am Med Assoc* 2007; **297**: 1901-8.
37. Habbe N, Koorstra JBM, Mendell JT, Offerhaus GJ, Ryu JK, Feldmann G, et al. MicroRNA miR-155 is a biomarker of early pancreatic neoplasia. *Cancer Biol Ther* 2009; **8**: 340-6.
38. du Rieu MC, Torrisoni J, Selves J, Al Saati T, Souque A, Dufresne M, et al. MicroRNA-21 Is Induced Early in Pancreatic Ductal Adenocarcinoma Precursor Lesions. *Clin Chem* 2010; **56**: 603-12.
39. Kong XY, Du YQ, Wang GK, Gao J, Gong YF, Li L, et al. Detection of Differentially Expressed microRNAs in Serum of Pancreatic Ductal Adenocarcinoma Patients: miR-196a Could Be a Potential Marker for Poor Prognosis. *Dig Dis Sci* 2011; **56**: 602-9.
40. Ho AS, Huang X, Cao HB, Christman-Skieller C, Bennewith K, Le QT, et al. Circulating miR-210 as a Novel Hypoxia Marker in Pancreatic Cancer. *Transl Oncol* 2010; **3**: 109-13.
41. Wang J, Chen JY, Chang P, LeBlanc A, Li DH, Abbruzzese JL, et al. MicroRNAs in Plasma of Pancreatic Ductal Adenocarcinoma Patients as Novel Blood-Based Biomarkers of Disease. *Cancer Prev Res* 2009; **2**: 807-13.
42. Shi XB, Xue L, Yang J, Ma AH, Zhao J, Xu M, et al. An androgen-regulated miRNA suppresses Bak1 expression and induces androgen-independent growth of prostate cancer cells. *Proc Natl Acad Sci U S A* 2007; **104**: 19983-8.
43. Bonci D, Coppola V, Musumeci M, Addario A, Giuffrida R, Memmo L, et al. The miR-15a-miR-16-1 cluster controls prostate cancer by targeting multiple oncogenic activities. *Nat Med* 2008; **14**: 1271-7.
44. Saini S, Majid S, Yamamura S, Tabatabai L, Suh SO, Shahryari V, et al. Regulatory Role of mir-203 in Prostate Cancer Progression and Metastasis. *Clin Cancer Res* 2011; **17**: 5287-98.
45. Hagman Z, Larne O, Edsjo A, Bjartell A, Ehrnstrom RA, Ulmert D, et al. miR-34c is downregulated in prostate cancer and exerts tumor suppressive functions. *Int J Cancer* 2010; **127**: 2768-76.
46. Spahn M, Kneitz S, Scholz CJ, Stenger N, Rudiger T, Strobel P, et al. Expression of microRNA-221 is progressively reduced in aggressive prostate cancer and metastasis and predicts clinical recurrence. *Int J Cancer* 2010; **127**: 394-403.
47. Mitchell PS, Parkin RK, Kroh EM, Fritz BR, Wyman SK, Pogossova-Agadjanyan EL, et al. Circulating microRNAs as stable blood-based markers for cancer detection. *Proc Natl Acad Sci U S A* 2008; **105**: 10513-8.
48. Brase JC, Johannes M, Schlomm T, Falth M, Haese A, Steuber T, et al. Circulating miRNAs are correlated with tumor progression in prostate cancer. *Int J Cancer* 2011; **128**: 608-16.
49. Zhang HL, Yang LF, Zhu Y, Yao XD, Zhang SL, Dai B, et al. Serum miRNA-21: Elevated Levels in Patients With Metastatic Hormone-Refractory Prostate Cancer and Potential Predictive Factor for the Efficacy of Docetaxel-Based Chemotherapy. *Prostate* 2011; **71**: 326-31.
50. Agaoglu FY, Kovancilar M, Dizdar Y, Darendeliler E, Holdenrieder S, Dalay N, et al. Investigation of miR-21, miR-141, and miR-221 in blood circulation of patients with prostate cancer. *Tumor Biology* 2011; **32**: 583-8.
51. Bryant RJ, Pawlowski T, Catto JWF, Marsden G, Vessella RL, Rhee B, et al. Changes in circulating microRNA levels associated with prostate cancer. *Br J Cancer* 2012; **106**: 768-74.
52. Kluiver J, Poppema S, de Jong D, Blokzijl T, Harms G, Jacobs S, et al. BIC and miR-155 are highly expressed in Hodgkin, primary mediastinal and diffuse large B cell lymphomas. *J Pathol* 2005; **207**: 243-9.
53. Huang ZH, Huang D, Ni SJA, Peng ZL, Sheng WQ, Du X. Plasma microRNAs are promising novel biomarkers for early detection of colorectal cancer. *Int J Cancer* 2010; **127**: 118-26.
54. Cheng HY, Zhang LN, Cogdell DE, Zheng H, Schetter AJ, Nykter M, et al. Circulating Plasma MiR-141 Is a Novel Biomarker for Metastatic Colon Cancer and Predicts Poor Prognosis. *PLoS One* 2011; **6**: e17745.
55. Ferracin M, Pedriali M, Veronese A, Zagatti B, Gafa R, Magri E, et al. MicroRNA profiling for the identification of cancers with unknown primary tissue-of-origin. *J Pathol* 2011; **225**: 43-53.
56. Gupta RA, Shah N, Wang KC, Kim J, Horlings HM, Wong DJ, et al. Long non-coding RNA HOTAIR reprograms chromatin state to promote cancer metastasis. *Nature* 2010; **464**: 1071-6.
57. Geng YJ, Xie SL, Li Q, Ma J, Wang GY. Large Intervening Non-coding RNA HOTAIR is Associated with Hepatocellular Carcinoma Progression. *J Int Med Res* 2011; **39**: 2119 - 28.
58. Yu W, Gius D, Onyango P, Muldoon-Jacobs K, Karp J, Feinberg AP, et al. Epigenetic silencing of tumour suppressor gene p15 by its antisense RNA. *Nature* 2008; **451**: 202-6.
59. Chen W, Böcker W, Brosius J, Tiedge H. Expression of neural BC200 RNA in human tumours. *J Pathol* 1997; **183**: 345-51.
60. Iacoangeli A, Lin Y, Morley EJ, Muslimov IA, Bianchi R, Reilly J, et al. BC200 RNA in invasive and preinvasive breast cancer. *Carcinogenesis* 2004; **25**: 2125-33.
61. Chung S, Nakagawa H, Uemura M, Piao L, Ashikawa K, Hosono N, et al. Association of a novel long non-coding RNA in 8q24 with prostate cancer susceptibility. *Cancer Sci* 2011; **102**: 245-52.
62. Gabory A, Jammes H, Dandolo L. The H19 locus: role of an imprinted non-coding RNA in growth and development. *Bioessays* 2010; **32**: 473-80.
63. Hibi K, Nakamura H, Hirai A, et al. Loss of H19 imprinting in esophageal cancer. *Cancer Res* 1996; **56**: 480-2.
64. Fellig Y, Ariel I, Ohana P, Schachter P, Sinelnikov I, Birman T, et al. H19 expression in hepatic metastases from a range of human carcinomas. *J Clin Pathol* 2005; **58**: 1064-8.
65. Matouk IJ, DeGroot N, Mezan S, Ayesh S, Abu-lail R, Hochberg A, et al. The H19 non-coding RNA is essential for human tumor growth. *PLoS One* 2007; **2**: e845.
66. Arima T, Matsuda T, Takagi N, Wake N. Association of IGF2 and H19 imprinting with choriocarcinoma development. *Cancer Genet Cytogenet* 1997; **93**: 39-47.
67. Berteaux N, Lottin S, Monte D, Pinte S, Quatannens B, Coll J, et al. H19 mRNA-like noncoding RNA promotes breast cancer cell proliferation through positive control by E2F1. *J Biol Chem* 2005; **280**: 29625-36.
68. Barsyte-Lovejoy D, Lau SK, Boutros PC, Khosravi F, Jurisica I, Andrusil IL, et al. The c-Myc oncogene directly induces the H19 noncoding RNA by allele-specific binding to potentiate tumorigenesis. *Cancer Res* 2006; **66**: 5330-7.
69. Tsai MC, Manor O, Wan Y, Mosammamaparast N, Wang JK, Lan F, et al. Long noncoding RNA as modular scaffold of histone modification complexes. *Science* 2010; **329**: 689-93.
70. Yang Z, Zhou L, Wu LM, Lai MC, Xie HY, Zhang F, et al. Overexpression of long non-coding RNA HOTAIR predicts tumor recurrence in hepatocellular carcinoma patients following liver transplantation. *Ann Surg Oncol* 2011; **18**: 1243-50.
71. Matouk IJ, Abbasi I, Hochberg A, Galun E, Dweik H, Aklawi M. Highly upregulated in liver cancer noncoding RNA is overexpressed in hepatic colorectal metastasis. *Eur J Gastroenterol Hepatol* 2009; **21**: 688-92.
72. Panzitt K, Tschernatsch MM, Guelly C, Moustafa T, Stradner M, Strohmaier HM, et al. Characterization of HULC, a novel gene with striking up-regulation in hepatocellular carcinoma, as noncoding RNA. *Gastroenterology* 2007; **132**: 330-42.
73. Guffanti A, Iacono M, Pelucchi P, Kim N, Solda G, Croft LJ, et al. A transcriptional sketch of a primary human breast cancer by 454 deep sequencing. *BMC Genomics* 2009; **10**: 163.

74. Yamada K, Kano J, Tsunoda H, Yoshikawa H, Okubo C, Ishiyama T, et al. Phenotypic characterization of endometrial stromal sarcoma of the uterus. *Cancer Sci* 2006; **97**: 106-12.
75. Lin R, Maeda S, Liu C, Karin M, Edgington TS. A large noncoding RNA is a marker for murine hepatocellular carcinomas and a spectrum of human carcinomas. *Oncogene* 2007; **26**: 851-8.
76. Luo JH, Ren B, Keryanov S, Tsang GC, Reo UNM, Monga SP, et al. Transcriptomic and genomic analysis of human hepatocellular carcinomas and hepatoblastomas. *Hepatology* 2006; **44**: 1012-24.
77. Gejman R, Batista DL, Zhong Y, Zhou Y, Zhang X, Swearingen B, et al. Selective loss of MEG3 expression and intergenic differentially methylated region hypermethylation in the MEG3/DLK1 locus in human clinically non-functioning pituitary adenomas. *J Clin Endocrinol Metab* 2008; **93**: 4119-25.
78. Benetatos L, Vartholomatos G, Hatzimichael E. MEG3 imprinted gene contribution in tumorigenesis. *Int J Cancer* 2011; **129**: 773-9.
79. Polisenio L, Salmena L, Zhang J, Carver B, Haveman WJ, Pandolfi PP. A coding-independent function of gene and pseudogene mRNAs regulates tumour biology. *Nature* 2010; **465**: 1033-8.
80. Khaithan D, Dinger ME, Mazar J, Crawford J, Smith MA, Mattick JS, et al. The melanoma-upregulated long noncoding RNA SPRY4-IT1 modulates apoptosis and invasion. *Cancer Res* 2011; **71**: 3852-62.
81. Lanz RB, Chua SS, Barron N, Soder BM, DeMayo F, O'Malley BW. Steroid Receptor RNA Activator Stimulates Proliferation as Well as Apoptosis In Vivo. *Mol Cell Biol* 2003; **23**: 7163-76.
82. Chooniedass-Kothari S, Vincett D, Yan Y, Cooper C, Hamedani MK, Myal Y, et al. The protein encoded by the functional steroid receptor RNA activator is a new modulator of ER alpha transcriptional activity. *FEBS Lett* 2010; **584**: 1174-80.
83. Wang F, Li X, Xie X, Zhao L, Chen W. UCA1, a non-protein-coding RNA up-regulated in bladder carcinoma and embryo, influencing cell growth and promoting invasion. *FEBS Lett* 2008; **582**: 1919-27.
84. Wang XS, Zhang Z, Wang HC, Cai JL, Xu QW, Li MQ, et al. Rapid identification of UCA1 as a very sensitive and specific unique marker for human bladder carcinoma. *Clin Cancer Res* 2006; **12**: 4851-8.
85. de Kok JB, Verhaegh GW, Roelofs RW, Hessels D, Kiemeneys LA, Aalders TW, et al. DD3(PCA3), a very sensitive and specific marker to detect prostate tumors. *Cancer Res* 2002; **62**: 2695-89.
86. Mourtada-Maarabouni M, Pickard MR, Hedge VL, Farzaneh F, Williams GT. GASS, a non-protein-coding RNA, controls apoptosis and is downregulated in breast cancer. *Oncogene* 2009; **28**: 195-208.
87. Yap KL, Li S, Munoz-Cabello AM, Raguz S, Zeng L, Mujtaba S, et al. Molecular interplay of the noncoding RNA ANRIL and methylated histone H3 lysine 27 by polycomb CBX7 in transcriptional silencing of INK4a. *Mol Cell* 2010; **38**: 662-74.
88. Rajaram V, Knezevich S, Bove KE, Perry A, Pfeifer JD. DNA sequence of the translocation breakpoints in undifferentiated embryonal sarcoma arising in mesenchymal hamartoma of the liver harboring the t(11;19)(q11;q13.4) translocation. *Genes Chromosom Cancer* 2007; **46**: 508-13.
89. Lai MC, Yang Z, Zhou L, Zhu QQ, Xie HY, Zhang F, et al. Long non-coding RNA MALAT-1 overexpression predicts tumor recurrence of hepatocellular carcinoma after liver transplantation. *Med Oncol* 2012; **29**: 1810-6.
90. Kino T, Hurt DE, Ichijo T, Nader N, Chrousos GP. Noncoding RNA gas5 is a growth arrest- and starvation-associated repressor of the glucocorticoid receptor. *Sci Signal* 2010; **3**: ra8.
91. Marks LS, Fradet Y, Deras IL, Blase A, Mathis J, Aubin SMJ, et al. PCA3 molecular urine assay for prostate cancer in men undergoing repeat biopsy. *Urology* 2007; **69**: 532-5.
92. Tinzl M, Marberger M, Horvath S, Chypre C. DD3PCA3 RNA Analysis in Urine – a new perspective for detecting prostate cancer. *Eur Urol* 2004; **46**: 182-7.
93. Neves AF, Dias-Oliveira JDD, Araujo TG, Marangoni K, Goulart LR. Prostate cancer antigen 3 (PCA3) RNA detection in blood and tissue samples for prostate cancer diagnosis. *Clin Chem Lab Med* 2013; **51**: 881-7.
94. Oberg AL, French AJ, Sarver AL, Subramanian S, Morlan BW, Riska SM, et al. miRNA Expression in Colon Polyps Provides Evidence for a Multihit Model of Colon Cancer. *PLoS One* 2011; **6**: e20465.
95. Kent OA, Mendell JT. A small piece in the cancer puzzle: microRNAs as tumor suppressors and oncogenes. *Oncogene* 2006; **25**: 6188-96.
96. Kota SK, Balasubramanian S. Cancer therapy via modulation of micro RNA levels: a promising future. *Drug Discov Today* 2010; **15**: 733-40.
97. Bader AG, Brown D, Stoudemire J, Lammers P. Developing therapeutic microRNAs for cancer. *Gene Ther* 2011; **18**: 1121-6.
98. Broderick JA, Zamore PD. MicroRNA therapeutics. *Gene Ther* 2011; **18**: 1104-10.
99. Croce CM. Causes and consequences of microRNA dysregulation in cancer. *Nat Rev Genet* 2009; **10**: 704-14.
100. Bader AG, Brown D, Winkler M. The Promise of MicroRNA Replacement Therapy. *Cancer Res* 2010; **70**: 7027-30.
101. Dolinsek T, Markelc B, Sersa G, Coer A, Stimac M, Lavrencak J, et al. Multiple Delivery of siRNA against Endoglin into Murine Mammary Adenocarcinoma Prevents Angiogenesis and Delays Tumor Growth. *PLoS One* 2013; **8**: e58723.
102. Todorovic V, Sersa G, Cemazar M. Gene electrotransfer of siRNAs against CD146 inhibits migration and invasion of human malignant melanoma cells SK-MEL28. *Cancer Gene Ther* 2013; **20**: 208-10.
103. Si ML, Zhu S, Wu H, Lu Z, Wu F, Mo YY. miR-21-mediated tumor growth. *Oncogene* 2007; **26**: 2799-803.
104. Ebert MS, Neilson JR, Sharp PA. MicroRNA sponges: competitive inhibitors of small RNAs in mammalian cells. *Nature Methods* 2007; **4**: 721-6.
105. Ma L, Young J, Prabhala H, Pan E, Mestdagh P, Muth D, et al. miR-9, a MYC/MYCn-activated microRNA, regulates E-cadherin and cancer metastasis. *Nat Cell Biol* 2010; **12**: 247-52.
106. Trang P, Medina PP, Wiggins JF, Ruffino L, Kelnar K, Omotola M, et al. Regression of murine lung tumors by the let-7 microRNA. *Oncogene* 2010; **29**: 1580-7.
107. Kumar MS, Erkeland SJ, Pester RE, Chen CY, Ebert MS, Sharp PA, et al. Suppression of non-small cell lung tumor development by the let-7 microRNA family. *Proc Natl Acad Sci U S A* 2008; **105**: 3903-8.
108. Ji Q, Hao X, Meng Y, Zhang M, DeSano J, Fan DM, et al. Restoration of tumor suppressor miR-34 inhibits human p53-mutant gastric cancer tumorspheres. *BMC Cancer* 2008; **8**: 266.
109. Gutschner T, Baas M, Diederichs S. Noncoding RNA gene silencing through genomic integration of RNA destabilizing elements using zinc finger nucleases. *Genome Res* 2011; **21**: 1944-54.
110. Borralho PM, Simoes AES, Gomes SE, Lima RT, Carvalho T, Ferreira DMS, et al. miR-143 Overexpression Impairs Growth of Human Colon Carcinoma Xenografts in Mice with Induction of Apoptosis and Inhibition of Proliferation. *PLoS One* 2011; **6**: e23787.
111. Mizrahi A, Czerniak A, Levy T, Amiur S, Gallula J, Matouk I, et al. Development of targeted therapy for ovarian cancer mediated by a plasmid expressing diphtheria toxin under the control of H19 regulatory sequences. *J Transl Med* 2009; **7**: 69.

Emerging clinical importance of the cancer biomarkers kallikrein-related peptidases (KLK) in female and male reproductive organ malignancies

Manfred Schmitt¹, Viktor Magdolen¹, Feng Yang¹, Marion Kiechle¹, Jane Bayani², George M. Yousef^{3,4}, Andreas Scorilas⁵, Eleftherios P. Diamandis^{3,5}, Julia Dorn¹

¹ Clinical Research Unit, Department of Obstetrics and Gynecology, Klinikum rechts der Isar, Technische Universität München, Munich, Germany

² Ontario Institute for Cancer Research, Transformative Pathology Department, Toronto, Canada

³ Department of Laboratory Medicine and Pathobiology, University of Toronto, Toronto, Canada

⁴ Department of Laboratory Medicine and the Keenan Research Centre in the Li KaShing Knowledge Institute, St Michael's Hospital, Toronto, Canada

⁵ Department of Biochemistry and Molecular Biology, University of Athens

⁶ Department of Pathology and Laboratory Medicine, Mount Sinai Hospital, Toronto, Canada

Radiol Oncol 2013; 47(4): 319-329.

Received 10 July 2013

Accepted 25 July 2013

Correspondence to: Prof. Dr. Manfred Schmitt, Klinische Forschergruppe der Frauenklinik der Technischen Universität München, Ismaninger Strasse 22, 81675 München, Germany. E-mail: manfred.schmitt@LRZ.tum.de

Disclosure: The authors have no conflict of interest to disclose.

The paper was presented at the 7th Conference of Experimental and Translational Oncology, 20-24th April 2013, Portoroz, Slovenia (www.ceto.si) co-organised and supported by COST TD1104 Action (www.electroporation.net).

Background. Tumor tissue-associated KLKs (kallikrein-related peptidases) are clinically important biomarkers that may allow prognosis of the cancer disease and/or prediction of response/failure of cancer patients to cancer-directed drugs. Regarding the female/male reproductive tract, remarkably, all of the fifteen KLKs are expressed in the normal prostate, breast, cervix uteri, and the testis, whereas the uterus/endometrium and the ovary are expressing a limited number of KLKs only.

Conclusions. Most of the information regarding elevated expression of KLKs in tumor-affected organs is available for ovarian cancer; depicting them as valuable biomarkers in the cancerous phenotype. In contrast, for breast cancer, a series of KLKs was found to be downregulated. However, in breast cancer, KLK4 is elevated which is also true for ovarian and prostate cancer. In such cases, selective synthetic KLK inhibitors that aim at blocking the proteolytic activities of certain KLKs may serve as future candidate therapeutic drugs to interfere with tumor progression and metastasis.

Key words: cancer; proteases; endometrium; ovary; uterus; prostate; testis; cervix; breast

Introduction

The human genome encompasses close to 600 different proteases, with about 180 serine proteases (<http://degradome.uniovi.es/numbers.html>). Serine proteases, *e.g.* plasmin, thrombin, urokinase (uPA), and the KLKs (kallikrein-related serine

peptidases) regulate diverse biological processes such as general protein turnover, embryogenesis and pregnancy, blood coagulation, complement activation, and wound healing.¹ More specifically, serine proteases are involved in cell proliferation and cell signaling, cell migration and invasion, apoptosis and cell death, not only under physiologi-

cal conditions but also in cancer. Proteases can be released from tissues into the blood, ascitic fluid, alveolar fluid, and cerebrospinal fluid.

KLKs, belonging to the protease clan PA, protease family S1 with subfamily A, located on chromosome 19q13.3-q13.4, are novel, well-suited cancer biomarkers. KLKs are supposed to be of clinical value to identify low- versus high-risk cancer patients, and to predict the course of the cancer disease and response to cancer therapeutics of male and female patients afflicted with reproductive tract malignancies, in addition to cancers of the lung, brain, skin, head and neck, kidney, urinary bladder, and the gastrointestinal tract. In high-risk cancer patient groups, these proteases cannot only be biomarkers for prognosis and therapy response but also act as valuable targets for small size cancer therapeutics, eventually resulting in reduction of the process of tumor cell dissemination and metastasis.²

The present, often inefficient, approach to systemic treatment of cancer is commonly referred to as a “trial and error” or “one size fits all” tactic. However, to achieve personalized treatment for cancer patients, one needs meaningful tissue-related or blood-borne biomarkers for the characterization of cancer subgroups, to determine prognosis, response to cancer therapeutics, and to predict severe toxicity related to treatment.³ For the cancer biomarkers in focus, a number of the fifteen members of the KLK family are thought to serve as such prognostic and predictive biomarkers, for patients afflicted with various solid malignant tumors.

Highly acknowledged, published evidence supports a strong clinical value of various KLKs to predict the course of certain cancer diseases and in these groups of patients, response to cancer therapy.¹ Since most of the published data have been collected for ovarian, breast, and prostate cancer, this review focusses on the clinical utility of KLKs for female and male reproductive organ malignancies and the current state-of-the-art regarding incidence of KLKs in afflicted reproductive organs and their potential to predict a patient’s risk to experience untimely disease recurrence, early death, or response/failure to adjuvant or palliative cancer therapy.

In the male urogenital tract, remarkably, all of the KLKs are expressed in the normal prostate and the testes, whereas in females this is only the case for the breast but not for the uterus/endometrium or the ovaries. Most of the information regarding mRNA and/or protein expression of KLKs in tumor-affected organs is available for ovarian cancer; all of the twelve KLKs tested so far were found to

be elevated in the malignant state, depicting them as valuable biomarkers to distinguish between the normal and the cancerous phenotype. In contrast, for breast cancer, at the mRNA level, eleven KLKs were found to be down regulated, while *KLK4* and *KLK15* mRNAs were overexpressed compared to normal breast tissue. Interestingly, *KLK4* is also overexpressed in cancer of the endometrium, ovary, and the prostate.

In the western world, the incidence of gynecological malignancies is highest for endometrial cancer, followed by cervical and ovarian cancer, while the mortality rate is highest for ovarian cancer, followed by cervical and endometrial cancer.² For cancers of the male reproductive tract encompassing those of the prostate, testis, and penis, prostate cancer is the most frequent cancer in men of older age whereas testicular cancer is most common in younger men.^{3,4}

KLKs are known to be involved in hormone-dependent cancers of the reproductive system of male or female patients, *e.g.* that of the ovary, breast, prostate.⁵⁻⁸ Remarkably, in women, the clinical impact of KLK family members as novel biomarkers for screening, diagnosis, prognosis, or therapy response prediction has been mainly studied in ovarian cancer patients.^{5,9-17}

KLK expression in ovarian cancer

Prognosis of tumors of the ovary is poor, owing to late diagnosis and often inefficient primary debulking surgery of this rare malignancy, but because of rapidly developing chemoresistance as well. In general, the term “ovarian cancer” describes epithelial-surface-type tumors of the ovary, accounting for more than 80% of all solid ovarian tumors. Others, such as sex cord-stromal tumors, germ cell tumors, and metastases from for example gastrointestinal tumors are less common. Two-third of the ovarian cancer patients will develop chemoresistance and disease recurrence within the first 5 years after primary surgery. The therapy of choice is paclitaxel plus carboplatin polychemotherapy. Neither vaginal ultrasonography nor analysis of the tumor-associated antigen CA125 in serum, nor other protein or gene expression analyses of the blood or tumor tissue (*e.g.* ROMA and OVA1) are sufficiently specific to predict the course of the disease or response to systemic adjuvant therapy.¹⁸⁻²⁰

The stage of ovarian cancer according to the International Federation of Gynecology and

Obstetrics (FIGO I-IV) at the time of diagnosis of the disease represents the major traditional prognostic factor. The 5-year survival of early FIGO stage I patients is more than 90%, while survival of patients with FIGO stage III and IV is only 25%. Other important traditional prognostic factors are size of residual tumor mass after cytoreductive surgery histology of the tumor tissue, tumor grade, and presence of ascitic fluid.^{21,22} Apart from that, tumor tissue-based biomarkers for screening and risk-group sub classification of early (FIGO I, II) or advanced (FIGO III, IV) ovarian cancer patients reflecting the biology of the tumor are urgently needed.

In this respect, in the last decade, mRNA and protein expression of various members of the KLK family has been studied extensively in a variety of normal and diseased human tissues, including the ovary and ovarian cancer.^{5,9,23} In normal human ovary tissues, *KLK* expression at the mRNA level is highest for *KLK6-8* and *10*, whereas low to moderate expression was noted for *KLK1, 9, 11, 13* and *14* with no expression for *KLK2-5, 12*, and *15*. (Table 1, Figure 1). At the protein level, low to moderate amounts were found for *KLK1, 5-8*, and *10-14*; *KLK2-4, 9* and *15* proteins are not expressed (Table 1, Figure 1).²³ Compared to normal ovarian tissues, concomitant up regulation of twelve (*KLK3-11* and *13-15*) of the fifteen *KLKs* at the mRNA and/or protein expression level is characteristic for ovarian cancer (Table 1, Figure 2).²⁴⁻⁴⁰ Regarding the clinical impact of some of the *KLKs*, expression of *KLK4-7, 10* and *15* indicates poor prognosis; *KLK8, 9, 11, 13* and *14* are markers of a favorable prognosis. Furthermore, *KLK5-8, 10, 11* and *13* are judged as promising predictive ovarian cancer biomarkers.

Seven *KLKs* (*KLK5-8, 10, 11* and *14*) are released into the blood, six of these *KLKs* are also released into peritoneal ascitic fluid (*KLK5, 7, 8, 10, 11* and *14*) of ovarian cancer patients.⁴¹⁻⁴⁸ *KLK* proteins released into the blood or ascitic fluid may also predict the course of early and/or late stage ovarian cancer. *KLK8* protein present in blood (serum) indicates a favorable prognosis for the ovarian cancer patient while elevated protein levels of *KLK5, 6, 10* and *11* are markers of a poor clinical outcome.^{44,46-49}

KLK expression in cervical cancer

Owing to well-accepted screening programs and successful therapy of pre-malignant lesions and early stages of cervical cancer, this malignant dis-

TABLE 1. *KLKs* present in normal and tumor tissues of patients afflicted with ovarian cancer

OVARY, NORMAL

Expression level (mRNA)	KLK number
Absent	2-5, 12, 15
Low	9, 13
Moderate	1, 11, 14
High	6-8, 10

Expression level (protein)	KLK number
Absent	2-4, 9, 15
Low	8, 14
Moderate	1, 6, 7, 10, 11
Present	5, 12, 13

OVARY, CANCER

Expression level (mRNA)	KLK number
Not determined	1, 2, 9, 12
Decreased	14
Increased	3-8, 10, 11, 13, 15

Expression level (protein)	KLK number
Not determined	1, 2, 12
Increased	3-11, 13-15

ease has become a rare disease in the industrialized world, although, malignant tumors of the cervix uteri are still one of the leading causes of death of young women in other countries. Cervical cancer develops stepwise from infection with the human papilloma virus (HPV) and subsequent inefficient immune response to eliminate the virus followed by cervical dysplasia (CIN I-III), subsequently turning into an invasive type of cervical carcinoma.⁵⁰

One of the most important factors to predict the clinical outcome of cervical cancer is clinical stage at the time of diagnosis, thus management of cervical cancer is stage-dependent. Early invasive cervical cancers are subject to surgery, whereby total radical hysterectomy including dissection of the parametries and pelvic lymph nodes, and resection of the vaginal cuff is achieved. In advanced stages of cervical cancer, primary radio-chemotherapy is the therapy of choice⁵¹, while cancer biomarkers play a lesser role in the management of this can-

TABLE 2. KLKs present in normal and tumor tissues of patients afflicted with cervical cancer**CERVIX UTERI, NORMAL**

Expression level (mRNA)	KLK number
Absent	15
Low	2, 3, 12
Moderate	1, 14
High	4-11, 13

Expression level (protein)	KLK number
Absent	2, 3, 15
Low	1, 4-8, 10, 13, 14
Moderate	9, 11, 12

CERVIX UTERI, CANCER

Expression level (mRNA)	KLK number
Not determined	1-15

Expression level (protein)	KLK number
Not determined	1-6, 9-15
Increased	7, 8

cer disease. Undeniably, no effective prognostic or predictive cancer biomarkers have been established yet for any stage of cervical cancer.⁵²

For normal cervix tissue (Table 2, Figure 1), low to moderate mRNA levels were reported for *KLK1-3, 12* and *14*, high ones for *KLK4-11* and *13*; *KLK15* mRNA is not expressed.^{23,53,54} Low to moderate KLK protein levels were determined for *KLK1* and *4-14*; *KLK2, 3* and *15* proteins are not expressed. Although KLK mRNA or protein is present in normal cervix tissues, except *KLK15*, no data have been reported for any KLK mRNA expression in the malignant state (Table 2, Figure 2). Similar, in cervical cancer, no protein expression data were presented for most of the KLKs, except for *KLK7* and *8* which are up regulated compared to normal cervix tissue.^{55,56} It is worth mentioning that *KLK7* protein content increases with the severity of cervical lesions, *i.e.* from cervicitis to low-grade cervical intraepithelial neoplasia, high-grade cervical intraepithelial neoplasia, squamous cervical carcinomas, and even cervical adenocarcinomas.⁵⁷ Obviously, *KLK7* could evolve as a useful marker

TABLE 3. KLKs present in normal and tumor tissues of patients afflicted with endometrial cancer**ENDOMETRIUM, NORMAL**

Expression level (mRNA)	KLK number
Not determined	4, 5, 7, 9, 11-15
Present	1-3, 6, 8, 10

Expression level (protein)	KLK number
Not determined	2, 9, 15
Present	1, 3-8, 10-14

ENDOMETRIUM, CANCER

Expression level (mRNA)	KLK number
Not determined	2-5, 7, 9, 11-15
Decreased	1
Increased	6, 8, 10

Expression level (protein)	KLK number
Not determined	1-3, 5-7, 9-15
Increased	4, 8

additional to the PAP smear for screening of cervical precursor lesions.⁵⁷

KLK expression in endometrial cancer

Endometrial cancer, which is a malignancy of the elderly female, derives from the inner glandular layer of the uterus; luckily it is often diagnosed in an early stage of the disease, which leads to expect a favorable clinical outcome. The therapy of choice for endometrial cancer is hysterectomy with bilateral salpingo-oophorectomy, frequently associated with pelvic and paraaortal lymphadenectomy and/or followed by adjuvant radiotherapy. Systemic chemotherapy or endocrine therapy is predominantly administered in advanced stages of endometrial cancer, which are rare.⁵⁸

At present, no effective serological or tissue biomarkers do exist to classify endometrial carcinoma patients at risk. Notwithstanding this, immunoenzymometric testing revealed that for eight of the



FIGURE 1. Comparative mRNA and protein expression in normal tissues of the reproductive tract

fifteen KLKs low to moderate protein levels were determined in tissue extracts of the uterus (KLK1, 4, 6, 9 and 11-14), seven were not (Figure 1). At the mRNA level, low to moderate values for six of the KLKs were detected (KLK1, 3, 10-12 and 14) (Figure 1).

Informative data are available for KLK expression in the normal endometrium, at the mRNA and protein level (Table 3, Figure 1). Six KLK mRNAs (KLK1-3, 6, 8 and 10) were found to be expressed, for the other nine KLKs no mRNA expression data have been reported. Assessment by immunohistochemical staining demonstrated protein expression of twelve KLKs (KLK1, 3-8 and 10-14), no data are available regarding protein expression in the normal endometrium of the other three KLKs.⁵⁴ Not much of published information is available regarding the mRNA/protein expression patterns of KLKs in endometrial carcinoma (Table 3, Figure 2). At the mRNA level, KLK1 was found to be down-regulated whereas KLK6, 8 and 10 are up-regulated. KLK4 and 8 proteins are up-regulated; no data are available for this malignancy regarding protein expression of the other thirteen KLKs.

KLK expression in breast cancer

Even though treatment options such as surgery, radiotherapy, chemotherapy/ endocrine therapy, and immunotherapy are currently available, breast cancer remains the second leading cause of cancer-related deaths among women after lung cancer.⁵⁹ Development of breast cancer is a result of multiple genetic changes of epithelial cells and by environmental insults. Several factors may contribute to this malignant transformation process, e.g. oncogenes, tumor suppressor genes, hormones, growth factors, and proteases. Serum/plasma-based biomarkers would be helpful for the early diagnosis of breast cancer, for assessment of the course of the disease, prediction of response or resistance to cancer therapeutics, or monitoring of efficacy of therapy.

In fact, several serum-based biomarkers have been described in the literature and are in clinical application, such as CA 15-3, BR 27.29 (CA27.29), carcinoembryonic antigen (CEA), tissue polypeptide antigen, tissue polypeptide specific antigen, or p105HER2 (the shed extracellular domain of

TABLE 4. KLKs present in normal and tumor tissues of patients afflicted with breast cancer**BREAST, NORMAL**

Expression level (mRNA)	KLK number
Absent	15
Low	4, 9, 12
Moderate	2, 3, 5, 13
High	1, 6-8, 10, 11, 14

Expression level (protein)	KLK number
Absent	3 ^a , 10, 12
Low	1, 4, 7, 13
Moderate	2, 5, 6, 8, 14, 15
High	9, 11
Present	3 ^a

^a Depending on the patient, KLK3 can be expressed or absent.

BREAST, CANCER

Expression level (mRNA)	KLK number
Unchanged	3, 8, 11
Decreased	1, 2, 5-12, 14
Increased	4, 6, 14, 15
Present	13

Expression level (protein)	KLK number
Not determined	2, 7-9, 11-13, 15
Absent	3
Increased	4, 6, 14
Decreased	3, 6, 14
Present	1, 5, 10

HER2).⁶⁰ Although none of these markers is specific or sensitive enough to allow early diagnosis of malignant breast cases or prognosis regarding the clinical course of the breast cancer disease.⁶¹ Thus, prognostic breast cancer biomarkers in regular clinical practice mainly encompass histomorphological markers (TNM status: tumor size, nodal status, incidence of metastasis, nuclear grading, histological subtype, lymphovascular invasion) plus determination of protein expression of receptors for the steroid hormones estrogen and progesterone but also newer cancer biomarkers such as the

TABLE 5. KLKs present in normal and tumor tissues of patients afflicted with prostate cancer**PROSTATE, NORMAL**

Expression level (mRNA)	KLK number
Low	5, 6, 9, 13
Moderate	4, 7, 8, 12
High	1-3, 10, 11, 14, 15

Expression level (protein)	KLK number
Absent	8
Low	4, 5, 13-15
High	1-3, 9, 11
Present	6, 7, 10, 12

PROSTATE, CANCER

Expression level (mRNA)	KLK number
Not determined	1, 6, 8, 9, 12
Decreased	3, 5, 7, 10, 11
Increased	2, 4, 13-15

Expression level (protein)	KLK number
Not determined	1, 5, 8, 9
Decreased	2, 3, 6, 7, 10, 11, 13, 15
Increased	2, 4, 12-14

multigene panel Oncotype DX and tumor invasion factors uPA/PAI-1.⁶²

Extracellular proteases such as uPA, plasmin, matrix metalloproteases, cathepsins, and the KLKs mediate many of the changes in the tumor micro-environment during tumor progression in disrupting the tumor nest-surrounding the basement membrane and the adjacent extracellular matrix (tumor stroma). With the recent discovery of all of the fifteen members of the KLK family, increasing evidence has indicated that KLKs may play pivotal roles in breast cancer progression and metastasis (Table 4, Figure 1,2).⁶³⁻⁶⁵ In normal breast tissue, all fifteen KLKs have been identified, either at the mRNA and/or the protein level.^{23,66} *KLK15* mRNA is not expressed by normal breast tissue, low to moderate mRNA levels are detected for *KLK2-5, 9, 12 and 13*, high ones for *KLK1, 6-8, 10, 11 and 14*. No expression of *KLK10* and *12* protein was determined but

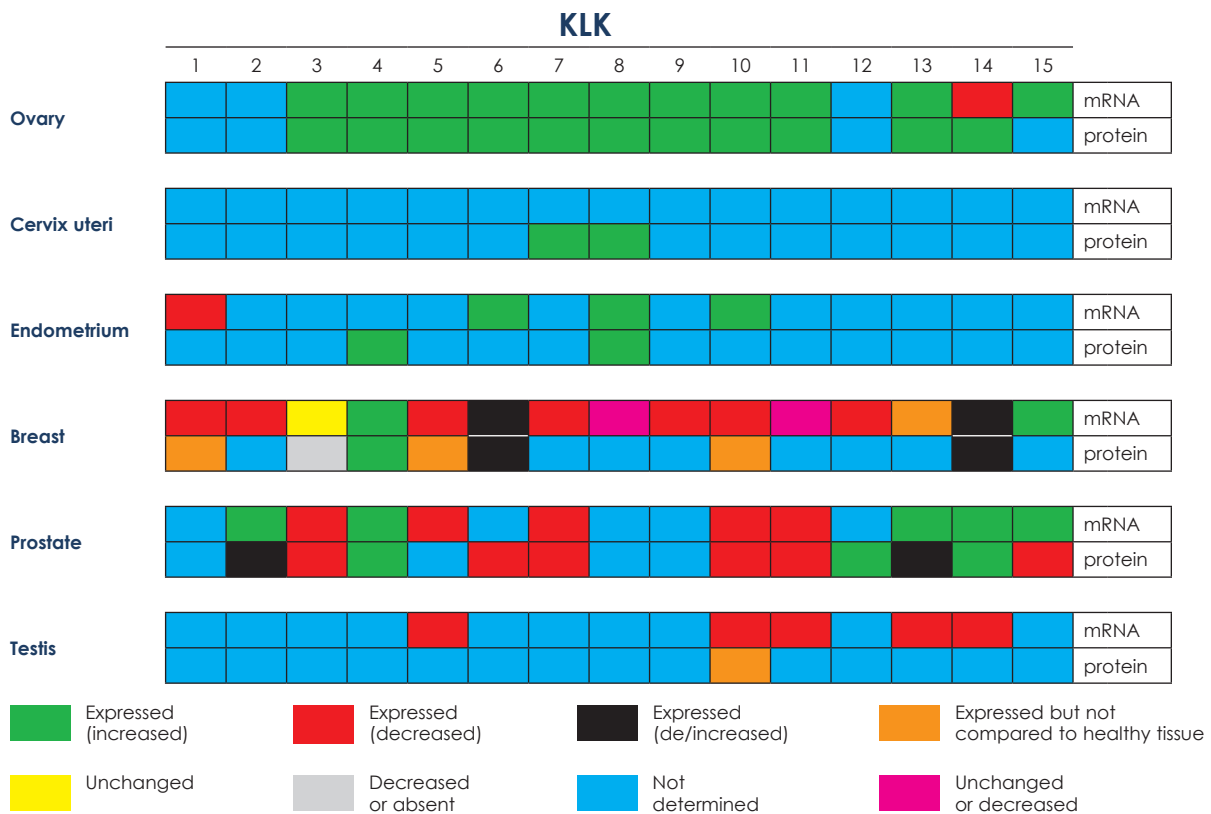


FIGURE 2. Comparative mRNA and protein expression in cancerous tissues of the reproductive tract

low to moderate levels for KLK1, 4-8 and 13-15 and high levels of KLK9 and 11. Interestingly, KLK3 is not prostate-specific but expressed in a wide variety of other tissues as well, including the breast of about one third of the women.^{23,67,68} The KLKs are mainly expressed in the breast's glandular epithelium and some are released into breast secretions, e.g. milk of lactating women, breast cyst fluid, and nipple aspirate fluid.^{23,69}

KLKs are not only involved in breast tissue development but also in various stages of breast cancer development and progression, indicating a regulating role of KLKs in tumor growth and metastasis. In this cancer, most of the KLKs, except KLK4 and KLK15, show reduced mRNA and/or protein expression levels compared to expression of the KLKs in normal breast tissue.^{9,23,66,70,71} KLK3, 8 and 11 mRNA expression is not changed in malignant breast tissue compared to normal breast tissue; KLK1, 2, and 5-12 mRNA expression is decreased; KLK4 and 15 are increased. KLK13 mRNA is expressed in breast cancer tissue but comparison with normal breast tissue has not been made available. For KLK6 and 14 both increases and decreases in mRNA expression have been reported. At the

protein expression level, only KLK4 is elevated compared to normal breast tissue; KLK6 and 14 protein levels were reported either to be lowered or elevated, depending on the study. KLK3 is decreased or absent in breast cancer tumor tissue. Limited data are available for KLK1, 5 and 10 protein expression since expression levels were not compared to expression levels of those proteins in the normal breast tissue. Several other KLKs (KLK2, 7-9, 11-13 and 15) have not been assessed for protein expression in breast cancer tumor tissue yet.

Nine of the fifteen members of the KLK family are considered potential prognostic and/or predictive cancer biomarkers in breast cancer. Five KLKs predict favorable prognosis (KLK3, 9, 12, 13 and 15), four indicate unfavorable, poor prognosis (KLK5, 7, 10 and 14).^{5,12,72} KLK3 and KLK10 are also predictive markers of response to endocrine therapy.^{48,73,74} Furthermore, breast cancer risk is associated with presence of single nucleotide polymorphisms (SNP) of KLK2 (Ex5 p 118C>T) or KLK4 (4207C>G).⁷⁵ No data are available regarding any possible prognostic/predictive value of KLK1, 2, 4, 6, 8 and 11 in breast cancer.

TABLE 6. KLKs present in normal and tumor tissues of patients afflicted with testicular/seminal cancer**TESTIS, NORMAL**

Expression level (mRNA)	KLK number
Low	9, 12
Moderate	1-3, 13, 15
High	4-8, 10, 11, 14

Expression level (protein)	KLK number
Absent	15
Low	1, 2, 4-8, 10, 11, 13
Moderate	3, 9
Present	12, 14

TESTIS, CANCER

Expression level (mRNA)	KLK number
Not determined	1-4, 6-9, 12, 15
Decreased	5, 10, 11, 13, 14

Expression level (protein)	KLK number
Not determined	1-9, 11-15
Present	10

KLKs in prostate cancer

Following lung cancer, prostate cancer is the second most common cancer and cause of cancer-related deaths in men worldwide.² At time of bioptic diagnosis, tumor stage and Gleason score⁷⁶ plus serum PSA (prostate-specific antigen, also known as kallikrein-related peptidase 3, KLK3) are the most accepted predictors of prognosis of prostate cancer. Treatment strategies may include active surveillance for those cancers that are considered aggressive, surgery with or without a combination of radiation, endocrine therapy or chemotherapy is recommended. Molecular profiling at the genomic, transcriptomic, or proteomic level have identified several potential markers that may distinguish between indolent and aggressive prostate cancers, including *NKX3.1*, *PTEN*, *ETS*, *MYC*, *TP53*, *AR*, *RB1*, and *APC* plus miRNAs as potential prognostic biomarkers.⁷⁷⁻⁸²

In normal prostate tissue, all of the KLKs are expressed at the mRNA level and, except for KLK8,

at the protein level as well (Table 5, Figure 1).^{23,54} Low to moderate KLK mRNAs levels are found for *KLK4-9*, 12 and 13, high levels for *KLK1-3*, 10, 11, 14 and 15. Low KLK protein expression is reported for KLK4, 5 and 13-15, high ones for KLK1-3, 9 and 11. KLK6, 7, 10 and 12 are expressed as well but expression levels were not scored. In prostate cancer, elevated levels of KLK2, 4 and 13-15 mRNA and/or protein have been reported; KLK3, 5, 7, 10 and 11 are decreased compared to nonmalignant tissue counterparts (Table 5, Figure 2). mRNA expression levels of *KLK 1, 6, 8, 9* and 12 were not determined yet. At the protein level, no information is available for KLK 1, 5, 8 and 9 but for the others with increased levels for KLK4, 12 and 14 versus decreased levels for KLK3, 6, 7, 10, 11 and 15. Conflicting results were reported for KLK2 and 13. Increase of three KLKs (KLK2, 14 and 15) is associated with poor prognosis; KLK4 is a marker of a favorable prognosis. Decreased mRNA or protein levels of KLK2, 3, 5-7, 10, 11, 13 and 15 have been reported of which KLK3 and 15 are markers of a poor prognosis and KLK5 and 11 markers of a favorable prognosis.^{70,83,84}

KLK2 and 3 possess steroid hormone binding sites while KLK1 and 4 possess putative steroid binding elements regulating KLK expression in prostate cancer⁸⁵⁻⁸⁷; the remaining KLKs do not contain such defined elements.^{85,86} DNA-methylation is also involved in KLK regulation as well as non-coding miRNAs.^{9,88-91}

KLKs in testicular cancer

Testicular cancer, which is affecting men between age 15 and 35 is relatively uncommon in Asia and Africa, but common among Caucasians; the incidence of this cancer increased during the last century for unknown reasons. Testicular cancer is treatable by surgery, radiotherapy, or chemotherapy with a cure rate of ~95%.^{92,93} Even if metastasized to other organs or lymph nodes, the 5-year survival rate is still high (~72%). For this type of cancer, α -fetoprotein, β -human chorionic gonadotropin, and lactate dehydrogenase serum markers are useful biomarkers to detect minimal residual disease. Novel biomarkers under investigation, e.g. glypican 3, SALL4, OCT3/4, SOX2, SOX17, OCT3/4, NANOG HMGA1, HMGA2, PATZ1, GPR30, and Aurora B are thought to discriminate between testicular cancer subgroups.⁹⁴⁻⁹⁸

In the normal testis, all of the fifteen KLKs are expressed at the mRNA level, this is also true for

KLK protein expression, except for KLK15 which is not expressed (Table 6, Figure 1).^{23,54} Some of the testicular cancer KLK mRNAs have been shown to be of clinical value, such as *KLK5*, *10*, *11*, *13* and *14*, which are all decreased compared to normal tissue expression.⁹⁹⁻¹⁰⁴ KLK5 is supposed to be a marker indicating a favorable prognosis.¹⁰⁰ To date, no study results relating to testicular cancer mRNA expression have been presented for the other ten KLKs; and no results are available relating to the testicular tumor KLK protein levels except for KLK10 (Table 6, Figure 2).

Future perspectives

KLKs are not only known for their strong biomarker value in prostate, ovarian, breast, and gastrointestinal cancers, regarding prediction of the course of the disease and response to cancer therapy, several KLKs appear to be of clinical value in other malignancies as well, e.g. in cancer of the lung, brain, head and neck, the kidney, urinary bladder the endometrium, cervix uteri, and the testes. For several of these malignancies, the tumor tissue-associated KLKs may serve as novel cancer biomarkers in allowing tumor sub classification, diagnosis and prognosis of the cancer disease or prediction of response/failure to cancer-directed drugs. Since, regarding their clinical utility, for most of the KLKs only single reports have been published, validation of KLK gene and protein expression data in independent patient sets on the basis of standard-operating-procedures is a prerequisite before recommendation which of the fifteen KLKs, and for which cancer disease, should be considered for clinical management to support individualized cancer care and treatment. Likewise, in this context, harmonization of methodologies, tools, reagents, and statistics to assess KLK expression in tumors and bodily fluids (plasma/serum, ascitic fluid, lavages) have to be pursued.

At first glance, the KLK peptidases are characterized by high sequence similarities, yet, they show significant differences in their substrate specificities, which will facilitate development of targeted KLK inhibitors. We envision that selective inhibitors to certain KLKs will be developed for future therapeutic application, that aim at blocking their enzymatic activity, in order to interfere with KLK-mediated degradation or activation of other proteins. Nonetheless, one has to bear in mind that KLKs may exist in different enzymatic active and inactive molecular forms. Since reports about the

enzymatic state of the various KLKs in different healthy and malignant tissues are scarce at present, the clinical utility of such new synthetic or biological therapeutics is not yet apparent.

References

- Schmitt M, Magdolen V. Using kallikrein-related peptidases (KLK) as novel cancer biomarkers. *Thromb Haemost* 2009; **101**: 222-4.
- GLOBOCAN 2008. Estimated cancer incidence, mortality, prevalence and disability-adjusted life years (DALYs) worldwide in 2008. Available at: <http://globocan.iarc.fr/>
- Siegel R, Naishadham D, Jemal A. Cancer statistics, 2012. *CA Cancer J Clin* 2012; **62**: 10-29.
- Siegel R, DeSantis C, Virgo K, Stein K, Mariotto A, Smith T, et al. Cancer treatment and survivorship statistics, 2012. *CA Cancer J Clin* 2012; **62**: 220-41.
- Borgoño CA, Diamandis EP. The emerging roles of human tissue kallikreins in cancer. *Nat Rev Cancer* 2004; **4**: 876-90.
- Krenzer S, Peterziel H, Mauch C, Blaber SI, Blaber M, Angel P, et al. Expression and function of the kallikrein-related peptidase 6 in the human melanoma microenvironment. *J Invest Dermatol* 2011; **131**: 2281-8.
- Pampalakis G, Sotiropoulou G. Tissue kallikrein proteolytic cascade pathways in normal physiology and cancer. *Biochim Biophys Acta* 2007; **1776**: 22-31.
- Sidiropoulos M, Pampalakis G, Sotiropoulou G, Katsaros D, Diamandis EP. Downregulation of human kallikrein 10 (KLK10/NES1) by CpG island hypermethylation in breast ovarian and prostate cancers. *Tumour Biol* 2005; **26**: 324-36.
- Avgeris M, Mavridis K, Scorilas A. Kallikrein-related peptidase genes as promising biomarkers for prognosis and monitoring of human malignancies. *Biol Chem* 2010; **391**: 505-11.
- Clements JA. Reflections on the tissue kallikrein and kallikrein-related peptidase family—from mice to men—what have we learnt in the last two decades? *Biol Chem* 2008; **389**: 1447-54.
- Clements JA, Willemsen NM, Myers SA, Dong Y. The tissue kallikrein family of serine proteases: functional roles in human disease and potential as clinical biomarkers. *Crit Rev Clin Lab Sci* 2004; **41**: 265-312.
- Emami N, Diamandis EP. Utility of kallikrein-related peptidases (KLKs); as-cancer biomarkers. *Clin Chem* 2008; **54**: 1600-7.
- Mavridis K, Scorilas A. Prognostic value and biological role of the kallikrein-related peptidases in human malignancies. *Future Oncol* 2010; **6**: 269-5.
- Oikonomopoulou K, Diamandis EP, Hollenberg MD. Kallikrein-related peptidases: proteolysis and signaling in cancer the new frontier. *Biol Chem* 2010; **391**: 299-310.
- Paliouras M, Diamandis EP. The kallikrein world: an update on the human tissue kallikreins. *Biol Chem* 2006; **387**: 643-562.
- Schmitt M Magdolen V. Using kallikrein-related peptidases (KLK) as novel cancer biomarkers. *Thromb Haemost* 2009; **101**: 222-4.
- Yousef GM, Diamandis EP. The human kallikrein gene family: new biomarkers for ovarian cancer. *Cancer Treat Res* 2009; **149**: 165-87.
- Baggerly KA, Morris JS, Edmonson SR, Coombes KR. Signal in noise: evaluating reported reproducibility of serum proteomic tests for ovarian cancer. *J Natl Cancer Inst* 2005; **97**: 307-9.
- Lu KH, Patterson AP, Wang L, Marquez RT, Atkinson EN, Baggerly KA, et al. Selection of potential markers for epithelial ovarian cancer with gene expression arrays and recursive descent partition analysis. *Clin Cancer Res* 2004; **10**: 3291-300.
- Skates SJ, Menon U, MacDonald N, Rosenthal AN, Oram DH, Knapp RC, et al. Calculation of the risk of ovarian cancer from serial CA-125 values for preclinical detection in postmenopausal women. *J Clin Oncol* 2003; **21**(10 Suppl): 206s-10s.

21. Polterauer S, Vergote I, Concin N, Braicu I, Chakerov R, Mahner S, et al. Prognostic value of residual tumor size in patients with epithelial ovarian cancer international FIGO Stages IIA-IV: analysis of the OVCAD data. *Int J Gynecol Cancer* 2012; **22**: 380-5.
22. Elattar A, Bryant A, Winter-Roach BA, Hatem M, Naik R. Optimal primary surgical treatment for advanced epithelial ovarian cancer. *Cochrane Database Syst Rev* CD007565; 2011.
23. Shaw JL, Diamandis EP. Distribution of 15 human kallikreins in tissues and biological fluids. *Clin Chem* 2007; **53**: 1423-32.
24. Dorn J, Harbeck N, Kates R, Magdolen V, Grass L, Soosaipillai A, et al. Disease processes may be reflected by correlations among tissue kallikrein proteases but not with proteolytic factors uPA and PAI-1 in primary ovarian carcinoma. *Biol Chem* 2006; **387**: 1121-8.
25. Dorn J, Schmitt M, Kates R, Schmalfeldt B, Kiechle M, Scorilas A, et al. Primary tumor levels of human tissue kallikreins impact surgical success and survival in ovarian cancer patients. *Clin Cancer Res* 2007; **13**: 1742-8.
26. Shan SJ, Scorilas A, Katsaros D, Rigault de la Longrais I, Massobrio M, Diamandis EP. Unfavorable prognostic value of human kallikrein 7 quantified by ELISA in ovarian cancer cytosols. *Clin Chem* 2006; **52**: 1879-86.
27. Yousef GM, Polymeris ME, Yacoub GM, Scorilas A, Soosaipillai A, Popalis C, et al. Parallel overexpression of seven kallikrein genes in ovarian cancer. *Cancer Res* 2003; **63**: 2223-7.
28. Zheng Y, Katsaros D, Shan SJ, de la Longrais IR, Porpiglia M, Scorilas A, et al. A multiparametric panel for ovarian cancer diagnosis prognosis response to chemotherapy. *Clin Cancer Res* 2007; **13**: 6984-92.
29. Adib TR, Henderson S, Perrett C, Hewitt D, Bourmpoulia D, Ledermann J, et al. Predicting biomarkers for ovarian cancer using gene-expression microarrays. *Br J Cancer* 2004; **90**: 686-92.
30. Bignotti E, Tassi RA, Calza S, Ravaggi A, Romani C, Rossi E, et al. Differential gene expression profiles between tumor biopsies and short-term primary cultures of ovarian serous carcinomas: identification of novel molecular biomarkers for early diagnosis and therapy. *Gynecol Oncol* 2006; **103**: 405-16.
31. Dong Y, Kaushal A, Brattsand M, Nicklin J, Clements JA. Differential splicing of KLK5 and KLK7 in epithelial ovarian cancer produces novel variants with potential as cancer biomarkers. *Clin Cancer Res* 2003; **9**: 1710-20.
32. Dong Y, Kaushal A, Bui L, Chu S, Fuller PJ, Nicklin J, et al. Human kallikrein 4 (KLK4; is highly expressed in serous ovarian carcinomas. *Clin Cancer Res* 2001; **7**: 2363-71.
33. Gilks CB, Vanderhyden BC, Zhu S, van de Rijn M, Longacre TA. Distinction between serous tumors of low malignant potential and serous carcinomas based on global mRNA expression profiling. *Gynecol* 2005; **96**: 684-94.
34. Shvartsman HS, Lue J, Lillie J, Deavers MT, Clifford S, Wolf JK, et al. Overexpression of kallikrein 10 in epithelial ovarian carcinomas. *Gynecol Oncol* 2003; **90**: 44-50.
35. Tanimoto H, Underwood LJ, Shigemasa K, Parmley TH, O'Brien TJ. Increased expression of protease M in ovarian tumors. *Tumour Biol* 2001; **22**: 11-8.
36. Tanimoto H, Underwood LJ, Shigemasa K, Yan MS, Clarke J, Parmley TH, et al. The stratum corneum chymotryptic enzyme that mediates shedding and desquamation of skin cells is highly overexpressed in ovarian tumor cells. *Cancer* 1999; **86**: 2074-82.
37. White NM, Mathews M, Yousef GM, Prizada A, Popadiuk C, Doré JJ. KLK6 and KLK13 predict tumor recurrence in epithelial ovarian carcinoma. *Br J Cancer* 2009; **101**: 1107-13.
38. Yousef GM, Magklara A, Chang A, Jung K, Katsaros D, Diamandis EP. Cloning of a new member of the human kallikrein gene family KLK14 which is down-regulated in different malignancies. *Cancer Res* 2001; **61**: 3425-31.
39. Yousef GM, Fracchioli S, Scorilas A, Borgoño CA, Iskander L, Puopolo M, et al. Steroid hormone regulation and prognostic value of the human kallikrein gene 14 in ovarian cancer. *Am J Clin Pathol* 2003; **119**: 346-55.
40. Yousef GM, Scorilas A, Katsaros D, Fracchioli S, Iskander L, Borgoño C, et al. Prognostic value of the human kallikrein gene 15 expression in ovarian cancer. *J Clin Oncol* 2003; **21**: 3119-26.
41. Bandiera E, Zanotti L, Bignotti E, Romani C, Tassi R, Todeschini P, et al. Human kallikrein 5: an interesting novel biomarker in ovarian cancer patients that elicits humoral response. *Int J Gynecol Cancer* 2009; **19**: 1015-21.
42. Borgoño CA, Grass L, Soosaipillai A, Yousef GM, Petraki CD, Howarth DH, et al. Human kallikrein 14: a new potential biomarker for ovarian and breast cancer. *Cancer Res* 2003; **63**: 9032-41.
43. Diamandis EP, Borgoño CA, Scorilas A, Yousef GM, Harbeck N, Dorn J, et al. Immunofluorometric quantification of human kallikrein 5 expression in ovarian cancer cytosols and its association with unfavorable patient prognosis. *Tumour Biol* 2003; **24**: 299-309.
44. Diamandis EP, Scorilas A, Fracchioli S, van Gramberen M, de Bruijn H, Henrik A, et al. Human kallikrein 6 (hK6): a new potential serum biomarker for diagnosis and prognosis of ovarian carcinoma. *J Clin Oncol* 2003; **21**: 1035-43.
45. Dorn J, Magdolen V, Gkazepis A, Gerte T, Harlozinska A, Sedlaczek P, et al. Circulating biomarker tissue kallikrein-related peptidase KLK5 impacts ovarian cancer patients' survival. *Ann Oncol* 2011; **22**: 1783-90.
46. Kishi T, Grass L, Soosaipillai A, Scorilas A, Harbeck N, Schmalfeldt B, et al. EP. Human kallikrein 8 a novel biomarker for ovarian carcinoma. *Cancer Res* 2003; **63**: 2771-4.
47. Koh SC, Razvi K, Chan YH, Narasimhan K, Ilancheran A, Low JJ, et al. The Ovarian Cancer Research Consortium of SE Asia. The association with age human tissue kallikreins 6 and 10 and hemostatic markers for survival outcome from epithelial ovarian cancer. *Arch Gynecol Obstet* 2011; **284**: 183-90.
48. Luo LY, Diamandis EP, Look MP, Soosaipillai AP, Foekens JA. Higher expression of human kallikrein 10 in breast cancer tissue predicts tamoxifen resistance. *Br J Cancer* 2002; **86**: 1790-6.
49. Oikonomopoulou K, Li L, Zheng Y, Simon I, Wolfert RL, Valik D, et al. Prediction of ovarian cancer prognosis and response to chemotherapy by a serum-based multiparametric biomarker panel. *Br J Cancer* 2008; **99**: 1103-13.
50. zur Hausen H. Papillomaviruses - to vaccination and beyond. *Biochemistry (Mosc)* 2008; **5**: 498-503.
51. Rose PG, Bundy BN, Watkins EB, Thigpen JT, Deppe G, Maiman MA, et al. Concurrent cisplatin-based radiotherapy and chemotherapy for locally advanced cervical cancer. *N Engl J Med* 1999; **15**: 1144-53.
52. Micke O, Bruns F, Schäfer U, Prott FJ, Willich N. The impact of squamous cell carcinoma (SCC) antigen in patients with advanced cancer of uterine cervix treated with (chemo)-radiotherapy. *Anticancer Res* 2005; **25A**: 1663-6.
53. Tian X, Shigemasa K, Hirata E, Gu L, Uebaba Y, Nagai N, et al. Expression of human kallikrein 7 (hK7/SCCE) and its inhibitor antileukoprotease (ALP/SLPI) in uterine endocervical glands and in cervical adenocarcinomas. *Oncol Rep* 2004; **12**: 1001-6.
54. Petraki CD, Papanastasiou PA, Karavana VN, Diamandis EP. Cellular distribution of human tissue kallikreins: immunohistochemical localization. *Biol Chem* 2006; **387**: 653-63.
55. Santin AD, Cane S, Bellone S, Bignotti E, Palmieri M, de las Casas LE, et al. The serine protease stratum corneum chymotryptic enzyme (kallikrein 7) is highly overexpressed in squamous cervical cancer cells. *Gynecol Oncol* 2004; **2**: 283-8.
56. Santin AD, Cane S, Bellone S, Bignotti E, Palmieri M, De Las Casas LE, et al. The novel serine protease tumor-associated differentially expressed gene-14 (KLK8/neurosp/ovasin) is highly overexpressed in cervical cancer. *Am J Obstet Gynecol* 2004; **1**: 60-6.
57. Termini L, Maciag PC, Soares FA, Nonogaki S, Pereira SM, Alves VA, et al. Analysis of human kallikrein 7 expression as a potential biomarker in cervical neoplasia. *Int J Cancer* 2010; **2**: 485-90.
58. Bovicelli A, D'Andrilli G, Giordano A, de Iaco P. Conservative treatment of early endometrial cancer. *J Cell Physiology* 2012; **228**: 1154-8.
59. Stuckey A. Breast cancer: epidemiology and risk factors. *Clin Obstet Gynecol* 2011; **54**: 96-102.
60. Marić P, Ozretić P, Levant S, Oresković S, Antunac K, Beketić-Oresković L. Tumor markers in breast cancer—evaluation of their clinical usefulness. *Coll Antropol* 2011; **35**: 241-7.
61. Duffy MJ. Serum tumor markers in breast cancer: are they of clinical value? *Clin Chem* 2006; **52**: 345-51.
62. Harris L, Fritsche H, Mennel R, Norton L, Ravdin P, Taube S, et al. American Society of Clinical Oncology 2007 update of recommendations for the use of tumor markers in breast cancer. *J Clin Oncol* 2007; **25**: 5287-312.

63. Naidoo S, Raidoo DM. Angiogenesis in cervical cancer is mediated by HeLa metabolites through endothelial cell tissue kallikrein. *Oncol Rep* 2009; **22**: 285-93.
64. Sher YP, Chou CC, Chou RH, Wu HM, Wayne Chang WS, Chen CH, et al. Human kallikrein 8 protease confers a favorable clinical outcome in non-small cell lung cancer by suppressing tumor cell invasiveness. *Cancer Res* 2006; **66**: 11763-70.
65. Tham SM, Ng KH, Pook SH, Esuvaranathan K, Mahendran R. Tumor and microenvironment modification during progression of murine orthotopic bladder cancer. *Clin Dev Immunol* 2011; **2011**: 865684.
66. Mangé A, Desmetz C, Berthes ML, Maudelonde T, Solassol J. Specific increase of human kallikrein 4 mRNA and protein levels in breast cancer stromal cells *Biochem Biophys Res Commun* 2008; **375**: 107-12.
67. Monne M, Croce CM, Yu H, Diamandis EP. Molecular characterization of prostate-specific antigen messenger RNA expressed in breast tumors. *Cancer Res* 1994; **54**: 6344-7.
68. Yu H, Levesque MA, Clark GM, Diamandis EP. Prognostic value of prostate-specific antigen for women with breast cancer: a large United States cohort study. *Clin Cancer Res* 1998; **4**: 1489-97.
69. Petraki CD, Papanastasiou PA, Karavana VN, Diamandis EP. Cellular distribution of human tissue kallikreins: immunohistochemical localization. *Biol Chem* 2006; **387**: 653-63.
70. Avgeris M, Mavridis K, Scorilas A. Kallikrein-related peptidases in prostate breast and ovarian cancers: from pathobiology to clinical relevance. *Biol Chem* 2012; **393**: 301-17.
71. Yousef GM, Yacoub GM, Polymeris ME, Popalis C, Soosaipillai A, Diamandis EP. Kallikrein gene downregulation in breast cancer. *Br J Cancer* 2004; **90**: 167-72.
72. Obiezu CV, Diamandis EP. Human tissue kallikrein gene family: applications in cancer. *Cancer Lett* 2005; **224**: 1-22.
73. Foekens JA, Diamandis EP, Yu H, Look MP, Meijer-van Gelder ME, van Putten WL, Klijn J. Expression of prostate-specific antigen (PSA) correlates with poor response to tamoxifen therapy in recurrent breast cancer. *Br J Cancer* 1999; **79**: 888-94.
74. Diamandis EP, Helle SI, Yu H, Melegos DN, Lundgren S, Lonning PE. Prognostic value of plasma prostate specific antigen after megestrol acetate treatment in patients with metastatic breast carcinoma. *Cancer* 1999; **85**: 891-8.
75. Lee JY, Park AK, Lee KM, Park SK, Han S, Han W, et al. Candidate gene approach evaluates association between innate immunity genes and breast cancer risk in Korean women. *Carcinogenesis* 2009; **30**: 1528-31.
76. Epstein JI, Allsbrook WC Jr, Amin MB, Egevad LL. Update on the Gleason grading system for prostate cancer: results of an international consensus conference of urologic pathologists. *Adv Anat Pathol* 2006; **13**: 57-9.
77. Barbieri CE, Baca SC, Lawrence MS, Demichelis F, Blattner M, Theurillat JP, et al. Exome sequencing identifies recurrent SPOP FOXA1 and MED12 mutations in prostate cancer. *Nat Genet* 2012; **44**: 685-9.
78. Berger MF, Lawrence MS, Demichelis F, Drier Y, Cibulskis K, Sivachenko AY, et al. The genomic complexity of primary human prostate cancer. *Nature* 2011; **470**: 214-20.
79. Beroukhi R, Mermel CH, Porter D, Wei G, Raychaudhuri S, Donovan J, et al. The landscape of somatic copy-number alteration across human cancers. *Nature* 2010; **463**: 899-905.
80. Grasso CS, Wu YM, Robinson DR, Cao X, Dhanasekaran SM, Khan AP, Quist MJ, et al. The mutational landscape of lethal castration-resistant prostate cancer. *Nature* 2012; **487**: 239-43.
81. Taylor BS, Schultz N, Hieronymus H, Gopalan A, Xiao Y, Carver BS, et al. Integrative genomic profiling of human prostate cancer. *Cancer Cell* 2010; **18**: 11-22.
82. Fendler A, Jung M, Stephan C, Honey RJ, Stewart RJ, Pace KT, et al. miRNAs can predict prostate cancer biochemical relapse and are involved in tumor progression. *Int J Oncol* 2011; **39**: 1183-92.
83. Nam RK, Diamandis EP, Toi A, Trachtenberg J, Magklara A, Scorilas A, et al. Serum human glandular kallikrein-2 protease levels predict the presence of prostate cancer among men with elevated prostate-specific antigen. *J Clin Oncol* 2000; **18**: 1036-42.
84. Mavridis K, Avgeris M, Koutalellis G, Stravodimos K, Scorilas A. Expression analysis and study of the KLK15 mRNA splice variants in prostate cancer and benign prostatic hyperplasia. *Cancer Sci* 2010; **101**: 693-9.
85. Yousef GM, Diamandis EP. The new human tissue kallikrein gene family: structure function and association to disease. *Endocr Rev* 2001; **22**: 184-204.
86. Lawrence MG, Lai J, Clements JA. Kallikreins on steroids: structure function and hormonal regulation of prostate-specific antigen and the extended kallikrein locus. *Endocr Rev* 2010; **31**: 407-46.
87. Lai J, Myers SA, Lawrence MG, Odorico DM, Clements JA. Direct progesterone receptor and indirect androgen receptor interactions with the kallikrein-related peptidase 4 gene promoter in breast and prostate cancer. *Mol Cancer Res* 2009; **7**: 129-41.
88. Olkhov-Mitsel E, van der Kwast T, Kron KJ, Ozcelik H, Briollais L, Massey C, et al. Quantitative DNA methylation analysis of genes coding for kallikrein-related peptidases 6 and 10 as biomarkers for prostate cancer. *Epigenetics* 2012; **7**: 1037-45.
89. Pampalakis G, Diamandis EP, Sotiropoulou G. The epigenetic basis for the aberrant expression of kallikreins in human cancers. *Biol Chem* 2006; **387**: 795-9.
90. Pasic MD, Olkhov E, Bapat B, Yousef GM. Epigenetic regulation of kallikrein-related peptidases: there is a whole new world out there. *Biol Chem* 2012; **393**: 319-30.
91. White NM, Youssef YM, Fendler A, Stephan C, Jung K, Yousef GM. The miRNA-kallikrein axis of interaction: a new dimension in the pathogenesis of prostate cancer. *Biol Chem* 2012; **393**: 379-89.
92. Viatori M. Testicular cancer. *Semin Oncol Nurs* 2012; **28**: 180-9.
93. Okamoto K. Epigenetics: a way to understand the origin and biology of testicular germ cell tumors. *Int J Urol* 2012; **19**: 504-11.
94. Barlow LJ, Badalato GM, McKiernan JM. Serum tumor markers in the evaluation of male germ cell tumors. *Nat Rev Urol* 2010; **7**: 610-7.
95. Salem M, Gilligan T. Serum tumor markers and their utilization in the management of germ-cell tumors in adult males. *Expert Rev Anticancer Ther* 2011; **11**: 1-4.
96. Emerson RE, Ulbright TM. Intratubular germ cell neoplasia of the testis and its associated cancers: the use of novel biomarkers. *Pathology* 2010; **42**: 344-55.
97. Favilla V, Cimino S, Madonia M, Morgia G. New advances in clinical biomarkers in testis cancer. *Front Biosci* 2010; **2**: 456-77.
98. Chieffi P. New prognostic markers and potential therapeutic targets in human testicular germ cell tumors. *Curr Med Chem* 2011; **18**: 5033-40.
99. Luo LY, Yousef G, Diamandis EP. Human tissue kallikreins and testicular cancer. *APMIS* 2003; **111**: 225-32.
100. Yousef GM, Obiezu CV, Jung K, Stephan C, Scorilas A, Diamandis EP. Differential expression of kallikrein gene 5 in cancerous and normal testicular tissues. *Urology* 2002; **60**: 714-8.
101. Luo LY, Rajpert-de Meyts ER, Jung K, Diamandis EP. Expression of the normal epithelial cell-specific 1 (NES1; KLK10) candidate tumour suppressor gene in normal and malignant testicular tissue. *Br J Cancer* 2001; **85**: 220-4.
102. Chang A, Yousef GM, Jung K, Rajpert-de Meyts E, Diamandis EP. Identification and molecular characterization of five novel kallikrein gene 13 (KLK13; KLK-L4; splice variants: differential expression in the human testis and testicular cancer. *Anticancer Res* 2001; **21**: 3147-52.
103. Yousef GM, Magklara A, Chang A, Jung K, Katsaros D, Diamandis EP. Cloning of a new member of the human kallikrein gene family KLK14 which is down-regulated in different malignancies. *Cancer Res* 2001; **61**: 3425-31.
104. Arsanious A, Bjarnason GA, Yousef GM. From bench to bedside: current and future applications of molecular profiling in renal cell carcinoma. *Mol Cancer* 2009; **8**: 20.

Expansive growth of two glioblastoma stem-like cell lines is mediated by bFGF and not by EGF

Neza Podergajs¹, Narve Brekka², Bernhard Radlwimmer³, Christel Herold-Mende⁴, Krishna M. Talasila², Katja Tiemann⁵, Uros Rajcevic^{1,6}, Tamara T. Lah^{1,7}, Rolf Bjerkvig^{2,5}, Hrvoje Miletic^{2,8}

¹ Department of Genetic Toxicology and Cancer Biology, National Institute of Biology, Ljubljana, Slovenia

² Department of Biomedicine, University of Bergen, Bergen, Norway

³ German Cancer Research Centre, Division of Molecular Genetics, Heidelberg, Germany

⁴ Division of Neurosurgical Research, Department of Neurosurgery, University of Heidelberg, Heidelberg, Germany

⁵ NorLux Neuro-Oncology Laboratory, Centre de Recherche Public de la Santé, Luxembourg

⁶ Blood Transfusion Centre of Slovenia, Ljubljana, Slovenia

⁷ Department of Biochemistry, Faculty of Chemistry and Chemical Engineering, University of Ljubljana, Ljubljana, Slovenia

⁸ Department of Pathology, Haukeland University Hospital, Bergen, Norway

Radiol Oncol 2013; 47(4): 330-337.

Received 2 July 2013

Accepted 1 September 2013

Correspondence to: Hrvoje Miletic, M.D., Ph.D., Department of Pathology, Haukeland University Hospital, Jonas Lies vei 65, 5021 Bergen, Norway. E-mail: Hrvoje.miletic@biomed.uib.no

Disclosure: No potential conflicts of interest were disclosed.

The paper was presented at the 7th Conference of Experimental and Translational Oncology, 20-24th April 2013, Portoroz, Slovenia (www.ceto.si) co-organised and supported by COST TD1104 Action (www.electroporation.net).

Background. Patient-derived glioblastoma (GBM) stem-like cells (GSCs) represent a valuable model for basic and therapeutic research. GSCs are usually propagated in serum-free Neural Basal medium supplemented with bFGF and EGF. Yet, the exact influence of these growth factors on GSCs is still unclear. Recently it was suggested that GBM stem-like cells with amplified EGFR should be cultured in stem cell medium without EGF, as the presence of EGF induced rapid loss of EGFR amplification. However, patient biopsies are usually taken into culture before their genomic profiles are defined. Thus, an important question remains whether GBM cells without EGFR amplification also can be cultured in stem cell medium without EGF.

Materials and methods. To address this question, we used two heterogeneous glioblastoma GSC lines (NCH421k and NCH644) that lack EGFR amplification.

Results. Although both cell lines showed very low EGFR expression under standard growth conditions, bFGF stimulation induced higher expression of EGFR in NCH644. In both cell lines, expression of the stem cell markers nestin and CD133 was higher upon stimulation with bFGF compared to EGF. Importantly, bFGF stimulated the growth of both cell lines, whereas EGF had no effect. We verified that the growth stimulation by bFGF was either mediated by proliferation (NCH421k) or resistance to apoptosis (NCH644).

Conclusions. We demonstrate that GSC cultures without EGFR amplification can be maintained and expanded with bFGF, while the addition of EGF has no significant effect and therefore can be omitted.

Key words: glioblastoma; bFGF; EGF; EGFR; stem cell cultures

Introduction

Glioblastoma (GBM) is the most frequent and most malignant primary brain tumor. Despite improvement of surgical removal, chemotherapy and radiotherapy, the majority of patients live only less

than 16 months after diagnosis.¹ The hypothesis that so-called cancer stem-like cells (CSCs) are responsible for tumor development has gained considerable attention, albeit with controversial views.^{2,3} These cells may reflect characteristics of normal neural stem cells, such as self-renewal, ex-

pression of neural stem cell markers, and the capacity to differentiate into phenotypes resembling neuronal and glial cell lineages.^{4,6} It has been postulated that CSCs are responsible for tumor recurrence after treatment⁷, which makes them highly relevant targets. Although the presence of GBM stem-like cells (GSCs) in human tumors is debated^{8,9}, GSCs cultured in Neurobasal (NB) medium supplemented with epidermal growth factor (EGF) and basic fibroblast growth factor (bFGF) currently represent the standard model in GSC research. The presence of EGF and bFGF in NB medium have been regarded as necessary supplements to maintain the stem cell-like features and also to stimulate their growth.¹⁰ Moreover, it has been shown that GSCs cultured under these conditions preserve the genetic profile and characteristics of the human tumor of origin much better than cells cultured in serum monolayer conditions.^{11,12} However, research is still needed to define optimal conditions for GSCs cultures.

In this respect, an open question remains about the influence of EGF and bFGF on GSC cultures and whether both of these growth factors are really required. Recently, Schulte *et al.*¹³ demonstrated that GBMs with EGF-receptor (EGFR) amplification are preserved much better in NB medium with bFGF, but without EGF. This observation is highly relevant since the tyrosine kinase receptor EGFR is often amplified or mutated in GBMs. About 40-50% of GBM patients show *EGFR* amplification and half of these harbor also the mutated EGFRvIII.^{14,15} Yet, over 50% of GBMs do not have amplifications or mutations of the EGFR. Thus, the optimal culture conditions irrespective of the genotype need to be defined in order to study important aspects of GBM biology within individual, genotypically preserved cultures.

In the present study, we investigated the impact of EGF and bFGF on GSCs without EGFR amplification in order to define whether the GSC culture conditions should be changed in general, as suggested by Schulte *et al.*¹³ We demonstrated that the presence of bFGF in the culture medium is crucial for GSC growth, whereas EGF had no significant stimulatory effects on these cells.

Materials and methods

Cell lines

Two GSC lines, NCH644 and NCH421k, which have been isolated as described previously¹⁶, were used in this study. The cells were grown as sus-

pension spheroids in NB medium (Invitrogen, Life Tech., Grand Island, NY) containing 2 mM L-glutamine, 1x penicillin/streptomycin (both from Lonza, Basel, Switzerland), 1x B-27 (Invitrogen, Life Tech., Grand Island, NY) and 1 U/ml heparin (Sigma-Aldrich, Steinheim, Germany). 20ng/ml bFGF and/or EGF (both from PeproTech, Inc., Rocky Hill, NJ) were added to NB medium to create different growth conditions as used for the experiments described in this section. NB medium with addition of EGF and bFGF is referred to as complete medium. Before the start of experiments, the NCH644 and NCH421k cells were initially cultured for 7 and 10 passages in complete medium, respectively. Neurospheres were dissociated mechanically when they reached approximately 200 μ m in diameter.

Comparative genomic hybridization (CGH)

Both cell lines used for this experiment were grown in complete NB medium. Array-CGH profiling was performed as previously reported.¹⁷ Data were analyzed based on Ensembl (version 69) using packages of the Bioconductor project¹⁸ implemented in our in-house developed ChipYard framework for microarray data analysis (<http://www.dkfz.de/genetics/ChipYard/>). The array-CGH analyses of NCH421k had previously been published¹¹ and were re-analysed for this study. The array-CGH analyses of NCH644 were performed exclusively for the present study.

Flow cytometry

Before the FACS analysis, cells were grown for ten days in NB medium without growth factors. The cells were then treated with EGF and/or bFGF for 48h. The cells were washed with PBS, stained with an anti-EGFR antibody diluted in 1:50 ratio (Santa Cruz Biotechnology, Inc., Santa Cruz, CA) for 30 minutes at 4°C, washed twice with PBS and stained with secondary Alexa Fluor 488[®] antibody diluted in 1:200 ratio (Invitrogen, Life Tech., Grand Island, NY) for 30 minutes at 4°C. Finally, the cells were washed twice, resuspended in PBS, and analyzed by FACSCalibur[™] (BD Biosciences, San Jose, California).

Western blotting

Prior to the experiment, cells were grown in complete NB medium. On the day of the experiment,

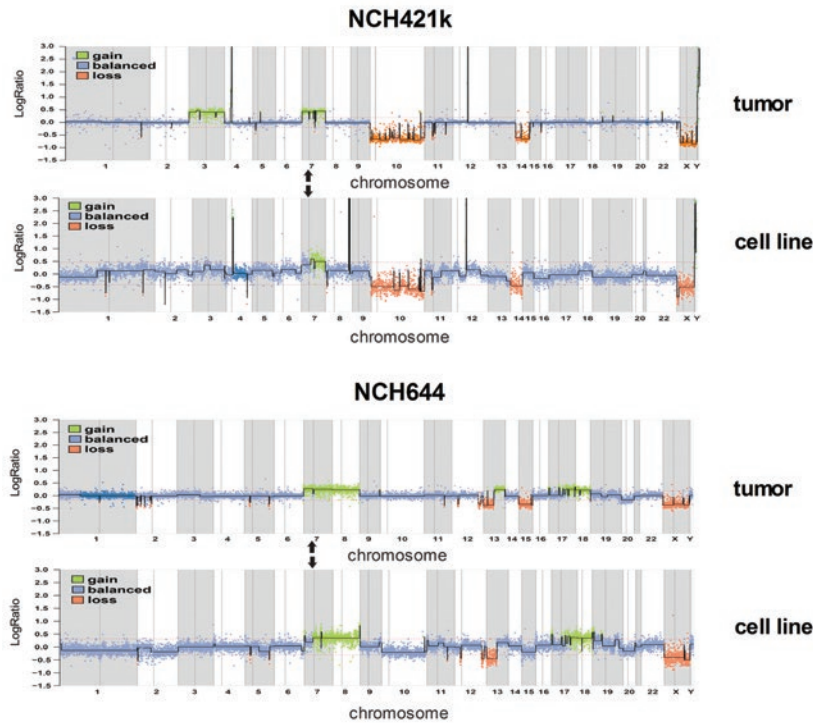


FIGURE 1. Array CGH profile of NCH421k and NCH644 cells and corresponding biopsies. Array-CGH analysis of NCH421k¹¹ and NCH644 primary tumors and the respective cell lines showing typical GBM aberrations that are preserved in the cell lines, and consistent absence of EGFR amplification. Panels on the right show NCH644 primary tumor (top) and cell line (bottom). The relative DNA copy number of genome fragments are plotted on the Y-axis in order of their chromosome mapping positions (X-axis). Arrows mark the mapping position of the EGFR locus on chromosome 7p.

the cells were divided into four groups and grown under different conditions for 14 days as stated in the results section. For protein isolation, spheroids were washed with PBS and lysed in lysis buffer (20 mM MOPS, pH 7.0, 2mM EGTA, 5mM EDTA, 30 mM NaF, 60 mM β -glycerophosphate, pH 7.2 20 mM sodium pyrophosphate, 1 mM sodium orthovanadate, 1 mM phenylmethylsulfonylfluoride, 3 mM benzamidine, 5 μ M pepstatin A, 10 μ M leupeptin, 1% Triton X-100, 1mM DTT). Proteins were quantified using Pierce BCATM Protein Assay Kit (Pierce Biotechnology, Rockford, IL). 20 μ g of protein was loaded on NuPage[®] Novex 4-12% Bis-Tris gels, run in MOPS running buffer (both from Invitrogen, Life Tech., Grand Island, NY) and blotted on nitrocellulose membrane (EMD Millipore, Massachusetts, USA). The nitrocellulose membrane was blocked for 1 hour at room temperature and incubated overnight at 4°C in buffer (PBS with 0.1% Tween 20 and 5% milk powder) containing the following

primary antibodies: anti-nestin diluted in 1:1000 ratio (EMD Millipore, Massachusetts, USA), anti-CD133/1 clone AC133 diluted in 1:100 ratio (Miltenyi, Auburn, CA), anti-SOX2 diluted in 1:200 ratio (R&D Systems, Abingdon, UK), anti-EGFR diluted in 1:500 ratio (Santa Cruz Biotechnology, Inc., Santa Cruz, CA), and anti-GAPDH antibody diluted in 1:2500 ratio (Abcam, Cambridge, UK). Secondary antibodies anti-mouse IgG HRP diluted in 1:10000 ratio (Santa Cruz Biotechnology, Inc., Santa Cruz, CA) or anti-rabbit IgG HRP diluted in 1:2500 ratio (Promega, Fitchburg, Wisconsin) and WestFemto Chemiluminescent Substrate (Pierce Biotechnology, Rockford, IL) were used for chemiluminescence detection. CD133, nestin and SOX2 expression results obtained from western blots were quantified using Image J software, version 1.46r (National Institutes of Health, <http://rsbweb.nih.gov/ij/>), following the developer's instructions (<http://rsb.info.nih.gov/ij/docs/index.html>) for the analysis of the data. The quantification of results are expressed as relative protein expression.

Cell growth assay

Cells were grown in NB medium without growth factors for ten days. 14 days before the start of the experiment, cells were divided into four groups and grown under different conditions as stated in the results section. On the starting day of the experiment, 1×10^4 of cells were seeded onto T25 plates. Neurospheres were dissociated mechanically and counted every four days for the following twenty days under a light microscope (Olympus CKX31, Southend-on-Sea, UK) using 100x magnification.

Cell cycle analysis

Cells, grown in NB medium without growth factors for ten days, were treated with EGF or bFGF and harvested 48 hours after the treatment. The preparation of the cells and cell cycle analysis were performed as described previously.¹⁹

Apoptosis assay

Cells, grown in NB medium without growth factors for ten days, were treated with EGF or bFGF and harvested 48 hours after the treatment. The cells were washed with PBS and analyzed using Annexin V kit (Molecular Probes, Life Tech., Grand Island, NY) following the manufacturer's instructions. Propidium iodide (PI; 50 μ g/ml) and a FITC

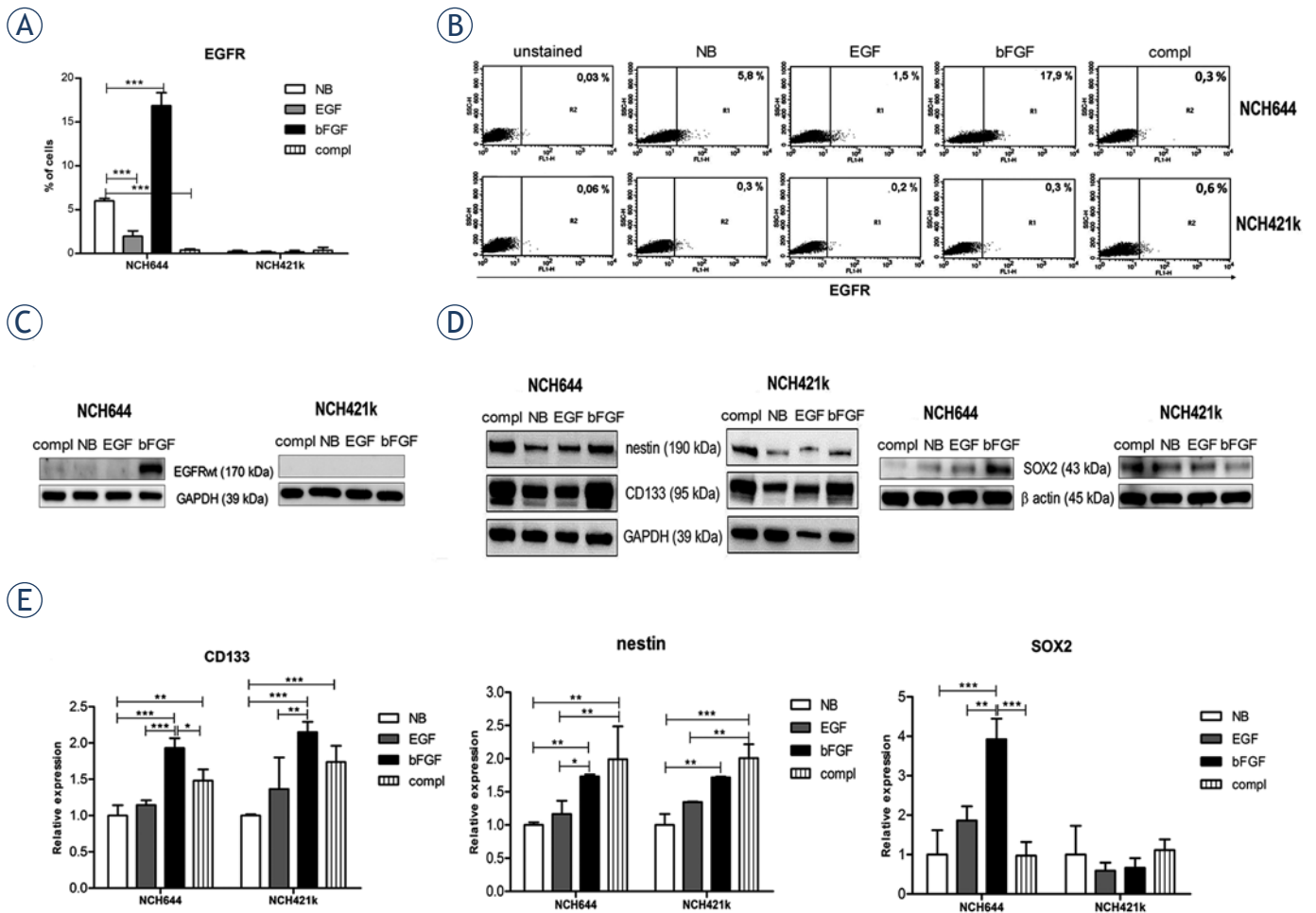


FIGURE 2. bFGF increases EGFR and stem cell marker expression in GSCs. **(A, B)** Flow cytometry analysis of EGFR expression in GSCs, grown in the presence of EGF and/or bFGF for 48 hours. bFGF alone increased the fraction of EGFR expressing cells in the NCH644 cell line, but not in the NCH421k, compared to medium without growth factors. Data shown are mean \pm SD of three independent experiments, ***: $p < 0.001$. **(C)** Western blots of GSCs cultured under different conditions. Presence of bFGF in culturing medium for 14 days upregulated the expression of EGFR in NCH644, but not in NCH421k. **(D)** Western blots of GSCs. Presence of bFGF in culturing medium for 14 days increased the expression of stem cell markers CD133 and nestin in both cell lines compared to unstimulated cells whereas the expression of SOX2 was increased only in NCH644 cells. EGF had no effect. **(E)** Quantification of western blots confirmed the significant higher expression of CD133 and nestin in both cell lines and a significant higher expression of SOX2 only in NCH644 cell line under bFGF stimulation. Data shown are mean \pm SD of three independent experiments, *: $p < 0.05$; **: $p < 0.01$; ***: $p < 0.001$. Labels: NB=Neurobasal medium without growth factors; compl=NB with EGF and bFGF; EGF=NB with EGF; bFGF=NB with bFGF.

conjugated Annexin V protein were used for detection of apoptotic and necrotic cells by Accuri[®] C6 Flow Cytometer (BD Biosciences, San Jose, California).

Statistical analysis

One-way ANOVA test with Bonferroni post-hoc test was used to detect significant differences of groups. All statistical analyses were performed using GraphPad Prism version 5.01 for Windows (GraphPad Software, La Jolla, CA). P values < 0.05 were considered significant. Independent experiments were performed in triplicates.

Results

Stimulation of GSCs with bFGF increases expression of EGFR and stem cell markers

In this study, we used two different, heterogeneous GSC lines, NCH421k and NCH644. These cell lines were derived from primary GBMs that showed typical GBM aberrations (*e.g.* loss of chromosome 10 and/or gain of chromosome 7) as indicated by DNA copy-number profiling by array-CGH. NCH421k additionally carried amplifications of the *PDGFRA* and *CDK4* gene loci. These copy number aberrations were well preserved in the

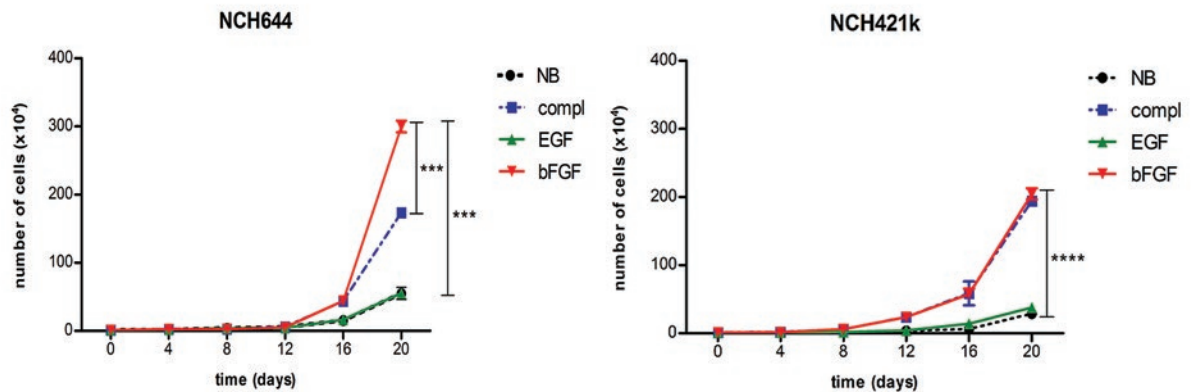


FIGURE 3. bFGF stimulates growth of GSCs. Growth curves of cells cultured in stem cell media differing in the presence of EGF and/or bFGF. Both cell lines showed the fastest growth upon bFGF stimulation, either alone or in complete medium with both growth factors whereas EGF alone did not significantly stimulate cell growth compared to medium without growth factors. Labels: NB=plain Neurobasal medium without growth factors; compl=NB with EGF and bFGF; EGF=NB with EGF; bFGF=NB with bFGF. Data shown are mean \pm SD of three independent experiments with the following significant changes: ****: $p < 0.0001$ for NCH421k (NB vs compl, NB vs bFGF, EGF vs compl, EGF vs bFGF); ***: $p < 0.001$ for NCH644 (NB vs compl, NB vs bFGF, EGF vs compl, bFGF vs compl, EGF vs bFGF).

cell lines (Figure 1). Both primary tumors as well as the NCH421k and NCH644 cell lines derived from them lack amplification of the *EGFR* gene locus (position indicated by arrows in Figure 1). Both cell lines belong to the proneural category according to the classification by Verhaak *et al.*²⁰ (data not shown). Recently it has been shown that the presence of EGF in the culture medium leads to reduced EGFR expression in tumor cells with EGFR amplification.¹³ However, cells without EGFR amplification might also express EGFR. Therefore, we first determined the expression level of EGFR by flow cytometry in both cell lines under different growth conditions. Before the experiment, cells were cultured in NB medium without growth factors for 10 days and then divided into different groups for growth factor treatment as indicated in Figure 2. FACS analysis for EGFR revealed that $0.4 \pm 0.14\%$ of NCH644 cells and $0.35 \pm 0.35\%$ of NCH421k cells stimulated by both EGF and bFGF (complete NB medium) were positive. However, while stimulation with EGF alone, bFGF alone or medium without growth factors did not alter the expression of EGFR in NCH421k cells, there was a change in NCH644 cells under the defined conditions as shown in Figure 2A and B. bFGF stimulation for 48 hours substantially increased the fraction of EGFR expressing NCH644 cells to $16.85 \pm 1.48\%$ ($p < 0.001$), while the absence of growth factors or EGF stimulation alone revealed only $6.00 \pm 0.28\%$ ($p < 0.001$) or $1.95 \pm 0.64\%$ ($p < 0.001$) EGFR expressing cells, respectively. Thus, bFGF stimulation alone had the strongest positive effect on EGFR expression, while complete medium containing both growth factors

and EGF had a negative effect. The upregulation of EGFR in NCH644 was verified by western blot, where cells were stimulated with bFGF for 14 days (Figure 2C). The difference in response to bFGF between the two cell lines might be explained by the variable levels of EGFR that are initially present in GBMs without EGFR amplification. Only a fraction of GBMs without EGFR amplification naturally expresses EGFR.²¹

In addition, we investigated the impact of EGF and bFGF on stem cell marker expression, such as CD133, nestin and SOX2. Expression levels of CD133 and nestin were significantly increased in both cell lines upon bFGF stimulation whether alone or in complete medium whereas EGF alone did not affect stem cell marker expression (Figure 2D and E). In NCH644 cells only, SOX2 expression levels were significantly increased upon bFGF stimulation. These results show that bFGF alone as well as both growth factors in combination are able to maintain high stem cell marker expression in both GSC lines.

bFGF, but not EGF, stimulates growth of GSCs

To define how bFGF and EGF affected the growth of the two cell lines, we cultured the cells in NB medium without growth factors for 10 days and then divided them into different groups for growth factor treatment as indicated in Figure 3. NCH421k and NCH644 cells formed spheroids under all conditions and there was no change in morphology of the cells as analyzed by light microscopy (data

not shown). We generated growth curves over 20 days, which clearly showed that bFGF alone and complete medium increased growth of both cell lines by 5.5-fold ($p < 0.001$) and 7.2-fold ($p < 0.001$) for NCH644 and NCH421k, respectively (Figure 3), compared to EGF and medium without growth factors. Further, bFGF significantly increased growth of NCH644 cells over complete medium ($p < 0.001$). Thus, bFGF appeared to be the most effective growth factor to culture and expand GSCs without EGFR amplification.

GSCs proliferation and resistance to apoptosis are stimulated by bFGF

We then determined how bFGF and EGF affect cell cycle parameters and apoptosis. Cells were stimulated for 48 hours with bFGF or EGF. We observed that NCH421k cells showed a significant ($p < 0.01$) increase in cells entering the S phase upon bFGF stimulation, verifying that the growth of NCH421k cells is stimulated by bFGF (Figure 4A). Stimulation with EGF had no effect on the cell cycle in NCH421k. Surprisingly, NCH644 cells did not show a significant difference upon stimulation with bFGF or EGF. Therefore, we used a cell death assay to analyze whether there is a difference in apoptosis. We observed 1.1-fold ($p < 0.01$) less apoptotic NCH644 cells upon bFGF stimulation compared to unstimulated cells. EGF stimulation did not have this effect. In contrast to NCH644, the NCH421k cell line did not show any significant differences in the apoptosis assay (Figure 4B). Thus, in both GSC lines bFGF stimulated growth by either enhancing proliferation (NCH421k) or mediating resistance to apoptosis (NCH644), while EGF showed no effects.

Discussion

An important prerequisite for culturing tumor cells from human biopsies is that the cultured cells should preserve the geno- and phenotype of the original tumor they were derived from. Culture media have an important impact as shown by Lee *et al.*¹², where GBM derived stem-like cells cultured in serum-free medium with EGF and bFGF showed more similarities to the primary tumors compared to serum cultured cells. However, Schulte *et al.*¹³ reported that stem cell medium without EGF better preserved original tumor levels of EGFR amplification. Moreover, under high EGF concentrations, tumor cells did not retain EGFR amplification and lost tumorigenicity *in vivo*. This highlights the im-

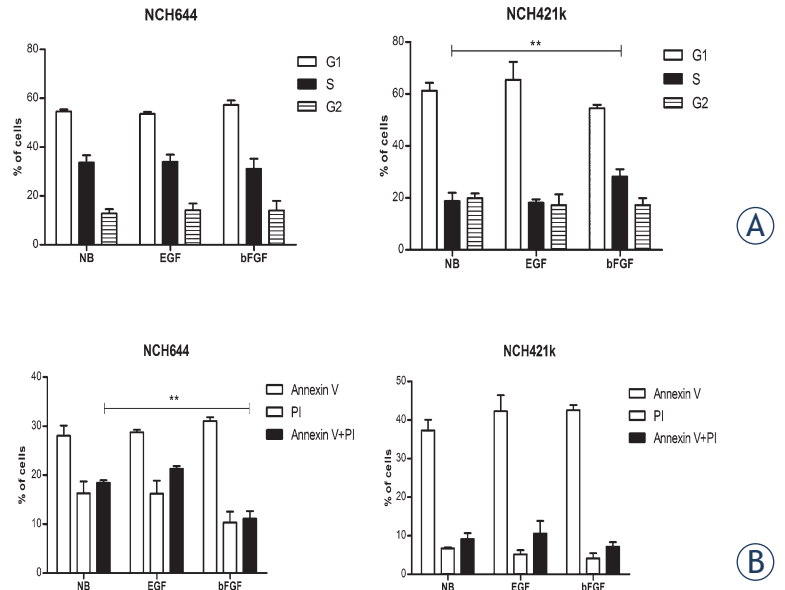


FIGURE 4. bFGF stimulates growth of GSCs due to increased viability or proliferation. **(A)** Cell cycle analysis of cells grown in the presence of EGF or bFGF. The relative changes in the cell number in G1, S and G2 phase were measured as indicators of cell proliferation. bFGF increased the number of cells in S phase in NCH421k cells, while there were no effects on the cell cycle in NCH644 cells. **(B)** Apoptosis assay of cells double labeled with Annexin V-FITC and PI. Percentages of cells in each histogram are representative of early apoptosis (labeled Annexin V), necrosis (labeled PI) and late apoptosis (labeled Annexin V+PI). Number of apoptotic NCH644 cells was decreased in presence of bFGF, but not in the presence of EGF. No significant changes upon EGF or bFGF stimulation were observed in the NCH421k cell line compared to the medium without growth factors. Labels: NB= Neurobasal medium without growth factors; comp1=NB with EGF and bFGF; EGF=NB with EGF; bFGF=NB with bFGF. Data shown are mean \pm SD of three independent experiments. **: $p < 0.01$.

portance of the right choice of growth factors in serum-free culture media. In laboratory practice, human tumor biopsies are most often cultured before the genomic profile of the patient tumor is known. Thus, it would be an important advantage if culture conditions for EGFR non-amplified and EGFR amplified primary GBMs would be identical in order to preserve their characteristics and the original tumor genotype. GSCs in such cultures would thus represent a better model for studying the impact of different genetic abnormalities.

Here, we used two cancer stem-like cell lines, NCH644 and NCH421k, derived from patient GBMs without EGFR amplification, to define which growth factors are needed in the culture medium to maintain and expand GSCs. Importantly, we demonstrated that bFGF was the main growth stimulator of these GSC lines, while EGF did not have a significant effect. We verified that the cell growth effects of bFGF were mediated by an increased proliferation (NCH421k) or a decreased apoptotic rate

(NCH644). This clearly shows that bFGF was able to induce expansion of GSC cultures in contrast to EGF. Investigating the effect of autocrine factors on glioblastoma growth, Kelly *et al.*²² claimed that glioma cells could also be effectively cultured without any growth factors as they have autocrine loops to stimulate proliferation. However, in our hands the GSCs without any growth factor stimulation were growing at a very slow rate, which is not sufficient for a considerable expansion of cells needed to effectively study GSCs.

When analyzing EGFR expression in the two GSC cell lines, we showed that only bFGF stimulation significantly increased the fraction of EGFR expressing cells compared to non-stimulated cells, whereas the presence of EGF alone or both growth factors in the culture medium significantly decreased this fraction. As this effect was observed in NCH644 only, the change in EGFR expression might also explain the significantly higher growth rate of NCH644 in bFGF only compared to complete medium, which was not observed in NCH421k. Upregulation of EGFR, which is a well characterized oncogene, might lead to a higher proliferation rate of cells. Thus, even in cells without EGFR amplification, EGFR expression can be better preserved when EGF is not present. This result was confirmed in a recent study by Mazzoleni *et al.*²³ showing that reduction of EGF levels in culture media resulted even in re-expression of EGFR in previously negative cells. Taken together this may indicate either a transcriptional downregulation of the receptor induced by EGF or the presence of a negative regulatory feedback loop, activated upon excessive EGF binding, which may result in endocytosis and degradation of EGF-EGFR complexes.²⁴ Although in cancer this loop may be normally bypassed in order to provide continuous oncogenic signaling, the chronic stimulation by EGF in stem cell media might result in an overstimulation of receptor activity, triggering its degradation. In contrast, upon bFGF stimulation, the increased EGFR expression which was observed in our experiments, may be induced by a cross-talk between EGFR and FGFR signaling pathways which often overlap.²⁵ FGFR activation upon bFGF binding may stimulate similar signaling transducers as binding of EGF to EGFR. Therefore, it is possible that FGFR activation through bFGF induces a positive feedback loop to increase EGFR expression.

Investigating the effects of both growth factors on expression of GSC stem cells markers, we showed that bFGF stimulation increased the expression of CD133 and nestin, while EGF did not.

This contradicts the findings by Soeda *et al.*²⁶ showing that EGF increased CD133 expression in a dose dependent manner. However, the stem-like tumor cells used in their study expressed high levels of EGFR in contrast to the NCH644 and NCH421k cells. Further, long-term stimulation of EGFR amplified/highly expressing tumor cells with EGF would result in down-regulation of EGFR and in the worst case loss of tumorigenicity¹³, eliminating EGF as a candidate growth factor for long-term stimulation of EGFR expressing cells. The present work indicates that bFGF alone is sufficient to preserve stem cell markers in GSCs, such as CD133 and nestin, which is important in order to study characteristics of the GSC phenotype.

In summary, using two different GSC lines without EGFR amplification, we demonstrated significant stimulatory effects of bFGF on the expression of stem cell markers and expansion of these cells. In contrast, EGF did not have any measurable effect. Moreover, EGF seemed to down-regulate EGFR expression, similar as reported for EGFR amplified GSCs^{13,23}, suggesting that GSCs should be cultured in stem cell medium supplemented with bFGF only to better preserve the original GSC genotype.

Acknowledgments

We thank Ingrid Gavlen and Bodil Hansen for expert technical assistance. This work was supported by the Research Council of Norway (grant 186492 to HM), the Bergen Medical Research Foundation, the Norwegian Cancer Society, Helse Vest, and Haukeland University Hospital. This work was also supported by the young researcher grant to NP (ARRS), Slovene Human Resources Development and Scholarship Fund (grants 11012-12/2009 and 11012-2/2011), Centre of the Republic of Slovenia for Mobility and European Educational and Training Programmes (grant 2009-6581) as well as by ARRS project J1-2095 (granted to TLT).

References

1. Stupp R, Mason WP, van den Bent, MJ, Weller M, Fisher B, Taphoorn MJ, et al. Radiotherapy plus concomitant and adjuvant temozolomide for glioblastoma. *N Engl J Med* 2005; **352**: 987-96.
2. Reya T, Morrison SJ, Clarke MF, Weissman IL. Stem cells, cancer, and cancer stem cells. *Nature* 2001; **414**: 105-11.
3. Valent P, Bonnet D, De Maria R, Lapidot T, Copland M, Melo JV, et al. Cancer stem cell definitions and terminology: the devil is in the details. *Nat Rev Cancer* 2012; **12**: 767-75.

4. Bjerkvig R, Johansson M, Miletic H, Niclou SP. Cancer stem cells and angiogenesis. *Semin Cancer Biol* 2009; **19**: 279-84.
5. Strojnik T, Røsland GV, Sakariassen PO, Kavalari R, Lah TT. Neural stem cell markers, nestin and musashi proteins, in the progression of human glioma: correlation of nestin with prognosis of patient survival. *Surg Neurol* 2007; **68**: 133-44.
6. Visvader JE, Lindeman GJ. Cancer stem cells in solid tumours: accumulating evidence and unresolved questions. *Nat Rev Cancer* 2008; **8**: 755-68.
7. Rahman M, Deleyrolle L, Vedam-Mai V, Azari H, Abdel-Barr M, et al. The cancer stem cell hypothesis: failures and pitfalls. *Neurosurgery* 2011 **68**: 531-45.
8. Tysnes BB, Bjerkvig R. Cancer initiation and progression: involvement of stem cells and the microenvironment. *Biochim Biophys Acta* 2007; **1775**: 283-97.
9. Van Meir EG, Hadjipanayis CG, Norden AD, Shu HK, Wen PY, Olson JJ. Exciting new advances in neuro-oncology: the avenue to a cure for malignant glioma. *CA Cancer J Clin* 2010; **60**: 166-93.
10. Chaichana K, Zamora-Berridi G, Camara-Quintana J, Quiñones-Hinojosa A. Neurosphere assays: growth factors and hormone differences in tumor and nontumor studies. *Stem Cells* 2006; **24**: 2851-7.
11. Ernst A, Hofmann S, Ahmadi R, Becker N, Korshunov A, Engel F, et al. Genomic and expression profiling of glioblastoma stem cell-like spheroid cultures identifies novel tumor-relevant genes associated with survival. *Clin Cancer Res*. 2009; **15**: 6541-50.
12. Lee J, Kotliarova S, Kotliarov Y, Li A, Su Q, et al. Tumour stem cells derived from glioblastomas cultured in bFGF and EGF more closely mirror the phenotype and genotype of primary tumours than do serum-cultured cell lines. *Cancer Cell* 2006; **9**: 391-403.
13. Schulte A, Günther HS, Martens T, Zapf S, Riethdorf S, et al. Glioblastoma stem-like cell lines with either maintenance or loss of high-level EGFR amplification, generated via modulation of ligand concentration. *Clin Cancer Res* 2012; **18**: 1901-13.
14. Loew S, Schmidt U, Unterberg A, Halatsch ME. The epidermal growth factor receptor as a therapeutic target in glioblastoma multiforme and other malignant neoplasms. *Anticancer Agents Med Chem* 2009; **9**: 703-15.
15. Ekstrand AJ, James CD, Cavenee WK, Seliger B, Pettersson RF, Collins VP. Genes for epidermal growth factor receptor, transforming growth factor alpha, and epidermal growth factor and their expression in human gliomas in vivo. *Cancer Res* 1991; **51**: 2164-72.
16. Campos B, Wan F, Farhadi M, Ernst A, Zeppernick F, Tagscherer KE, et al. Differentiation therapy exerts antitumor effects on stem-like glioma cells. *Clin Cancer Res* 2010; **16**: 2715-28.
17. Mendrzyk F, Radlwimmer B, Joos S, Kokocinski F, Benner A, Stange DE, et al. Genomic and protein expression profiling identifies CDK6 as novel independent prognostic marker in medulloblastoma. *J Clin Oncol* 2005; **23**: 8853-62.
18. Gentleman RC, Carey VJ, Bates DM, Bolstad B, Dettling M, Dudoit S, et al. Bioconductor: open software development for computational biology and bioinformatics. *Genome Biol* 2004; **5**: R80.
19. Prestegarden L, Svendsen A, Wang J, Sleire L, Skafnesmo KO, Bjerkvig R, et al. Glioma cell populations grouped by different cell type markers drive brain tumor growth. *Cancer Res* 2010; **70**: 4274-9.
20. Verhaak RG, Hoadley KA, Purdom E, Wang V, Qi Y, Wilkerson MD, et al. Integrated genomic analysis identifies clinically relevant subtypes of glioblastoma characterized by abnormalities in PDGFRA, IDH1, EGFR, and NF1. *Cancer Cell* 2010; **17**: 98-110.
21. Schlegel J, Stumm G, Brandle K, Merdes A, Mechttersheimer G, Hynes NE, et al. Amplification and differential expression of members of the erbB-gene family in human glioblastoma. *J Neurooncol* 1994; **22**: 201-7.
22. Kelly JJ, Stechishin O, Chojnacki A, Lun X, Sun B, et al. Proliferation of human glioblastoma stem cells occurs independently of exogenous mitogens. *Stem Cells* 2009; **27**: 1722-33.
23. Mazzoleni S, Politi LS, Pala M, Cominelli M, Franzin A, et al. Epidermal growth factor receptor expression identifies functionally and molecularly distinct tumor-initiating cells in human glioblastoma multiforme and is required for gliomagenesis. *Cancer Res* 2010; **70**: 7500-13.
24. Avraham R, Yarden Y. Feedback regulation of EGFR signalling: decision making by early and delayed loops. *Nat Rev Mol Cell Biol* 2011; **12**: 104-17.
25. Schlessinger J. Common and distinct elements in cellular signaling via EGF and FGF receptors. *Science* 2004; **306**: 1506-7.
26. Soeda A, Inagaki A, Oka N, Ikegami Y, Aoki H, et al. Epidermal growth factor plays a crucial role in mitogenic regulation of human brain tumor stem cells. *J Biol Chem* 2008; **283**: 10958-66.

Heterogeneity of uroplakin localization in human normal urothelium, papilloma and papillary carcinoma

Dasa Zupancic and Rok Romih

Institute of Cell Biology, Faculty of Medicine, Ljubljana, Slovenia

Radiol Oncol 2013; 47(4): 338-345.

Received 29 May 2013
Accepted 12 July 2013

Correspondence to: Assist.Prof. Daša Zupančič, Ph.D., Institute of Cell Biology, Vrazov trg 2, SI-1000 Ljubljana, Slovenia.
E-mail: dasa.zupancic@mf.uni-lj.si

Disclosure: The authors have no conflict of interest to disclose.

The paper was presented at the 7th Conference of Experimental and Translational Oncology, 20-24th April 2013, Portoroz, Slovenia (www.ceto.si) co-organised and supported by COST TD1104 Action (www.electroporation.net).

Background. Uroplakins are differentiation-related membrane proteins of urothelium. We compared uroplakin expression and ultrastructural localization in human normal urothelium, papilloma and papillary carcinoma. Because of high recurrence rate of these tumours, treated by transurethral resection, we investigated urothelial tumour, resection border and uninvolved urothelium.

Patients and methods. Urinary bladder samples were obtained from tumour free control subjects and patients with papilloma and papillary carcinoma. Immunohistochemical and immunoelectron labelling of uroplakins were performed.

Results. In normal human urothelium with continuous uroplakin-positive superficial cell layer uroplakins were localized to flattened mature fusiform vesicles and apical plasma membrane of umbrella cells. Diverse uroplakin expression was found in papilloma and papillary carcinoma. Three aberrant differentiation stages of urothelial cells, not found in normal urothelium, were recognized in tumours. Diverse uroplakin expression and aberrant differentiation were occasionally found in resection border and in uninvolved urothelium.

Conclusions. We demonstrated here that uroplakin expression and localization in urothelial tumours is altered when compared to normal urothelium. In patients with papilloma and papillary carcinoma immunolabelling of uroplakins at ultrastructural level shows aberrant urothelial differentiation. It is possible that aberrant differentiation stages of urothelial cells in resection border and in uninvolved urothelium contribute to high recurrence rate.

Key words: human urothelium; papilloma; papillary carcinoma; uroplakins; immunoelectron microscopy; immunohistochemistry

Introduction

Urothelium is the source of most urinary bladder cancers, which are the ninth most common malignancy worldwide.¹ Among all bladder urothelial cancers, more than half represent the papilloma and the papillary carcinoma.² Tumours, which are cytopathologically and recently even cytogenetically diagnosed by the examination of urine or bladder washing³, are usually resected during the transurethral resection of the urinary bladder

(TURB).⁴ However the recurrence rate of this malignancies is nearly 70%.⁵

Four uroplakins (UPIa, UPIb, UPII and UPIIIa)^{6,7} are the major differentiation products of urothelium^{8,9}, however their expression is not strictly correlated with pathological stage and grade.¹⁰⁻¹⁴ Uroplakins are transmembrane proteins, which form complex membrane structures, called urothelial plaques^{15,16}, which represent the ultimate marker for terminal differentiation of superficial umbrella cells of normal urothelium. Urothelial plaques

cover up to 90% of the apical plasma membrane and fusiform vesicles.¹⁵ Fusiform vesicle undergoes distinct stages of maturation, from small, rounded uroplakin-positive transporting vesicles to discoidal immature fusiform vesicles and flattened mature fusiform vesicles, which are incorporated into the apical plasma membrane.^{17,18} In partially differentiated intermediate urothelial cells only uroplakin-positive transporting vesicles and immature fusiform vesicles are formed.^{17,18} Ultrastructural localisation of uroplakins is therefore closely related to the differentiation stage of urothelial cell. We have shown recently that ultrastructural localization of uroplakins is preserved in preneoplastic urothelium¹⁹, but the ultrastructural localization of uroplakins in urothelial tumour cells is not known.

The aim of the present study was to explore uroplakin expression and ultrastructural localization of uroplakins in normal urothelial cells and in urothelial cells of papilloma and papillary carcinoma from patients which underwent TURB. We analysed the tumour, the urothelium positioned next to the resected tumour, which we termed "resection border", and the urothelium away from the removed tumour, which we termed "uninvolved urothelium". We showed that ultrastructural localization of differentiation-related uroplakins may be featuring different urothelial regions in patients with urothelial tumours.

Materials and methods

Patients and sampling

The study was approved by the Slovenian National Medical Ethics Committee, No. 80/11/99, and was conducted in accordance with the Helsinki Declaration. The study population consisted of 25 patients with bladder cancer who underwent TURB and 4 tumour free control subjects who underwent transurethral resection of the prostate. Patients were histopathologically diagnosed as papilloma (5 patients; 41 to 76 y-old; mean age 55,6 y), papillary urothelial carcinoma - pTa (15 patients; 9 patients with G1, 3 patients with G1-2, 2 patients with G2 and 1 patient with G2-3; 46 to 77 y-old; mean age 65,8 y), and papillary urothelial carcinoma with lamina propria invasion - pT1 (5 patients; 1 patient with G1-2, 3 patients with G2 and 1 patient with G2-3; 64 to 73 y-old; mean age 67,3 y). The 1998 "World Health Organization/International Society of Urological Pathology consensus classification of urothelial (transitional cell) neoplasms of the urinary bladder" was used for pathologic stag-

ing and grading.²⁰ All control subjects were diagnosed as benign prostatic hyperplasia.

From each control and papilloma one sample was obtained. From papillary urothelial carcinoma (pTa, pT1) three samples were acquired: (i) the urothelial tumour, (ii) the urothelium positioned next to the resected tumour, *i.e.* "resection border", and (iii) the urothelium away from the removed tumour, *i.e.* "uninvolved urothelium". Each sample was cut into 2 halves immediately after biopsy, one being processed for light and the other for the electron microscopy.

Immunohistochemical labelling of uroplakins

For light microscopy, samples were immersed in Bouin solution for 24 h, dehydrated and embedded in paraffin wax. Paraffin sections were cut from at least two different parts of each sample. Sections were incubated in the anti-uroplakins antibody.⁶ Sections were then labelled with biotinylated swine anti-rabbit immunoglobulins (Dako, Glostrup, Denmark), followed by ABC/HRP complex (Vector Laboratories, Burlingame, CA), developed by DAB (Sigma, Taufkirchen, Germany) and counterstained with haematoxylin. For negative controls, the incubation with primary antibody was omitted or the specific primary antibody was replaced by a non-relevant antibody. Sections were examined with a Nikon Eclipse TE300 microscope.

Immunoelectron microscopy

For immunoelectron microscopy, samples were cut into 1mm³ pieces and fixed in 2% paraformaldehyde plus 0.05% glutaraldehyde. Samples were dehydrated by increasing the concentration of ethanol while simultaneously decreasing the temperature and then they were embedded in Lowicryl HM20 resin at - 50°C. The resin was polymerized by ultraviolet light. Semithin and ultrathin sections were cut. Semithin sections were immunolabelled first in order to find appropriate region for immunoelectron microscopy. Both sections were treated according to the same protocol. Non-specific labelling was blocked by the PBS buffer containing 0.1% fish gelatin, 0.8% bovine serum albumin and 5% fetal calf serum (blocking buffer). Sections were incubated with anti-uroplakins antibody in the blocking buffer. After washing in washing buffer (blocking buffer without fetal calf serum) primary antibody was detected with goat anti-rabbit IgG conjugated to either 5 nm or 10 nm colloidal

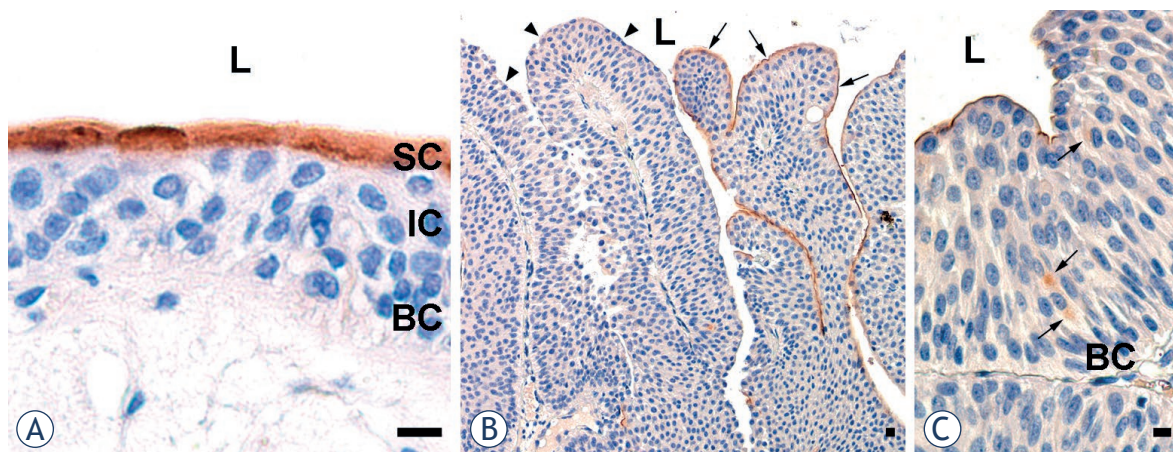


FIGURE 1. Immunohistochemical labelling of uroplakins in normal urothelium and in papilloma (A) Brown reaction products shows that superficial cells (SC) with high uroplakin expression form a continuous layer in normal urothelium from control subjects. Underlying intermediate (IC) and basal cells (BC) are uroplakin-negative. (B) In the urothelium of a patient with papilloma, superficial cells of some papillae are uroplakin-positive (arrows), while others are uroplakin-negative (arrowhead). (C) Individual intermediate urothelial cells of papillae are uroplakin-positive (arrows). L – lumen. Scale bars: 10 µm.

gold, diluted 1:50 in blocking buffer. Sections were washed in washing buffer followed by ultrapure water. The 5 nm gold was silver enhanced with IntenSE (Amersham, U.K.). The enhancement times were 24 min and 4 min for semithin and ultrathin sections, respectively. Semithin sections were counterstained with toluidin blue and examined under an epi-polarization microscope in transmitted bright-field (Axioscop 20, Carl Zeiss). Ultrathin sections were counterstained with uranyl acetate and lead citrate and viewed in a Philips CM100 transmission electron microscope.

Results

Different immunohistochemical labelling of uroplakins is displayed in human normal urothelium, papilloma and papillary carcinoma

According to WHO consensus classification²⁰, control subjects with benign prostatic hyperplasia had a normal urothelium, with no cytological atypia, but with slight hyperplasia in some areas, which was in agreement with previous studies.^{12,21} Several areas of urothelium showed normal morphology with three to five cell layers and large superficial umbrella cells, while other areas of urothelium consisted of up to seven cell layers with smaller superficial cells. No other premalignant or malignant changes were observed.

Consistent with the notion that uroplakins are expressed in terminally differentiated umbrella cells^{8,9}, we considered as normal urothelium only the regions where immunohistochemical labelling

of uroplakins was positive in all superficial cells (Figure 1A).

Papilloma was defined as a discrete papillary growth with a central fibrovascular core lined by urothelium of normal thickness and cytology.²⁰ The apical cell layer of papillae was composed of uroplakin-positive and uroplakin-negative regions (Figure 1B). Although all basal cells and the majority of intermediate cells of papillae were uroplakin-negative, rare intermediate cells exhibited positive uroplakin labelling (Figure 1C).

Papillary carcinomas showed no direct correlation between uroplakin expression and carcinoma staging and grading, which was consistent with previously published data.^{12,13} In order to compare uroplakin expression in different urothelial regions, immunohistochemical labelling of uroplakins was performed on the paraffin sections from (i) the urothelial tumour, (ii) resection border and (iii) uninvolved urothelium. In general, uroplakin expression was lower in all patients compared to normal urothelium. (i) Urothelium of urothelial tumours showed three distinct types of uroplakin labelling patterns. In the first type, urothelium was covered by continuous layer of uroplakin-positive superficial cell and it also contained individual uroplakin-positive intermediate cells (Figure 2A). In the second type, urothelium was completely uroplakin-negative (Figure 2B). In the third type, urothelium contained individual uroplakin-positive cells, which were scattered throughout all cell layers (Figure 2C). (ii) Urothelium of resection borders also revealed heterogeneous labelling patterns, which could be placed into three categories. One

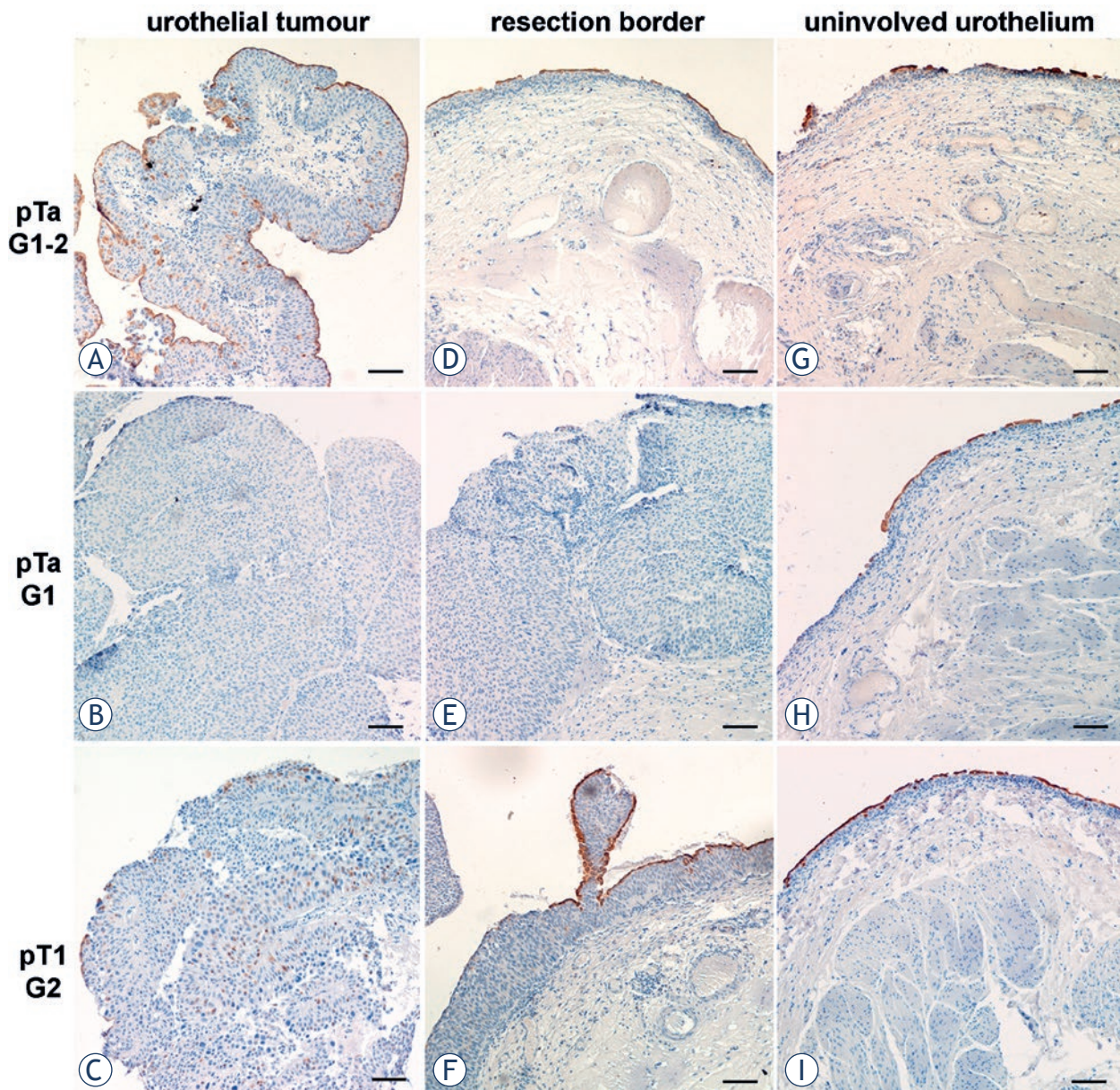


FIGURE 2. Immunohistochemical labelling of uroplakins (brown reaction products) in urothelial tumour (**A-C**), resection border (**D-F**) and uninvolved urothelium (**G-I**) from patients with noninvasive (pTa) or lamina propria invasive (pT1) papillary carcinomas. Urothelial tumour with (**A**) uroplakin-positive superficial cell layer and individual uroplakin-positive intermediate cells, (**B**) uroplakin-negative urothelium and (**C**) urothelium containing rare uroplakin-positive cells. Resection border with (**D,F**) uroplakin-positive and uroplakin-negative regions of urothelium and (**E**) completely uroplakin-negative urothelium. Uninvolved urothelium with (**G,H**) small and (**I**) large regions of uroplakin-positive superficial cells. In the region with uroplakin-positive superficial cells, some intermediate cells are also uroplakin-positive. Scale bars: 100 μ m.

type of resection border contained urothelium with normal histology, but discontinuous uroplakin expression in the superficial cell layer (Figure 2D). Another type of resection border was composed of urothelium, which had the same histopathologic characteristics as tumours. Here, urothelium was also completely uroplakin-negative as was the case in the neighbouring tumour (Figure 2E). Yet another type of resection border contained hyper-

plastic urothelium, which was covered with large stretches of uroplakin-positive superficial cells, alternating with large stretches of uroplakin-negative superficial cells. Urothelial regions covered with uroplakin-positive superficial cells contained uroplakin-positive intermediate cells. These uroplakin-positive cells were always found just beneath the superficial cell layer (Figure 2F). (iii) Uninvolved urothelia exhibited normal histology; however their

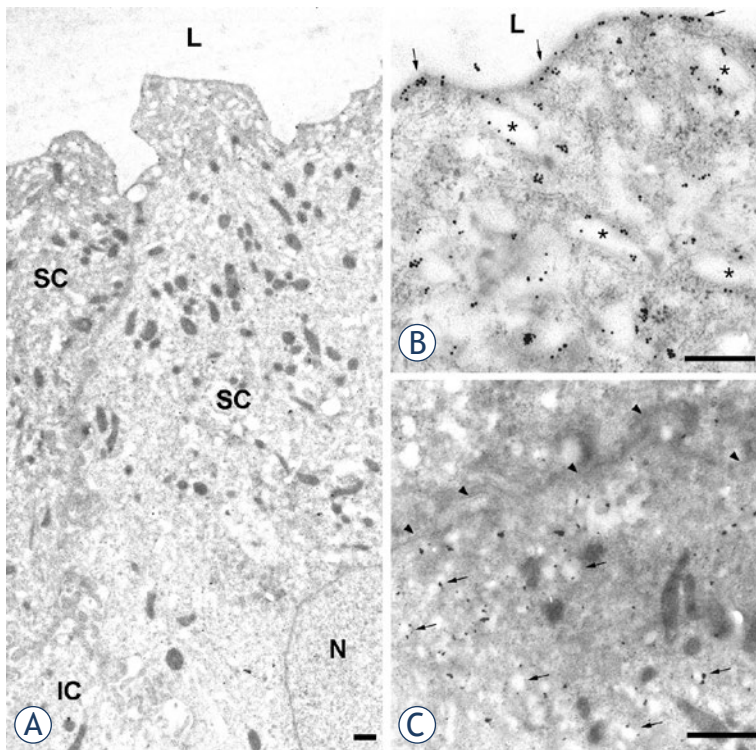


FIGURE 3. Immunoelectron microscopy of uroplakins in normal urothelium. (A) Two neighbouring superficial umbrella cells (SC), contain numerous mature fusiform vesicles. A part of underlying intermediate cell (IC) is also seen. (B) In umbrella cell uroplakin-positive apical plasma membrane (arrows) and uroplakin-positive mature fusiform vesicles (asterisks) are heavily labelled with colloidal gold particles. (C) Intermediate cell contains uroplakin-positive transporting vesicles (arrows). The basolateral plasma membrane (arrowheads) is uroplakin-negative. N – nucleus, L – lumen. Scale bars: 1 μ m.

superficial cells were either uroplakin-positive or uroplakin-negative (Figure 2G-I). The extent of uroplakin-positive versus uroplakin-negative regions varied to a great degree. As described for tumours and resection borders, uninvolved urothelium also contained individual uroplakin-positive intermediate cells, usually underlying uroplakin-positive superficial cells (Figure 2I).

Uroplakin ultrastructural localization in papilloma and papillary carcinoma is altered in comparison to normal human urothelium

Because immunohistochemical labelling of uroplakins is insufficient for determination of urothelial cell's differentiation stage, we performed immunoelectron microscopy to determine ultrastructural localization of uroplakins in human normal and tumour urothelial samples.

Normal urothelium was covered with superficial cells, which contained uroplakin-positive large flattened mature fusiform vesicles and uroplakin-positive apical plasma membrane (Figure 3A, B).

These superficial cells were terminally differentiated and they shared characteristics with umbrella cells described in other species.^{16,18} Intermediate cells of normal urothelium were generally uroplakin-negative, except for some intermediate cells that contained small, round uroplakin-positive transporting vesicles. Their plasma membrane was always uroplakin-negative (Figure 3C), which is also in agreement with observations in other species.¹⁸

Immunoelectron microscopy of uroplakins confirmed the results of immunohistochemical labelling of urothelial tumours. We observed uroplakin-positive (Figure 4A, B) and uroplakin-negative (Figure 4C) superficial cells in papilloma and in all regions (tumour, resection border, uninvolved urothelium) of pTa and pT1 papillary carcinoma. Uroplakin-positive superficial cells had uroplakins in their apical plasma membranes and cytoplasmic vesicles. These uroplakin-positive vesicles were smaller and weakly labelled (Figure 4B) when compared to mature fusiform vesicles of normal urothelium (Figure 3B), and therefore represented immature fusiform vesicles. Importantly, mature fusiform vesicles were not detected in any of the samples taken from patients with urothelial tumours, not even in uninvolved urothelium. Uroplakin-negative superficial cells had microvilli on their apical surface and small, rounded vesicles in their cytoplasm (Figure 4C).

Also in agreement with immunohistochemical labelling, we observed uroplakin-positive intermediate cells in urothelial tumours (Figure 4A,D,E). One type of uroplakin-positive intermediate cells had uroplakin-positive transporting vesicles and uroplakin-negative plasma membranes (Figure 4D). This type of intermediate cells therefore had all the characteristics of corresponding intermediate cells of normal urothelium (Figure 3C). There was another type of uroplakin-positive intermediate cells that had never been described before. This type of cells was characterized by the presence of numerous mitochondria, uroplakin-positive transporting vesicles and uroplakin-positive plasma membranes (Figure 4E). However, the majority of intermediate (as well as all basal cells) were uroplakin-negative. All the described types of intermediate cells could be found in papilloma and in all samples from patients with papillary carcinoma.

Discussion

The majority of knowledge about normal urothelium originates from the studies on laboratory

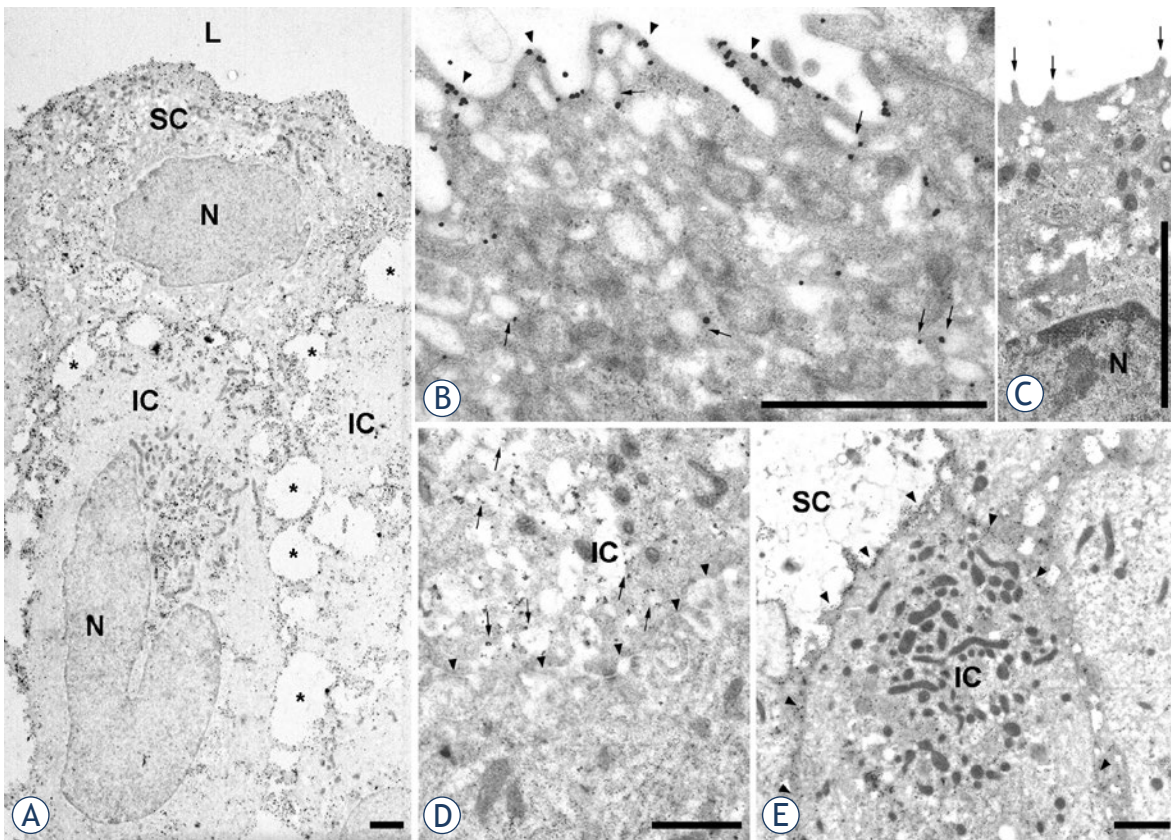


FIGURE 4. Immunoelectron microscopy of uroplakins in urothelial tumours. (A,B) papilloma, (C) tumour region of pTa G1, (D) tumour region of pT1 G1-2, (E) uninvolved urothelium of pTa G1-2. (A) Uroplakin-positive superficial (SC) and uroplakin-positive intermediate cells (IC) are shown. Note dilatations of intercellular spaces (asterisks) and prominent cytoplasmic processes that interconnect neighbouring cells. (B) Superficial cell with uroplakin-positive apical plasma membrane (arrowheads) and weakly positive immature fusiform vesicles (arrows). (C) Uroplakin-negative superficial cell with microvilli (arrows) on the apical surface. (D) Intermediate cell with uroplakin-positive transporting vesicles (arrows) and uroplakin-negative plasma membrane (arrowheads). (E) Intermediate cell with numerous mitochondria, uroplakin-positive transporting vesicles and uroplakin-positive plasma membrane (arrowheads). N – nucleus, L – lumen. Scale bars: 1 μ m.

animals. In the normal human urothelium, urothelial plaques and fusiform vesicles has not yet been extensively studied, partially due to the fact that urothelium is obtained from patients and not from healthy individuals. The definition from WHO/ISUP consensus²⁰ proposes that “Flat lesions with benign cytology and minimal disorder should not be designated as mild dysplasia but rather as normal urothelium”. In our study we adopted more stringent criteria for normal urothelium, which must contain undisrupted layer of superficial umbrella cells expressing uroplakins. Umbrella cells have uroplakins in their apical plasma membrane and contain mature fusiform vesicles (Table 1), which are flat and strongly uroplakin-positive vesicles. Minority of urothelial regions fulfil this demand. This is probably because urothelia are from control subjects with benign prostatic hyperplasia,

which decrease the differentiation stage of superficial urothelial cells in some areas.¹² Intermediate urothelial cells have uroplakin-positive transporting vesicles, but their plasma membranes are uroplakin-negative. This is consistent with the normal mouse urothelium, where uroplakin-positive transporting vesicles are found, but plasma membrane of partially differentiated intermediate cells does not contain uroplakins.¹⁷ We assume that at least some intermediate cells synthesize uroplakins, which accumulate in uroplakin-positive transporting vesicles (Table 1). It seems that these vesicles cannot fuse with the plasma membrane.

Since identification of uroplakins as the major differentiation products of normal urothelium^{8,9} their altered expression in urothelial carcinomas has been studied. We demonstrate here, that in papilloma only some regions of apical surface and

TABLE 1. Uroplakin-positive structures in the urothelial cells of human normal urothelium, papilloma and papillary carcinoma (urothelial tumour, resection border and uninvolved urothelium of pTa and pT1).

Histology	Superficial cells	Intermediate cells	Basal cells		
normal urothelium	mFV, iFV, UPTV,	aPM	UPTV*	uroplakin	
papilloma	iFV*,	aPM*	UPTV*,	PM*	negative
papillary carcinoma					

mFV = mature fusiform vesicles, iFV = immature fusiform vesicles, UPTV = uroplakin-positive transporting vesicles, aPM = apical plasma membrane, PM = plasma membrane

* individual cells (the majority of cells is uroplakin negative)

extremely rare intermediate cells express uroplakins. On the other hand, papillary carcinoma elaborates heterogeneous uroplakin distribution. Some tumours are almost entirely covered with superficial cells expressing uroplakins and they also contain individual intermediate cells expressing uroplakins. Other tumours express no uroplakins, while several of them exhibit numerous intermediate cells and rare superficial cells expressing uroplakins. Uroplakins are located in the apical plasma membrane as in normal urothelium, while no mature fusiform vesicles are detected in the cytoplasm of these superficial urothelial cells. The cytoplasm of these superficial urothelial cells contains immature fusiform vesicles (Table 1), similar to partially differentiated intermediate cells of normal mouse urothelium.¹⁸ Therefore, we assume that uroplakin expressing superficial urothelial cells of papilloma and papillary carcinoma take alternative pathway of differentiation and elaborate special aberrant differentiation stage. This might be interpreted as compensatory effect of upregulating major differentiation products to counter the proliferative effects of the tumour cells.¹³ Urothelial plaques may retain smaller as observed in preneoplastic mouse urothelium.¹⁹ In the majority of intermediate cells of papilloma uroplakins are absent, indicating their low differentiation stage. Rare intermediate cells, which express uroplakins, exhibit them in uroplakin-positive transporting vesicles and also in their plasma membrane (Table 1). These cells represent another unique aberrant differentiation stage. Similarly, in another type of intermediate cells of papillary carcinoma, uroplakins are localized in uroplakin-positive transporting vesicles and not in the plasma membrane. To sum up, cells of urothelial tumours, which express uroplakins, could follow diverse aberrant differentiation pathways as observed by uroplakin localization analysis. This is probably due to the fact that uroplakin expression and transport is subject to different

regulatory mechanisms, which need to be further exploited.

Urothelial tumours have high recurrence rates⁵, however the exact reasons for that are not yet known. Our study revealed that uninvolved urothelia and resection borders have disrupted uroplakin-positive superficial cell layer and therefore does not fulfil all the criteria for normal urothelium. Since resection borders are usually not removed during TURB, even more pronounced concern represents our finding, that the majority of them were composed of hyperplastic urothelium or even urothelium, which had architectural and cytological characteristics and uroplakin expression similar to that in the tumour. Therefore it is possible that although the main portion of urothelial tumour is removed during TURB, potentially dangerous parts of urothelium are often left behind.

In conclusion, when carefully selected regions of normal human urothelium are examined, umbrella cells develop uroplakin-positive apical plasma membrane and mature fusiform vesicles. Uroplakin expression in the urothelial tumour cells results in heterogeneity of uroplakin ultrastructural localization and contribute to diverse unique aberrant cell differentiation. We assume that such cells in resection border and uninvolved urothelium might represent potential source of new malignant growth and probably contribute to high recurrence rate of this kind of tumours.

Acknowledgment

We are grateful to Prof. T.T. Sun of New York University School of Medicine for donating primary antibodies used in this study. We thank Nada Pavlica, Sabina Železnik, Sanja Čabraja, and Linda Štrus for their technical assistance. We express gratitude to Boris Sedmak and Igor Sterle from

Department of Urology, University Medical Centre Ljubljana, for collecting the samples. This study was supported by a grant from Ministry of Higher Education, Science and Technology, Republic of Slovenia (P3-0108).

20. Epstein JI, Amin MB, Reuter VR, Mostofi FK. The World Health Organization/International Society of Urological Pathology consensus classification of urothelial (transitional cell) neoplasms of the urinary bladder. *Am J Surg Pathol* 1998; **22**: 1435-48.
21. Romih R, Korosec P, Sedmak B, Jezernik K. Mitochondrial localization of nitric oxide synthase in partially differentiated urothelial cells of urinary bladder lesions. *Appl Immunohistochem Mol Morphol* 2008; **16**: 239-45.

References

1. Ploeg M, Aben KKH, Kiemeneij LA. The present and future burden of urinary bladder cancer in the world. *World J Urol* 2009; **27**: 289-93.
2. Eble JN, Sauter G, Epstein J, Sesterhenn IA. *World Health Organization Classification of Tumours: Tumours of the Urinary System and Male Genital Organs*. Lyon: IARC Press; 2004.
3. Fležar MS. Urine and bladder washing cytology for detection of urothelial carcinoma: standard test with new possibilities. *Radiol Oncol* 2010; **44**: 207-14.
4. Shen Z, Shen T, Wientjes MG, O'Donnell MA, Au JL-S. Intravesical treatments of bladder cancer: Review. *Pharm Res* 2008; **25**: 1500-10.
5. Schenk-Braat EA, Bangma CH. Immunotherapy for superficial bladder cancer. *Cancer Immunol Immunother* 2005; **54**: 414-23.
6. Wu XR, Manabe M, Yu J, Sun TT. Large scale purification and immunolocalisation of bovine uroplakins I, II, and III. Molecular markers of urothelial differentiation. *J Biol Chem* 1990; **265**: 1775-84.
7. Wu XR, Lin JH, Walz T, Häner M, Yu J, Aebi U, et al. Mammalian uroplakins. A group of highly conserved urothelial differentiation-related membrane proteins. *J Biol Chem* 1994; **269**: 13716-24.
8. Sun TT, Liang FX, Wu XR. Uroplakins as markers of urothelial differentiation. *Adv Exp Med Biol* 1999; **462**: 7-18; discussion 103-14.
9. Romih R, Veranic P, Jezernik K. Appraisal of differentiation markers in urothelial cells. *Appl. Immunohistochem. Mol Morphol* 2002; **10**: 339-43.
10. Wu R-L, Osman I, Wu X-R, Lu M-L, Zhang Z-F, Liang F-X, et al. Uroplakin II Gene Is Expressed in Transitional Cell Carcinoma But Not in Bilharzial Bladder Squamous Cell Carcinoma: Alternative Pathways of Bladder Epithelial Differentiation and Tumor Formation. *Cancer Res* 1998; **58**: 1291-7.
11. Ogawa K, St John M, Luiza de Oliveira M, Arnold L, Shirai T, Sun TT, et al. Comparison of uroplakin expression during urothelial carcinogenesis induced by N-butyl-N-(4-hydroxybutyl)nitrosamine in rats and mice. *Toxicol Pathol* 1999; **27**: 645-51.
12. Romih R, Korošec P, Jezernik K, Sedmak B, Tršinar B, Deng F-M, et al. Inverse expression of uroplakins and inducible nitric oxide synthase in the urothelium of patients with bladder outlet obstruction. *BJU Int* 2003; **91**: 507-12.
13. Huang HY, Shariat SF, Sun TT, Lopor H, Shapiro E, Hsieh JT, et al. Persistent uroplakin expression in advanced urothelial carcinomas: implications in urothelial tumors progression and clinical outcome. *Hum Pathol* 2007; **38**: 1703-13.
14. Zupančič D, Ovčak Z, Vidmar G, Romih R. Altered expression of UPLa, UPLb, UPLII, and UPLIII during urothelial carcinogenesis induced by N-butyl-N-(4-hydroxybutyl)nitrosamine in rats. *Virchows Arch* 2011; **458**: 603-13.
15. Hicks RM, Ketterer B. Hexagonal lattice of subunits in the thick luminal membrane of the rat urinary bladder. *Nature* 1969; **224**: 1304-5.
16. Koss LG. The asymmetric unit membranes of the epithelium of the urinary bladder of the rat. An electron microscopic study of a mechanism of epithelial maturation and function. *Lab Invest* 1969; **21**: 154-68.
17. Hudoklin S, Jezernik K, Neumüller J, Pavelka M, Romih R. Urothelial plaque formation in post-Golgi compartments. *PLoS One* 2011; **6**(8): e23636.
18. Hudoklin S, Jezernik K, Neumüller J, Pavelka M, Romih R. Electron tomography of fusiform vesicles and their organization in urothelial cells. *PLoS One* 2012; **7**(3): e32935.
19. Zupančič D, Zakrajšek M, Zhou G, Romih R. Expression and localization of four uroplakins in urothelial preneoplastic lesions. *Histochem Cell Biol* 2011; **136**: 491-500.

Biological evaluation of trans-dichloridoplatinum(II) complexes with 3- and 4-acetylpyridine in comparison to cisplatin

Lana Filipovic¹, Sandra Arandelovic¹, Nevenka Gligorijevic¹, Ana Krivokuca¹, Radmila Jankovic¹, Tatjana Srdic-Rajic¹, Gordana Rakic², Zivoslav Tesic², Sinisa Radulovic¹

¹ Institute for Oncology and Radiology of Serbia, Belgrade, Serbia

² Faculty of Chemistry, University of Belgrade, Belgrade, Serbia

Radiol Oncol 2013; 47(4): 346-357.

Received 29 March 2013

Accepted 25 June 2013

Correspondence to: Siniša Radulović, M.D., Ph.D., Scientific Director, Department for Experimental Oncology, Institute for Oncology and Radiology of Serbia, Pasterova 14, Belgrade 11000, Serbia. Tel: +38111 2067 434; Fax: +381 11 2067 294; E-mail: sinisar@ncrc.ac.rs

Disclosure: No potential conflicts of interests were disclosed.

The paper was presented at the 7th Conference of Experimental and Translational Oncology, 20-24th April 2013, Portoroz, Slovenia (www.ceto.si) coorganised and supported by COST TD1104 Action (www.electroporation.net).

Background. In our previous study we reported the synthesis and cytotoxicity of two *trans*-platinum(II) complexes: *trans*-[PtCl₂(3-acetylpyridine)₂] (**1**) and *trans*-[PtCl₂(4-acetylpyridine)₂] (**2**), revealing significant cytotoxic potential of **2**. In order to evaluate the mechanism underlying biological activity of both *trans*-Pt(II) isomers, comparative studies versus cisplatin were performed in HeLa, MRC-5 and MS1 cells.

Materials and methods. The cytotoxic activity of the investigated complexes was determined using SRB assay. The collagenolytic activity was determined using gelatin zymography, while the effect of platinum complexes on matrix metalloproteinases 2 and 9 mRNA expression was evaluated by quantitative real-time PCR. Apoptotic potential and cell cycle alterations were determined by FACS analyses. Western blot analysis was used to evaluate the effect on expression of DNA-repair enzyme ERCC1, and quantitative real-time PCR was used for the ERCC1 mRNA expression analysis. *In vitro* antiangiogenic potential was determined by tube formation assay. Platinum content in intracellular DNA and proteins was determined by inductively coupled plasma-optical emission spectrometry.

Results. Compound **2** displayed an apparent cytoselective profile, and flow cytometry analysis in HeLa cells indicated that **2** exerted antiproliferative effect through apoptosis induction, while **1** induced both apoptosis and necrosis. Action of **1** and **2**, as analyzed by quantitative real-time PCR and Western blot, was associated with down-regulation of ERCC1. Both *trans*-complexes inhibited MMP-9 mRNA expression in HeLa, while **2** significantly abrogated *in vitro* tubulogenesis in MS1 cells.

Conclusions. The ability of **2** to induce multiple and selective *in vitro* cytotoxic effects encourages further investigations of *trans*-platinum(II) complexes with substituted pyridines.

Key words: angiogenesis; apoptosis; MMPs; MRC-5; *trans*-platinum(II)

Introduction

Cisplatin (CDDP) represents the basis of combination chemotherapy regimens in solid tumors, although main drawbacks to its successful application are development of resistance and toxic side effects.^{1,2} Search for CDDP analogues with improved pharmacological properties by manipu-

lation of the structure of ligands, has achieved a reduction in toxicity, but obtained limited success in broadening spectrum of activity.³⁻⁵ However, novel classes of platinum complexes including *trans*-Pt(II) compounds with planar amine ligands are able to exert cytotoxicity, equivalent or better to that of CDDP, and possess different mechanisms of antitumor action.⁶⁻¹⁰ Cytotoxicity data of 107

platinum compounds from the NCI human tumor panel recognized *trans*-platinum complexes, of structural formula $[\text{PtCl}_2(\text{L})(\text{L}')]]$ with planar amine ligands (L and L' may be the same or different), as unique group of *trans*-platinum drugs that had cytotoxicities similar to that of their *cis*-isomers and CDDP, and possessed a novel cytotoxicity profile.¹¹ Search for new platinum compounds with the complementary or wider range of activity than CDDP, whose actions would be more selective toward cancer comparing to normal cells, and which would possess different targets than the traditional CDDP, is always attractive topic.⁷ Formation and persistence of DNA-adducts are considered vital in platinum drug induced cytotoxicity, and type of DNA-damage is determined by the nature of platinum-coordinating ligands.^{4,12,13} However, cellular sensitivity to platinum complexes is multifactorial, with some of major mechanisms being the proficiency of the cellular mechanism for adducts recognition and repair, and the ability of cells to reduce intracellular platinum, due to deactivation by sulphur-containing biomolecules and/or drug efflux.¹⁴⁻¹⁶ Numerous studies imply the significance of copper transporters in regulating cellular pharmacology of CDDP by mediating its uptake and efflux in different cell lines.¹⁷

Structure-activity studies up to date demonstrated that bulky amine carrier ligands, such as pyridine, appear to sterically hinder approach of incoming nucleophiles to the axial positions of the platinum center, thus reducing deactivation of platinum by sulphur-containing biomolecules.¹⁸ *Trans*-orientation of planar pyridines seems to contribute to greater affinity of complexes for interstrand cross-link formation and DNA conformational distortion, comparing to *cis*-isomers, leading to activation of different DNA-repair mechanisms.¹⁹⁻²¹

Recent studies demonstrated that fine tuning of the biological activity of *trans*-platinum pyridines may be achieved by different positioning of the substituents such as: methyl-group and 3- or 4-hydroxymethyl-group, on the pyridine ring.^{19,20,22}

In our previous investigations, we have synthesized and characterized two *trans*-platinum(II) complexes, of structural formula $trans\text{-}[\text{PtCl}_2(\text{L})_2]$ with substituted pyridine ligands, L=n-acetylpyridine, (n = 3 or 4) (Figure 1). Cytotoxicity evaluation on the panel of tumor cell lines revealed potential of $trans\text{-}[\text{PtCl}_2(4\text{-acetylpyridine})_2]$ to exert activity in low micromolar range, with the highest cytotoxicity in HeLa cells, comparable to that of CDDP.²³ Aim of this study was to investigate the molecular mechanisms underlying the *in vitro* biological activity of

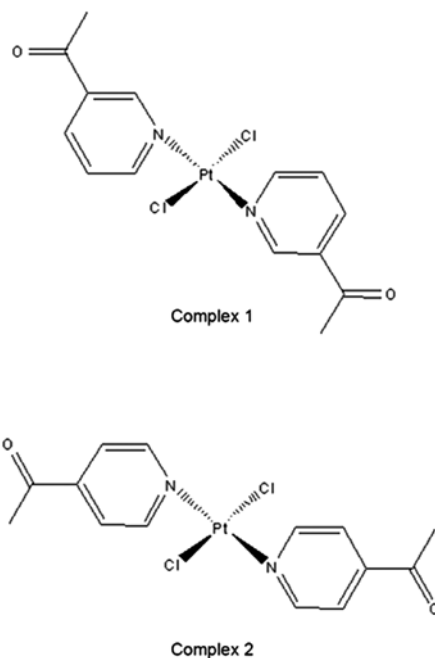


FIGURE 1. Structures of the investigated *trans*-platinum(II) complexes: $trans\text{-}[\text{PtCl}_2(3\text{-acetylpyridine})_2]$ **1**; $trans\text{-}[\text{PtCl}_2(4\text{-acetylpyridine})_2]$ **2**.

$trans\text{-}[\text{PtCl}_2(4\text{-acetylpyridine})_2]$ (complex **2**) and its less cytotoxic structural isomer $trans\text{-}[\text{PtCl}_2(3\text{-acetylpyridine})_2]$ (complex **1**), and to understand possible relations to their structural characteristics, such as the position of the acetyl substituent on the pyridine ring. Mechanistic studies were performed in comparison to CDDP in human cervix carcinoma cell line (HeLa), and two other cell lines: human normal lung fibroblast (MRC-5) cell line, which was used as a non-cancerous model system for *in vitro* toxicity evaluation, and murine endothelial cells immortalized by infection with a retrovirus encoding SV40 large T antigen (MS1), as a model system for *in vitro* testing of antiangiogenic effect.²⁴ In order to test if the cytotoxic responses produced by compounds **1** and **2** in HeLa cells correlated with the platinum content in cellular DNA and to evaluate the mechanism of cytotoxic action, we studied the ability of complexes to bind intracellular DNA and proteins, and to induce DNA-damage related response, cell cycle alterations and apoptosis.

Based on the literature data reporting inhibitory effect of some platinum(II) compounds on matrix metalloproteinases (MMP) activity, we assumed that $trans\text{-}[\text{PtCl}_2(n\text{-acetylpyridine})_2]$ (n = 3 or 4), may possess ability to modulate diverse cellular processes, including those related to the cancer cell angiogenic and metastatic behaviour.²⁵⁻²⁷ Thus, in the final part of our study, we analyzed if the tested

complexes affected gelatinolytic activity and mRNA expression of secreted forms of MMP-2 and MMP-9, or abrogated process of angiogenesis *in vitro*.

Materials and methods

Synthesis

Platinum complexes *trans*-[PtCl₂(3-acetylpyridine)₂] (complex 1) and *trans*-[PtCl₂(4-acetylpyridine)₂] (complex 2) (Figure 1) were synthesized and characterized by IR and NMR, as previously described.²³

Cytotoxic activity

Cell culture

HeLa and MRC-5 cells were maintained as monolayer culture in nutrient medium, Roswell Park Memorial Institute 1640 medium (RPMI1640), (Sigma-Aldrich Co).²⁸ MS1 cells were maintained as monolayer culture in nutrient medium, Dulbecco's Modified Eagle Medium (DMEM), (Sigma-Aldrich Co). Nutrient medium conditions and cell maintenance procedures were explained previously.²⁹

In vitro cytotoxicity assay (SRB)

Cells were seeded into 96-well plates (Thermo Scientific Nunc™), in number of 7000 cells per well (c/w) for MS1 and 5000 cells per well for MRC-5, and left for 24 h before complexes 1, 2 and CDDP were added. Preparation of test solutions was performed immediately before experiments by dissolving in DMSO. The cells were treated with serial dilutions of the studied compounds for 48 h. Final concentrations achieved per wells were 1 μM, 3 μM, 10 μM, 30 μM and 100 μM. Each concentration was tested in triplicates, and the final concentration of DMSO solvent never exceeded 0.33%. Cytotoxicity of the investigated platinum complexes, and CDDP as a referent compound, was evaluated after 48 h of continuous action, using sulforhodamine B (Sigma-Aldrich Co.) colorimetric assay.³⁰ The percentages of surviving cells relative to untreated controls were determined. The IC₅₀ value, defined as the concentrations of the compound causing 50% cell growth inhibition, was estimated from the dose-response curves.

Flow cytometric analysis of cell cycle phase distribution

Quantitative analysis of cell cycle phase distribution was performed by flow-cytometric analysis of the DNA content in fixed HeLa cells, after stain-

ing with propidium iodide (PI).³¹ Cells were seeded at density of 2×10⁵ into 6-well plates (Thermo Scientific Nunc™), and grown in nutrient medium. After 24 h cells were exposed to the investigated compounds 1, 2 and CDDP for 24 h, at concentrations corresponding to IC₅₀ or 1.5×IC₅₀. The detailed procedure was previously described.²⁹ Cell cycle phase distribution was analyzed using a fluorescence activated cell sorting (FACS) Calibur Becton Dickinson flow cytometer and Cell Quest computer software.

Statistical analysis

Calculations of mean, SD, and p values were performed on triplicate experiments. The Student t-test was used to calculate p-values for comparison. The significant statistics was set at a p-value <0.05 (Stata Software).

Annexin V-FITC apoptotic assay

Quantitative analysis of apoptotic and necrotic cell death induced by the investigated platinum complexes and CDDP, as a referent compound, was performed by Annexin V-FITC apoptosis detection kit, according to the manufacturer's instructions (BD Biosciences). Precisely, 2×10⁵ HeLa cells treated with 1×IC₅₀ of the tested compounds and CDDP for 4 and 24 h and the analysis was performed as previously reported.²⁹

Measurement of platinum binding to intracellular DNA or proteins using ICP-OES

Binding of platinum(II) to cellular DNA and proteins was analyzed in HeLa cells, using inductively coupled plasma optical emission spectrometry (ICP-OES). 6×10⁶ cells were seeded into 75 cm² dish (Thermo Scientific Nunc™) and treated with the investigated complexes in concentrations corresponding to 0.5×IC₅₀. Following 6 or 24 h, cells were harvested by scraping, washed by ice cold PBS and cell pellet was collected by centrifugation at 2000 rpm, 10 min. DNA and proteins were isolated using TRI Reagent® (Sigma-Aldrich Co.) according to the manufacturer's procedure and concentrations were determined spectrophotometrically by measuring absorbance at A260 and A280 nm respectively (Eppendorf BioPhotometer 6131). Platinum(II) levels were determined in isolated DNA and protein fractions according to the standard procedure, using Thermo Scientific iCAP 6500 Duo ICP (Thermo Fisher Scientific).

Quantitative real-time PCR (qRT-PCR)

Sample preparation for qRT-PCR; RNA extraction and cDNA synthesis

6x10⁶ HeLa cells were seeded in nutrient medium and after 24 h treated with the investigated complexes 1, 2 or CDDP at concentrations corresponding to 0.5xIC₅₀ for 6 and 24 hours. After treatment, cells were washed with ice cold PBS and harvested by scraping, while cell pellet was collected by centrifugation. Total RNA was isolated using TRI Reagent® (Sigma-Aldrich Co.) according to manufacturer's recommendations. RNA extraction in details and cDNA synthesis were described earlier.²⁹

Quantitative real-time PCR

The analysis of gene expression level of several genes and GAPDH (endogenous control) was done by using TaqMan® Gene Expression Assays for human genes (assay ID Applied Biosystem, listed as following: Hs_01012155_g1 (ERCC1); Hs_01548727_m1 (MMP-2); Hs_00234579_m (MMP-9); Hs_00355782_m1 (GAPDH)) on ABI PRISM® 7500 PCR instrument (Applied Biosystems). PCR was performed as previously reported.²⁹

Western blot

HeLa cells were treated with the investigated platinum complexes 1 and 2 or CDDP for 6 h, at concentrations corresponding to the 0.5xIC₅₀ values obtained for 48 h of continuous treatment. Cells maintained in nutrient medium were used as the untreated control. Sample preparation and the analysis were performed as described in the previous study.^{29,32} Purified mouse anti-human ERCC1 monoclonal antibody (1:500 dilution) (BD Biosciences Pharmingen) was used, as well as the secondary anti-mouse IgG-peroxidase conjugated antibody (1:2000 dilution) (Sigma-Aldrich Co.).

Gelatin zymography

Effect of the investigated *trans*-Pt(II) complexes and CDDP on gelatinolytic activity of secreted matrix metalloproteinases MMP-2 and MMP-9 in HeLa was analyzed by zymography in 10% SDS-polyacrylamide gels impregnated with 0.1% gelatin.³³ HeLa cells were treated with the complexes (0.5xIC₅₀) for 6 h in serum-free medium and the precise conditions, as well as the procedure have been given previously.²⁹ The gelatinolytic activities were visualized as clear transparent bands against

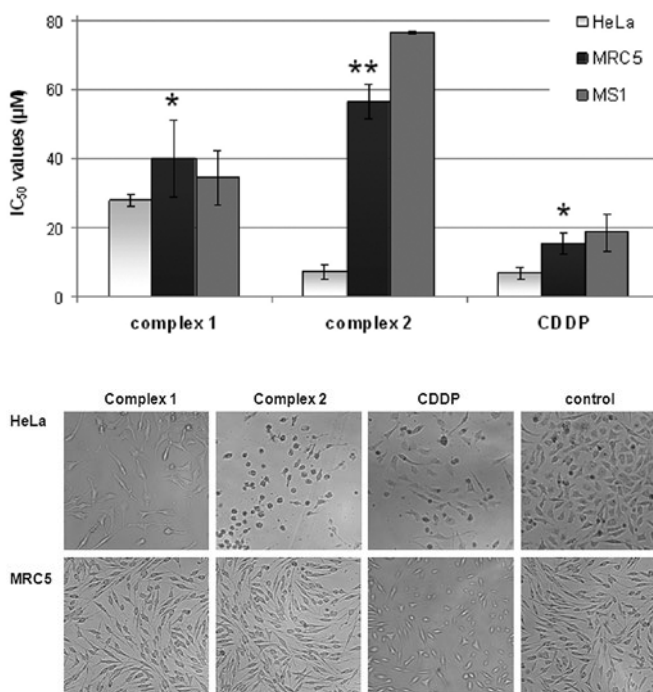


FIGURE 2. A Diagram presenting cytotoxicity of the tested agents and cisplatin in terms of IC₅₀ values, obtained for 48 h of drug action, by SRB assay. IC₅₀ values present average (±SD) obtained from three or more independent experiments. Asterisks denotes p values, when comparing MRC-5 cells to HeLa cells, by ANOVA test: **1** (*) p > 0.05; **2** (**) p < 0.001; CDDP (*) p > 0.05; **B** Micrographs of HeLa cells or MRC-5 cells exposed to equimolar (5 mM) concentration of tested platinum complexes 1, 2 or CDDP, following 24 h treatment, versus control (non treated cells). Micrographs are one representative experiment selected of three and were obtained with Olympus digital camera connected to the inverted microscope (Carl Zeiss, Jena, Germany, objective 6.3/0.20).

the blue background of Coomassie brilliant blue-stained gelatin.

Tube formation assay (in vitro angiogenesis assay)

Potential of *trans*-platinum(II) complexes and CDDP to inhibit angiogenesis *in vitro* was analyzed by tube formation assay in MS1 cells. MS1 cells, when plated into gel of basement membrane proteins, rapidly organize into multicellular tube-like structures, while antiangiogenic effect of the tested compounds is observed as the reduction of tube formation.²⁴ Briefly, 24-well plates were coated with collagen and allowed to solidify at 37°C 1 h. MS1 cells were seeded into wells (1x10⁵ c/w) in nutrient medium. Complexes 1 and 2 were added 2 h after cells settled, at concentrations corresponding to 0.03xIC₅₀, which was non-toxic to the cells. Tube formation was observed periodically over time under microscope and representative pictures were

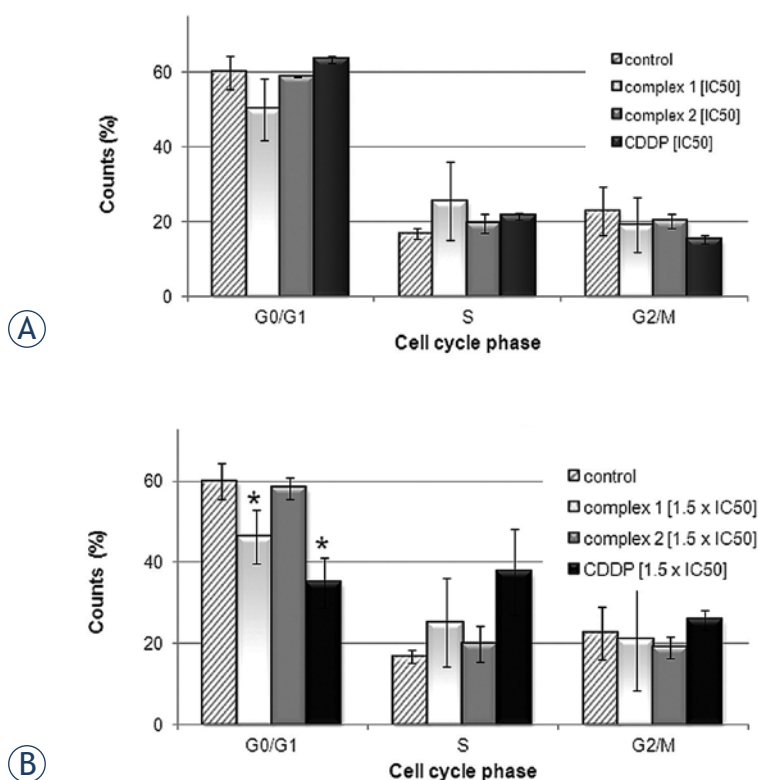


FIGURE 3. Diagrams presenting cell cycle phase distribution of treated HeLa cells, obtained by flow-cytometric analysis of the DNA content in fixed cells, after staining with PI. HeLa cells were collected following 24 h treatment with tested complexes or cisplatin at concentration corresponding to **A** IC₅₀ and **B** 1.5xIC₅₀. Bar graphs represent mean ± SD in at least three independent experiments. Asterisks (*) denotes p values < 0.05, calculated by Student t-test, indicating statistically significant differences (Stata Software).

taken after 24 h incubation with Olympus digital camera connected to the inverted microscope (Carl Zeiss, Jena, Germany, objective 6.3/0.20).

Morphological examination by light microscopy

HeLa cells (50000 c/w) and MRC-5 cells (125000 c/w), were seeded into 6-well plates (Thermo Scientific Nunc™), in the corresponding nutrient medium, and after 24 h of growth cells were exposed to complexes **1**, **2** or CDDP, at equimolar concentrations of 5 mM. Following 24 h of treatment, cells were observed under the light microscope and photographs were taken with Olympus digital camera connected to the inverted microscope (Carl Zeiss, Jena, Germany, objective 6.3/0.20)..

Statistical analysis

Statistical comparison of IC₅₀ values in MRC-5 cell line versus HeLa and MS1 cell line, was performed

using one way statistical analysis of variance (one-way ANOVA - GraphPad Software). IC₅₀ values were determined as mean ± SD (standard deviation) of three or more independent experiments.

Results

In vitro cytotoxicity assay (SRB)

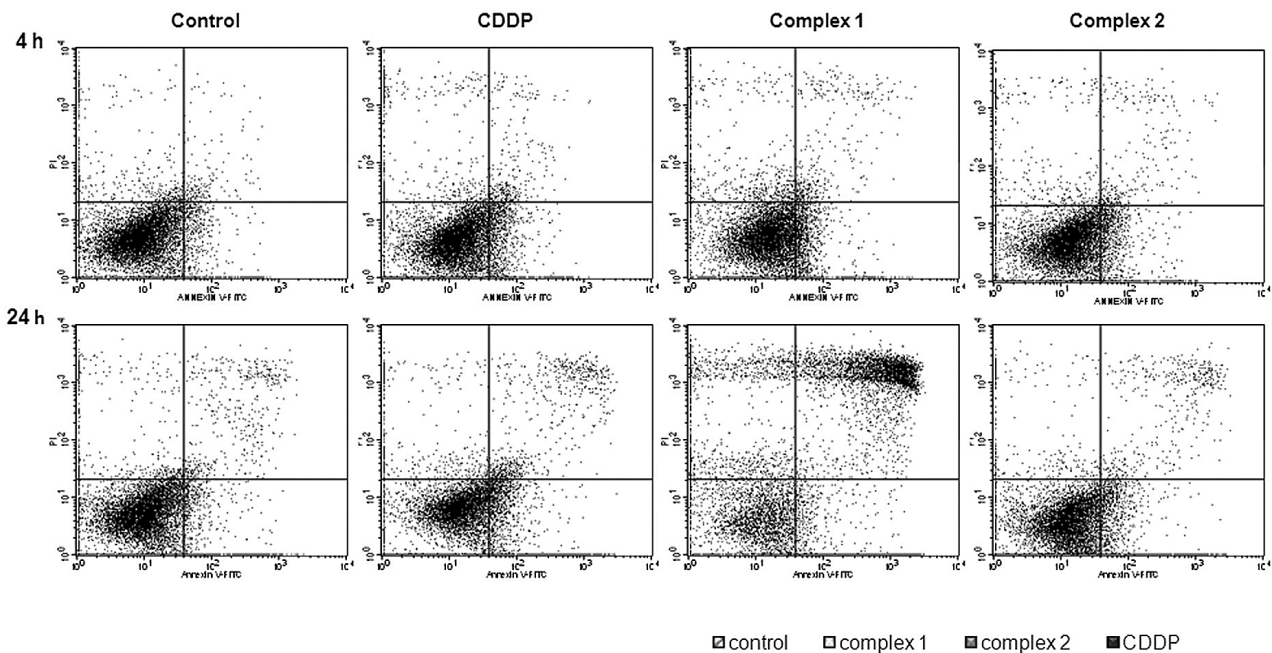
In order to further investigate cytotoxic and cytototoxic potential of the two *trans*-platinum isomers, in comparison to CDDP, growth inhibitory study was performed in MRC-5 cells, which were used as non-cancerous model for *in vitro* toxicity evaluation; and MS1 cells as *in vitro* model for testing of antiangiogenic effect. Cytotoxicity of the complexes summarized in terms of IC₅₀ values, is presented in Figure 2A. IC₅₀ values (mM) obtained for 48 h of continuous drug action in MRC-5 cells, may be arranged in increasing order as following: 15.4 ± 3.1 mM, for CDDP; 40.0 ± 11.1 mM for complex **1**; and 56.4 ± 5.0 mM for **2**, indicating lower toxicity of *trans*-complexes in non-cancerous cell model comparing to CDDP. Particularly, complex **2** exerted less cytotoxicity in MRC-5 cells than in HeLa, by a factor of approximately four-fold, indicating significant cytototoxic potential toward neoplastic cells (p < 0.001). Both *trans*-complexes exhibited poor activity, in MS1 cells with IC₅₀ values being: 76.3 ± 0.5 mM for complex **2**; 34.5 ± 7.8 mM for complex **1**; comparing to CDDP (IC₅₀ 18.6 ± 5.4 mM).

Morphological examination

The results of the morphological analysis of HeLa and MRC-5 cells are presented in Figure 2B, as micrographs obtained following 24 h agents action. Results indicated that in the presence of 5 mM of complex **2**, concentration which corresponded to IC₅₀ value in HeLa cells, viability of MRC-5 cells was not significantly altered, suggesting cytototoxic potential toward neoplastic HeLa cells. Oppositely, complex **1** haven't exerted cytototoxic potential, as observed in Figure 2B. Morphological changes of MRC-5 cells, such as: cell shrinkage and detachment, following equimolar treatment with CDDP, were indicative for apoptosis.

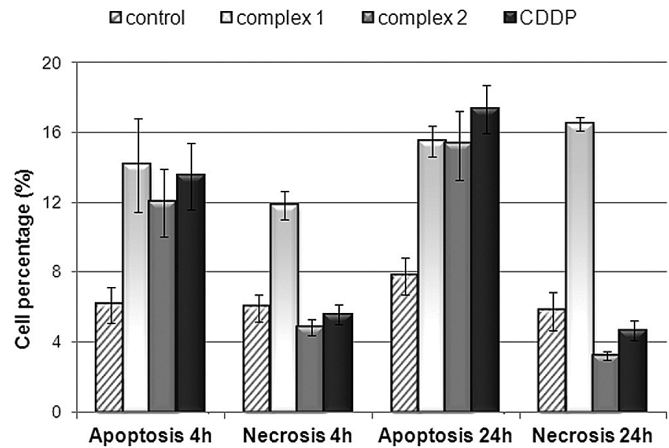
Determination of cell cycle perturbation by flow cytometry

The potential of the tested complexes to induce cell cycle alterations in comparison to CDDP in HeLa cells, was examined by flow cytometry using staining with PI. Results are presented as diagrams of



(A)

FIGURE 4. A Dot plot diagrams obtained by flow-cytometric analysis of treated HeLa cells after dual staining with Annexin V-FITC and PI. Annexin V-FITC/PI staining was monitored overtime, following 4 and 24 hours in HeLa cells exposed to complex 1, 2 or CDDP at concentrations corresponding to IC_{50} . Representative dot plots of three independent experiments are given, presenting intact cells at lower-left quadrant, FITC(-)/PI(-); early apoptotic cells at lower-right quadrant, FITC(+)/PI(-); late apoptotic or necrotic cells at upper-right quadrant, FITC(+)/PI(+); and necrotic cells at upper-left quadrant, FITC(-)/PI(+). **B** Apoptosis and necrosis were quantified by FACS after Annexin V-FITC and PI labeling; bar graphs represent mean \pm SD in at least three independent experiments.



(B)

cell distribution over the cell cycle phases after 24 h of agent action, where Figure 3A shows effects of the complexes at concentration corresponding to IC_{50} , and Figure 3B shows effects of the complexes at concentration corresponding to $1.5 \times IC_{50}$. Complex 1, induced arrest in the S phase of cell cycle at concentrations corresponding to $1.5 \times IC_{50}$, but less than CDDP (Figure 3B). Complex 1 induced decrease of cell percentage in the G0/G1 phase in concentration dependent manner, comparing to the non-treated control. CDDP induced dose-dependent arrest in the S phase of cell cycle, and decrease of cell progression through G2/M phase (Figures 3A and 3B).

The Student t-test showed that the difference is considered to be statistically significant only for G0/G1 cells when two groups of cell cycle results were compared (control cells compared to cells treated

with $1.5 \times IC_{50}$ complex 1, and control cells compared to cells treated with $1.5 \times IC_{50}$ CDDP ($p < 0.05$, Stata Software)).

Quantification of apoptosis by annexin V-FITC binding

Potential of the investigated complex to induce apoptosis in HeLa cells was assessed by flow cytometry using Annexin V-FITC and PI dual staining. Dot plots are presented in Figure 4A, while Figure 4B reports the results of a representative experiment as percentages of apoptotic cells (Annexin V-FITC positive and PI negative) and necrotic cells (Annexin V-FITC negative and PI positive) measured periodically at 4 and 24 h. Data obtained indicated that complex 2 caused 15.5% of apoptosis in HeLa cells following 24 h of action, while the per-

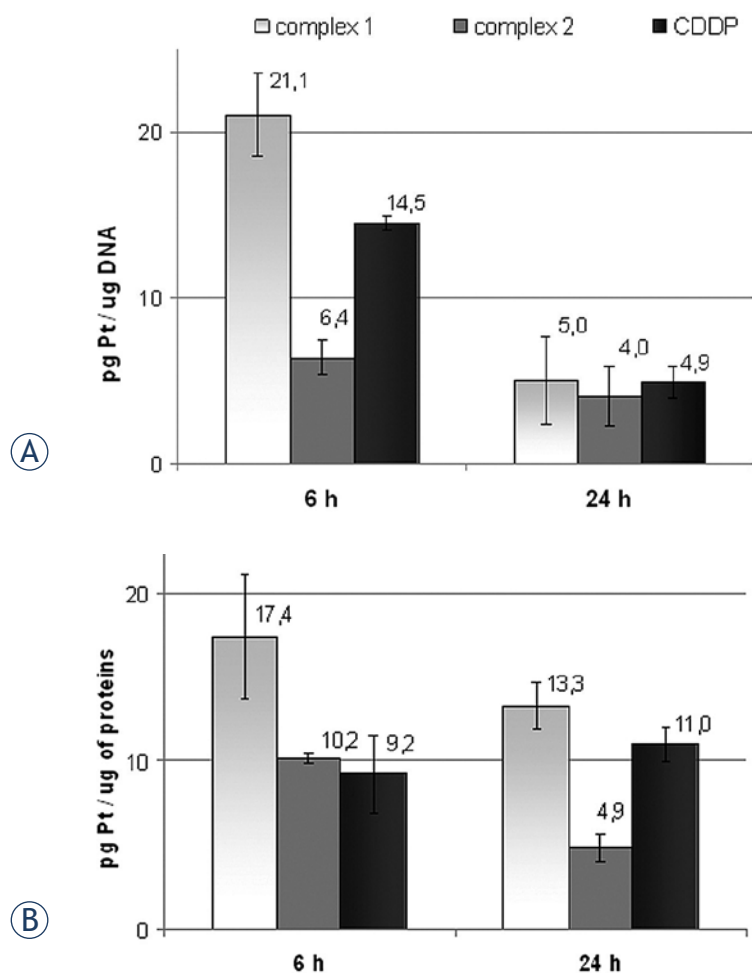


FIGURE 5. Diagrams presenting quantitative determination of platinum(II) content in DNA and proteins in HeLa cells, obtained by ICP-OES analysis, following 6 h and 24 h of action of **1**, **2** or CDDP; **A** Platinum content in cellular DNA; **B** Platinum content in cellular protein fraction (pg Pt/mg proteins). Bar graph represent mean \pm SD of three independent experiments.

centage of necrotic cells was negligible. Kinetics, as well as the degree of apoptosis induction, was comparable to CDDP. Complex **1** at concentration of IC_{50} initiated early apoptotic cell death after 4 and 24 h action, where apoptotic cell population represented 14.2% and 15.5% of total cells, respectively. Though, after 24 h of action more than 50% of total cell population underwent cell death in either apoptotic or necrotic manner.

Determination of the platinum(II) binding to intracellular DNA and proteins

Intracellular platinum(II) distribution among DNA and protein fractions in HeLa cells treated with equitoxic concentrations of investigated complexes for 6 and 24 h, was analyzed using ICP-OES analy-

sis, and results are presented in Figure 5. Levels of platinum(II)-DNA binding (Figure 5A), varied between the investigated complexes, especially following short-term (6 h) treatment, when platinum content (pg Pt/mg DNA) decreased in order: 21 ± 2.5 (complex **1**); 14.5 ± 0.4 (CDDP) and 6.4 ± 1.1 (complex **2**). Both CDDP and **1** seemed to be more efficient in promoting cellular DNA binding comparing to complex **2**, though differences in double-stranded DNA platination affinity between complex **2** and CDDP were in accordance to the recent study.³⁴ Platinum(II)-DNA content, decreased in time-dependent manner, and reached comparable levels following 24 h of action. Results of the ICP-OES analysis of platinum(II) content in the protein fraction (Figure 5B), indicated that **1** exhibited the highest affinity for protein binding following both 6 h and 24 h treatment, while **2** exhibited the lowest binding affinity. Time dependent decrease of protein binding, indicated reversible nature of interactions of **1** and **2**, oppositely to CDDP.

Protein and mRNA expression of ERCC1

DNA excision repair protein ERCC1 is an important component of NER (Nucleotide Excision Repair) which is primarily induced in the repair of bulky platinum-DNA adducts.³⁵ In order to evaluate whether investigated complexes induce ERCC1-dependent cell response as the result of cytotoxic DNA lesions, we investigated mRNA and protein expression level of ERCC1. Data obtained on HeLa cells after 6 h of continuous treatment with equitoxic concentrations of tested *trans*-platinum complexes or CDDP indicated negative modulation of ERCC1 expression on both mRNA and protein levels (results presented in Figure 6). Complexes **1**, **2** and CDDP decreased ERCC1 mRNA level for 45%, 40% and 36%, respectively, comparing to the non treated control (Figure 6A). Western blot analysis (Figure 6B) showed reduction of ERCC1 protein levels, following both *trans*-complexes **1** and **2** action, while there were no obvious changes associated with CDDP treatment.

Tube formation assay (*in vitro* angiogenesis assay)

In order to determine the potency of the investigated complexes to restrict the angiogenesis of cancer cells, we performed an *in vitro* tube formation assay in mouse endothelial cells MS1. In our experiment, MS1 endothelial cells were treated with sub-toxic concentrations of the investigated complexes in or-

der to distinguish among growth inhibitory effect and their potential to inhibit the formation of tube-like structures. Antiangiogenic effect was observed for both tested *trans*-platinum complexes, and results are presented in Figure 7A. *Trans*-complexes, particularly complex 2, showed inhibitory effect on the formation of cell-cell contact and tube-like structures, at very low sub-toxic concentration corresponding to $0.03 \times IC_{50}$ while CDDP did not exhibit any significant effect in this assay.

Gelatin zymography and determination of MMP-9 and MMP-2 expression on mRNA level

We investigated whether tested complexes were able to modulate mRNA expression of MMP-2 and MMP-9 or affect their gelatinolytic activity *in vitro*. The effect of 1 and 2 on the activity of the secreted forms of MMP-2 and MMP-9 in HeLa cells, was examined following 6 h action, by gelatin zymography and the results are presented in Figure 7B. Quantitative analysis of the gelatin zymography was performed by Image J software, and is presented in Figure 7B. Results obtained indicated that complex 1 induced moderate decrease of gelatinolytic activity of MMP-2 and MMP-9 in comparison to the control (non treated cells), when applied at concentration of $0.5 \times IC_{50}$ (Figure 7C). CDDP failed to show effect in this assay, while complex 2 induced minor enhancement of metalloproteinases activity. Results obtained by qRT-PCR indicated that *trans*-complexes reduced level of MMP-9 mRNA, comparing to the control, following 6 h treatment (Figure 7D). Complex 2 and CDDP, when applied at equitoxic concentrations corresponding to $0.5 \times IC_{50}$ upregulated MMP-2 mRNA, while complex 1 did not induce obvious alteration of MMP-2 mRNA expression.

Discussion

In our previous study we have reported synthesis, structural characterization and cytotoxic potential of two *trans*-platinum complexes of structural formula *trans*-[PtCl₂(*n*-acetylpyridine)₂] (*n* = 3 or 4, complex 1 or 2, respectively), revealing significant cytotoxic potential of complex 2 on several tumor cell lines, with the highest potential in HeLa cells.²³ In the current study we investigated the mechanism underlying *in vitro* antitumor activity of both isomers, in order to understand possible relations to their structural differences, such as position of

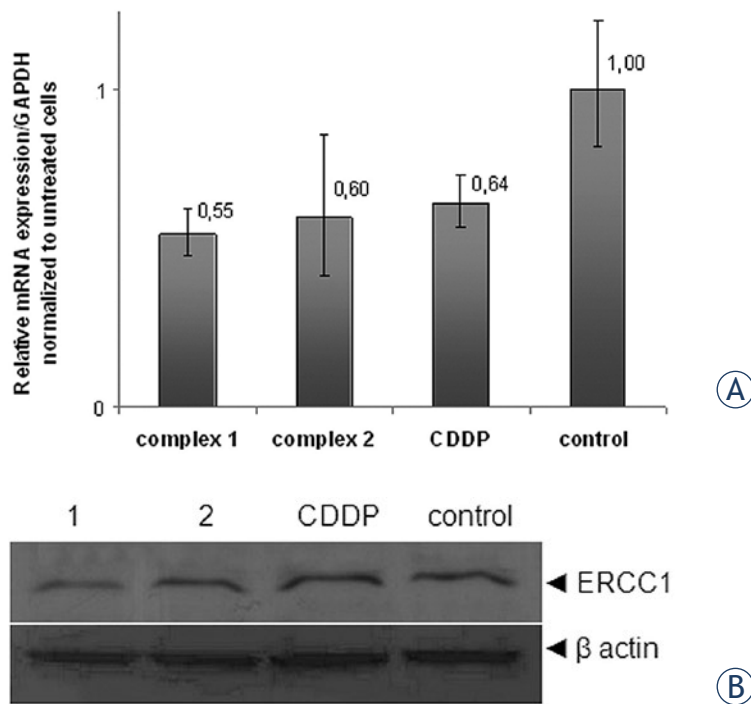


FIGURE 6. A Results of the qRT-PCR analysis of ERCC1 mRNA presented as diagrams showing relative expression level of ERCC1 mRNA, normalized with the GAPDH; Bar graph represent mean \pm SD of three independent experiments; **B** Protein expression levels of ERCC1 determined by Western blot, and normalized with b-actin. Tested agents 1, 2 and CDDP were applied at concentration of $0.5 \times IC_{50}$. Western blot results show one representative experiment selected of three.

the acetyl substituent on pyridine ligand. Study was performed in comparison to CDDP as referent compound.

Cytotoxicity evaluation in MRC-5 cells, which were used as *in vitro* non-cancerous cell model, showed feature of the tested *trans*-platinum isomers to exert less toxicity in MRC-5, than in HeLa. Particularly complex 2 with 4-acetylpyridine, exhibited significant cytoselective potential toward neoplastic cells (HeLa) relative to normal cells (MRC-5), cells ($p < 0.001$), comparing to CDDP ($p > 0.05$).

According to the results of flow cytometry, anti-proliferative action of complex 1, was associated to minor cell cycle arrest in the G0/G1 and S phase, and consequent initiation of cell death. When tested at equitoxic concentrations (IC_{50}), complex 1 induced significant percentage of necrotic cells, comparing to complex 2 and CDDP, observed already after 4 h of action. Complex 2 exhibited the rate and kinetics of apoptosis induction similar to that of CDDP.

Mechanism of anticancer activity of platinum drugs is believed to be associated with their binding with cellular DNA. The level of DNA-binding

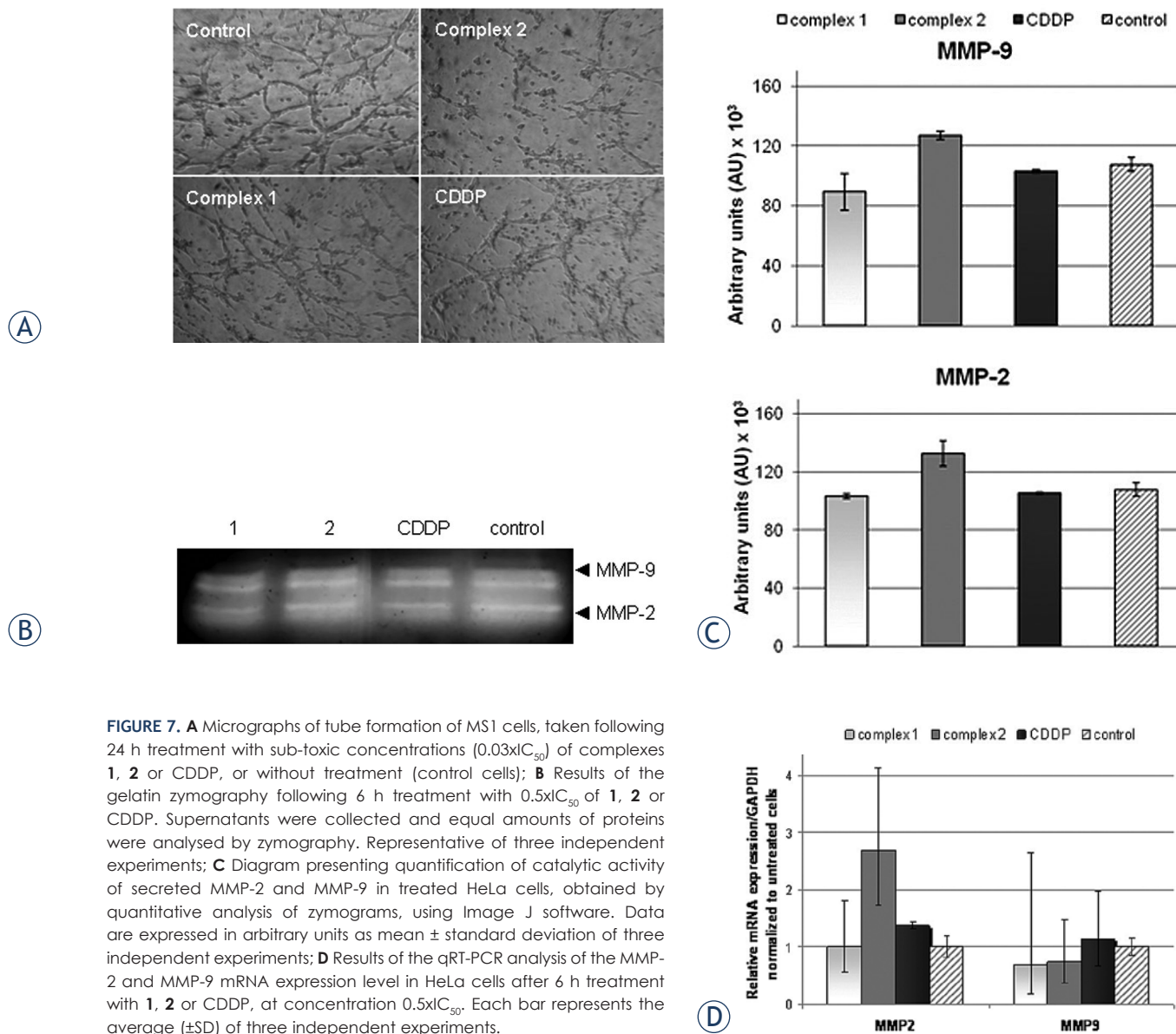


FIGURE 7. A Micrographs of tube formation of MS1 cells, taken following 24 h treatment with sub-toxic concentrations ($0.03 \times IC_{50}$) of complexes **1**, **2** or CDDP, or without treatment (control cells); **B** Results of the gelatin zymography following 6 h treatment with $0.5 \times IC_{50}$ of **1**, **2** or CDDP. Supernatants were collected and equal amounts of proteins were analysed by zymography. Representative of three independent experiments; **C** Diagram presenting quantification of catalytic activity of secreted MMP-2 and MMP-9 in treated HeLa cells, obtained by quantitative analysis of zymograms, using Image J software. Data are expressed in arbitrary units as mean \pm standard deviation of three independent experiments; **D** Results of the qRT-PCR analysis of the MMP-2 and MMP-9 mRNA expression level in HeLa cells after 6 h treatment with **1**, **2** or CDDP, at concentration $0.5 \times IC_{50}$. Each bar represents the average (\pm SD) of three independent experiments.

is considered to provide more meaningful information (related to activity) than total cellular uptake especially as platinum drugs may undergo complexation with cellular platinumophiles, so that only a very small fraction of the drugs actually binds with DNA.³⁶

The results of the present work, demonstrating nuclear DNA binding affinity of compounds **1** and **2**, are consistent with the hypothesis that the minor structural modifications of carrier ligands in *trans*-mononuclear platinum complexes could modulate the DNA binding affinity, resulting in the altered biological (pharmacological) activity of these new platinum complexes in tumor cells, relative to CDDP.³⁷ Results of the analysis of the

actual platination of DNA, presented in terms of pg Pt/mg DNA, showed that **2** exhibited the lowest DNA binding following 6 h treatment, with platinum content being less by a factor of approximately threefold comparing to **1**, though reaching similar level of DNA binding as **1** and CDDP following 24 h treatment. Structure-activity correlation suggests that the acetyl-group in the para-position on the planar pyridine rings (4-acetylpyridine) in complex **2**, may additionally hamper positioning of the non-leaving moieties in the adducts of this analogue, that would be entirely favorable for its interaction with the double helix.³⁷ It should be noted that complex **2** platinum-DNA level just slightly decreased during 24 h treatment comparing to complex **1** and

CDDP, suggesting on the other side sustainable nature of platinum-DNA lesion. Different studies support the assumption that long-lived DNA-adducts, formed by mononuclear *trans*-platinum(II) complexes containing planar ligands such as quinoline or pyridine constitute potential cytotoxic lesions.³⁸ The higher cytotoxicity of **2** comparing to **1**, may be attributed to its ability to form different DNA conformational distortions and lesions which are differentially processed by DNA damage recognition/repair proteins, and to the ability of compound to induce different cellular response.²¹ Lower level of unfavorable interactions with proteins may be additional determinant of enhanced cytotoxicity of complex **2** in comparison to **1**.

On the other side, meta-position of the acetyl substituent on the pyridine ring (3-acetylpyridine) in complex **1**, allowed reactivity with intracellular DNA and proteins, though in reversible manner.

Complex **1** platinum levels in cellular DNA decreased from 6 h to 24 h time points, indicating that **1** treated cells partially recovered from the initial cytotoxic stress, which may be due to an early DNA damage response and removal of the platinum-DNA lesions.¹³

In order to evaluate role of DNA-damage repair in mediating differences in cytotoxicity of the tested complexes, we further evaluated expression of ERCC1 on mRNA and protein level. Nucleotide excision repair is one of the DNA-repair mechanisms primarily activated in response to cisplatin induced genotoxic stress.³⁹⁻⁴² In the case of CDDP, cycle cycle arrest in the phase G0/G1 (also caused by investigated complex **1**) and G2/M arrest, may be indicative for activation of NER repair proteins.²⁰ Nevertheless, western blot and gene expression analysis in the current study, revealed reduction of ERCC1 mRNA and protein levels, following short-term treatment with **1** and **2**, while there was discordance in mRNA and protein levels following CDDP treatment. It is likely that ERCC1 might not play fundamental role in mediating sensitivity to *trans*-platinum complexes, as well as to the investigated complexes in the current settings, but additional studies need to be directed toward understanding of the molecular mechanism underlying expression status of ERCC1 (mRNA and protein), and its correlation to *trans*-platinum-based drug sensitivity.^{15,43}

In the separate part of our study we investigated the potential of tested complexes to modulate processes related to angiogenic and metastatic potential of tumor cells *in vitro*. Pathological angiogenesis is a hallmark of cancer and represents

an important step in the development of metastasis.⁴⁴⁻⁴⁶ Significant efforts in the area of anticancer drug research are focused on the development of a drug, which would be able to limitate angiogenesis of cancer cells. Study in MS1 cells revealed potential of **2** to inhibit formation of tube-like structures and tumor cell-cell contacts, at very low subtoxic concentration (0.03 IC₅₀), while CDDP failed to show effect in this assay. Our results indicated potential of complex **2** to act on multiple processes in cancer cells, and that exposure to DNA-damaging agents at subtoxic concentrations may alter tumor cell behavior. More direct experiments would be required to confirm the observed antiangiogenic potential of **2** *in vitro*.

Matrix metalloproteinases 2 and 9, which are frequently over expressed in tumor cells, play a critical role in modulation of extra cellular matrix, and its role in tumor cell migration, formation of tumor cell contacts and angiogenesis transition is extensively investigated. Thus, MMPs represent a promising target for antitumor drug design.^{25,45} Our investigations of the effect of tested complexes on gelatinolytic activity of secreted matrix metalloproteinases MMP-2 and MMP-9 and their mRNA expression levels, showed that both **1** and **2** caused decrease of MMP-9 mRNA, for 6 h action, though for the time point observed (6 h), inhibitory effect on the enzyme activity level was minor.⁴⁴ Only complex **1** showed moderate inhibitory effect on MMP-2 and MMP-9 activity. Reduction of functional levels of MMP-9 by **1** and **2** was in correlation to the reduction of the enzyme mRNA-level, which might represent the indirect effect of genotoxic stress.

Although two investigated complexes of structural formula *trans*-[PtCl₂(n-acetylpyridine)₂] (n = 3 or 4) represent close structural isomers, their interactions with cellular targets and consequently induced cellular responses are different. Results obtained suggest that structural settings play a fundamental role, since they are responsible for the interaction between *trans*-Pt drug and cellular DNA and proteins and the consequent biological effects. Higher cytotoxicity of **2** compared to the **1** analogue, may be attributed to its ability to form different DNA-lesions, produce different cellular effects related to damage-processing and signal activation pathways, and induce multiple cellular responses. Our study demonstrated that complex **2** is particularly interesting since it exhibited cytotoxic and apoptotic potential in HeLa cells comparable to that of CDDP, though showing differences in terms of reactivity to DNA and proteins, cytoselectivity.

tivity toward tumor cells and potential for *in vitro* angiogenesis inhibition. Further explorations are needed to determine a possible differential mechanism of action and elucidate antitumor potential of complex *in vivo*.

Altogether, properties of complexes of structural formula *trans*-[PtCl₂(*n*-acetylpyridine)₂] (*n* = 3 or 4), encourage further investigation of substituted *trans*-platinum pyridines in search for compound with different modalities of action toward cancer cells in comparison to CDDP.

Acknowledgements

This work was supported by the Ministry of Science, Republic of Serbia, Grant, No.III 41026 and Grant, No 172017 (URL address: <http://www.mpn.gov.rs/sajt/>).

References

- O'Dwyer PJ, Stevenson JP, Johnson SW. Clinical status of cisplatin, carboplatin and other platinum-based antitumor drugs. In: Lippert B, editor. *Cisplatin: chemistry and biochemistry of the leading anticancer drug*. Weinheim, Germany: Wiley-VCH; 1999. p. 30-70.
- Kelland L. The resurgence of platinum-based cancer chemotherapy. *Nat Rev Cancer* 2007; **7**: 573-84.
- Desoize B, Madoulet C. Particular aspects of platinum compounds used at present in cancer treatment. *Crit Rev Oncol Hematol* 2002; **42**: 317-25.
- Reedijk J. Metal-ligand exchange kinetics in platinum and ruthenium complexes. *Platinum Metals Rev* 2008; **52**: 2-11.
- Wang, X. Fresh platinum complexes with promising antitumor activity. *Anti-Cancer Agents Med Chem* 2010; **10**: 396-411.
- Farrell N, Kelland LR, Robert JD, Van Beusichem M. Activation of the *trans* geometry in platinum antitumor complexes: a survey of the cytotoxicity of *trans* complexes containing planar ligands in murine L1210 and human tumor panels and studies on their mechanism of action. *Cancer Res* 1992; **52**: 5065-72.
- Quiroga AG. Understanding *trans* platinum complexes as potential antitumor drugs beyond targeting DNA. *J Inorg Biochem* 2012; **114**: 106-12.
- Coluccia M, Nassi A, Loseto F, Boccarelli A, Mariggio MA, Giordano D, et al. A *trans*-platinum complex showing higher antitumor activity than the *cis* congeners. *J Med Chem* 1993; **36**: 510-2.
- Radulović S, Tesić Ž, Manić, S. *Trans*-platinum complexes as anticancer drugs: recent developments and future prospects. *Curr Med Chem* 2002; **9**: 1611-8.
- Pérez JM, Montero EI, González AM, Solans X, Font-Bardia M, Fuertes MA, et al. X-Ray structure of cytotoxic *trans*-[PtCl₂(dimethylamine)(isopropylamine)]: interstrand cross-link efficiency, DNA sequence specificity, and inhibition of the B-Z transition. *J Med Chem* 2000; **43**: 2411-8.
- Arandjelović S, Tesić Ž, Juranić Z, Radulović S, Vrvic M, Potkonjak B, et al. Antiproliferative activity of some *cis*-/*trans*-platinum(II) complexes on HeLa cells. *J Exp Clin Cancer Res* 2002; **21**: 519-26.
- Aris SM, Farrell N. Towards antitumor active *trans*-platinum compounds. *Eur J Inorg Chem* 2009; **10**: 1293-302.
- Wang, X. Fresh platinum complexes with promising antitumor activity. *Anti-Cancer Agents Med Chem* 2010; **10**: 396-411.
- Cubo L, Quiroga AG, Zhang J, Thomas DS, Carnero A, Navarro-Ranninger C, et al. Influence of amine ligands on the aquation and cytotoxicity of *trans*-diamine platinum(II) anticancer complexes. *Dalton Trans* 2009; **18**: 3457-66.
- Reed E. ERCC1 and clinical resistance to platinum-based therapy. *Clin Cancer Res* 2005; **11**: 6100-2.
- Manić S, Gatti L, Carenini N, Fumagalli G, Zunino F, Perego P. Mechanisms controlling sensitivity to platinum complexes: role of p53 and DNA mismatch repair. *Curr Cancer Drug Targets* 2003; **3**: 21-9.
- Kalayda GV, Wagner CH, Jaehde U. Relevance of copper transporter 1 for cisplatin resistance in human ovarian carcinoma cells. *J Inorg Biochem* 2012, **116**: 1-10.
- Sadler PJ. Protein recognition of platinated DNA. *ChemBioChem* 2009; **10**: 73-4.
- Ravera M, Gabano E, Sardi M, Ermondi G, Caron G, McGlinchey MJ, et al. Synthesis, characterization, structure, molecular modeling studies and biological activity of sterically crowded Pt(II) complexes containing bis(imidazole) ligands. *J Inorg Biochem* 2011; **105**: 400-9.
- Ramos-Lima FJ, Moneo V, Quiroga AG, Carnero A, Navarro-Ranninger C. The role of p53 in the cellular toxicity by active *trans*-platinum complexes containing isopropylamine and hydroxymethylpyridine. *Eur J Med Chem* 2010; **45**: 134-41.
- Huq F, Yu JQ, Daghriri H, Beale P. Studies on activities, cell uptake and DNA binding of four *trans*-planar amine platinum(II) complexes of the form: *trans*-PtL(NH₃)Cl₂, where L=2-hydroxypyridine, imidazole, 3-hydroxypyridine and imidazo(1,2- α)pyridine. *J Inorg Biochem* 2004; **98**: 1261-70.
- Aris SM, Knott KM, Yang X, Gewirtz DA, Farrell NP. Modulation of transplatinamine platinum complex reactivity by systematic modification of carrier and leaving groups. *Inorg Chim Acta* 2009; **362**: 929-34.
- Rakić GM, Grgurić-Sipka S, Kaluderović GN, Gómez-Ruiz S, Bjelogrić SK, Radulović SS, et al. Novel *trans*-dichloridoplatinum(II) complexes with 3- and 4-acetylpyridine: Synthesis, characterization, DFT calculations and cytotoxicity. *Eur J Med Chem* 2009; **44**: 1921-5.
- Kim KY, Jeong SY, Won J, Ryu PD, Nam MJ. Induction of angiogenesis by expression of soluble type II transforming growth factor-beta receptor in mouse hepatoma. *J Bio Chem* 2001; **276**: 38781-6.
- Muscella A, Calabriso N, Vetrugno C, Urso L, Fanizzi FP, De Pascali SA, et al. Sublethal concentrations of the platinum(II) complex [Pt(O,O'-acac)(gamma-acac)(DMS)] alter the motility and induce anoikis in MCF-7 cells. *Br J Pharmacol* 2010; **160**: 1362-77.
- Sasanelli R, Boccarelli A, Giordano D, Laforgia M, Arnesano F, Natile G, et al. Platinum complexes can inhibit matrix metalloproteinase activity: platinum-diethyl[(methylsulfinyl)methyl]phosphonate complexes as inhibitors of matrix metalloproteinases 2, 3, 9, and 12. *J Med Chem* 2007; **50**: 3434-41.
- Montiel M, Urso L, de la Blanca EP, Marsigliante S, Jiménez E. Cisplatin reduces endothelial cell migration via regulation of type 2-matrix metalloproteinase activity. *Cell Physiol Biochem* 2009; **23**: 441-8.
- Jacobs JP, Jones CM, Baille JP. Characteristics of a human diploid cell designated MRC-5. *Nature* 1970; **227**: 168-70.
- Gligorijević N, Arandelović S, Filipović L, Jakovljević K, Janković R, Grgurić-Sipka S, et al. Picolinate ruthenium(II)-arene complex with in vitro antiproliferative and antimetastatic properties: comparison to a series of ruthenium(II)-arene complexes with similar structure. *J Inorg Biochem* 2012; **108**: 53-61.
- Skehan P, Storeng R, Scudiero D, Monks A, McMahon J, Vistica D, et al. New colorimetric cytotoxicity assay for anticancer-drug screening. *J Natl Cancer Inst* 1990; **82**: 1107-12.
- Ormerod MG. *Flow Cytometry, a Practical Approach*. New York: Oxford University Press; 1994.
- Bradford MM. A rapid and sensitive method for the quantitation of microgram quantities of protein utilizing the principle of protein-dye binding. *Anal Biochem* 1976; **72**: 248-54.
- Snoek-van Beurden PA, Von den Hoff JW. Zymographic techniques for the analysis of matrix metalloproteinases and their inhibitors. *BioTechniques* 2005; **38**: 73-83.
- Musetti C, Nazarov AA, Farrell NP, Sissi C. DNA reactivity profile of *trans*-platinum planar amine derivatives. *Chem Med Chem* 2011; **6**: 1283-90.

35. Altaha R, Liang X, Yu JJ, Reed E. Excision repair cross complementing-group 1: gene expression and platinum resistance. *Int J Mol Med* 2004; **14**: 959-70.
36. Zorbas H, Keppler BK. Cisplatin damage: are DNA repair proteins saviors or traitors to the cell? *Chem Bio Chem* 2005; **6**: 1157-66.
37. Ramos-Lima FJ, Vrána O, Quiroga AG, Navarro-Ranninger C, Halámiková A, Rybníčková H, et al. Structural characterization, DNA interactions, and cytotoxicity of new transplatin analogues containing one aliphatic and one planar heterocyclic amine ligand. *J Med Chem* 2006; **49**: 2640-51.
38. Bierbach U, Sabat M, Farrell N. Inversion of the cis geometry requirement for cytotoxicity in structurally novel platinum(II) complexes containing the bidentate N,O-donor pyridin-2-yl-acetate. *Inorg Chem* 2000; **39**: 1882-90.
39. Wang QE, Milum K, Han C, Huang YW, Wani G, Thomale J, et al. Differential contributory roles of nucleotide excision and homologous recombination repair for enhancing cisplatin sensitivity in human ovarian cancer cells. *Mol Cancer* 2011; **10**: 24.
40. Perego P, Giarola M, Righetti SC, Supino R, Caserini C, Delia D, et al. Association between cisplatin resistance and mutation of p53 gene and reduced bax expression in ovarian carcinoma cell systems. *Cancer Res* 1996; **56**: 556-62.
41. Todd RC, Lippard SJ. Inhibition of transcription by platinum antitumor compounds. *Metallomics* 2009; **1**: 280-91.
42. Seetharam RN, Sood A, Basu-Mallick A, Augenlicht LH, Mariadason JM, Goel S. Oxaliplatin resistance induced by ERCC1 up-regulation is abrogated by siRNA-mediated gene silencing in human colorectal cancer cells. *Anticancer Res* 2010; **30**: 2531-8.
43. Kasparkova J, Marini V, Najajreh Y, Gibson D, Brabec V. DNA binding mode of the cis and trans geometries of new antitumor nonclassical platinum complexes containing piperidine, piperazine, or 4-picoline ligand in cell-free media. Relations to their activity in cancer cell lines. *Biochemistry* 2003; **42**: 6321-32.
44. Arkell J, Jackson CJ. Constitutive secretion of MMP9 by early-passage cultured human endothelial cells. *Cel Biochem Funct* 2003; **21**: 381-6.
45. Ulukaya E, Ari F, Dimas K, Ikitimur KI, Yilmaz VT. Anti-cancer activity of a novel palladium(II) complex on human breast cancer cells *in vitro* and *in vivo*. *Eur J Med Chem* 2011; **46**: 4957-63.
46. Kiran MS, Viji RJ, Kumar SV, Prabhakaran AA, Sudhakaran PR. Changes in expression of VE-cadherin and MMPs in endothelial cells: Implications for angiogenesis. *Vasc Cell* 2011; **3**: 6.

Dual time point imaging fluorine-18 flourodeoxyglucose positron emission tomography for evaluation of large loco-regional recurrences of breast cancer treated with electrochemotherapy

Louise Wichmann Matthiessen¹, Helle Hjorth Johannesen², Kristin Skougaard¹, Julie Gehl¹, Helle Westergren Hendel³

¹ Center for Experimental Drug and Gene Electrotransfer (C*EDGE), Department of Oncology, Copenhagen University Hospital Herlev, Copenhagen University Hospital Herlev, Herlev, Denmark

² Department of Radiology, Copenhagen University Hospital Herlev, Herlev, Denmark

³ Department of Clinical Physiology and Nuclear Medicine, Copenhagen University Hospital Herlev, Herlev, Denmark

Radiol Oncol 2013; 47(4): 358-365.

Received 19 April 2013
Accepted 30 June 2013

Correspondence to: Julie Gehl, Dr. Med. Sci., M.D., Department of Oncology, Copenhagen University Hospital Herlev, Herlev Ringvej 75, DK-2730 Herlev, Copenhagen, Denmark. E-mail: julie.gehl@regionh.dk. Phone: +45 38 68 29 81

Disclosure: No potential conflicts of interests were disclosed.

The paper was presented at the 7th Conference of Experimental and Translational Oncology, 20-24th April 2013, Portoroz, Slovenia (www.ceto.si) coorganised and supported by COST TD1104 Action (www.electroporation.net).

Background. Electrochemotherapy is a local anticancer treatment very efficient for treatment of small cutaneous metastases. The method is now being investigated for large cutaneous recurrences of breast cancer that are often confluent masses of malignant tumour with various degrees of inflammation. To this end 18-Flourine-Flourodeoxyglucose-Positron Emission Tomography/Computed Tomography (FDG-PET/CT) could be a method for response evaluation. However, a standard FDG-PET/CT scan cannot differentiate inflammatory tissue from malignant tissue. Dual point time imaging (DTPI) FDG-PET has the potential of doing so. The purpose of this study was to investigate if DTPI FDG-PET/CT could assess response to electrochemotherapy and to assess the optimal timing of imaging.

Patients and methods. Within a phase II clinical trial 11 patients with cutaneous recurrences had FDG-PET/CT scans at three time points: 60 min, 120 min and 180 min after FDG injection. The scans were performed before and 3 weeks after electrochemotherapy.

Results. A significant reduction in maximum standard uptake value at 60 min post injection was seen after treatment. Furthermore a change in the FDG uptake pattern was observed; from increasing uptake in up to 180 min post injection before treatment to stabilization of FDG uptake at 120 min post injection after treatment. The change in FDG uptake pattern over time lead to change of response in three target lesions; two lesions changed from stable metabolic disease to partial metabolic response and one lesion changed from partial metabolic response to stable metabolic disease. To ensure detection of the change in uptake pattern, scanning 60 and 180 min post injection seems optimal.

Conclusions. The present study shows that FDG-PET/CT 60 and 180 min after tracer injection is a promising tool for response evaluation of cutaneous recurrences of breast cancer treated with electrochemotherapy.

Key words: dual time point FDG PET; breast cancer; electrochemotherapy; response assessment; cutaneous metastases

Introduction

Could dual time point imaging (DTPI) fluorine-18 flourodeoxyglucose positron emission tomogra-

phy combined with computed tomography (FDG-PET/CT) be a useful tool for imaging of recurrent breast cancer treated with electrochemotherapy? The 5-year incidence of loco-regional recurrence

of breast cancer is reported to be between 6% and 23% following mastectomy and approximately 6% after breast conserving surgery and radiotherapy.¹ In spite of treatment, subsequent loco-regional recurrence occurs in 25-35% of patients² and of these it is reported that an estimated 30% will suffer from significant morbidity because of their local recurrence.³ Treatment of recurrent loco-regional breast cancer can be a clinical challenge. Local tumour control, in spite of any distant metastases, is important as the presence of uncontrolled loco-regional recurrence can cause severe patient distress due to large ulcerating and secreting tumours (Figure 1).

Electrochemotherapy is a local treatment using electric pulses to transiently permeabilize the cell membrane.⁴ It augments the effect of chemotherapy, by enabling passage over the cell membrane of otherwise non-permeating chemotherapeutic drugs.⁵ For the chemotherapeutic agent bleomycin, the effect is enhanced several hundred fold, enabling high efficacy after one or few treatments.⁶ Electrochemotherapy has proven highly effective in palliative treatment of cutaneous metastases less than 3 cm in diameter⁷⁻¹³ and has shown promising results in terms of efficacy and alleviation of symptoms in heavily pre-treated breast cancer patients with loco-regional recurrence (Figure 1).^{12,14,15} Furthermore electrochemotherapy is currently being evaluated for deep seated tumours.¹⁶⁻¹⁸ Loco-regional recurrence of breast cancer that has previously been treated with radiotherapy and surgery is often a confluent mass of tumour and a varying degree of chronic and acute inflammation. Response evaluation of cutaneous loco-regional recurrences of breast cancer poses a challenge because inflammation cannot be distinguished from malignancy. Clinical evaluation with measurement of lesion extension has proven unsuitable for response evaluation after electrochemotherapy as it does not visualize deeper parts of the lesion and is not able to differentiate between inflammation, ulceration and tumour.¹⁴ Thus other methods for response evaluation of electrochemotherapy are needed.

FDG-PET/CT scan is a highly accurate method for staging of breast cancer recurrence.^{19,20} The technique provides metabolic information that can complement inconclusive findings derived from anatomical imaging and may better characterize disease extent. Furthermore, FDG-PET/CT can assess the response to ongoing therapy early as metabolic response prelude morphological changes. Uptake of FDG is however not specific to tumour

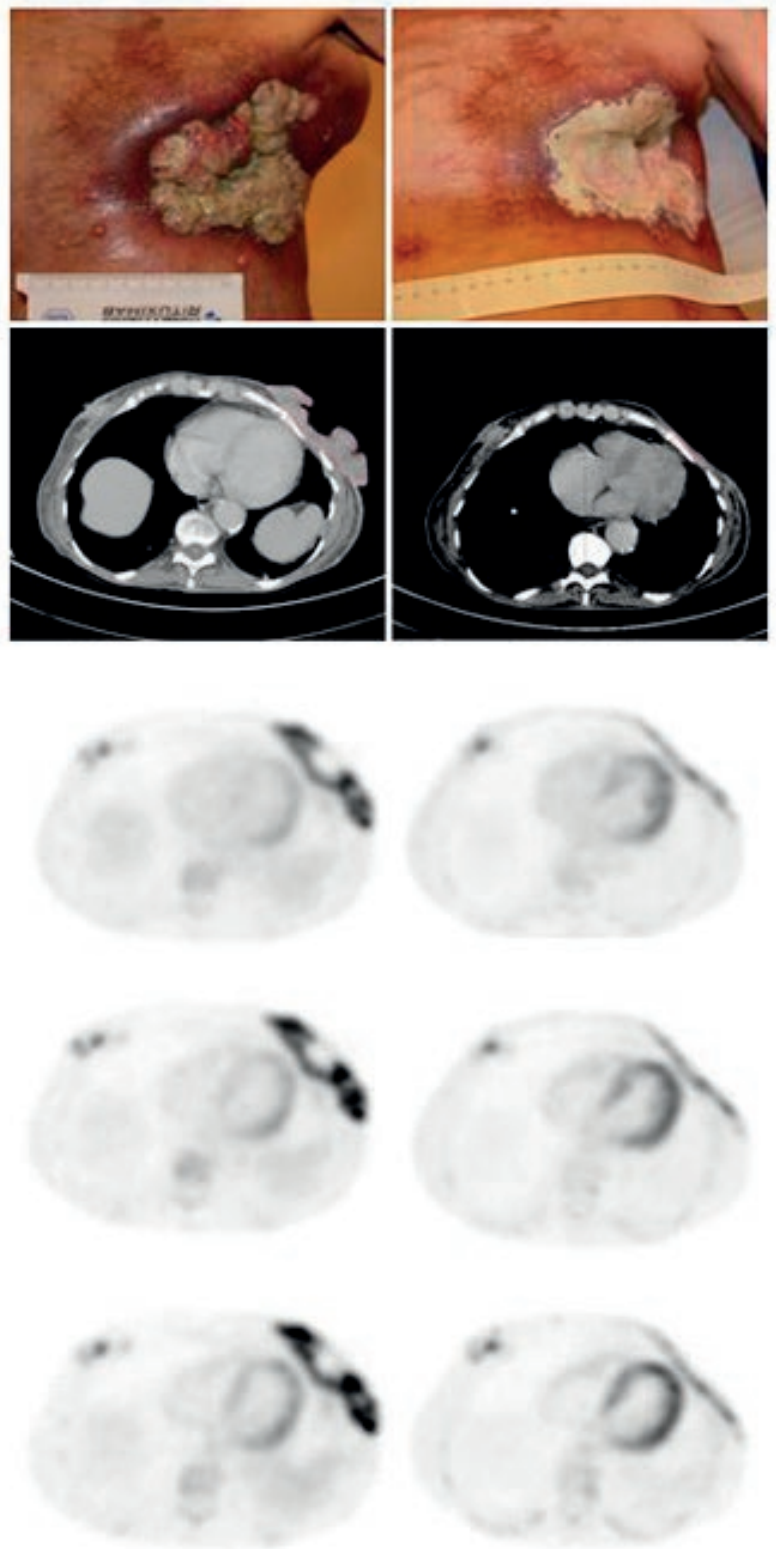


FIGURE 1. Large recurrence with varying depth and inflammation on the left chest wall of 68 y female. Left column shows from the top clinical presentation, CT-scan, PET scan at 60 min p.i., PET scan at 120 min p.i. and PET scan 180 min p.i. Right column. Same patients after one treatment. Change in SUVmax in target lesion at baseline compared to follow up was 29.7% at 60 min p.i., 71.2% at 120 min p.i., and 83.1% at 180 min p.i.

cells as inflammatory cells also take up FDG.²¹ Studies have shown that the FDG uptake increases for several hours in malignant lesions,²¹⁻²³ which is rarely seen in inflammatory lesions and normal tissue.²⁴ Thus, the difference in time course when using DTPI may improve the differentiation between inflammation, known to be present and viable malignant tumour.

In this study we investigated DTPI FDG-PET/CT as a possible method for response evaluation of loco-regional recurrent breast cancer treated with electrochemotherapy. This was done in order to evaluate if the method can assess treatment response to therapy and to determine the optimal timing of imaging FDG uptake in the loco-regional recurrence of breast cancer in this setting.

Petients and methods

Patients and treatment

In the period October 2008 to October 2010 patients with cutaneous loco-regional recurrence of breast cancer were prospectively accrued for a phase II investigator initiated electrochemotherapy protocol.¹⁴ Seventeen patients were included and treated within the protocol. Patients were separately asked if they would be willing to have DTPI FDG-PET/CT. Twelve patients completed DTPI FDG-PET/CT before (baseline) and after (follow up) electrochemotherapy. DTPI FDG-PET/CT was performed median 5 days (range, 2-15) before electrochemotherapy and 24 days (range, 17-59 days) after electrochemotherapy. Eleven patients were evaluable while one patient was not evaluable due to lack of contrast enhancement and lack of metabolic activity in the target lesions, making them indistinguishable from the surrounding tissue.

Electrochemotherapy was considered when no other treatment options were available and patients had symptoms from large (> 3 cm) cutaneous loco-regional recurrence of breast cancer. All patients gave informed written consent and the protocol was approved by the Regional Research Ethics Committee, The Danish Medicines Agency (clinicaltrials.gov identifier: NCT00744653), and the Data Protection Agency.

Electrochemotherapy was performed according to the standard operating procedures.²⁵ General anaesthesia was induced in all patients. Bleomycin was administered intravenously using a standard dose of 15.000 IU/m².

Data acquisition

Clinical examination

The cutaneous loco-regional recurrences to be treated were defined as target lesions. According to protocol loco-regional recurrences smaller than 3 cm were not considered target lesions.

Clinical examination was performed at baseline and at follow up. The longest diameter of the target lesions was recorded using a ruler and verified with digital photography.

FDG-PET/CT-scanning

A combined FDG-PET 60 min post-tracer injection (p.i.) and contrast enhanced CT scan of the thorax was performed in each patient at baseline and at follow up. Furthermore, PET scanning was performed 120 min p.i. and 180 min p.i. at baseline and at follow up. Patients fasted for at least 6 hours before the examination. A blood sample determined glucose level (Ascension Contour, Bayer Health Care, Germany) before FDG administration to ensure the inclusion criteria of euglycemia (concentrations below 120 mg/dL). All examinations were performed with a Gemini PET/CT system (Philips Medical, The Netherlands), consisting of a dedicated germanium oxyorthosilicate full-ring PET scanner and a dual-slice helical CT scanner. After intravenous injection of 18F-FDG (370 MBq), the patients rested in a quiet room for 45 min. The scans were performed with the patients in supine position with arms over the head and were initiated with a low-dose CT scan (20 mA, 140 kV, 512 × 512 matrix) covering the thorax and used for attenuation correction. Thereafter, emission measurements were performed in the 3-dimensional mode with a 144 × 144 matrix (60 min p.i.). Emission scan time per bed position was 2 min; 4 bed positions (field of view: 155 mm) were acquired. After the first emission scan, a diagnostic CT scan of the thorax was performed after automated intravenous injection (100 mL 5 mL/sec) of iodine-containing contrast medium (Omnipaque 350 mg/mL, GE Healthcare Deutschland GmbH). Scan delay after injection was 50 seconds. Diagnostic dual-slice CT with an axial field of view of 600 mm and a matrix of 512 × 512 was performed in the spiral mode under continuous acquisition at 120 kV and 145 mA (slice thickness of 5.0 mm, increment of 2.5 mm/seconds, rotation time of 0.5 seconds, and pitch index of 1). The patients were then resting in comfortable chairs in the waiting room for two further emission scans of the thorax at 120 and 180 min p.i. The average examination time (including rest periods) was

TABLE 1. Response evaluation with clinical examination, CT and PET/CT-scans

Patient no (lesion no)	Clinical response evaluation			Response evaluation on CT scans			Response evaluation with PET scans 60 min post tracer injection.			Response evaluation with PET scans 120 min post tracer injection.			Response evaluation with PET scans 180 min post tracer injection.		
	Base-line (cm)	Follow up (cm)	Response	Base-line (cm)	Follow up (cm)	Response	Baseline SUV-max 60 min	FUP SUV- max 60 min	Response	Baseline SUV-max 120 min	FUP SUV- max 120 min	Re-sponse	Baseline SUV-max 180 min	FUP SUV- max 180 min	Response
1*	7.5	6.3	SD	10.6	6.3	PR	2.6	2.4	SMD	3.1	2.4	SMD	ND		
2 (a)	3.7	0.0	CR	1.4	0.0	CR	0.6	0.0	CMR	0.8	0.0	CMR	0.6	0.0	CMR
2 (b)	3.2	0.0	CR	0.7	0.0	CR	0.7	0.0	CMR	0.6	0.0	CMR	0.5	0.0	CMR
3	6.5	6.5	SD	1.0	1.3	PD	1.6	2.1	PMD	1.5	3.0	PMD	2.6	4.5	PMD
4	10.0	10.0	SD	11.0	10.5	SD	22.6	19.3	SMD	30.7	25.6	SMD	34.9	23.4	PMR
5 (a)	12.0	9.5	SD	11.8	9.1	SD	11.7	9.6	SMD	16.6	14.8	SMD	19.9	14.0	PMR
5 (b)	3.5	2.5	SD	3.9	2.7	PR	11.4	4.0	PMR	14.1	5.5	PMR	17.5	6.6	PMR
5 (c)	3.5	2.5	SD	3.9	1.2	PR	8.3	2.3	PMR	10.3	3.2	PMR	12.7	3.4	PMR
5 (d)	6.0	5.0	SD	7.1	4.3	PR	9.6	9.2	SMD	13.6	11.9	SMD	15.6	12.5	SMD
5 (e)	3.5	1.5	PR	4.2	1.2	PR	10	2.3	PMR	12.8	3.2	PMR	14.2	3.0	PMR
6	9.0	11.0	PD	10.0	14.8	PD	11.8	10.9	SMD	15.9	14.9	SMD	16.6	16.5	SMD
8	11.0	12.0	SD	11.9	8.0	PR	6.7	4.7	PMR	7.9	2.3	PMR	9.1	1.5	PMR
9	3.2	3.2	SD	2.4	2.5	SD	5.0	2.8	PMR	6.5	3.2	PMR	6.7	3.2	PMR
10	25.0	16.5	PR	19.7	10.8	PR	5.6	4.6	SMD	7.1	5.6	SMD	10.5	5.6	PMR
12	9.0	5.5	PR	15.2	16.0	SD	17.9	8.9	PMR	21.8	10.3	PMR	25.0	3.9	PMR
15	20.0	20.0	SD	16.3	13.7	SD	12.4	8.1	PMR	13.5	9.2	PMR	13.9	10.8	SMD
Mean	8.5	7.0		8.2	6.4		8.7	5.7		11.0	7.2		13.4	7.3	
S.D.	6.3	5.8		6.0	5.5		6.1	5.0		8.2	6.9		9.2	6.8	

Responses recorded for single lesions evaluated with clinical evaluation, CT and PET/CT scans at 60, 120 and 180 minutes after FDG injection are presented. For patient number 4 and 10 the observed response evaluated with PET/CT changes from SMD at 60 and 120 min to PMR at 180 min. For patient number 8 the observed response evaluated with PET/CT changes from SMD at 60 min to PMR at 120 and 180 min. (CMR: complete metabolic response, PMR: Partial metabolic response, SMD: Stable metabolic disease, PMD: progressive metabolic disease). ND: Not done

Patient numbers refers to numbers given consecutively when patients were included in the trial.

* Scan at 180 min was not performed at baseline

approximately 4 hours. Total time spent in the scanner was approximately 30 min.

Response evaluation

Clinical Evaluation:

Assessment of tumour response in target lesions was done in accordance with RECIST 1.0: ²⁶ Complete response (CR) was defined as disappearance of the target lesion, partial response (PR) was defined as at least 30% decrease in the diameter of the target lesion, progressive disease (PD) was defined as at least 20% increase in the diameter of the target lesion and stable disease (SD) as neither sufficient shrinkage to qualify for PR or sufficient increase to qualify for PD. Non-target lesions and systemic disease was not addressed.

FDG-PET/CT-scans

CT scans were analysed by an experienced radiologist using Eclipse Cone Planning version 8.9

(Varian Medical Systems Inc., California, USA), standardly used for radiotherapy planning. The largest diameter of target lesions in the axial plane was recorded and the sum of the diameters evaluated in accordance to RECIST.²⁶

PET data were reconstructed iteratively with a method based on the row action maximum-likelihood algorithm (RAMLA) using the PETView software (Philips Medical, The Netherlands). Image analysis and measurements were performed by a specialist in nuclear medicine in collaboration with the oncologist responsible for the treatment. Tumour tracking in the Brilliance Workspace software package (Philips, The Netherlands) was used. This allowed simultaneous viewing and analysis of the PET scans acquired at 60, 120 and 180 min p.i. Scans at baseline and follow up were analysed separately. The FDG uptake in target lesions were assessed semiquantitatively by measuring the maximum standardized uptake value (SUVmax) within a three dimensional ellipsoidal volume of interest

TABLE 2. SUVmax values before and after treatment

	60 min	120 min	180 min	RI ₁₂₀₋₆₀	RI ₁₈₀₋₆₀	RI ₁₈₀₋₁₂₀
Before treatment (n = 16)	8.7 ± 6.1	11.0 ± 8.2	13.4 ± 9.2	22.5% ± 14.7 %	41.1% ± 29.6 %	15.3% ± 24.4%
Background before treatment (n=11)	1.7 ± 0.3	1.4 ± 0.2	1.3 ± 0.4	-16.3% ± 12.5%	-27.3% ± 29.7%	-9.0% ± 40.7%
After treatment (n = 16)	5.7 ± 5.0	7.2 ± 6.9	7.3 ± 6.5	30.3% ± 16.8%	26.8% ± 41.1%	-1.3% ± 32.5%
Background after treatment (n = 11)	1.8 ± 0.4	1.5 ± 0.4	1.4 ± 0.5	-16.3% ± 16.7%	-24.2% ± 24.6%	-7.0% ± 33.7%

Table 2 shows the SUVmax values for lesions before and after treatment with electrochemotherapy. The corresponding values for background measured as SUVmax in a 1.2 cm spherical ROI in the Aortic arch is also shown. Eleven patients with 16 target lesions were scanned. All data are presented as mean ± S.D.

RI: Retention index.; RI₁₂₀₋₆₀: (SUV_{60min}-SUV_{120min})/SUV_{60min} × 100%; RI₁₈₀₋₆₀: (SUV_{60min}-SUV_{180min})/SUV_{60min} × 100%; RI₁₈₀₋₁₂₀: (SUV_{120min}-SUV_{180min})/SUV_{120min} × 100%

(VOI) covering the target. SUV's normalized to body weight were automatically drawn by isocontouring in the selected VOI. SUV of 2.5 was used as cut off for the isocounting. Background activity was determined as the SUVmax in the aortic arch using a spherical VOI with a diameter of 1.2 cm. Lesions outside the treated area and new lesions were not considered in this study. SUVmax in each target lesion was recorded at baseline and at follow up at 60, 120 and 180 min p.i. A complete metabolic response (CMR) was considered as visual disappearance of tumour activity in the target lesion, so that it became indistinguishable from surrounding normal tissue. Partial metabolic response (PMR) was considered when more than a 25% decline in SUVmax was observed, progressive metabolic disease (PMD) was considered when more than a 25% increase in SUVmax was observed and stable metabolic disease (SMD) was defined as not CMR, PMR or PMD as suggested limits in the EORTC criteria.²⁷

Statistics

All of the quantitative values were expressed in terms of mean ± SD. A paired t-test was applied to determine the difference in SUVmax at baseline and at follow up. Repeated measurement analysis using general linear model was applied to determine the difference in SUVmax at 60, 120, and 180 min p.i. A p value of <0.05 was considered significant. Statistical analyses were performed using SPSS for windows version 16.0.

Results

Patients

The eleven evaluable patients with cutaneous loco-regional recurrence of breast cancer presented with a total of 16 target lesions (median 1 lesion per patient, range, 1-5). Baseline DTPI FDG-PET/CT was

performed five days (range, 2-15) before electrochemotherapy and follow up DTPI FDG-PET/CT was performed 23 days (range, 17-35 days) after electrochemotherapy.

Clinical evaluation

Before treatment the mean tumour diameter was 8.5 ± 6.3 and after treatment the mean tumour diameter was 7.0 ± 5.8 cm with a mean difference of 1.5 ± 2.5 cm (p=0.024). Observed responses were CR in two lesions, PR in three lesions, SD in 10 lesions, and PD in one lesion, resulting in objective response in 5 out of 16 lesions (31%) (Table 1).

CT-scans

Axial diameter and volume of the treated lesions were measured at baseline (median 5 days (range, 2-15) before electrochemotherapy) and at follow up (24 days (range, 17-59 days) after electrochemotherapy). Mean tumour diameter at baseline was 8.2 ± 6.0 cm and at follow up 6.4 ± 5.5 cm with a mean difference of 1.8 ± 2.9 cm (p=0.026).

Observed responses were CR in 2 lesions, PR in 7 lesions, SD in 5 lesions, and PD in 1 lesion, resulting in objective response of 9 out of 16 lesions (56%) (Table 1).

PET-scans

Baseline PET

At baseline (median 5 days (range, 2-15) before electrochemotherapy) mean SUVmax in target lesions was 8.7 ± 6.1 at 60 min p.i., 11.0 ± 8.2 at 120 min p.i., and 13.4 ± 9.2 at 180 min p.i. The corresponding mean SUVmax for background was 1.7 ± 0.3 at 60 min p.i., 1.4 ± 0.2 at 120 min p.i., and 1.3 ± 0.4 at 180 min p.i. (Table 2). Mean percentage change in SUVmax in target lesion between 60 and 120 min p.i. was 22.5 ± 14.7% (p=0.002), between 60 and 180

min p.i. $41.1 \pm 29.6\%$ ($p=0.001$), and between 120 and 180 min p.i. $15.3 \pm 24.4\%$ ($p=0.001$). The corresponding percentage change in SUVmax for background was $-16.3 \pm 12.5\%$ ($p=0.004$), $-27.3 \pm 29.7\%$ ($p=0.058$), and $-9.0 \pm 40.7\%$ ($p=1.000$) (Table 2).

Follow-up PET

At follow up (24 days (range, 17-59 days) after electrochemotherapy) mean SUVmax in target lesion was 5.7 ± 5.0 , 7.2 ± 6.9 , and 7.3 ± 6.8 at 60, 120, and 180 min p.i. respectively. The corresponding mean SUVmax for background was 1.8 ± 0.4 , 1.5 ± 0.4 , and 1.4 ± 0.5 (Table 2). Mean percentage change of SUVmax in target lesions between 60 and 120 min p.i. was $30.3 \pm 16.8\%$ ($p=0.008$) between 60 and 180 min p.i. $36.8 \pm 41.1\%$ ($p=0.052$), and between 120 and 180 min p.i. $-1.3 \pm 32.5\%$ ($p=1.000$). The corresponding change in SUVmax for background was $-16.3 \pm 16.7\%$ ($p=0.019$), $-24.2 \pm 24.6\%$ ($p=0.059$), and $-7.0 \pm 33.7\%$ ($p=1.000$) (Table 2).

Change between baseline and follow-up PET

The mean changes in SUVmax between baseline and follow-up scans were 3.1 ± 3.1 , 3.8 ± 3.8 , and 5.9 ± 6.0 at 60, 120, and 180 min p.i. respectively. Mean percentage changes of SUVmax between baseline and follow up scans were $38 \pm 38\%$ ($p=0.001$), $37 \pm 47\%$ ($p=0.001$), and $47 \pm 46\%$ ($p=0.002$) at 60, 120 and 180 scans respectively.

At the 60 min p.i. scans CMR was observed in 2 lesions, PMR in 7 lesions, SMD in 6 lesions, and PMD in 1 lesion. The corresponding responses observed at the 120 min p.i. scans were CMR in 2 lesions, PMR in 7 lesions, SMD in 6 lesions, and PMD in 1 lesion. Observed responses at the 180 min p.i. was CMR in 2 lesions, PMR in 9 lesions, SMD in 3 lesions, and PMD in 1 lesion (Table 1). One patient did not have the baseline 180 min post tracer injection scan and was therefore not evaluated at 180 min p.i. The changes in SUVmax over time are illustrated in Figure 2 and an example is given in Figure 1.

Discussion

In this study of 11 patients with cutaneous loco-regional recurrent breast cancer, 16 lesions were treated with electrochemotherapy and evaluated with DTPI FDG-PET/CT. We observed two changes between the baseline and follow-up PET-scan: a significant reduction in SUVmax 60 min p.i. after electrochemotherapy (standard imaging protocol) and a change in the SUVmax pattern from a

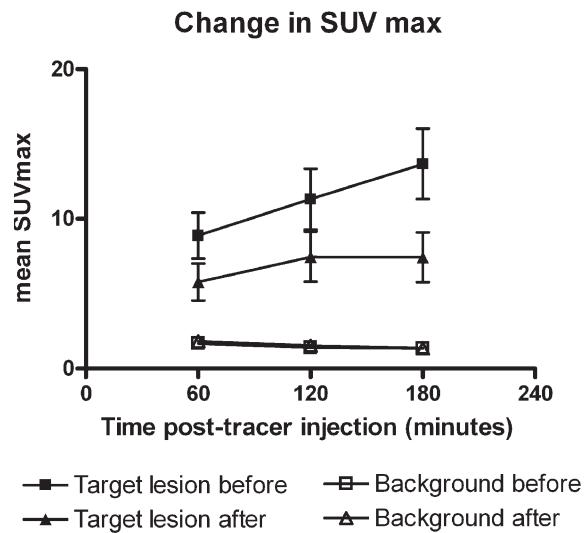


FIGURE 2. Change in SUVmax over time in target lesions and background. There was significant increase in mean SUVmax over time in target lesions before treatment whereas the mean SUVmax in target lesions after treatment stabilized at 120 min after FDG injection. Mean SUVmax in background (measured in the aortic arch) did not increase over time.

steadily increasing SUVmax in up to 180 min before electrochemotherapy to a stabilization at 120 min p.i. on the after electrochemotherapy, making the difference in SUVmax before and after electrochemotherapy more pronounced using the 180 min p.i. scan. A significant reduction of SUVmax 60 min p.i. is in routine anti-cancer treatment monitoring used as a surrogate parameter for tumour response and we interpret it as response to the electrochemotherapy in our study. This interpretation is strongly supported by the change in uptake pattern: after treatment the SUVmax stabilizes after 120 min in contrast to the baseline scans, where there is a steadily increased uptake in up to 180 min. This might indicate more tissue with inflammatory cells than with malignant cells at follow up as the SUVmax reaches a plateau in inflammatory cells faster than in malignant cells.²² This perception is in accordance with Boerner *et al.*²⁸ who recommend a three hour protocol for detection of breast cancer and Caprio *et al.*²⁹ who observed an increase SUVmax over time in primary breast malignancies using DTPI FDG-PET/CT. We observed continuous uptake of FDG in target lesions at baseline scans for at least three hours suggesting 180 min p.i. could be the optimal time for imaging of FDG uptake in lesions such as cutaneous loco-regional recurrence of breast cancer. The difference between SUVmax at baseline and follow-up was significantly larger at the 180 min p.i. scans com-

pared to the 60 min p.i. scans. Therefore the 180 min p.i. scans might enable visualization of smaller differences in SUVmax changes compared to the 60 min p.i. scans and provide useful information in the event that re-treatment needs to be planned.

Clinical examination with measurement of lesion extension is used for evaluation of electrochemotherapy and was also done in this study. CR was observed in two target lesions, PR in three, SD in 10 lesions and PD in one lesion using this method. It is difficult to measure the extent of the lesions in a clinical setting. The FDG-PET/CT scans showed a different picture from the clinical evaluation with more patients having partial response than patients having stable disease.¹⁴ This illustrates that clinical evaluation of response in highly heterogeneous lesions such as a loco-regional recurrence of breast cancer treated with electrochemotherapy may not be suitable and that FDG-PET/CT may be more precise methods for response evaluation. CT-scans can illustrate the anatomical extent of the lesions but may include scar tissue, inflammatory tissue and thickened skin that cannot be differentiated from malignant tissue. PET-scans help in this differentiation by adding biological important information of metabolic activity to CT-scans.

Other forms of PET scanners such as the Positron Emission Mammography has shown high accuracy and appears useful in biopsy guidance, surgical planning and surveillance for recurrence³⁰, but is unsuitable for patients with cutaneous loco-regional recurrence of breast cancer as most of these have had mastectomy.

With DTPI PET the time course of FDG uptake can be used to differentiate inflammation from malignancy which further improves the evaluation of response. The change in FDG uptake over time did change the response in three target lesions; in two lesions from SMD to PMR and in one lesion from PMR to SMR compared to the 60 min scan. To confirm our observations further studies could include biopsies, to determine the extent of inflammation and malignant tissue after treatment. Induction of inflammatory papules in the skin could also be of interest in evaluating the control time course of FDG uptake in inflammatory tissue. This was not done in this primary study.

Although DTPI FDG-PET/CT is an experimental, expensive and time consuming investigation not favourable for routine clinical application, we do find it a promising non-invasive method for response evaluation of cutaneous loco-regional recurrent breast cancer treated with electrochemotherapy. Furthermore it can be of use in deep seat-

ed tumours^{31,32}, in the neoadjuvant setting³³ and investigated for other local treatments such as irreversible electroporation³⁴ or radio-frequency ablation as well. Carbon-11-thymidine has shown to be promising in measurement and prediction of early response to chemotherapeutic agents and could also be considered in these types of treatments as it is not taken up by inflammatory cells.

In conclusion, this study indicates that not only FDG-PET/CT but also DTPI FDG-PET/CT is promising for evaluation and planning of electrochemotherapy and could be useful for other localized anti-cancer treatments as well. Although further studies are needed, a planned scan time at 180 min would be feasible and could add important information in particular when inflammation and cancer are superposed.

Acknowledgement

We would like to thank the staff of the PET division at Department of Clinical Physiology and Nuclear Medicine, Copenhagen University Hospital Herlev for assistance. This was an investigator initiated study and partly funded by a grant from the Capital Region of Denmark. Julie Gehl is a research fellow of the Royal Swedish Academy, supported by the Acta Oncologica Foundation.

References

1. Clarke M, Collins R, Darby S, Davies C, Elphinstone P, Evans E, et al. Effects of radiotherapy and of differences in the extent of surgery for early breast cancer on local recurrence and 15-year survival: an overview of the randomised trials. *Lancet* 2005; **366**: 2087-106.
2. van Tienhoven G., Voogd AC, Peterse JL, Nielsen M, Andersen KW, Mignolet F, et al. Prognosis after treatment for loco-regional recurrence after mastectomy or breast conserving therapy in two randomised trials (EORTC 10801 and DBCG-82TM). EORTC Breast Cancer Cooperative Group and the Danish Breast Cancer Cooperative Group. *Eur J Cancer* 1999; **35**: 32-8.
3. Bedwinek JM, Fineberg B, Lee J, Ocwieza M. Analysis of failures following local treatment of isolated local-regional recurrence of breast cancer. *Int J Radiat Oncol Biol Phys* 1981; **7**: 581-85.
4. Gehl J. Electroporation: theory and methods, perspectives for drug delivery, gene therapy and research. *Acta Physiol Scand* 2003; **177**: 437-47.
5. Gehl J, Skovsgaard T, Mir LM. Enhancement of cytotoxicity by electroporation: an improved method for screening drugs. *Anti-Cancer Drugs* 1998; **9**: 319-25.
6. Gothelf A, Mir LM, Gehl J. Electrochemotherapy: results of cancer treatment using enhanced delivery of bleomycin by electroporation. *Cancer Treat Rev* 2003; **29**: 371-87.
7. Marty M, Sersa G, Garbay JR, Gehl J, Collins CG, Snoj M, et al. Electrochemotherapy, An easy, highly effective and safe treatment of cutaneous and subcutaneous metastases: Results of ESOP (European Standard Operating Procedures of Electrochemotherapy) study. *EJC Supplements* 2006; **4**: 3-13.

8. Campana LG, Mocellin S, Basso M, Puccetti O, De Salvo GL, Chiarion-Sileni V, et al. Bleomycin-based electrochemotherapy: clinical outcome from a single institution's experience with 52 patients. *Ann Surg Oncol* 2009; **16**: 191-9.
9. Belehradec M, Domenge C, Luboiniski B, Orlowski S, Belehradec J, Jr, Mir LM. Electrochemotherapy, a new antitumor treatment. First clinical phase I-II trial. *Cancer* 1993; **72**: 3694-700.
10. Curatolo P, Quaglino P, Marengo F, Mancini M, Nardo T, Mortera C, et al. Electrochemotherapy in the Treatment of Kaposi Sarcoma Cutaneous Lesions: A Two-Center Prospective Phase II Trial. *Ann Surg Oncol* 2011; **19**: 192-80.
11. Heller R, Jaroszeski MJ, Glass LF, Messina JL, Rapaport DP, DeConti RC, et al. Phase I/II trial for the treatment of cutaneous and subcutaneous tumors using electrochemotherapy. *Cancer* 1996; **77**: 964-71.
12. Matthiessen LW, Chalmers RL, Sainsbury DC, Veeramani S, Kessel G, Humphreys AC, et al. Management of cutaneous metastases using electrochemotherapy. *Acta Oncol* 2011; **50**: 621-9.
13. Quaglino P, Mortera C, Osella-Abate S, Barberis M, Illengo M, Rissone M, et al. Electrochemotherapy with intravenous bleomycin in the local treatment of skin melanoma metastases. *Ann Surg Oncol* 2008; **15**: 2215-22.
14. Matthiessen LW, Johannesen HH, Hendel HW, Moss T, Kamby C, Gehl J. Electrochemotherapy for large cutaneous recurrence of breast cancer: a phase II clinical trial. *Acta Oncol* 2012; **51**: 713-21.
15. Sersa G, Cufer T, Paulin SM, Cemazar M, Snoj M. Electrochemotherapy of chest wall breast cancer recurrence. *Cancer Treat Rev* 2012; **38**: 379-86.
16. Agerholm-Larsen B, Iversen HK, Ibsen P, Moller JM, Mahmood F, Jensen KS, et al. Preclinical validation of electrochemotherapy as an effective treatment for brain tumors. *Cancer Res* 2011; **71**: 3753-62.
17. Linnert M, Gehl J. Bleomycin treatment of brain tumors: an evaluation. *Anticancer Drugs* 2009; **20**: 157-64.
18. Edhemovic I, Gadzije EM, Breclj E, Miklavcic D, Kos B, Zupanic A et al. Electrochemotherapy: a new technological approach in treatment of metastases in the liver. *Technol Cancer Res Treat* 2011; **10**: 475-85.
19. Jansson T, Westlin JE, Ahlstrom H, Lilja A, Langstrom B, Bergh J. Positron emission tomography studies in patients with locally advanced and/or metastatic breast cancer: a method for early therapy evaluation? *J Clin Oncol* 1995; **13**: 1470-77.
20. Bassa P, Kim EE, Inoue T, Wong FC, Korkmaz M, Yang DJ, et al. Evaluation of preoperative chemotherapy using PET with fluorine-18-fluorodeoxyglucose in breast cancer. *J Nucl Med* 1996; **37**: 931-8.
21. Hamberg LM, Hunter GJ, Alpert NM, Choi NC, Babich JW, Fischman AJ. The dose uptake ratio as an index of glucose metabolism: useful parameter or oversimplification? *J Nucl Med* 1994; **35**: 1308-12.
22. Lodge MA, Lucas JD, Marsden PK, Cronin BF, O'Doherty MJ, Smith MA. A PET study of 18FDG uptake in soft tissue masses. *Eur J Nucl Med* 1999; **26**: 22-30.
23. Matthies A, Hickeyson M, Cuchiara A, Alavi A. Dual time point 18F-FDG PET for the evaluation of pulmonary nodules. *J Nucl Med* 2002; **43**: 871-5.
24. Zhuang H, Pourdehnad M, Lambright ES, Yamamoto AJ, Lanuti M, Li, P et al. Dual time point 18F-FDG PET imaging for differentiating malignant from inflammatory processes. *J Nucl Med* 2001; **42**: 1412-7.
25. Mir LM, Gehl J, Sersa G, Collins CG, Garbay JR, Billard V, et al. Standard operating procedures of the electrochemotherapy: Instructions for the use of bleomycin or cisplatin administered either systemically or locally and electric pulses delivered by the Cliniporator™ by means of invasive or non-invasive electrodes. *EJC Supplements* 2006; **4**: 14-25.
26. Therasse P, Arbuck SG, Eisenhauer EA, Wanders J, Kaplan RS, Rubinstein L, et al. New guidelines to evaluate the response to treatment in solid tumors. European Organization for Research and Treatment of Cancer, National Cancer Institute of the United States, National Cancer Institute of Canada. *J Natl Cancer Inst* 2000; **92**: 205-16.
27. Young H, Baum R, Cremerius U, Herholz K, Hoekstra O, Lammertsma AA, et al. Measurement of clinical and subclinical tumour response using [18F]-fluorodeoxyglucose and positron emission tomography: review and 1999 EORTC recommendations. European Organization for Research and Treatment of Cancer (EORTC) PET Study Group. *Eur J Cancer* 1999; **35**: 1773-82.
28. Boerner AR, Weckesser M, Herzog H, Schmitz T, Audretsch W, Nitz U, et al. Optimal scan time for fluorine-18 fluorodeoxyglucose positron emission tomography in breast cancer. *Eur J Nucl Med* 1999; **26**: 226-30.
29. Caprio MG, Cangiano A, Imbriaco M, Soscia F, Di Martina G, Farina A et al. Dual-time-point [18F]-FDG PET/CT in the diagnostic evaluation of suspicious breast lesions. *Radiol Med* 2010; **115**: 215-24.
30. Weinberg IN. Applications for positron emission mammography. *Phys Med* 2006; **21** (Suppl 1): 132-37.
31. Linnert M, Iversen HK, Gehl J. Multiple brain metastases - current management and perspectives for treatment with electrochemotherapy. *Radiol Oncol* 2012; **46**: 271-78.
32. Miklavcic D, Sersa G, Breclj E, Gehl J, Soden D, Bianchi G, et al. Electrochemotherapy: technological advancements for efficient electroporation-based treatment of internal tumors. *Med Biol Eng Comput* 2012; **50**: 1213-25.
33. Mozzillo N, Caraco C, Mori S, Di Monta G, Botti G, Ascierio PA, et al. Use of neoadjuvant electrochemotherapy to treat a large metastatic lesion of the cheek in a patient with melanoma. *J Transl Med* 2012; **10**: 131.
34. Neal RE, Rossmelil JH, Jr, Garcia PA, Lanz OI, Henao-Guerrero N, Davalos RV. Successful treatment of a large soft tissue sarcoma with irreversible electroporation. *J Clin Oncol* 2011; **29**: e372-7.

Electrochemotherapy as a new therapeutic strategy in advanced Merkel cell carcinoma of head and neck region

Daniele Scelsi¹, Niccolò Mevio¹, Giulia Bertino¹, Antonio Occhini¹, Valeria Brazzelli², Patrizia Morbini³, Marco Benazzo¹

¹ Department of Otolaryngology Head Neck Surgery, ² Institute of Dermatology, ³ Department of Molecular Medicine, Section of Pathology, University of Pavia, IRCCS Policlinico S. Matteo Foundation, Pavia, Italy

Radiol Oncol 2013; 47(4): 366-369.

Received 10 May 2013
Accepted 11 July 2013

Correspondence to: Daniele Scelsi, M.D., Department of Otolaryngology Head Neck Surgery, University of Pavia, IRCCS Policlinico S. Matteo Foundation, P.le Golgi 19, 27100-Pavia (PV), Italy. E-mail: daniele.scelsi@gmail.com

Disclosure: The authors have no conflict of interest to disclose.

The paper was presented at the 7th Conference of Experimental and Translational Oncology, 20-24th April 2013, Portoroz, Slovenia (www.ceto.si) co-organised and supported by COST TD1104 Action (www.electroporation.net).

Background. Merkel Cell Carcinoma (MCC) is a rare and aggressive tumour, arising from a cutaneous mechanoreceptor cell located in the basal layer of epidermis, with poor prognosis. The treatment of choice for the initial stage of the disease is surgery and/or radiotherapy. The treatment of recurrent or advanced disease is still controversial.

Case report. We report a case of 84 years old woman with a recurrent MCC of the chin treated with electrochemotherapy (ECT). During the period of 20 months, four sessions of ECT were employed, which resulted in an objective response of the tumour and good quality of residual life.

Conclusions. Our case shows the effectiveness of ECT in the treatment of locally advanced MCC of the head and neck region in a patient not suitable for standard therapeutic options.

Key words: electrochemotherapy; head and neck cancer; Merkel cell carcinoma; palliative treatment

Introduction

Merkel Cell Carcinoma (MCC) is a rare and aggressive cancer described for the first time in 1972 by Toker *et al.*¹ Clinically it is characterized by a rapidly increasing red or bluish nodule. It frequently occurs in the head and neck area (41-50%), followed by upper and lower limbs (32-38%) and trunk (12-14%). This neuroendocrine neoplasia arises from a cutaneous mechanoreceptor cell (Merkel cell), located in the basal layer of epidermis.¹ The annual incidence in the Caucasian population is 0.23 per 100,000 individuals and 61% of these cases are men. MCC affects more frequently elderly and immunocompromised patients with a previously history of damaging sun exposure.² The prognosis

is poor due to the fast local growth and high local recurrence, regional lymph node metastases and distant metastases rates, occurring even after the prompt treatment.³

The main treatment modality for the early stage tumours is surgery and/or radiotherapy, while chemotherapy with etoposide and cisplatin or carboplatin finds a role only in patients with systemic metastases. Due to the low incidence of MCC, the experiences with recurrent lesions or advanced stage tumours are scarce.^{3,4}

We report the case of a 84 years old woman affected by a extensive recurrence of MCC of the chin treated with multiple sessions of electrochemotherapy (ECT).

Case report

A 84 years old woman with hypertension, chronic vascular disease, chronic cardiac ischemia was admitted because of a dome-shaped bluish skin lesion in her chin of 2x2 cm, characterized by rapid growth. A skin biopsy showed poorly differentiated cells with scarce cytoplasm and vesicular nuclei with inconspicuous nucleoli. High mitotic index and apoptotic figures were present. Immunohistochemical reactions were positive for cytokeratin 8 and 20 and neuroendocrine markers chromogranin, synaptophysin and CD56/N-CAM; TTF-1 was not expressed. A diagnosis of MCC was established (Figure 1).

Total body computed tomography scan and bone scintigraphy excluded mandibular infiltration, regional or systemic metastases. The lesion was staged cT2N0M0. The patient underwent surgical excision of the tumour, bilateral selective neck dissection (levels I-III) and reconstruction with radial forearm free flap. The histopathological examination of resected specimen confirmed a stage IIA (pT2N0M0) MCC and surgical margins free of tumour. The patient refused proposed postoperative radiotherapy, whereas the systemic therapy was not indicated due to co-morbidities.

Two months after the treatment, mass in the area of previous surgery extending into a submandibular region was documented. A biopsy of the mass confirmed recurrent MCC (Figure 2). The re-operation was not an option because of the tumour extension, and radiotherapy was again refused by the patient. She was offered a palliative treatment with ECT. The treatment was performed according to the standard operating procedures of the ESOPE.⁵ Intravenous bleomycin infusion of 15.000 IU/m² was administered eight minutes before delivery of electric pulses under general anaesthesia by means of a hexagonal electrode (length 25 mm) connected to a generator (Cliniporator™ - IGEA srl, Carpi, [MO], Italy). The lesion with 1 cm tumour-free margin was treated by multiple direct insertions of the electrode. The pulses were completed within 28 minutes after the infusion of bleomycin.

The patient was evaluated four weeks after the treatment: 50% reduction of the original tumour volume was observed, corresponding to a partial response according to RECIST criteria.⁶ The next ECT treatment resulted in 80% volume reduction compared to the original lesion (Figure 3).

Due to the good response and tolerability of the procedure, two additional ECT treatments were performed during the following sixteen months,

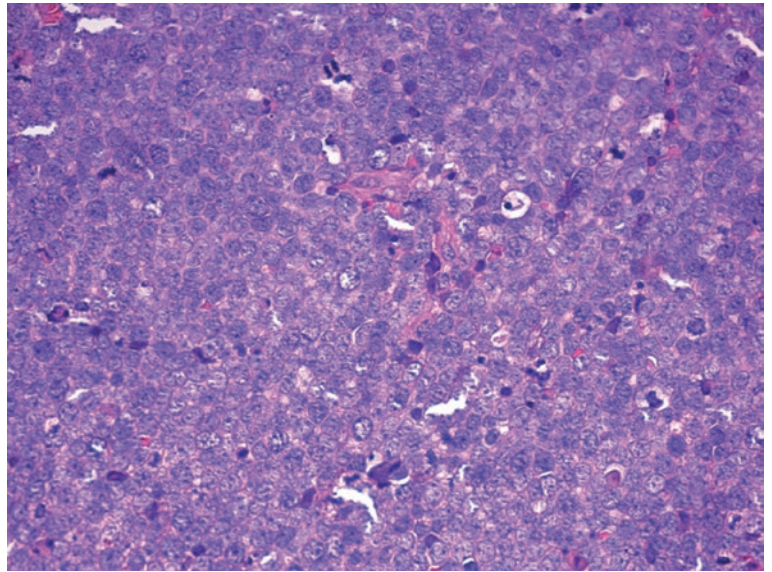


FIGURE 1. Tumour biopsy showing poorly differentiated cells with scarce cytoplasm and vesicular nuclei with inconspicuous nucleoli. High mitotic index and apoptotic figures were present. Immunohistochemical reactions were positive for cytokeratin 8 and 20 and neuroendocrine markers (chromogranin, synaptophysin and CD56/N-CAM); TTF-1 was not expressed (H&E stain, 40x).



FIGURE 2. Before first electrochemotherapy: voluminous bluish lesion of the chin.



FIGURE 3. Reduction of 80% of the volume to the initial lesion after 2 treatments.



FIGURE 4. Follow up after four electrochemotherapy applications and 16 months.

which resulted in a good local control of the tumour (Figure 4).

Unfortunately, just after the fourth ECT treatment (and 20 months after the first ECT session), lung metastases were diagnosed. The patient died one month later due to heart failure which was unrelated to MCC.

No major complications were observed during or after ECT treatments. The only recorded side effect was moderate pain after the first ECT session, easily managed with peroral non-opioids. The patient reported a good quality of life until the last two months before she died when severe pain, controlled by opioids, appeared.

Discussion

The management of patients with MCC of the head and neck region is still challenging due to poor prognosis. According to the National Comprehensive Cancer Network guidelines⁷, surgery is commonly considered the treatment of choice and significantly improves the overall survival, if associated with adjuvant radiotherapy.⁸ In the head and neck area where it is difficult to obtain safety margins wide enough, radiotherapy can be the first treatment option.³ Because of the high incidence of occult regional metastasis, patients with clinical and radiographically negative necks should undergo elective dissection, irradiation, or preferably sentinel lymph node biopsy. Chemotherapy is an option for patients with an incurable recurrent, heavily pre-treated disease or for those with systemic metastases although without proven effect on the overall survival.⁹

In the last years, ECT has been proposed as a novel therapeutic weapon for the control of recurrent cutaneous, subcutaneous or mucosal neoplastic lesions of different histologies.⁵ In the literature, few data exist about the effectiveness of this procedure in the treatment of head and neck cancers; the reported rates of objective response (OR) seem promising, ranging from 56% to 100%, depending on the tumour size.¹⁰⁻¹⁶ To the best of our knowledge there is only one case of MCC treated with ECT documented in the literature. The authors reported a complete response (CR) of the tumour to ECT after a follow up time of six months.¹²

The choice of using ECT in our patient was determined by the existing comorbidities and the patient's refusal of radiotherapy. With ECT we were able to reach a good local tumour control, with no significant adverse events, nor functional or aesthetic, which resulted in a good quality of the rest of her life. This case demonstrates that ECT can be considered as an effective palliative treatment option for patients with recurrent or advanced-stage tumour, not suitable for conventional treatments.¹⁰⁻¹⁴

References

1. Toker C. Trabecular carcinoma of the skin. *Arch Dermatol* 1972; **105**: 107-10.
2. Pellitteri PK, Takes RP, Lewis JS Jr, Devaney KO, Harlor EJ, Strojan P, et al. Merkel cell carcinoma of the head and neck. *Head Neck* 2012; **34**: 1346-54.
3. Pectasides D, Pectasides M, Economopoulos T. Merkel cell cancer of the skin. *Ann Oncol* 2006; **17**: 1489-95.
4. Eng TY, Boersma MG, Fuller CD, Cavanaugh SX, Valenzuela F, Hermann TS. Treatment of merkel cell carcinoma. *Am J Clin Oncol* 2004; **27**: 510-5.
5. Mir LM, Gehl G, Sersa G, Collins C, Garbay G-R, Billard V, et al. Standard operating procedures of the electrochemotherapy: Instructions for the use of bleomycin or cisplatin administered either systemically or locally and electric pulses delivered by the Cliniporator™ by means of invasive or non-invasive electrodes. *EJC Suppl* 2006; **4**: 14-25.
6. Eisenhauer EA, Therasse P, Bogaerts J, Schwartz LH, Sargent D, Ford R, et al. New response evaluation criteria in solid tumours: revised RECIST guideline (version 1.1). *Eur J Cancer* 2009; **45**: 228-47.
7. National Comprehensive Cancer Network, NCCN Guidelines™, Version 1.2012, Merkel Cell Carcinoma. Available at: <http://www.merkelcell.org/usefullinfo/documents/NccnMcc2012.pdf>
8. Tai PT, Yu E, Tonita J, Gilchrist J. Merkel cell carcinoma of the skin. *J Cutan Med Surg* 2000; **4**: 186-95.
9. Suarez C, Rodrigo JP, Ferlito A, Devaney KO, Rinaldo A. Merkel cell carcinoma of the head and neck. *Oral Oncol* 2004; **40**: 773-9.
10. Gargiulo M, Moio M, Monda G, Parascandolo S, Cubicotti G. Electrochemotherapy: actual considerations and clinical experience in head and neck cancers. *Ann Surg* 2010; **251**: 773.
11. Panje WR, Hier MP, Garman GR, Harrel E, Goldman A, Bloch I. Electroporation therapy of head and neck cancer. *Ann Otol Rhinol Laryngol* 1998; **107**: 779-85.
12. Curatolo P, Mancini M, Clerico R, Ruggiero A, Frascione P, Di Marco P, et al. Remission of extensive Merkel cell carcinoma after electrochemotherapy. *Arch Dermatol* 2009; **145**: 494-5.
13. Sersa G. The state-of-the-art of electrochemotherapy before the ESOPE study; advantages and clinical uses. *EJC Suppl* 2006; **4**: 52-9.
14. Mevio N, Bertino G, Occhini A, Scelsi D, Tagliabue M, Mura F, et al. Electrochemotherapy for the treatment of recurrent head and neck cancers: preliminary results. *Tumori* 2012; **98**: 308-13.
15. Landström FJ, Nilsson CO, Crafoord S, Reinzenstein JA, Adamsson GB, Löfgren LA. Electroporation therapy of skin cancer in the head and neck area. *Dermatol Surg* 2010; **36**: 1245-50.
16. Mali B, Miklavcic D, Campana LG, Cemazar M, Sersa G, Snoj M, et al. Tumor size and effectiveness of electrochemotherapy. *Radiol Oncol* 2013; **47**: 32-41.

Minimally invasive treatment of peristomal metastases from gastric cancer at an ileostomy site by electrochemotherapy

Luca G. Campana¹, Marco Scarpa², Antonio Sommariva¹, Elena Bonandini³, Sara Valpione⁴, Leonardo Sartore⁵, Carlo R. Rossi¹

¹ Sarcoma and Melanoma Unit, Veneto Institute of Oncology (IOV-IRCCS), Padova, Italy

² Surgical Oncology Unit, Veneto Institute of Oncology (IOV-IRCCS), Padova, Italy

³ Department of Pathology, University of Padova, Padova, Italy

⁴ Melanoma Cancer Unit, Veneto Institute of Oncology (IOV-IRCCS), Padova, Italy

⁵ Plastic Surgery Unit, University of Padova, Padova, Italy

Radiol Oncol 2013; 47(4): 370-375.

Received 3 June 2013

Accepted 2 July 2013

Correspondence to: Luca G. Campana, M.D. Ph.D., Veneto Oncology Institute (IOV-IRCCS), Via Gattamelata, 64 - 35128, Padova, Italy, Phone: +39(0)49.8215526; Fax: +39(0)49.8218349; Mail: maximizing@hotmail.com

Disclosure: No potential conflicts of interest were disclosed.

The paper was presented at the 7th Conference of Experimental and Translational Oncology, 20-24th April 2013, Portoroz, Slovenia (www.ceto.si) coorganised and supported by COST TD1104 Action (www.electroporation.net).

Background. Peristomal metastases are rare, but potentially associated with relevant morbidity. Surgical resection, followed by stoma relocation, represent the gold standard in most patients. We describe electrochemotherapy (ECT), a minimally invasive method for locally-enhancing drug delivery by means of electric pulses, as an alternative approach.

Patient and methods. A 49-year-old man with advanced gastric cancer developed skin metastases around an ileostomy site. The ulcerated and oozing tumor growth impaired patient's quality of life due to continuous trouble in fitting the ostomy appliance, its poor adherence and consequent stools spillage. ECT consisted of a 20-minute course under mild general sedation. A bleomycin bolus of 15 000 IU/m² was followed by the percutaneous application of multiple, 1.5 ms -long electric pulses by means of a needle electrode.

Results. Post ECT course was uneventful and the patient was discharged on the same day. After one week, tumor nodules were flattened and partial tumor regression was appreciable at one-month follow-up. More importantly, peristomal skin conditions significantly improved, thus allowing for an effective application of the ostomy appliance during the following months, until patient's death.

Conclusions. This report suggests the feasibility of ECT as a minimally invasive approach for peristomal tumors. In selected cases, ECT, by achieving a rapid tumor control, may ensure effective ostomy management and preserve patients' quality of life.

Key words: stomach neoplasms; ileostomy; electrochemotherapy; skin care; palliative care

Introduction

Despite the introduction of combined treatment strategies, gastric cancer (GC) remains one of the leading causes of cancer-related death worldwide.¹ The most common metastatic sites are lymph nodes, liver, ovary and peritoneal cavity. The oc-

currence of skin metastases is a rare event, generally found at a very late stage of disease²⁻⁴ and, occasionally, as the initial clinical manifestation.⁵⁻⁸ Isolated superficial metastases have been also described following invasive procedures (*i.e.* laparoscopic surgery).^{9,10} Peristomal metastases represent an even rarer, but challenging finding, due to pos-

sible bowel obstruction and trouble in ostomy management. Wide local excision and stoma relocation, when feasible, represent the gold standard treatment for these patients. Unfortunately, only few of them are still considered resectable when skin metastases occur, due to disease extension and poor general conditions. Electrochemotherapy (ECT) is a minimally-invasive approach which is gaining increasing acceptance in patients with unresectable or refractory superficial metastases, thanks to its sustained antitumor activity in different tumor histotypes, rapid patient's recovery and favorable short-term outcomes.^{11,12} ECT mechanism relies on the association of an anticancer agent, bleomycin (BLM) or cisplatin (CDDP), with transient tumor permeabilization by means of brief, high-voltage, electric pulses (electroporation).¹³ The drug can be administered as an intravenous bolus or, alternatively, by the intratumoral route, according to disease burden.¹⁴ Tumor electroporation is achieved by the application of suitable plate or needle electrodes. Electric pulses open multiple, reversible pores on cell membrane, throughout which an increased number of chemotherapy molecules entry into the cell and exert their selective cytotoxic activity (Figure 1). We here report on the first case featuring ECT as an alternative treatment in a patient with symptomatic skin metastases from GC at an ileostomy site.

Case report

A 49-year-old man with peritoneal carcinomatosis from GC, who previously required the construction of an end-ileostomy due to bowel obstruction, presented with multiple peristomal metastases that were confluent in a 10 x 10 cm area on the abdominal wall (Figure 2). In 2008 the patient was diagnosed with stage IV GC with peritoneal dissemination. He received 3 cycles of epirubicin, oxaliplatin and 5-fluorouracil, before undergoing total gastrectomy, D2 lymphadenectomy, distal pancreatectomy and splenectomy. Histopathological examination was T4aN3aM1, signet ring cells, HER2 negative, gastric adenocarcinoma. Additional 5 cycles of adjuvant chemotherapy were administered after surgical treatment. In April 2010, chemotherapy with epirubicin, oxaliplatin and 5-fluorouracil was started and then shifted to docetaxel, cisplatin plus 5-fluorouracil. In September 2011, an ileostomy was created in the lower right abdominal quadrant in order to palliate the progressively worsening symptoms of bowel obstruction. Third line

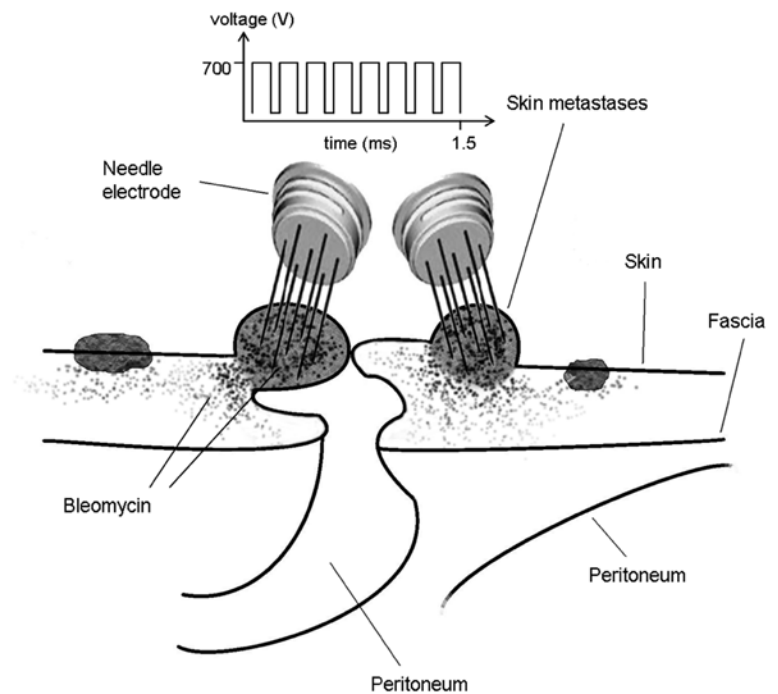


FIGURE 1. Electrochemotherapy of peristomal skin metastases. Eight minutes after intravenous injection, bleomycin molecules are equally distributed in body tissues. Tumor nodules are briefly exposed to a train of eight consecutive, high voltage (1000 V/cm), square-wave, 100-ms electric pulses, delivered at a repetition frequency of 5000 Hz by means of a needle electrode inserted into tumor tissue and connected to a pulse generator. As a consequence, transient pores open on the cell membrane and enable bleomycin concentration and entrapment, thus increasing its cytotoxic activity.

monochemotherapy with irinotecan was ongoing at the time of our first evaluation, on October 2011. Given patient's low performance status according to the Eastern Cooperative Oncology Group scale, peritonectomy associated with intraperitoneal chemotherapy was deemed contraindicated. On the other hand, peristomal tumor growth was highly symptomatic, since cutaneous metastases caused a continuous burning sensation that was exacerbated by the contact with liquid and slightly caustic stools at the ileostomy site. Moreover, tumor nodules were oozing and partially bleeding and the abundant exudate engendered continuous troubles in ileostomy management, due to difficult application of the pouching bag. At physical examination, ileostomy outer mucosa appeared macroscopically normal (Figure 2B). Mild stricture was present, but repetitive manual expansions maintained its patency and digital exploration was negative for tumor infiltration. ECT was offered with a palliative intent to improve disease-related complaints and everyday ileostomy management. The patient signed an informed consent.



FIGURE 2. Peristomal skin tumor infiltration from gastric cancer at the ileostomy site. Baseline clinical presentation (A, B). The histological examination (E.E.) showed a dermal infiltration of neoplastic cells with atypical and eccentric nuclei, with nucleoli and pale cytoplasm and a signet ring aspect (C), immunoreaction for CAM5.2 (D).



FIGURE 3. Electrochemotherapy treatment. The patient in the operating room and the electric pulse generator (arrow) (A). The ECT field (B). The application of electric pulses by means of the needle electrode (arrow) (C). Early postoperative skin conditions, with slight erythema at the electrode insertion sites (arrowheads) and partial tumor bluish coloration due to voltage-induced vasoconstriction (arrows) (D).

ECT procedure lasted 20 min and was performed under mild general sedation (Figure 3A). Tumor site was rinsed and prepared with sterile drapes; a silicon tube was placed into the ileostomy in order to drain stools and keep the operative field clean. (Figure 3B) Chemotherapy consisted of an intravenous bolus of BLM (15 000 IU/m²). After 8 minutes, necessary for drug biodistribution in accordance

with the European Standard Operating Procedures on Electrochemotherapy (ESOPE)¹⁵, electric pulses were delivered by percutaneously inserting a 2-cm long needle electrode into skin nodules (Figure 3C). The electrode is composed of seven metal needles arranged in a hexagonal fashion (Figure 1) and is maneuvered by means of a handle connected to an electric pulse generator (Cliniporator™, Igea, Modena, Italy) (Figure 3A). Complete tumor coverage was achieved by means of multiple electrode placements delivering a 1.5 ms-long electric pulse. At the end of the procedure, local toxicity consisted of slight skin marks at the site of electrode insertion (Figure 3D). There was no sign of bleeding, rather the thicker portion of the tumor turned to a bluish coloration due to local vasoconstriction (Figure 3D). After treatment, electroporated skin was carefully cleaned and covered with a healing powder (Figure 4A). Moreover, a custom-sized hydrocolloid dressing (DuoDERM®, ConvaTech, Inc.) was applied over the ECT field (Figure 4B) and the space between ileostomy and peristomal skin was sealed by means of a stoma paste (Stomahesive® Paste, ConvaTech, Inc.) in order to prevent stools leakage over inflamed tissues (Figure 3C). Additionally, a silicon catheter was placed into the stoma in order to drain stools directly into the ostomy bag (Figure 4 C,D). The postoperative course was uneventful and the patient was discharged on the same day with the prescription for a course of metronidazole plus ciprofloxacin prophylactic therapy. After one week, tumor nodules were significantly flattened (Figure 5A). Skin care consisted of hydrocolloid dressing application combined with stools deviation by means of a silicon tube (Figure 5B). After three weeks, physical examination showed a normal appearing stoma with adjacent mild erythema and partially necrotic skin from the 12-o'clock to the 7-o'clock position (Figure 5C). Tumor nodules were partially regressed and electroporated skin was healing and dry, thus allowing for easy application and effective sealing of the ostomy flange and pouching bag (Figure 5D). The ileostomy function remained normal throughout this period and no sign of infection was present. In January 2011, one month after treatment, the patient returned to the outpatient clinic for a minor surgical debridement, during which the necrotic crusts were removed, leaving an underlying intact tissue that was suitable for the application of the ostomy flange. The ileostomy maintained its patency and, importantly, the adherence of the stoma appliance was preserved during the following four months, until patient's death.

Discussion

Peristomal tumors represent a rare late complication of surgery for gastrointestinal cancers¹⁶⁻¹⁸ and inflammatory bowel diseases.¹⁹⁻²² Sporadically, peristomal metastases have been reported also in patients with head and neck^{23,24} and genitourinary tumors.²⁵ Besides harboring the risk of possible stoma obstruction, these lesions may interfere with peristomal skin care and application of the pouching systems. In patients with bowel deviation, all the conditions that produce a less than perfect adhesion of the stoma appliance may cause direct contact between stools and peristomal skin, thus affecting patient's quality of life.^{26,27} In fact, even minor consequences, such as peristomal dermatitis, need extra medical care that may significantly impair ostomy everyday management, patients' autonomy and ultimately increase the costs of the procedure.^{27,29} Wide local resection followed by stoma resiting, when feasible, represent the only potential effective treatment for peristomal metastases. Unfortunately, in our patient en bloc resection of the stoma together with surrounding soft tissues would have required abdominal wall repair by means of a complex reconstructive technique (*i.e.* long groin flap, anterolateral thigh flap or latissimus dorsi flap) that would have been likely associated with relevant morbidity in a patient with peritoneal carcinomatosis and poor general conditions. On the contrary, ECT procedure proved feasible and well tolerated. It ensured rapid local tumor control thus proving effective in palliating disease-related complaints. A single course of treatment led to an appreciable flattening of peristomal tumor nodules. As a result, the improved peristomal skin conditions allowed for the effective application of ileostomy bag and prevented stools spillage on the abdominal wall.

Since local inflammatory reaction and soft tissue ulceration are possible side effects of ECT application^{30,31}, one challenging aspect was played by peristomal skin protection from the ileostomy outflow. Our management strategy aimed at separating the electroporated skin from stools. For this purpose, a smooth silicon drain was placed into the ileostomy during the procedure and the first postoperative course. Moreover, a hydrocolloid dressing proved to be an effective barrier and a reliable support for the flange of the pouching system.

It is not clear to us why, despite the rapid and homogeneous tumor response after one week (Figure 4A), afterwards local response was rather inhomogeneous and some portions of the tumor

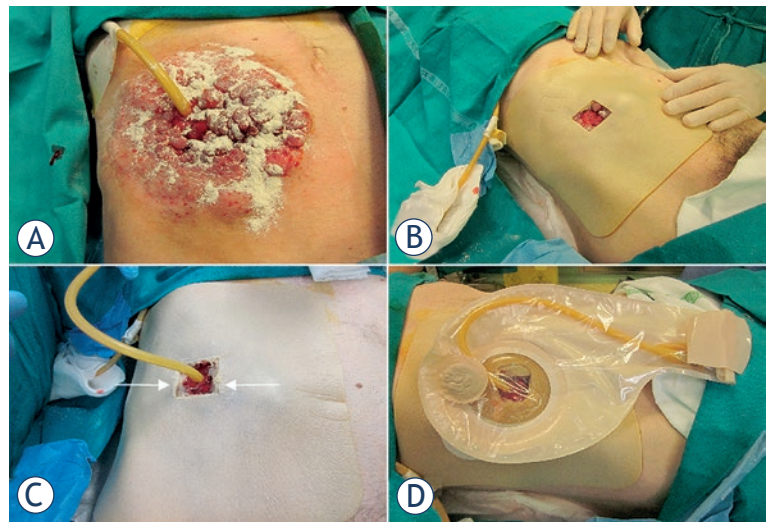


FIGURE 4. Post treatment wound dressing. Stoma powder application to absorb moisture from broken skin (A). Covering with an hydrocolloid dressing (B). Insertion of a silicon tube into the stoma to drain the stools and sealing of the hydrocolloid dressing with a stoma paste (arrows) (C). Effective application and sealing of the ileostomy flange and bag (D).

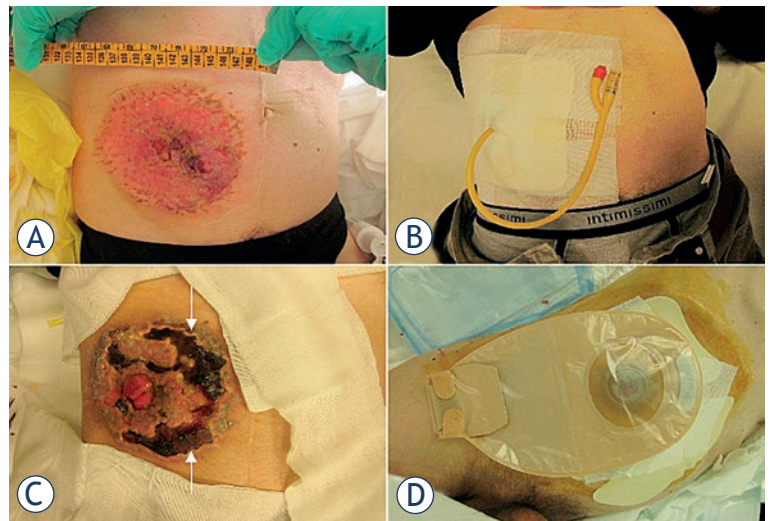


FIGURE 5. Follow-up. Clinical presentation one week after ECT (A). Application of the ileostomy bag on the hydrocolloid dressing (B). Clinical presentation three weeks after ECT (C). Effective application of the ileostomy bag on the abdominal wall (D).

were clearly necrotic, while others not (Figure 4C). Although BLM was given intravenously, in accordance with ESOPE guidelines¹⁴ which recommend systemic drug administration in case of multiple or large tumors, the irregular tumor vascularization and consequent inhomogeneous drug distribution could explain the jeopardized response to treatment in our patient.

TABLE 1. Primary peristomal skin/soft tissues tumors: summary of case reports from literature review

Author (year)	Disease	Ostomy	Interval (years)	Clinical presentation	Histotype	Treatment	Follow-up
Didolkar ³³ (1975)	RC	C	33	4-cm size peristomal ulceration	BCC	WLE + stoma resiting + split-thickness skin graft	2.5 years
O'Connell ³⁴ (1987)	CD	I	39	painful peristomal ulceration, 3.0 x 2.5 fungating lesion	SCC	WLE + stoma resiting + skin flap transposition	3 months
Wu ³⁵ (2000)	UC	I	44	Painful, 10-cm size, peristomal skin lesion	SCC	WLE + stoma resiting	1 year
Ramanujam ³⁶ (2002)	UC	I	51	4x3 cm peristomal ulcer, peristomal discomfort and bleeding	SCC	WLE + stoma resiting	28 months
Sewell ³⁷ (2008)	RC	C	33	slowly growing, ulcerated parastomal nodule	BCC	MMS	16 years
Fessa ³⁸ (2010)	RC	C	12	progressive erythematous patch	AS	WLE + stoma resiting	nr
Liu ³⁹ (2012)	UC	I	33	oozing peristomal erosions, difficult adherence of stoma appliance	Pageť	WLE + stoma revision	nr

Abbreviations: RC = rectal carcinoma; CD = Crohn disease; C = colostomy; BCC = basal cell carcinoma; WLE = wide local excision; I = ileostomy; SCC = squamous cell carcinoma; UC = ulcerative colitis; MMS = Mohs micrographic surgery; AS = angiosarcoma; nr = not reported

ECT has been recognized as a safe and effective option for patients with superficially disseminated metastases, mainly from malignant melanoma and breast cancer.^{30,31} Interestingly, several other tumor histotypes seem to be sensitive to electroporation-driven chemotherapy, thus potentially expanding the number of eligible patients.¹¹ If its efficacy and feasibility will be further confirmed, ECT could represent not only a valuable palliative option for peristomal metastases, but also an effective treatment for those patients with primary skin / soft tissue tumors arising at any ostomy site. Although rare, the occurrence of peristomal primary tumors have been described, especially in the setting of colorectal cancer or inflammatory bowel diseases (Table 1).³²⁻³⁸

Waiting for more evidence, in our opinion some precautions should be taken when applying ECT to peristomal lesions. First, since some peristomal tumors may represent metachronous intestinal cancers, which are not amenable with current ECT equipment (due to feasibility of electrode application and possible damage to intestinal wall), pre-operative clinical or endoscopic evaluation seems mandatory. Second, electrode insertion should be extremely careful and possibly image-guided, in order to avoid direct physical damage or late cytotoxic effects to the stoma. Finally, the assistance of an ostomy nursing staff represent a precious support to ensure adequate skin care and pouching system management.

In conclusion, we applied, for the first time, ECT in a very rare, but morbid condition such as skin tumor infiltration from GC at an ileostomy site. A single 20-minute treatment course led to rapid

tumor control, prevented stoma obstruction and improved peristomal skin conditions, thus ensuring effective application of the stoma flange and its long-term (as in a palliative setting) maintenance, without stools leakage. These results significantly improved patient's quality of life.

Acknowledgments

Fernando Gaion, MD, Medical Oncology Unit, and Ostomy Nursing Staff of Azienda ULSS 15 – Alta Padovana, Camposampiero, Italy, for the precious assistance in patient's care. Mr Matteo Vescuso, Anesthesiology Unit, Veneto Oncology Institute, Padova, Italy, for technical support.

The work described in this paper was supported by "Piccoli Punti" (www.piccolipunti.it), a charity supporting cancer research at Melanoma and Sarcoma Unit, Veneto Institute of Oncology, Padova.

References

- Guggenheim DE, Shah MA. Gastric cancer epidemiology and risk factors. *J Surg Oncol* 2013; **107**: 230-36.
- Gates O. Cutaneous metastases of malignant disease. *Am J Cancer* 1937; **30**: 718-30.
- Alcaraz I, Cerroni L, Rütten A, Kutzner H, Requena L. Cutaneous metastases from internal malignancies: a clinicopathologic and immunohistochemical review. *Am J Dermatopathol* 2012; **34**: 347-93.
- Takata T, Takahashi A, Tarutani M, Sano S. A rare case of cellulitis-like cutaneous metastasis of gastric adenocarcinoma. *Int J Dermatol* 2013; Epub ahead of print; doi: 10.1111/j.1365-4632.2012.05498.x.
- Qiao J, Fang H. Cutaneous nodule in a young man. *JAMA* 2012; **308**: 812-3.

6. Ozakyol AH, Sariçam T, Paşaoğlu O. A rare entity: cutaneous metastasis from gastric adenocarcinoma. *Am J Gastroenterol* 1999; **94**: 1118-9.
7. Sood A, Midha V, Sekhon JS, Sidhu SS. Generalized cutaneous metastases from carcinoma stomach. *Am J Gastroenterol* 1998; **93**: 1601.
8. Choi HM, Myung KB, Kook HI. Cutaneous metastatic adenocarcinoma of stomach: nodular and inflammatory carcinoma. *J Korean Med Sci* 1986; **1**: 49-52.
9. Früh M, Ruhstaller T, Neuweiler J, Cerny T. Resection of skin metastases from gastric carcinoma with long-term follow-up: an unusual clinical presentation. *Onkologie* 2005; **28**: 38-40.
10. García-González E, Alvarez-Paque L, Loyola-Zárate M, Lisker-Melman M. Seeding of gastric adenocarcinoma cells to the skin after invasive procedures. *J Clin Gastroenterol* 1998; **26**: 82-4.
11. Mali B, Jarm T, Snoj M, Sersa G, Miklavcic D. Antitumor effectiveness of electrochemotherapy: a systematic review and meta-analysis. *Eur J Surg Oncol* 2013; **39**: 4-16.
12. Sadadcharam M, Soden DM, O'sullivan GC. Electrochemotherapy: an emerging cancer treatment. *Int J Hyperthermia* 2008; **24**: 263-73.
13. Gothelf A, Mir LM, Gehl J. Electrochemotherapy: results of cancer treatment using enhanced delivery of bleomycin by electroporation. *Cancer Treat Rev* 2003; **29**: 371-87.
14. Mir LM, Gehl J, Sersa G, Collins CG, Garbay JR, Billard V, et al. Standard operating procedures of the Electrochemotherapy: instructions for the use of bleomycin or cisplatin administered either systemically or locally and electric pulses delivered by the Cliniporator by means of invasive or non-invasive electrodes. *EJC Suppl* 2006; **4**: 14-25.
15. Cava A, Román J, González Quintela A, Martín F, Aramburo P. Subcutaneous metastasis following laparoscopy in gastric adenocarcinoma. *Eur J Surg Oncol* 1990; **16**: 63-7.
16. Townley WA, Kothari MS, Meyrick-Thomas J. Metachronous stomal adenocarcinoma following abdominoperineal resection for rectal cancer. *Ann R Coll Surg Engl* 2005; **87**: 1-3.
17. Greenberg HL, Lopez L, Butler DF. Peristomal metastatic adenocarcinoma of the rectum. *Arch Dermatol* 2006; **142**: 1372-3.
18. Vijayasekar C, Noormohamed S, Cheetham MJ. Late recurrence of large peri-stomal metastasis following abdomino-perineal resection of rectal cancer. *World J Surg Oncol* 2008; **6**: 96.
19. Cuesta MA, Donner R. Adenocarcinoma arising at an ileostomy site: report of a case. *Cancer* 1976; **37**: 949-52.
20. Smart PJ, Sastry S, Wells S. Primary mucinous adenocarcinoma developing in an ileostomy stoma. *Gut* 1988; **29**: 1607-12.
21. Quah HM, Samad A, Maw A. Ileostomy carcinomas a review: the latent risk after colectomy for ulcerative colitis and familial adenomatous polyposis. *Colorectal Dis* 2005; **7**: 538-44.
22. Achneck HE, Wong IY, Kim PJ, Fernandes MA, Walther Z, Seymour NE, Jain D. Ileostomy adenocarcinomas in the setting of ulcerative colitis. *J Clin Gastroenterol* 2005; **39**: 396-400.
23. el Shennawy M, Fayek A, el Sharkawy L. A study of peristomal recurrence. *Rev Laryngol Otol Rhinol (Bord)* 2000; **121**: 117-20.
24. Fagan JJ, Loock JW. Tracheostomy and peristomal recurrence. *Clin Otolaryngol Allied Sci* 1996; **21**: 328-30.
25. Yoshida T, Takayama H, Uemura M, Nakai Y, Nonomura N, Tsujimura A. Solitary skin metastasis adjacent to ureterocutaneostomy 4 years after radical cystectomy for bladder cancer. *Jpn J Clin Oncol* 2012; **42**: 331-4.
26. Scarpa M, Ruffolo C, Boetto R, Pozza A, Sadocchi L, Angriman I. Diverting loop ileostomy after restorative proctocolectomy: predictors of poor outcome and poor quality of life. *Colorectal Disease* 2010; **12**: 914-20.
27. Scarpa M, Sadocchi L, Ruffolo C, Iacobone M, Filosa T, Prando D, et al. Rod in loop ileostomy: just an insignificant detail for ileostomy-related complications? *Langenbecks Arch Surg* 2007; **392**: 149-54.
28. Carlsen E, Bergen AB. Loop ileostomy: technical aspects and complications. *Eur J Surg* 1999; **165**: 140-3.
29. McLeod RS, Lavery IC, Leatherman JR, Maryland PA, Fazio VW, Jagelman DG, et al. Factors affecting quality of life with a conventional ileostomy. *World J Surg* 1986; **10**: 474-80.
30. Campana LG, Mocellin S, Basso M, Puccetti O, De Salvo GL, Chiarion-Sileni V, et al. Bleomycin-based electrochemotherapy: clinical outcome from a single institution's experience with 52 patients. *Ann Surg Oncol* 2009; **16**: 191-9.
31. Campana LG, Valpione S, Falci C, Mocellin S, Basso M, Corti L, et al. The activity and safety of electrochemotherapy in persistent chest wall recurrence from breast cancer after mastectomy: a phase-II study. *Breast Cancer Res Treat* 2012; **134**: 1169-78.
32. Didolkar MS, Douglass HO, Holyoke ED, Elias EG. Basal-cell carcinoma originating at the colostomy site: report of a case. *Dis Colon Rectum* 1975; **18**: 399-402.
33. O'Connell PR, Dozois RR, Irons GB, Scheithauer BW. Squamous cell carcinoma occurring in a skin-grafted ileostomy stoma. Report of a case. *Dis Colon Rectum* 1987; **30**: 475-8.
34. Wu JS, Sebek BA, Fazio VW. Images for surgeons. Parastomal squamous cell carcinoma in an ileostomy 44 years after proctocolectomy. *J Am Coll Surg* 2000; **191**: 107.
35. Ramanujam P, Venkatesh KS. An unusual case of squamous cell carcinoma arising at the stomal site: case report and review of the literature. *J Gastrointest Surg* 2002; **6**: 630-1.
36. Sewell LD, Marks VJ. Excision of a peristomal basal cell carcinoma using Mohs micrographic surgery. *Dermatol Surg* 2008; **34**: 971-3.
37. Fessa CK, Sharma R, Fernández-Peñas P. Cutaneous epithelioid angiosarcoma occurring at a peristomal site. *J Am Acad Dermatol* 2010; **63**: e55-6.
38. Liu X, Melton GB, Xie H, Dietz DW. Extramammary Paget disease in peristomal skin: report of a unique case. *J Gastrointest Surg* 2012; **16**: 1967-71.

Effect of ionizing radiation on human skeletal muscle precursor cells

Mihaela Jurdana¹, Maja Cemazar^{1,2}, Katarina Pegan^{3,4}, Tomaz Mars³

¹ University of Primorska, Faculty of Health Science, Izola, Slovenia

² Institute of Oncology Ljubljana, Department of Experimental Oncology, Ljubljana, Slovenia

³ University of Ljubljana, Faculty of Medicine, Institute of Pathophysiology, Ljubljana, Slovenia

⁴ Jožef Stefan Institute, Department of Biochemistry, Molecular and Structural Biology, Ljubljana, Slovenia

Radiol Oncol 2013; 47(4): 376-381.

Received 28 May 2013

Accepted 23 August 2013

Correspondence to: Tomaž Marš, M.D., Ph.D., Institute of Pathophysiology, Faculty of Medicine, University of Ljubljana, Zaloška cesta 4, SI-1000 Ljubljana, Slovenia. E-mail: tomaz.mars@mf.uni-lj.si

Disclosure: The authors have no conflict of interest to disclose.

The paper was presented at the 7th Conference of Experimental and Translational Oncology, 20-24th April 2013, Portoroz, Slovenia (www.ceto.si) co-organised and supported by COST TD1104 Action (www.electroporation.net).

Background. Long term effects of different doses of ionizing radiation on human skeletal muscle myoblast proliferation, cytokine signalling and stress response capacity were studied in primary cell cultures.

Materials and methods. Human skeletal muscle myoblasts obtained from muscle biopsies were cultured and irradiated with a Darpac 2000 X-ray unit at doses of 4, 6 and 8 Gy. Acute effects of radiation were studied by interleukin – 6 (IL-6) release and stress response detected by the heat shock protein (HSP) level, while long term effects were followed by proliferation capacity and cell death.

Results. Compared with non-irradiated control and cells treated with inhibitor of cell proliferation Ara C, myoblast proliferation decreased 72 h post-irradiation, this effect was more pronounced with increasing doses. Post-irradiation myoblast survival determined by measurement of released LDH enzyme activity revealed increased activity after exposure to irradiation. The acute response of myoblasts to lower doses of irradiation (4 and 6 Gy) was decreased secretion of constitutive IL-6. Higher doses of irradiation triggered a stress response in myoblasts, determined by increased levels of stress markers (HSPs 27 and 70).

Conclusions. Our results show that myoblasts are sensitive to irradiation in terms of their proliferation capacity and capacity to secrete IL-6. Since myoblast proliferation and differentiation are a key stage in muscle regeneration, this effect of irradiation needs to be taken into account, particularly in certain clinical conditions.

Key words: myoblasts; irradiation; proliferation; interleukin 6; muscle regeneration; apoptosis

Introduction

Maintenance of skeletal muscle mass and function depends on the process of muscle regeneration and the ability of satellite cells to activate into proliferative myoblasts, key cells responsible for muscle lesion repair and reconstruction.¹ Myokine interleukin 6 (IL-6) is released from activated myoblasts in response to injury and IL-6 is an important factor promoting myoblast proliferation and differentiation during muscle regeneration.²⁻⁵ Several studies have investigated radiation effects on skeletal mus-

cle, demonstrating that skeletal muscle damage after irradiation remains for many years. Adult skeletal muscle is considered to be radiation resistant, unless higher doses of radiation are applied.⁶⁻¹¹ However, radiation directly inhibits muscle regeneration by damaging satellite cells, which can lead to mitotic failure and cell death.¹² Impaired muscle regeneration following irradiation may thus be due to an insufficient number of activated satellite cells needed for fusion and repair of damaged muscle fibre. The lack of adequate muscle regeneration may also be due to impaired cytokine signalling and,

finally, differentiation.¹³ This indicates that skeletal muscle is sensitive to ionizing radiation during development, that is why radiotherapy in childhood may induce muscular atrophy, a fact that is attributed to the large number of radiosensitive satellite cells during a child's growth period.¹⁴ The underlying mechanism for radiation induced muscular atrophy has been insufficiently studied, so the main aim of this study was to evaluate the radiation dose-dependent effect on precursors of muscle regeneration, primary mononucleated human myoblasts, which are key cells involved in the development of adult muscle fibre and in the process of muscle regeneration. Two types of irradiation effects on human myoblast *in vitro* were studied: acute effects (determined 24 h post-irradiation) were followed by monitoring IL-6 secretion and stress response detected by the level of HSPs; long term effects (evaluated 72 h post-irradiation) were followed through proliferation capacity and cell death.

Materials and methods

Study design

The study was conducted at the Institute of Pathophysiology of the University of Ljubljana, where myoblast cell cultures were prepared and analysed, and at the Institute of Oncology Ljubljana, where cell cultures were exposed to ionizing radiation under controlled conditions. The experiments were approved by the Ethical Commission of the Ministry of Health of the Republic of Slovenia (permit numbers 63/01/99 and 71/05/12) and performed in compliance with the Helsinki Declaration and Good Laboratory Practice regulations. Experiments were performed on primary cultures of human myoblast that were prepared from three different donors (see below). Each primary culture was considered as independent experiment and all treatments of cells were performed at least in triplicate.

Myoblast cultures

Experiments were performed on cultures of human myoblasts prepared as previously described.^{5,15-16} Human myoblasts were derived from satellite cells obtained from muscle tissue routinely discarded during orthopaedic operations on donor patients aged 5, 11 and 20 years, without diagnosed muscular disease. After muscle tissue cleaning and trypsinization, released muscle satellite cells were grown in advanced Minimum Essential Medium (aMEM, Invitrogen, Grand Island, NY, USA) supplement-

ed with 10% fetal bovine serum (FBS, Invitrogen) at saturated humidity in a mixture of 5% CO₂-enriched air at 37°C. Myoblast colonies identified by morphological characteristics and devoid of fibroblast contamination were trypsinized and further expanded. Cells were plated in six-well dishes and grown for 3 days in aMEM supplemented with 10% FBS prior to the experiments.

Irradiation

Cells (1×10⁶ cells/ml aMEM) were plated in six-well dishes and irradiated with a dose rate of 2 Gy/min, with graded doses (2–8 Gy). A Darpac 2000 X-ray unit (Gulmay Medical Ltd, Shepperton, UK), operated at 220 kV, 10 mA, using 0.55 mm Cu filtration and 1.8 mm Al filtration was used for irradiation.

BrdU proliferation assay

The proliferation of cells was determined by BrdU Cell Proliferation Assay, Calbiochem, Merck, Darmstadt, Germany. Cells were plated on 96-well plates (1500 cells per well in 100 µl MEM), the next day they were irradiated and the proliferation test was performed 72 h later. 10 µM arabunifuranosyl cytidine (Ara C), an inhibitor of DNA synthesis, was added to the cells to produce the negative proliferation control. BrdU was allowed to incubate with cells for 18 h. BrdU labelled cells were visualized by Anti-BrdU Antibody diluted 1:100 (supplied with the kit). The diluted Peroxidase Goat Anti-Mouse IgG HRP Conjugate was filtered through 0.2 micron filter according to instructions. Fifteen minutes after adding the Substrate Solution absorbance was measured at 450 nm and 540 nm (Victor 3 plate reader from PerkinElmer, Shelton, CT, USA).

Assessment of apoptosis and necrosis

Cells were plated in white 24-well plates (10⁵ cells per well in 500 µl MEM) (Visiplate-24 TC, PerkinElmer, Shelton, CT, USA). After irradiation, the cells were treated for caspase detection and the culture media were collected and used to assess the release of lactate dehydrogenase (LDH, EC 1.1.1.27).

Apoptotic initiator caspase 9 (LEHD-ase) and executor caspase 3/7 (DEVD-ase) activity were measured using CaspaseGlo 9 Assay and CaspaseGlo 3/7 Assay Kits from Promega (Madison, WI, USA).

The level of necrotic cell death after cell irradiation was determined by measuring the activity of LDH in the cell culture media using a Cytotoxicity Detection Kit PLUS (Roche Diagnostics GmbH,

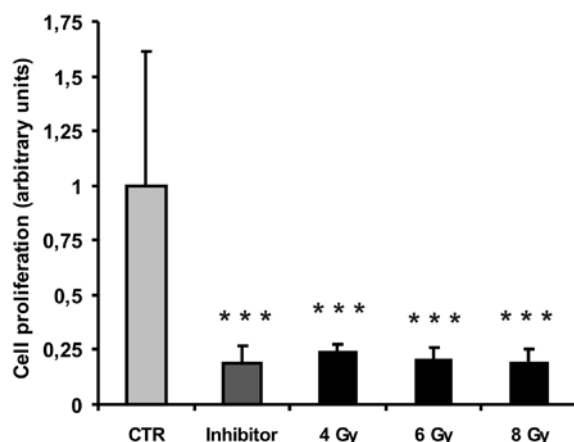


FIGURE 1. The effect of selected therapeutic doses of ionizing radiation (4 Gy, 6 Gy, 8 Gy) on the proliferation of human skeletal myoblasts assessed 72 h after irradiation. Columns and bars represent means \pm SD ($n=8$). Means are expressed as arbitrary units which are relative units of absorbance measurement at dual wavelengths of 450-540 nm. The control was used as the predetermined reference measurement. Statistically significant differences ($p < 0.001$) are indicated by ***. Control (CTR) – non-irradiated myoblast; Inhibitor – myoblasts treated with 10 μ M AraC, an inhibitor of cell proliferation; 4 Gy – myoblasts irradiated with 4 Gy; 6 Gy – myoblasts irradiated with 6 Gy; 8 Gy – myoblasts irradiated with 8 Gy.

Mannheim, Germany). Luminescence and absorbance (490 nm) were measured on a Victor 3 plate reader (PerkinElmer, Shelton, CT, USA) immediately after irradiation, 36 h and 72 h later.

IL-6 secretion analysis

Levels of secreted IL-6 in the culture supernatant collected from the cultures 24-h after exposure to irradiation were measured using an Enzyme-Linked Immunosorbent Assay (ELISA) kit (Endogen, Rockford, USA), according to the manufacturer's instructions and as described previously.¹⁷ IL-6 levels were calculated from concentrations of IL-6 measured in supernatants in each well.

Western Blot analysis for HSP 27 and HSP 70

Western blot analysis was performed as described in Katalinic *et al.*¹⁶ from myoblast samples collected from the cultures 24-h after exposure to irradiation. In brief, myoblasts were washed in ice-cold PBS and lysed. Protein content was determined in supernatants by the Bradford protein assay (Thermo Scientific Pierce, USA Rockford, IL). Homogenate samples were mixed with standard Laemmli buffer (3:1) (at 56°C, 20 min) and separated in 10% NuPage Novex Bis-Tris Gel (Invitrogen) by using the XCell SureLock electrophoresis system

(Invitrogen) and transferred to a PDVF membrane (Millipore, Billerica, MA, USA). Membranes with transferred samples were blocked in a blocking buffer (0.2% (w/v) I-Block (Applied Biosystems), 0.3% (v/v) Tween 20 (Sigma-Aldrich) prepared in phosphate buffered saline (PBS)) and incubated with selected primary antibodies against HSP 27 (rabbit polyclonal antibody PA1-516, ABR-Affinity BioReagents, USA Rockford, IL; diluted 1:200), HSP 70 (rabbit polyclonal antibody PA3-514, ABR-Affinity BioReagents; diluted 1:200) overnight at 4°C. Next day, the membranes were incubated with alkaline phosphatase-conjugated secondary antibodies (Sigma-Aldrich). Blots were developed in 2% (v/v) NBT/BCIP (Roche, Mannheim, Germany) solution prepared in developing buffer. Membrane quantification was performed with the Chemi Genius BioImaging System (Syngene, Cambridge, UK).

Statistical analysis

Results are presented as mean \pm SD. The differences among experimental groups were calculated using one-way ANOVA, followed by Bonferroni's post hoc test for multiple comparisons. SPSS 15.0 for Windows (SPSS, Chicago, IL, USA) was used for data analysis.

Results

Myoblast proliferation

Therapeutic doses of ionizing radiation used in the experiment effectively inhibited human myoblast proliferation. Irradiation at all doses statistically significantly inhibited myoblast proliferation to the same level (~0.2 of the untreated control) as the inhibitor of DNA synthesis Ara C (Figure 1).

Assessment of cell death

Irradiation of myoblasts did not cause necrotic cell death, measured by LDH activity, up to 36 h after treatment at all tested doses (Figure 2A). However, a statistically significant increase in necrotic cell death occurred 72 h after irradiation with 4 Gy. LDH activity in the media at this time point increased to 42 \pm 9%. Furthermore, a similar pattern was seen after irradiation with higher doses, although the increase in LDH activity was not statistically significant compared to control untreated cells.

Apoptosis of cells was measured by activation of caspases 3, 7 and 9. Irradiation of myoblasts did

not result in either increased activity of initiator caspase 9 (data not shown) or activation of execution caspases 3 and 7 (Figure 2 B).

Effects of irradiation on the secretion of IL-6

Levels of IL-6 were measured in supernatants of cultures 24-hours after exposure to different doses of irradiation. In control cultures that were kept in the same conditions as other cultures and were not exposed to irradiation, the constitutive level of IL-6 was 13,448 pg/ml (n=18). Exposure of myoblasts to irradiation resulted in a decreased level of IL-6 secretion in a dose dependent manner, being most pronounced in myoblasts irradiated with 4 Gy in comparison with myoblast irradiated with 6 Gy ($p < 0.05$) or with 8 Gy ($p < 0.05$). Irradiation of cells with 6 Gy also resulted in a statistically significant decrease of IL-6 secretion, while irradiation of myoblasts with the highest tested dose (8 Gy) did not result in decreased secretion of IL-6 (Figure 3).

Stress protein response in myoblast exposed to irradiation

The two most prominent stress proteins, HSP 27 and HSP 70, were followed in myoblasts 24-hours after irradiation. Levels of both proteins were increased in myoblasts exposed to irradiation in comparison with levels in control non-exposed myoblasts, although this increase was insignificant in myoblasts exposed to lower doses of irradiation (4 Gy and 6 Gy), while in myoblasts exposed to 8 Gy irradiation, the HSP 70 level was statistically significantly increased ($p < 0.05$) (Figure. 4).

Discussion

Radiation is thought to prevent mitosis of satellite cells, the primary stem cells in adult skeletal muscle, responsible for postnatal muscle growth and hypertrophy, causing breaks in strands of the cell's DNA and in this way inhibiting muscle regeneration.¹² Human muscle precursor myoblasts derived from satellite cells are responsible for muscle growth and regeneration.^{18,19} Radiation is well-known to affect muscle cells during development by impairing their activation, proliferation and differentiation.^{20,21} It also prevents muscle growth during development. The results of this study are the first to show a dose-dependent effect on human myoblast proliferation and regeneration capacity

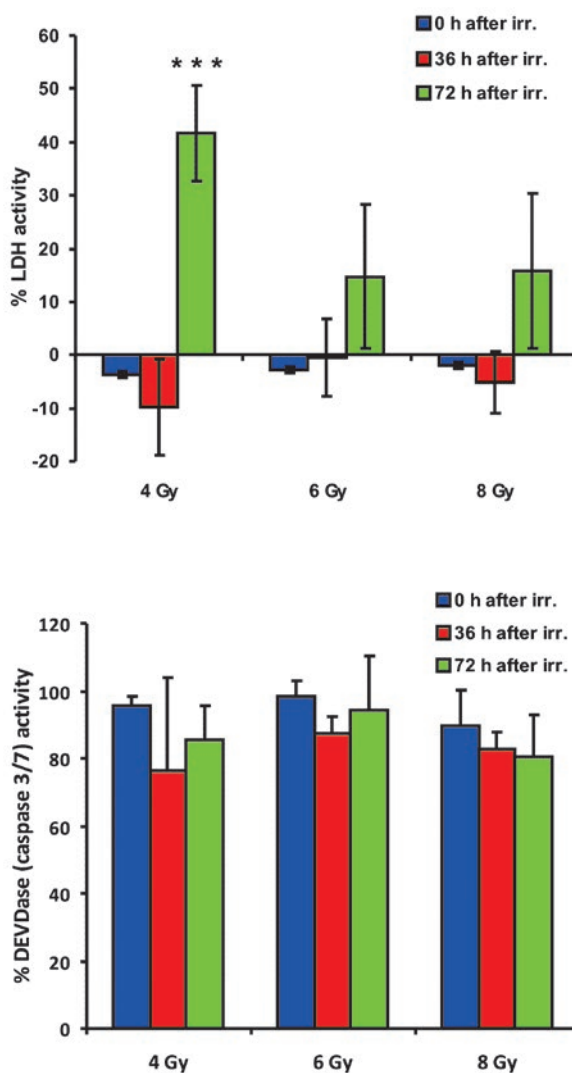


FIGURE 2. The effect of selected therapeutic doses of ionizing radiation (4 Gy, 6 Gy, 8 Gy) on cell death immediately after irradiation (0 h after IR.), 36 h after irradiation (36 h after IR.) and 72 h after irradiation (72 h after IR.). Columns and bars represent means \pm SD (n=4). (A) The assessment of myoblasts membranes integrity at different time points after irradiation is shown as the activity of lactate dehydrogenase (LDH) released in the medium. Statistically significant differences ($p \leq 0.001$) are indicated by ***. (B) The cleavage activity of the amino acid sequence DEVD (recognised and cleaved by apoptotic caspase 3 and 7) is shown at different time points after irradiation. There were no statistically significant differences among groups.

due to irradiation. These results indicate the occurrence of a significant change in myoblast proliferation and regeneration ability.

The myoblast stage of developing skeletal muscle is sensitive to ionizing radiation, and it is thus essential to devote particular attention to radiotherapy during infancy, while the sensitivity of adult skeletal muscle mass to ionizing radiation is still controversial. Most data suggest⁶⁻¹¹ that adult skeletal muscle is resistant to ionizing radia-

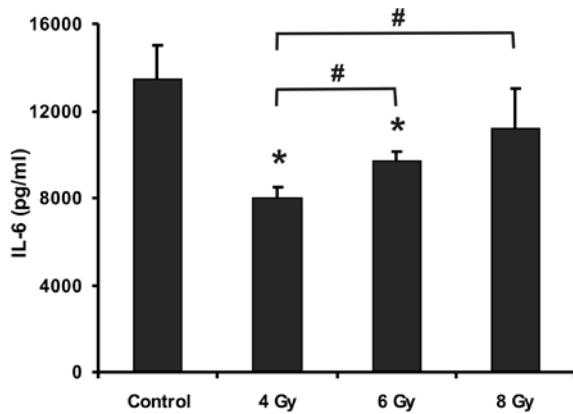


FIGURE 3. Effects of different doses of ionizing radiation on constitutive level of IL-6. Level of constitutive IL-6 secretion was estimated by ELISA in control myoblast cultures and compared with level of IL-6 secretion in myoblast cultures 24 hours after exposure to 4 Gy, 6 Gy and 8 Gy dose of irradiation. Data are means \pm SD ($n = 18$ in each independent experiment). * $p < 0.05$ (t-test) denotes difference in level of IL-6 in exposed cultures vs. respective level of control cultures, # significant difference between groups indicated $p < 0.05$ (t-test).

tion unless higher doses of radiation are applied. However, higher doses of radiation can cause myopathies and, in most cases, induced muscle atrophy. Skeletal muscle in cancer patients is often exposed to ionizing radiation during radiotherapeutic treatment. One of the most probable mechanisms contributing to post radiation myopathy and muscle atrophy is the inability of muscle to regenerate. Muscle regeneration is a key process, responsible for maintaining the integrity of the muscle mass and function throughout life and particularly after muscle injury.^{22,23} It has been demonstrated that autocrine secretion of IL-6 plays an important role in the regulation of myoblast proliferation and differentiation.²⁴ We observed an acute decrease in IL-6 secretion, which was more prominent when myoblasts were exposed to lower doses of irradiation. The less prominent decrease of IL-6 secretion in myoblasts exposed to higher doses of irradiation might be the result of IL-6 release from damaged cells, although we could not detect significantly increased levels of necrotic cell markers. In some *in vivo* and *in vitro* studies, it was shown that radiation increases cytokine IL-1 and IL-6 levels^{23,25}; higher levels of cytokines might be due to their release from cells other than muscle. Similarly, although more robust, a decrease in constitutive IL-6 secretion was also observed in primary myoblast culture after exposure to high doses of glucocorticoids or to environmental stress or organophosphates.^{16,17} Our results and the results of previous studies^{16,17}

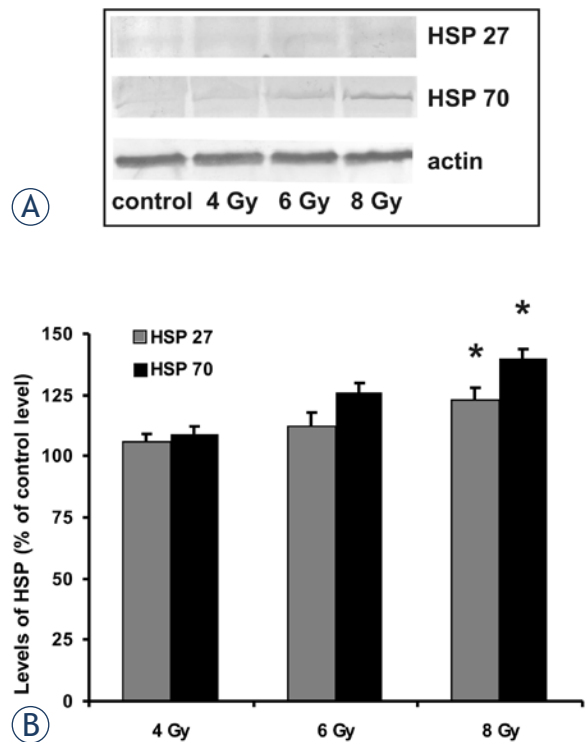


FIGURE 4. The effect of different doses of ionizing radiation on the HSP 27 and HSP 70 level in myoblasts 24 h after exposure. Representative Western blots for HSP 27 and HSP 70 (A). Relative levels of HSP 27 and HSP 70 shown as % of control level of proteins in myoblasts not exposed to irradiation (B), * $p < 0.05$ denotes significant difference in level of HSP in exposed myoblasts vs. level in control non-exposed myoblasts.

show high sensitivity of human myoblast to various chemical and physical factors. The mechanism of this myoblast response might involve transmission through highly conservative cytoprotective HSPs.^{26,27} In this connection, we observed increased levels of HSP 27 and HSP 70 as an acute myoblast response to irradiation; both HSPs are typically induced in cells when exposed to stress factors. In the light of the observed acute effects of irradiation, a long term effect might also be expected. In the long term, we observed a reduced proliferation capacity of myoblasts and subsequently also a higher rate of cell death, as detected by an increased level of LDH activity, which is a specific marker of cell damage and necrosis. These results are not unexpected, particularly due to the observed decreased level of secretion of IL-6 in myoblasts exposed to irradiation. IL-6 is a potent stimulator of myoblast proliferation and a decreased level of IL-6 secretion after irradiation might severely diminish autocrine and paracrine IL-6 activity.

In conclusion, our results show that myoblasts are sensitive to irradiation in terms of their prolifer-

eration capacity and capacity to secrete IL-6. Since myoblast proliferation and differentiation are a key stage in muscle regeneration, this effect of irradiation needs to be taken into account, particularly in certain clinical conditions.

References

- Chargé SB, Rudnicki MA. Cellular and molecular regulation of muscle regeneration. *Physiol Rev* 2004; **84**: 209-38.
- Austin L, Bower J, Kurek J, Vakakis N. Effects of leukaemia inhibitory factor and other cytokines on murine and human myoblast proliferation. *J Neurol Sci* 1992; **112**: 185-91.
- Serrano AL, Baeza-Raja B, Perdiguero E, Jardí M, Muñoz-Cánoves P. Interleukin-6 is an essential regulator of satellite cell-mediated skeletal muscle hypertrophy. *Cell Metab* 2008; **7**: 33-44.
- Baeza-Raja B, Munoz-Canoves P. p38 MAPK-induced nuclear factor-kappaB activity is required for skeletal muscle differentiation: role of interleukin-6. *Mol Biol Cell* 2004; **15**: 2013-26.
- Podbregar M, Lainscak M, Prelovsek O, Mars T. Cytokine response of cultured skeletal muscle cells stimulated with proinflammatory factors depends on differentiation stage. *Scientific World Journal* 2013; **2013(617170)**: 1-8.
- Lewis RB. Changes in striated muscle following single intense doses of x-rays. *Lab Invest* 1954; **3**: 48-55.
- Khan MY. Radiation-induced changes in skeletal muscle. An electron microscopic study. *J Neuropathol Exp Neurol* 1974; **33**: 42-57.
- Wirtz P, Loermans H, Rutten E. Effects of irradiation on regeneration in dystrophic mouse leg muscles. *Br J Exp Pathol* 1982; **63**: 671-9.
- Gulati AK. The effect of X-irradiation on skeletal muscle regeneration in the adult rat. *J Neurol Sci* 1987; **78**: 111-20.
- Wakeford S, Watt DJ, Partridge TA. X-irradiation improves mdx mouse muscle as a model of myofiber loss in DMD. *Muscle Nerve* 1991; **14**: 42-50.
- Olivé M, Blanco R, Rivera R, Cinos C, Ferrer I. Cell death induced by gamma irradiation of developing skeletal muscle. *J Anat* 1995; **187(Pt 1)**: 127-32.
- Rosenblatt JD, Yong D, Perry DJ. Satellite cell activity is required for hypertrophy of overloaded adult rat skeletal muscle. *Muscle Nerve* 1994; **17**: 608-13.
- Phelan JN, Gonyea WJ. Effect of radiation on satellite cell activity and protein expression in overloaded mammalian skeletal muscle. *The Anat Rec* 1997; **247**: 179-88.
- Jurdana M. Cancer cachexia-anorexia syndrome and skeletal muscle wasting. *Radiol Oncol* 2009; **43**: 65-75.
- Pirkmajer S, Filipovic D, Mars T, Mis K, Grubic Z. HIF-1alpha response to hypoxia is functionally separated from the glucocorticoid stress response in the in vitro regenerating human skeletal muscle. *Am J Physiol Regul Integr Comp Physiol* 2010; **299**: R1693-700.
- Katalinic M, Mis K, Pirkmajer S, Grubic Z, Kovarik Z, Mars T. The cholinergic and non-cholinergic effects of organophosphates and oximes in cultured human myoblasts. *Chem Biol Interact* 2013; **203**: 144-8.
- Prelovsek O, Mars T, Jevsek M, Podbregar M, Grubic Z. High dexamethasone concentration prevents stimulatory effects of TNF-alpha and LPS on IL-6 secretion from the precursors of human muscle regeneration. *Am J Physiol* 2006; **291**: 1651-6.
- Schultz E, McCormick KM. Skeletal muscle satellite cells. *Rev Physiol Biochem Pharmacol* 1994; **123**: 213-57.
- Hawke TJ, Garry DJ. Myogenic satellite cells: physiology to molecular biology. *J Appl Physiol* 2001; **91**: 534-51.
- Zeman W, Soloma M. Effects of radiation on striated muscle. In: Berdijis CC, editor. *Pathology of irradiation*. Baltimore: Williams & Wilkins; 1971. p.185.
- Prasad KN. *Handbook of radiobiology*. Radiation damage of other organ systems. Boca Raton: CRC press; 1995. p. 181-92.
- Bischoff R. The satellite cell and muscle regeneration. In: Engel AG, Frazini-Armstrong C, editors. *Myology*. New York: McGraw-Hill; 1994. p. 97-118.
- Husmann I, Soulet L, Gautron J, Martelly I, Barritault D. Growth factors in skeletal muscle regeneration. *Cytokine Growth Factor Rev* 1996; **7**: 249-58.
- Cantini M, Massimino ML, Rapizzi E, Rossini K, Catani C, Dallalibera L, et al. Human satellite cell-proliferation in vitro is regulated by autocrine secretion of IL-6 stimulated by a soluble factor(s) released by activated monocytes. *Biochem Biophys Res Commun* 1995; **216**: 49-53.
- Hodgetts SI, Grounds MD. Irradiation of dystrophic host tissue prior to myoblast transfer therapy enhances initial (but not long-term) survival of donor myoblasts. *J Cell Sci* 2003; **116**: 4131-46.
- Welch WJ. Mammalian stress response: cell physiology, structure/function of stress proteins, and implications for medicine and disease. *Physiol Rev* 1992; **72**: 1063-81.
- Wu T, Tanguay RM. Antibodies against heat shock proteins in environmental stresses and diseases: friend or foe? *Cell Stress Chaperones* 2006; **11**: 1-12.

Recombinant human erythropoietin alters gene expression and stimulates proliferation of MCF-7 breast cancer cells

Nina Trost¹, Tina Stepisnik², Sabina Berne², Anja Pucer³, Toni Petan³, Radovan Komel², Natasa Debeljak^{1,2}

¹ Center for Functional Genomics and Bio-chips, Institute of Biochemistry, Faculty of Medicine, University of Ljubljana, Slovenia

² Medical Center for Molecular Biology, Institute of Biochemistry, Faculty of Medicine, University of Ljubljana, Slovenia

³ Department of Molecular and Biomedical Sciences, Jožef Stefan Institute, Ljubljana, Slovenia

Radiol Oncol 2013; 47(4): 382-389.

Received: 18 June 2013

Accepted: 16 August 2013

Correspondence to: Assist. Prof. Dr. Nataša Debeljak, Institute of Biochemistry, Faculty of Medicine University of Ljubljana, Vrazov trg 2, SI-1000 Ljubljana, Slovenia. E-mail: natasa.debeljak@mf.uni-lj.si

Disclosure: No potential conflicts of interest were disclosed.

The paper was presented at the 7th Conference of Experimental and Translational Oncology, 20-24th April 2013, Portoroz, Slovenia (www.ceto.si) co-organised and supported by COST TD1104 Action (www.electroporation.net).

Background. Functional erythropoietin (EPO) signaling is not specific only to erythroid lineages and has been confirmed in several solid tumors, including breast. Three different isoforms of erythropoietin receptor (EPOR) have been reported, the soluble (EPOR-S) and truncated (EPOR-T) forms acting antagonistically to the functional EPOR. In this study, we investigated the effect of human recombinant erythropoietin (rHuEPO) on cell proliferation, early gene response and the expression of EPOR isoforms in the MCF-7 breast cancer cell line.

Materials and methods. The MCF-7 cells were cultured with or without rHuEPO for 72 h or 10 weeks and assessed for their growth characteristics, expression of early response genes and different EPOR isoforms. The expression profile of EPOR and EPOR-T was determined in a range of breast cancer cell lines and compared with their invasive properties.

Results. MCF-7 cell proliferation after rHuEPO treatment was dependent on the time of treatment and the concentration used. High rHuEPO concentrations (40 U/ml) stimulated cell proliferation independently of a preceding long-term exposure of MCF-7 cells to rHuEPO, while lower concentrations increased MCF-7 proliferation only after 10 weeks of treatment. Gene expression analysis showed activation of *EGR1* and *FOS*, confirming the functionality of EPOR. rHuEPO treatment also slightly increased the expression of the functional EPOR isoform, which, however, persisted throughout the 10 weeks of treatment. The expression levels of EPOR-T were not influenced. There were no correlations between EPOR expression and the invasiveness of MCF-7, MDA-MB-231, Hs578T, Hs578Bst, SKBR3, T-47D and MCF-10A cell lines.

Conclusions. rHuEPO modulates MCF-7 cell proliferation in time- and concentration-dependent manner. We confirmed *EGR1*, *FOS* and EPOR as transcription targets of the EPO-EPOR signaling loop, but could not correlate the expression of different EPOR isoforms with the invasiveness of breast cancer cell lines.

Key words: breast cancer; erythropoietin; erythropoietin receptor isoforms; proliferation; gene expression

Introduction

Erythropoietin (EPO) is a 34 kDa glycoprotein hormone that regulates erythroid maturation in bone marrow.¹ Its binding to the erythropoietin recep-

tor (EPOR) on the surface of erythroid progenitors triggers several downstream signaling pathways, including Janus kinase 2 (Jak2)/signal transducer and activator of transcription 5 (STAT5), phosphatidylinositol 3-kinase (PI3K)/protein kinase

TABLE 1. Details on the cohort of breast cancer cell lines as defined by ATCC. ESR, estrogen receptor; PGR, progesterone receptor; AC, adenocarcinoma; IDC, invasive ductal carcinoma; F, fibrocystic disease; PE, pleural effusion; P. Br, primary breast. Cell invasiveness increases with number (1 = the least invasive, 7 = the most invasive). Cells were cultured as described in Hevir *et al.*¹⁶

Cell line	Receptor status	Tissue source	Tumor type	Invasiveness
MCF-10A	ESR ⁻ , PGR ⁻		F	1
Hs578Bst	ESR ⁻ , PGR ⁻	Adjacent breast tissue		2
MCF-7	ESR ⁺ , PGR ⁺	PE	IDC	3
T-47D	ESR ⁺ , PGR ⁺	PE	IDC	4
SK-BR-3	ESR ⁻ , PGR ⁻ , HER2 ⁺	PE	AC	5
MDA-MB-231	ESR ⁻ , PGR ⁻	PE	AC	6
Hs578T	ESR ⁻ , PGR ⁻	P. Br	IDC	7

B (Akt), Ras/mitogen-activated protein kinase (MAPK) and protein kinase C (PKC) pathways.² EPO-EPOR signaling not only promotes erythroid proliferation and differentiation, but also protects erythroid progenitors against apoptosis.³ EPO has been shown to increase the frequency of S-phase burst-forming-units (BFUs) in human bone marrow.⁴ Furthermore, EPO increases the expression of anti-apoptotic proteins B-cell lymphoma 2 (Bcl-2) and B-cell lymphoma-extra large (Bcl-X_L) via the Jak2/STAT5 signaling pathway.⁵ Functional EPO-EPOR signaling is not limited only to erythroid lineages since EPOR expression has been confirmed in several non-hematopoietic cells and tissues, as well as in solid tumors.⁶ Recombinant forms of human erythropoietin (rHuEPO), used in clinical oncology settings to improve anemia, have been correlated with lower survival rates of patients undergoing rHuEPO treatment.² These observations raised concerns about EPO's potential in promoting cancer growth and development of more aggressive cancer phenotypes. Therefore, EPO-EPOR signaling has been studied in correlation to cancer progression in several laboratories. Their findings are conflicting and strongly depend on the used experimental models, as rHuEPO was reported to increase cancer cell proliferation^{7,8} or to have no significant effect.^{9,10} Contrasting effects might be explained by the presence of different EPOR isoforms. Three EPOR isoforms are listed in the UniProt database (<http://www.uniprot.org/uniprot/P19235>): a full-length functional (EPOR-F), a truncated isoform (EPOR-T) lacking the cytoplasmic region¹¹ and a soluble (EPOR-S) receptor that is missing the trans-membrane and cytoplasmic domains.¹² EPOR-S is secreted from the cell where it competes with EPOR-F for EPO binding.¹³ The EPOR-T and EPOR-S isoforms most probably act

as antagonists of EPOR-mediated signaling.¹⁴ All three isoforms were confirmed in breast cancer.¹⁵

The objective of our study was to investigate the effect of rHuEPO on cell proliferation, EPOR expression and early gene response in breast cancer cells. The effect of a long-term rHuEPO treatment of MCF-7 cells on cell proliferation, EPO-responsiveness and the expression of functional (EPOR), soluble (EPOR-S) and truncated (EPOR-T) receptor isoforms was assessed. Additionally, the expression profile of EPOR and EPOR-T was determined in a range of breast cancer cell lines and compared with their invasive properties.

Materials and methods

Cell lines

The breast cancer cell lines (Table 1) were from the American Type Culture Collection (ATCC; Manassas, VA, USA) and were cultured according to their recommendations in basic growth medium, supplemented with 10% fetal bovine serum (FBS) at 37°C in a humidified 5% (v/v) CO₂ atmosphere. The receptor status of a specific cell line and the tumor type are shown in Table 1. The MCF-7 cells were pretreated with rHuEPO up to 10 weeks (5 U/ml, NeoRecormon, Roche, Germany). In parallel, control cells were cultured in the same conditions, but without rHuEPO.

Proliferation assays

The effect of rHuEPO on cell proliferation was analyzed using the colorimetric 3-(4,5-dimethylthiazol-2-yl)-2,5-diphenyltetrazolium bromide (MTT, Sigma, USA) assay. rHuEPO pretreated (10 weeks) and non-pretreated cells were seeded in a volume

TABLE 2. Primers used in qPCR analysis of genes of interest and reference genes. Forward (Fw) and reverse (Rev) reverse oligonucleotide primers are shown; (NA) not available

Genes of interest					
Gene symbol	Gene name	Nucleotide sequence	Ref. seq.	Amplicon length	PCR Eff
EPOR		Fw: 5'-GCTGGAAGTTACCCITGTGG-3' Rev: 5'-CTCATCCTCGTGGTCATCCT-3'	NM_000121	148	1.920
EPOR-T	erythropoietin receptor, truncated form	Fw: 5'-GGTCCAGGTCGCTAGGCGTCAG-3' Rev: 5'-TGCTTCTGTCAGCCAAACTGC-3'	NM_000121	249	1.911
EPOR-S	erythropoietin receptor, soluble form	Fw: 5'-CTCCACCCTCTGTACGCTCCCTGC-3' Rev: 5'-ACGCCTAGCGGGCTGAAGC-3'	NM_000121	183	(NA)
FOS	FBJ murine osteosarcoma viral oncogene homolog	Fw: 5'-CTACCACTCACCCGCAGACT-3' Rev: 5'-AGGTCCGTGCAGAAAGTCCT-3'	NM_005252.2	72	2
JUN	jun-proto oncogene	Fw: 5'-CCAAAGGATAGTGCATGTTT-3' Rev: 5'-CTGTCCCTCTCCACTGCAAC-3'	NM_002228.2	62	2
NF-kB	nuclear factor of kappa light polypeptide gene enhancer in B-cells 1	Fw: 5'-GGTGCCTCTAGTAAAAGAACAAGA-3' Rev: 5'-GCTGGTCCCACATAGTTGCA-3'	NM_003998.3	68	1.722
FOSL1	FOS-like antigen 1	Fw: 5'-AACC GGAGGAAGGAAGTAC-3' Rev: 5'-CTGCAGCCCAGATTCTCAT-3'	NM_005438.3	75	2
EGR1	Early growth response 1	Fw: 5'-AGCCCTACGAGCACCTGAC-3'; Rev: 5'-GGTGGTGGGGTAACTG-3'	NM_001964.2	81	2
Reference genes					
Gene symbol	Gene name	Nucleotide sequence	Ref. seq.	Amplicon length	Primer Eff
RPLP0	ribosomal protein, large, P0	Fw: 5'-TCTACAACCCTGAAGTGCCTGAT-3' Rev: 5'-CAATCTGCAGACAGACTGG-3'	NM_001002.3	96	2.073
GAPDH	glyceraldehyde-3-phosphate dehydrogenase	Fw: 5'-AGCCACATCGCTCAGACAC-3' Rev: 5'-GCCCAATACGACCAAATCC-3'	NM_002046.3	66	1.999
SF3A1	Splicing factor 3a, subunit 1	NA	NM_005877	NA	1.799
TOP1	DNA Topoisomerase I	Fw: 5'-CCCTGACTTCATCGACAAGC-3' Rev: 5'-CCACAGTGCCGCTGTTTC-3'	NM_003286.2	NA	1.809
YWHAZ	Tyrosine 3-monooxygenase/tryptophan 5-monooxygenase activation protein, zeta polypeptide	NA	NM_003406	NA	1.887

of 100 μ l on a 96-well plate at a density of 5×10^3 cells per well. Cells seeded in six replicates were left to adhere for 24 h. Growth medium was then replaced with a medium supplemented with different concentrations of rHuEPO (0, 5, 40 U/ml). Cells were grown for 72 h and at specific time-points 15 μ l of MTT (5 mg/ml in PBS) was added to each well and the plate was incubated at 37°C for 3 h, according to the manufacturer's recommendations. Cell metabolic activity reflecting cell number and thus proliferation was measured daily and normalized to values obtained with control cells not exposed to rHuEPO.

Gene expression analysis

Sample preparation. MCF-7 cells pretreated with rHuEPO for 10 weeks (Figure 1C) and non-pre-

treated cells (Figure 1A) were cultured in basic growth medium in T-25 flasks at a density of 5×10^5 cells/ml and grown to 75% of confluency. Cells were serum starved for 24 h and exposed to 50 U/ml rHuEPO for 0, 4, 8, 16, 32 and 64 min. Following the stimulation with rHuEPO, cells were subjected to RNA isolation and analyzed for EPOR expression levels. The non-pretreated cells were further analyzed for early gene response. Cells were cultured in 6-well plates at a density of 3×10^5 cells/ml in serum-deprived media and cultured for 48 h. Cells were stimulated with 5 U/ml rHuEPO for 0, 30, 60 and 240 min, fast frozen in liquid nitrogen and subjected to RNA isolation (Figure 1B).

RNA isolation. Total RNA was isolated using the High Pure Total RNA Isolation Kit (Roche) or TRI Reagent (Sigma) following manufacturer's instructions. The Agilent Bioanalyzer 2100 (Agilent

Technologies, USA) was used for the determination of RNA concentrations and quality, assuring all RNA integrity numbers (RINs) were above 9.8. Total RNA was transcribed to cDNA using Transcriptor First Strand cDNA Synthesis Kit (Roche) and SuperScript III reverse transcriptase (Invitrogen, USA).

Quantitative real-time PCR (qPCR). Forward and reverse primers for *FOS*, *JUN*, *NFκB*, *FOSL1*, *EGR1*, *RPLP0* and *GAPDH* were designed to span intron-exon junctions using PrimerExpress software (Applied Biosystems, USA) and their specificity was checked using BLAST algorithm (Table 2). *RPLP0* and *GAPDH* were used as reference genes in the analysis of early gene response. Forward and reverse primers for functional (*EPOR*), soluble (*EPOR-S*) and truncated (*EPOR-T*) erythropoietin receptor were designed according to Arcasoy *et al.*¹⁵ Primers specific for *SF3A1* and *YWHAZ* genes from the Human geNorm Kit (Primer Design, UK) and for *TOP1*¹⁷ were chosen as reference genes in the analysis of the *EPOR* isoform expression. Primer validation was done by analyzing the slope of the standard curve and the presence of a single peak in the melting curve after qPCR analysis. qPCR was conducted on a 384-well plates using the LightCycler 480 Real-Time PCR System (Roche) and SYBR Green I Master chemistry (Roche). Amplification of specific PCR products was performed in triplicates in a total reaction mixture of 5 µl, containing 750 ng RNA equivalent cDNA template and 300 nM of each set of primers. The expression levels of the selected reference genes were used for normalization of expression data. Gene expression normalization factors were calculated for each sample based on geometric means of the selected reference genes.¹⁸ Minimum Information for Publication of Quantitative Real-Time PCR Experiments (MIQE) was followed in the performance and interpretation of the qPCR reactions.¹⁹

EPOR expression and cancer invasiveness

The invasiveness of breast cancer cell lines was compared with the expression of *EPOR* isoforms. Cell lines differing in cell invasiveness as represented in Table 1.

Statistical analysis

Statistical analysis of the data was performed using the Limma package²⁰ from Bioconductor analysis tools for R programming language.²¹ The effect of rHuEPO treatment on cell proliferation and gene

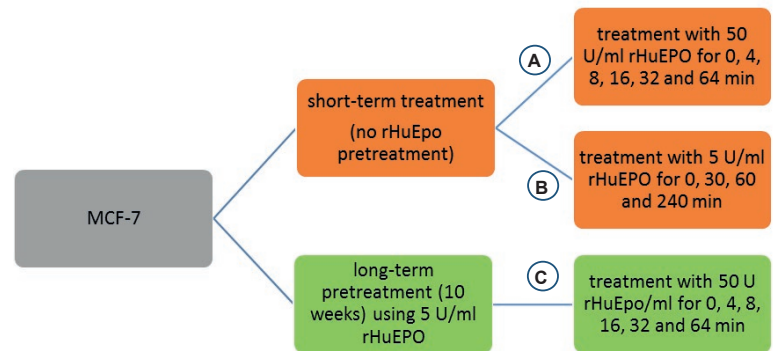


FIGURE 1. Protocol of treatment of MCF-7 cells with recombinant human erythropoietin for isolation of total RNA.

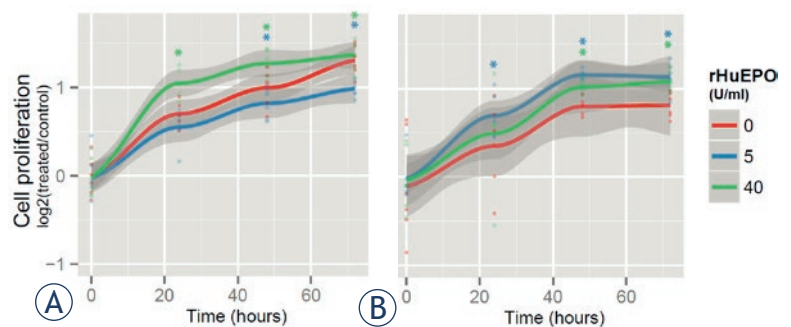


FIGURE 2. Differential effects of recombinant human EPO on MCF-7 cell proliferation (A) MCF-7 cells were cultured in complete medium in the presence of indicated concentrations of rHuEPO (short-term treated) (B) MCF-7 cells were cultured in complete medium in the presence of 5 U/ml of rHuEPO for 10 weeks (long-term pretreated cells), EPO was added to the pretreated cells at indicated concentrations. Asterisk (*) denotes statistical significance for Type 1 error $\alpha = 0.05$.

expression was assessed by Two-way analysis of variance (ANOVA). Multiple-testing correction using False discovery rate (FDR)²² was employed and $p < 0.05$ was considered as statistically significant.

Results

EPO alters the proliferation rate of MCF-7 breast cancer cells

MCF-7 cells were stimulated with rHuEPO (0, 5, 40 U/ml) and assessed for proliferation using the MTT assay. We found that MCF-7 cell proliferation is dependent on the concentration of rHuEPO used and the time of the treatment (Figure 2). Treatments with 40 U/ml rHuEPO led to increased MCF-7 cell proliferation independently of the length of cell exposure to rHuEPO. On the other hand, 5 U/ml rHuEPO affects MCF-7 cell proliferation in a time dependent manner; cell proliferation was reduced

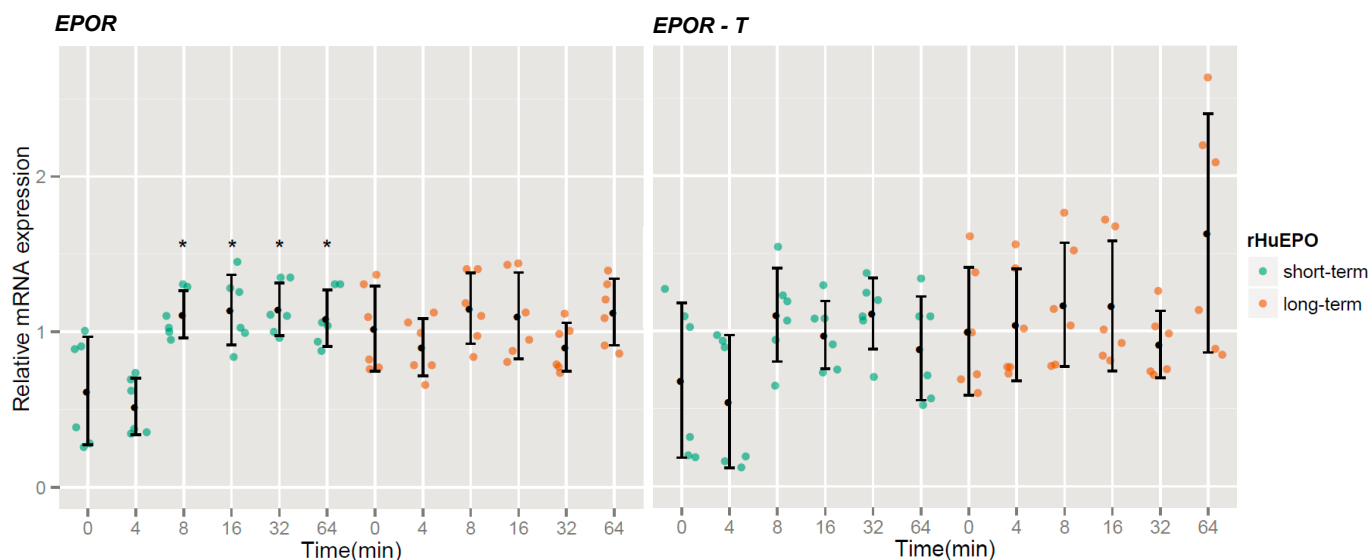


FIGURE 3. Effects of recombinant human EPO on relative *EPOR* and *EPOR-T* expression. MCF-7 cells were stimulated with 50 U/ml rHuEPO (short-term, green) or cultured in complete medium in the presence of 5 U/ml of rHuEPO for 10 weeks and stimulated with 50 U/ml rHuEPO (long-term, red). Error bars represent standard deviations (SD) between six replicate samples; asterisk (*) denotes statistical significance for Type 1 error $\alpha = 0.05$.

during a short-term treatment (Figure 2A), but was higher when rHuEPO was added to long-term rHuEPO-pretreated cells (Figure 2B).

EPO induces gene expression changes in MCF-7 cells

The expression of EPOR isoforms in EPO-treated cells. To determine the effects of rHuEPO on the expression of its receptor protein variants, mRNA expression levels of *EPOR*, *EPOR-S* and *EPOR-T* genes were analyzed in short (Figure 1A) and long-term (Figure 1C) rHuEPO-treated MCF-7 cells. The expression of *EPOR* and *EPOR-T* isoforms at specific time-points was confirmed by qPCR (Figure 3). On the other hand, we were not able to confirm the presence of *EPOR-S* (data not show). Short-term stimulation of MCF-7 cells with 50 U/ml rHuEPO leads to an increase in *EPOR* expression, while it has no statistically significant effect on *EPOR-T*. Interestingly, the addition of 50 U/ml rHuEPO to the long-term pretreated cells (5 U/ml rHuEPO) did not have any additional influence on the expression levels of *EPOR* and *EPOR-T*.

The expression of early response genes in EPO-treated cells. Since rHuEPO affected MCF-7 cell proliferation in a time-dependent manner only at the 5 U/ml concentration, MCF-7 cells were stimulated with 5 U/ml rHuEPO and analyzed for early gene response. The most pronounced changes were observed in the expression of *EGR1* and *FOS* (Figure 4). Both genes were up-regulated after

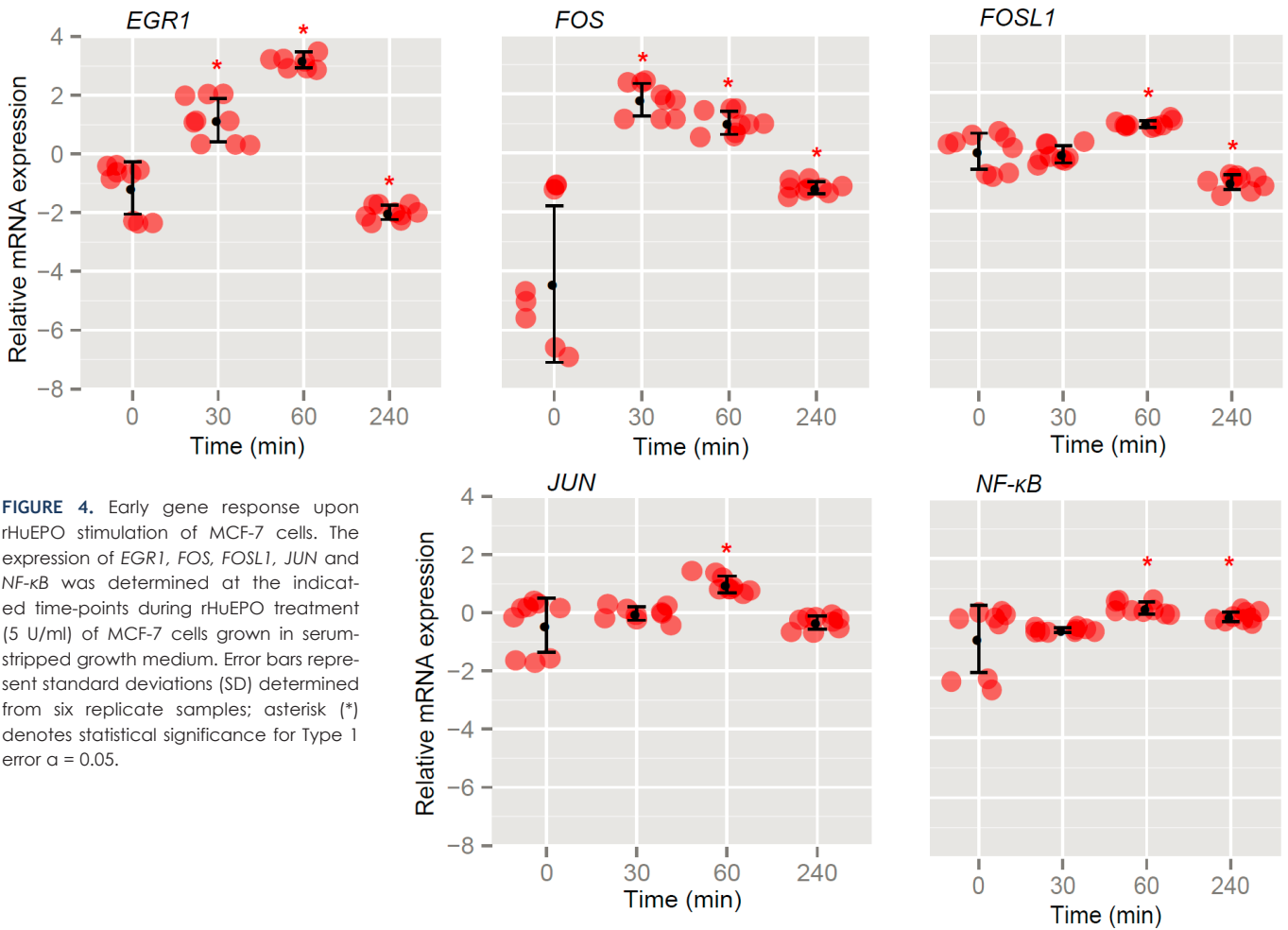
rHuEPO stimulation. rHuEPO only slightly modulated the expression of *FOSL1*, *JUN* and *NF- κ B* genes.

The expression of EPOR does not correlate with breast cancer cell invasiveness

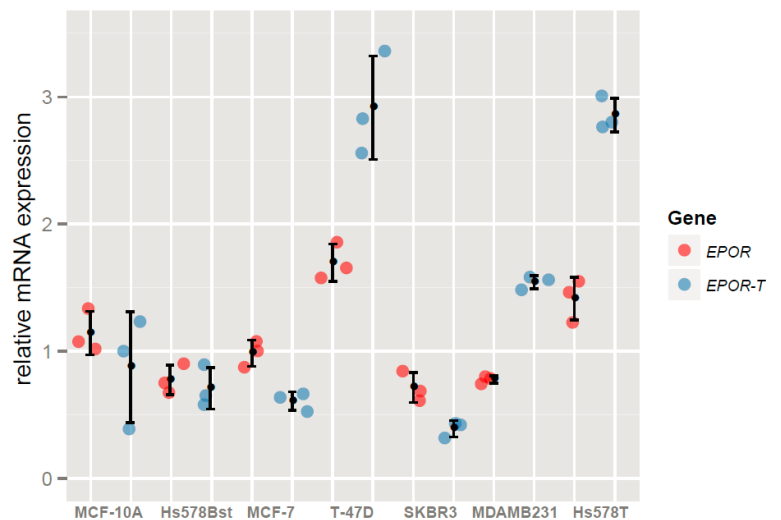
The expression of *EPOR* isoforms was paralleled with the invasiveness of cancer and epithelial-like breast cell lines included in the current study (Table 1). We found no association between the expression of *EPOR* (*EPOR* or *EPOR-T*) and the breast cell invasiveness. There were no significant differences in the level of *EPOR* expression between cell lines and its expression in a particular cell line did not correlate with its invasiveness, ESR, PGR or HER2 status (Figure 5).

Discussion

EPO is a key regulator of erythropoiesis and is gaining more significance also in other tissues^{2,6} and (patho)physiological processes. EPO is important for neuro-²³ and cardioprotection²⁴, while the functionality of EPO-EPOR signaling in cancer settings questions the suitability of its usage for the treatment of cancer or chemotherapy-related anemia.²⁵ EPOR activation is considered to influence cancer cell growth in terms of stimulated proliferation, prevention of apoptosis and increased resist-



ance to therapy. The mechanisms of EPO actions are not well understood, but it has been suggested that an active crosstalk with other growth factor receptors is involved, especially those from the estrogen family and HER2.^{26,27} It has been shown that the AP-1 (*FOS* and *JUN*) transcription factor is critical for growth and proliferation of breast cancer cells.²⁸ We therefore analyzed early gene response in MCF-7 cells stimulated with rHuEPO. We show that rHuEPO induces rapid up-regulation of *FOS* and *EGR1* gene expression, which is followed by an increase in the expression of *JUN* and *NF-κB* (Figure 4). Despite the up-regulation of *FOS*²⁹ and *EGR1*³⁰ genes, both considered a driving force for cell proliferation, we observed a decreased proliferation rate of short-term (72 h) treated MCF-7 cells after stimulation with rHuEPO (5 U/ml) (Figure 2). On the contrary, the effect was reversed after long-term pretreatment being in agreement with our previously published data.³¹ This suggests that a long-term treatment with low doses of rHuEPO



sensitizes the MCF-7 cells to further treatment with the growth factor. At a higher concentration of 40 U/ml, rHuEPO significantly increased cell proliferation independently of the any previous exposure of MCF-7 cells to the hormone.

Further, we analyzed the expression of functional *EPOR* and its antagonists, truncated (*EPOR-T*) and soluble *EPOR* (*EPOR-S*), in rHuEPO-treated MCF-7 cells and other breast cancer cell lines. The presence of *EPOR-S* was not confirmed, despite previous reports of its presence in MCF-7 cells.³² We found no association between the expression of *EPOR* (*EPOR* or *EPOR-T*) and the breast cell invasiveness. There were no significant differences in the level of *EPOR* expression between cell lines and its expression in a particular cell line did not correlate with its invasiveness, ESR, PGR or HER2 status (Figure 5).

Interestingly, we show here that rHuEPO can slightly up-regulate the expression of the functional *EPOR*, but has no effect on *EPOR-T*. The up-regulation of functional *EPOR* is very fast, it happens after 8 min of rHuEPO (50 U/ml) stimulation. The addition of 50 U/ml rHuEPO to the long-term pretreated cells (5 U/ml rHuEPO) did not have any additional influence on the *EPOR* expression levels. It seems the expression is slightly elevated throughout whole long-term treatment (Figure 3). Our results indicate that rHuEPO stimulation regulates the expression of *EPOR* but not *EPOR-T* in MCF-7 cells as indicated previously.³³ Finally, the analysis of *EPOR* mRNA levels in a panel of breast cancer cell lines suggests that the pattern of *EPOR* (functional and *EPOR-T*) expression does not correlate with the invasiveness of breast cancer cell lines (Figure 5).

Conclusions

Our study confirmed the functionality of EPO-*EPOR* signaling pathways in MCF-7 cells, indicating time- and concentration-dependent rHuEPO effects on cell proliferation. The 5 U/ml (physiological) rHuEPO concentration was shown to have an opposite effect on cell proliferation after 10 weeks versus 72 hours of treatment, most probably due to cell line sensibilization. Furthermore, two *EPOR* isoforms were confirmed, full-length functional *EPOR* and truncated *EPOR-T*, showing different expression profile upon rHuEPO treatment. The observed expression profiles are not correlated with the invasiveness of analyzed breast cancer cell lines.

Acknowledgement

Authors acknowledge the financial support of the Slovenian Research Agency; the study was supported by the P1-0104 and P1-0207 program grants, Z3-9402 grant to S.B., J3-0124 grant to N.D., and Young Researcher Grant to N.T. Authors also acknowledge Roche Slovenia for financial support.

Footnotes

Tina Stepišnik is currently employed at the Laboratory of Biocybernetics, Faculty of Electrical Engineering, University of Ljubljana, Slovenia.

Authors' contributions

SB, NT, ND, TP and RK contributed to the conception and design of the study. SB and TS carried out the cell proliferation and invasiveness experiments, the gene expression was assayed by SB, TS and NT. Total RNA from the cells with different invasiveness was provided by TP and AP. SB, TS, NT and ND have analyzed the data and interpreted the results. NT, TS and ND participated in drafting the article. All authors critically revised the manuscript and approved the submitted and revised version.

References

- Moritz KM, Lim GB, Wintour EM. Developmental regulation of erythropoietin and erythropoiesis. *Am J Physiol* 1997; **273**: R1829-44.
- Jelkmann W, Bohlius J, Hallek M, Sytkowski AJ. The erythropoietin receptor in normal and cancer tissues. *Crit Rev Oncol Hematol* 2008; **67**: 39-61.
- Koury MJ, Bondurant MC. The molecular mechanism of erythropoietin action. *Eur J Biochem* 1992; **210**: 649-63.
- Dessypris EN, Krantz SB. Effect of pure erythropoietin on DNA-synthesis by human marrow day 15 erythroid burst forming units in short-term liquid culture. *Br J Haematol* 1984; **56**: 295-306.
- Silva M, Grillot D, Benito A, Richard C, Nunez G, Fernandez-Luna JL. Erythropoietin can promote erythroid progenitor survival by repressing apoptosis through Bcl-XL and Bcl-2. *Blood* 1996; **88**: 1576-82.
- Elliott S, Sinclair AM. The effect of erythropoietin on normal and neoplastic cells. *Biologics* 2012; **6**: 163-89.
- Westenfelder C, Baranowski RL. Erythropoietin stimulates proliferation of human renal carcinoma cells. *Kidney Int* 2000; **58**: 647-57.
- Kumar SM, Acs G, Fang D, Herlyn M, Elder DE, Xu XW. Functional erythropoietin autocrine loop in melanoma. *Am J Pathol* 2005; **166**: 823-30.
- Selzer E, Wacheck V, Kodym R, Schlagbauer-Wadl H, Schlegel W, Pehamberger H, et al. Erythropoietin receptor expression in human melanoma cells. *Melanoma Res* 2000; **10**: 421-6.
- Ludwig H. rHuEPO and treatment outcomes: the preclinical experience. *Oncologist* 2004; **9** (Suppl 5): 48-54.

11. Nakamura Y, Komatsu N, Nakauchi H. A truncated erythropoietin receptor that fails to prevent programmed cell death of erythroid cells. *Science* 1992; **257**: 1138-41.
12. Todokoro K, Kuramochi S, Nagasawa T, Abe T, Ikawa Y. Isolation of a cDNA encoding a potential soluble receptor for human erythropoietin. *Gene* 1991; **106**: 283-4.
13. Sakanaka M, Wen TC, Matsuda S, Masuda S, Morishita E, Nagao M, et al. In vivo evidence that erythropoietin protects neurons from ischemic damage. *Proc Natl Acad Sci U S A* 1998; **95**: 4635-40.
14. Sinclair AM, Todd MD, Forsythe K, Knox SJ, Elliott S, Begley CG. Expression and function of erythropoietin receptors in tumors: implications for the use of erythropoiesis-stimulating agents in cancer patients. *Cancer* 2007; **110**: 477-88.
15. Arcasoy MO, Amin K, Karayal AF, Chou SC, Raleigh JA, Varia MA, et al. Functional significance of erythropoietin receptor expression in breast cancer. *Lab Invest* 2002; **82**: 911-8.
16. Hevir N, Trost N, Debeljak N, Rizner TL. Expression of estrogen and progesterone receptors and estrogen metabolizing enzymes in different breast cancer cell lines. *Chem Biol Interact* 2011; **191**: 206-16.
17. Mounier CM, Wendum D, Greenspan E, Flejou JF, Rosenberg DW, Lambeau G. Distinct expression pattern of the full set of secreted phospholipases A2 in human colorectal adenocarcinomas: sPLA2-III as a biomarker candidate. *Br J Cancer* 2008; **98**: 587-95.
18. Vandesompele J, De Preter K, Pattyn F, Poppe B, Van Roy N, De Paepe A, et al. Accurate normalization of real-time quantitative RT-PCR data by geometric averaging of multiple internal control genes. *Genome Biol* 2002; **3**: RESEARCH0034.
19. Bustin SA, Benes V, Garson JA, Hellems J, Huggett J, Kubista M, et al. The MIQE guidelines: minimum information for publication of quantitative real-time PCR experiments. *Clin Chem* 2009; **55**: 611-22.
20. Smyth GK. Limma: linear models for microarray data. In: Robert Gentleman VJC, Wolfgang Huber, Rafael A. Irizarry, Sandrine Dudoit editor. *Bioinformatics and computational biology solutions using R and bioconductor*. New York: Springer; 2005. p.397-420.
21. (2008) RDCT. *R: A language and environment for statistical computing*. Vienna: R Foundation for Statistical Computing; 2011.
22. Benjamini Y, Hochberg Y. Controlling the false discovery rate - a practical and powerful approach to multiple testing. *R Stat Soc Series B Stat Methodol* 1995; **57**: 289-300.
23. Noguchi CT, Asavaritikrai P, Teng R, Jia Y. Role of erythropoietin in the brain. *Crit Rev Oncol Hematol* 2007; **64**: 159-71.
24. Nishiya D, Omura T, Shimada K, Matsumoto R, Kusuyama T, Enomoto S, et al. Effects of erythropoietin on cardiac remodeling after myocardial infarction. *J Pharmacol Sci* 2006; **101**: 31-9.
25. Szenajch J, Wcislo G, Jeong JY, Szczylik C, Feldman L. The role of erythropoietin and its receptor in growth, survival and therapeutic response of human tumor cells From clinic to bench - a critical review. *Biochim Biophys Acta* 2010; **1806**: 82-95.
26. Liang K, Esteva FJ, Albarracin C, Stemke-Hale K, Lu Y, Bianchini G, et al. Recombinant human erythropoietin antagonizes trastuzumab treatment of breast cancer cells via Jak2-mediated Src activation and PTEN inactivation. *Cancer Cell* 2010; **18**: 423-35.
27. Trost N, Hevir N, Rizner TL, Debeljak N. Correlation between erythropoietin receptor(s) and estrogen and progesterone receptor expression in different breast cancer cell lines. *Int J Mol Med* 2013; **31**: 717-25.
28. Lu C, Shen Q, DuPre E, Kim H, Hilsenbeck S, Brown PH. cFos is critical for MCF-7 breast cancer cell growth. *Oncogene* 2005; **24**: 6516-24.
29. Liu WM, Powles T, Shamash J, Propper D, Oliver T, Joel S. Effect of haemopoietic growth factors on cancer cell lines and their role in chemosensitivity. *Oncogene* 2004; **23**: 981-90.
30. Vivacqua A, Bonfiglio D, Recchia AG, Musti AM, Picard D, Ando S, et al. The G protein-coupled receptor GPR30 mediates the proliferative effects induced by 17beta-estradiol and hydroxytamoxifen in endometrial cancer cells. *Mol Endocrinol* 2006; **20**: 631-46.
31. Trost N, Juvan P, Sersa G, Debeljak N. Contrasting effect of recombinant human erythropoietin on breast cancer cell response to cisplatin induced cytotoxicity. *Radiol Oncol* 2012; **46**: 213-25.
32. Arcasoy MO, Jiang X, Haroon ZA. Expression of erythropoietin receptor splice variants in human cancer. *Biochem Biophys Res Commun* 2003; **307**: 999-1007.
33. Singh S, Dev A, Verma R, Pradeep A, Sathyanarayana P, Green JM, et al. Defining an EPOR-regulated transcriptome for primary progenitors, including Tnfr-sf13c as a novel mediator of EPO-dependent erythroblast formation. *PLoS One* 2012; **7**: e38530.

The usefulness of F-18 FDG PET/CT-mammography for preoperative staging of breast cancer: comparison with conventional PET/CT and MR-mammography

Eun-Ha Moon^{1,3}, Seok Tae Lim^{1,2}, Yeon-Hee Han¹, Young Jin Jeong⁴, Yun-Hee Kang⁵, Hwan-Jeong Jeong^{1,2}, Myung-Hee Sohn^{1,2}

¹ Department of Nuclear Medicine, Chonbuk National University Medical School and Hospital, Jeonju, Jeonbuk, Korea

² Research Institute of Clinical Medicine, Chonbuk National University Medical School and Hospital, Jeonju, Jeonbuk, Korea

³ Department of Nuclear Medicine, Presbyterian Medical Center, Jeonju, Jeonbuk, Korea

⁴ Department of Nuclear Medicine, Dong-A University Medical Center, Busan, Korea

⁵ Department of Nuclear Medicine, Eulji University School of Medicine, Daejeon, Korea

Radiol Oncol 2013; 47(4): 390-397.

Received 20 November 2012

Accepted 14 April 2013

Correspondence to: Seok Tae Lim, Department of Nuclear Medicine, Chonbuk National University Medical School and Hospital, San 2-20 Geumam-Dong, Deokjin-Gu, Jeonju, Jeonbuk, 561-180, South Korea. Phone: +82-63-250-1174; Fax: +82-63-255-1172; E-mail: stlim@jbnu.ac.kr

Disclosure: No potential conflicts of interest were disclosed.

Background. The objective of the study was to compare the diagnostic efficacy of an integrated Fluorine-18 fluorodeoxyglucose (F-18 FDG) PET/CT-mammography (mammo-PET/CT) with conventional torso PET/CT (supine-PET/CT) and MR-mammography for initial assessment of breast cancer patients.

Patients and methods. Forty women (52.0 ± 12.0 years) with breast cancer who underwent supine-PET/CT, mammo-PET/CT, and MR-mammography from April 2009 to August 2009 were enrolled in the study. We compared the size of the tumour, tumour to chest wall distance, tumour to skin distance, volume of axillary fossa, and number of metastatic axillary lymph nodes between supine-PET/CT and mammo-PET/CT. Next, we assessed the difference of focality of primary breast tumour and tumour size in mammo-PET/CT and MR-mammography. Histopathologic findings served as the standard of reference.

Results. In the comparison between supine-PET/CT and mammo-PET/CT, significant differences were found in the tumour size (supine-PET/CT: 1.3 ± 0.6 cm, mammo-PET/CT: 1.5 ± 0.6 cm, $p < 0.001$), tumour to thoracic wall distance (1.8 ± 0.9 cm, 2.2 ± 2.1 cm, $p < 0.001$), and tumour to skin distance (1.5 ± 0.8 cm, 2.1 ± 1.4 cm, $p < 0.001$). The volume of axillary fossa was significantly wider in mammo-PET/CT than supine-PET/CT (21.7 ± 8.7 cm³ vs. 23.4 ± 10.4 cm³, $p = 0.03$). Mammo-PET/CT provided more correct definition of the T-stage of the primary tumour than did supine-PET/CT (72.5% vs. 67.5%). No significant difference was found in the number of metastatic axillary lymph nodes. Compared with MR-mammography, mammo-PET/CT provided more correct classification of the focality of lesion than did MR-mammography (95% vs. 90%). In the T-stage, 72.5% of cases with mammo-PET/CT and 70% of cases with MR-mammography showed correspondence with pathologic results.

Conclusions. Mammo-PET/CT provided more correct definition of the T-stage and evaluation of axillary fossa may also be delineated more clearly than with supine-PET/CT. The initial assessment of mammo-PET/CT would be more useful than MR-mammography because the mammo-PET/CT indicates similar accuracy with MR-mammography for decision of T-stage of primary breast tumour and more correct than MR-mammography for defining focality of lesion.

Key words: breast cancer; fluorodeoxyglucose; positron emission tomography; MRI; mammography

Introduction

Breast cancer is the most common cancer and the second leading cause of cancer-related death in women in western countries.¹ Currently, breast cancer is diagnosed by triple assessment of physical examination, radiologic evaluation, and histopathologic confirmation. In particular, radiologic evaluation is more important when the size of tumour is too small.^{2,3} Treatment strategy of breast cancer is dependent on the size of the breast, size or extent of the tumour, infiltration, and lymph node metastasis, et cetera. Therefore, once breast cancer is diagnosed, accurate staging of the tumour is extremely important as it influences appropriate treatment decision and determines prognosis.⁴

Initial breast cancer staging has been based on a multimodality approach: X-ray mammography, ultrasonography, MRI, sentinel lymph node biopsy, and bone scintigraphy.⁵ X-ray mammography is the most widely used technique for evaluation of the primary tumour in both symptomatic and asymptomatic patients.⁶⁻⁸ However, because of dense breasts, X-ray mammography is less sensitive for Korean women, and underestimates the size or focality of the primary tumour.^{2,3,9,10} Correlation of X-ray mammography findings with breast ultrasonography and MRI has been helpful for differential diagnosis of a primary breast lesion and for detection of occult breast tumours.¹¹⁻¹³ However, this multimodality approach is invasive, as well as time and cost consuming. Thus, a non-invasive, single-session approach for breast cancer staging may be desirable.¹⁴⁻¹⁶

Fluorine-18 fluorodeoxyglucose positron emission tomography/computed tomography (F-18 FDG PET/CT) allows for accurate staging of various types of malignancies and for acquisition of whole-body imaging.^{17,18} Thus, PET/CT has high sensitivity in detection of primary tumour and axillary lymph node metastasis, as well as distant metastasis, in patients with breast cancer. In addition, PET/CT is beneficial for use in monitoring of therapy. However, with CT as part of PET/CT, tumour delineation is more difficult to determine than with MRI up to now, PET/CT has been used predominantly for evaluation of distant metastases.¹⁹⁻²³ MR-mammography, as well as X-ray mammography, in conjunction with ultrasonography, has remained the method of choice for imaging of the primary tumour of the breast. Patient positioning, which is similar to that used in MR-mammography (PET/CT-mammography), may provide more accurate information on the primary tumour and axillary

lymph node in PET/CT. However, the diagnostic accuracy of this PET/CT-mammography algorithm has not yet been defined.

The purpose of this study was to assess the usefulness and feasibility of PET/CT-mammography for preoperative staging of breast cancer and to compare the capability of measurement and delineation of lesion of PET/CT-mammography to those of conventional torso F-18 FDG PET/CT and MR-mammography.

Patients and methods

Patients

Forty women (mean age; 52.0 ± 12.0 years) with breast cancer who underwent conventional torso F-18 FDG PET/CT (supine-PET/CT), PET/CT-mammography (mammo-PET/CT) (PET/CT-mammography was acquired after the conventional torso PET/CT), and MR-mammography from April 2009 to August 2009 were enrolled (mean interval between MR-mammography and PET/CT-mammography: 1.7 ± 3.9 days, range: 0-23 days). All patients were confirmed breast cancer by biopsy before the diagnostic imagings were acquired. We compared the primary tumour size (longest diameter of lesion in trans-axial image), tumour to thoracic wall distance (T-C distance, maximal distance from tumour to thoracic wall in trans-axial image), tumour to skin distance (T-S distance, maximal distance from tumour to skin in trans-axial image), volume of ipsilateral axillary fossa, and number of suspected metastatic axillary lymph nodes between supine-PET/CT and mammo-PET/CT, retrospectively. Next, we evaluated the difference of the focality of the primary tumour and the size of the tumour in mammo-PET/CT and MR-mammography, retrospectively. Histopathologic findings served as the standard of reference. The protocol was approved by the Institutional Review Board of Chonbuk National University Hospital.

Imaging protocol

Supine-PET/CT and mammo-PET/CT

Whole body F-18 FDG PET/CT scans were obtained on a BiographTruepoint 40 PET/CT (Siemens, Berlin, Germany). Patients fasted for at least 6 hours before receiving an intravenous injection of F-18 FDG (mean: 429.0 ± 59.0 MBq (11.6 ± 1.6 mCi), range: 259.0 – 592.0 MBq (7 – 16 mCi)). Prior to injection of F-18 FDG, blood glucose levels were checked in order to determine



FIGURE 1. Breast positioning device. The device is constructed for prone breast positioning.

whether the levels were within the reference range (< 150 mg/dL). PET/CT images were acquired at 50–60 minutes after intravenous administration of F-18 FDG. Torso PET/CT from the skull base to the upper thigh was performed while the patient was in supine position (5 bed position, 120 seconds per bed). An iodinated contrast agent containing 320 mg of iodine per millilitre was injected using an automated injector (2.0 ml/kg body weight at an injection rate of 1.6 ml/s). A limited breath-hold technique was used in order to avoid motion-induced artifacts near the diaphragm. Then, mammo-PET/CT was performed after repositioning the patient prone (2 bed position, 120 seconds per bed), using a special breast-positioning device (E-cam scintimammography pallet, Siemens) (Figure 1). That device allowed for a breast position similar to that for the MR-mammography used in a routine clinical setting. Mammo-PET/CT image acquisition started at approximately 75 minutes after intravenous injection of F-18 FDG. The PET images were reconstructed by standard 3D-iterative algorithm (ordered subset expectation maximization; OSEM).

MR-mammography

All patients underwent MR-mammography. Dynamic contrast-enhanced breast MRI (Magnetom Symphony 1.5T (Siemens, Berlin, Germany)) was performed while the patient was in prone position using a dedicated breast coil. The breast MRI protocol also includes a sagittal T1-weighted localizing sequence followed by a sagittal T2-weighted

sequence (3,200/96 [repetition time ms/echo time ms]). A T1-weighted 3-dimensional, fat-suppressed fast spoiled gradient-echo sequence (11.0/4.8; flip angle, 90°; bandwidth, 150 Hz) was then performed before and 4 times sequentially after a rapid bolus intravenous injection of 0.1 mmol/kg body weight of gadolinium at an injection rate of 2.0 ml/s. Image acquisition began immediately after administration of the contrast material and saline bolus.

Image analyses

Analysis of PET/CT images was performed by two nuclear medicine physicians and MR-mammography was read by two radiologists. The evaluating physicians were blinded to the results of the other imaging procedures.

Supine-PET/CT and mammo-PET/CT

Assessments of the primary tumour, axillary lymph node metastasis, and distant metastasis with PET/CT were based on qualitative and quantitative assessments. PET/CT data were assessed qualitatively for regions of focally increased glucose metabolism and semi-quantitatively by maximal standardized uptake values (SUVmax). A lesion was determined as malignancy or metastasis on PET/CT if FDG uptake was higher than that in the surrounding tissue on qualitative analysis; the SUVmax was checked for the corresponding lesions. We also calculated the SUVmax ratio of primary breast lesion (SUVmax of primary lesion/SUVmax of adjacent muscle) and suspected metastatic lymph node in the axillary fossa (SUVmax of ipsilateral, metastatic axillary lymph node/SUVmax of adjacent muscle).

A breast lesion was suspected as malignant if it showed contrast enhancement, compared with the surrounding tissue (attenuation measurement with regions of interest (ROI) and expressed in Hounsfield unit (HU)) and elevated FDG uptake, compared with the adjacent breast tissue. The volume of ipsilateral axillary fossa (cm³) was evaluated for potential lymph node metastasis. Axillary fossa was assessed by measuring the area of axillary fat (between the outer margin of the *latissimus-dorsi/major teres* muscle and *minor/major pectoralis* muscle).²⁴ Lymph nodes were graded as malignant or benign based on their size and morphologic pattern (cross-sectional short axis diameter of more than 10 mm, loss of fatty hilum or cortical thickening supported the diagnosis of lymph node metastasis). In addition, FDG uptake of axillary lymph node was assessed using qualitative and quantitative analyses.

TABLE 1. Comparison of conventional whole body PET/CT and PET/CT-mammography in characteristics of primary breast lesions and ipsilateral axillary area

	Whole Body PET/CT (n = 40)	PET/CT-mammography (n = 40)	p value
Tumour size (cm)	1.3 ± 0.6	1.5 ± 0.6	< 0.001
Mean T-C* (cm)	1.8 ± 0.9	2.2 ± 2.1	< 0.001
Mean T-S†(cm)	1.5 ± 0.8	2.1 ± 1.4	< 0.001
Axillary area (cm ³)	21.7 ± 8.7	23.4 ± 10.4	0.03
Compatibility with pathologic T-staging (%)	67.5 (27/40)	72.5 (29/40)	0.63

* Tumour-Chest wall distance; † Tumour-Skin distance; n = number of patients

Supine-PET/CT and mammo-PET/CT were compared for assessment of the primary tumour and axillary lymph nodes. All PET/CT images were reviewed in 3 orthogonal planes (axial, coronal, and sagittal).

MR-mammography

Determination of malignancy on MR-mammography was based on assessment of tumour morphological characteristics, as well as the pattern of contrast-enhancement. Breast lesions were rated according to the American College of Radiology Breast Imaging Reporting and Data System lexicon. Both the morphologic appearance (size, shape, and enhancement pattern) and the temporal enhancement pattern were evaluated. Time-signal-intensity curves (progressive, plateau, or washout) were generated for all enhancing lesions.

Evaluation and staging of malignant lesions was performed according to the American Joint Committee on Cancer (AJCC) staging classification. The 2 imaging modalities (PET/CT and MR-mammography) were compared for T stage and focality of the primary tumour. Findings of focality of the primary tumour with mammo-PET/CT and MR-mammography were classified as unifocal (a single lesion in 1 quadrant), multifocal (more than 2 lesions in the same quadrant), or multicentric lesions (more than 2 quadrants affected by breast cancer, or distance between breast cancer lesions more than 4 cm within 1 quadrant).

Data analyses

Accuracy for delineation of primary tumour and axillary lymph node metastasis among the supine-PET/CT, mammo-PET/CT, and MR-mammography was calculated. T stage of the primary tumour was assessed with supine-PET/CT, mammo-PET/CT, and MR-mammography. Axillary lymph node was

assessed between the supine-PET/CT and mammo-PET/CT. In addition, the ability for accurate differentiation of unifocal, multifocal, and multicentric lesions was compared between mammo-PET/CT and MR-mammography. The final diagnosis was served by the histopathologic results.

Statistical Analyses

Accuracy for assessment of the primary tumour and axillary lymph nodes was calculated according to a patient-based analysis. Differences between images and histopathologic results were evaluated using a paired t-test, Pearson chi-square test, and Fisher's exact test. A *p*-value of less than 0.05 indicated a significant difference. SPSS version 12.0 (IBM, New York, USA) was used in performance of all statistical analyses.

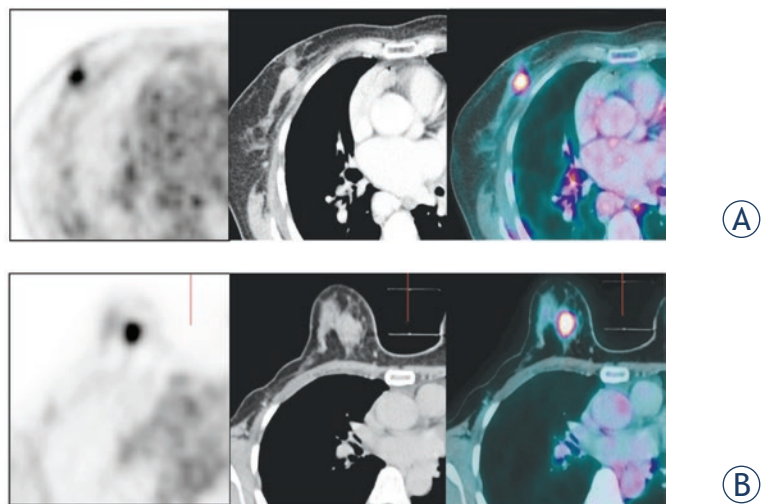


FIGURE 2. A woman with right breast cancer performed the supine-PET/CT and mammo-PET/CT. A The primary tumour was abutted on the chest wall in the supine-PET/CT. B The tumour could be more clearly distinguished from the chest wall in the mammo-PET/CT.

TABLE 2. T-stage of resected breast cancer and number of patients correctly staged with PET/CT-mammography and MR-mammography

T-stage	Pathologic Confirmation (n = 40)	Staged with PET/CT-mammography (n = 40)	Staged with MR-mammography (n = 40)
T1a	6	2 (33.3%)	-
T1b	1	1 (100%)	1 (100%)
T1c	21	18 (87.5%)	19 (90.5%)
T2	11	8 (72.7%)	8 (72.7%)
T3	1	-	-
T4	0	-	-
Total	40	29 (72.5%)	28 (70%)

Results

Assessment of the primary tumour

Pathologic biopsy showed that invasive ductal carcinoma, invasive lobular carcinoma and invasive micropapillary carcinoma were found 77.5% (31/40), 5% (2/40) and 5% (2/40) of patients. Ductal carcinoma in situ (DCIS) and the others (small cell carcinoma and tubular carcinoma) were found 7.5% (3/40) and 5% (2/40) of patients.

Comparison between supine-PET/CT and mammo-PET/CT

The mean size of primary tumour lesions, in the longest axis dimension, was significantly larger on mammo-PET/CT than on supine-PET/CT (supine-PET/CT: 1.3 ± 0.6 cm, mammo-PET/CT: 1.5 ± 0.6 cm, $p < 0.001$). The difference of tumour size between PET/CT imaging and histopathologic result was 0.5 ± 1.1 cm on supine-PET/CT and 0.2 ± 1.2 cm on mammo-PET/CT. Thus, the real size of the primary tumour was more accurate on mammo-PET/CT than on supine-PET/CT. The mean tumour to chest wall distance (supine-PET/CT: 1.8 ± 0.9 cm, mammo-PET/CT: 2.2 ± 2.1 cm, $p < 0.001$) and tumour to skin distance (supine-PET/CT: 1.5 ± 0.8 cm, mammo-PET/CT: 2.1 ± 1.4 cm, $p < 0.001$) were significantly longer on mammo-PET/CT than on supine-PET/CT, indicating better delineation of the tumour from the chest wall and skin (Figure 2, Table 1). The mean SUVmax of the primary tumour was 7.6 ± 5.8 (range: 1.4-20.8) on supine-PET/CT and 8.0 ± 6.2 (range: 1.8-21.4) on mammo-PET/CT ($p = 0.02$). The mean SUVmax ratio of the primary tumour showed 5.4 (range: 1.4-30.8) in the supine-PET/CT and 5.7 (1.3-23.4) in the mammo-PET/CT. No significant difference was showed between the supine-PET/CT and mammo-PET/CT statistically ($p = 0.18$).

Six patients were proven with T1a stage, and 1 patient with T1b, 21 patients with T1c, 11 patients with T2, and 1 patient with T3 by histopathologic confirmation. None of the patients had T4 stage of breast cancer. Characterization of T stage in breast cancer lesions was corrected in 27 (67.5%) of 40 patients on supine-PET/CT and 29 (72.5%) on mammo-PET/CT, compared with histopathologic confirmation (Table 1). No statistically significant difference was observed ($p = 0.63$).

Comparison between mammo-PET/CT and MR-mammography

In comparison of T stage, mammo-PET/CT provided correct classification of T stage of the primary tumour in 72.5% of cases. In patients with T1a, T1b, and T1c stage, mammo-PET/CT correctly found 2 (33.3%) of 6 patients, 1 (100%) of 1 patient, and 18 (87.5%) of 21 patients, respectively. Mammo-PET/CT also correctly found 8 (72.7%) of 11 patients in the T2 stage and none of the patients had T3 or T4 stage on mammo-PET/CT. MR-mammography provided correct characterization of T stage in a total of 28 (70%) of 40 patients. In patients with T1 (T1a-T1c) stage, MR-mammography found 1 (100%) of 1 patient with T1b, and 19 (90.5%) of 21 patients with T1c. In T2 stage patients, MR-mammography correctly found 8 (72.5%) of 11 patients and none of the patients had T3 or T4 stage in MR-mammography ($p = 0.81$) (Table 2). In measuring the size of primary tumour, one case showed more correct result in the mammo-PET/CT than the MR-mammography although the T stage was not changed.

In the focality of primary breast lesions, mammo-PET/CT provided correct characterization of 38 (95%) of 40 patients and MR-mammography found 36 (90%) of 40 patients. Solitary, multifocal, and multicentric lesions were found in 33, 2, and

TABLE 3. Comparison of PET/CT-mammography and MR-mammography in focality of primary breast lesions

Focality	Pathologic Confirmation (n = 40)	PET/CT-mammography (n = 40)	MR-mammography (n = 40)
Solitary	33	32	31
Multifocal	2	1	1
Multicentric	5	5	4
Total		38 (95%)	36 (90%)

5 patients in histopathologic confirmation. Finally, mammo-PET/CT found 32 of 33 patients with a solitary lesion, 1 of 2 patients with multifocal lesions, and 5 of 5 patients with multicentric lesions. MR-mammography correctly found 31 of 33 patients with a solitary lesion, 1 of 2 patients with multifocal lesions, and 4 of 5 patients with multicentric lesions ($p = 0.68$) (Table 3).

Axillary lymph node and distant metastasis

In axillary lymph node dissection, intra-axillary lymph node metastasis was histopathologically proven in 18 of 40 patients. PET/CT provided correct detection of intra-axillary metastatic lymph nodes in 14 of 18 patients and the other 4 patients showed no significant FDG uptake and negative imaging findings. No significant differences between supine-PET/CT and mammo-PET/CT were evaluated in the detection of the number of metastatic axillary lymph nodes. Sensitivity, specificity, and accuracy of PET/CT (supine-PET/CT and mammo-PET/CT) for detection of metastatic axillary lymph nodes were 77.8%, 86.4%, and 82.5%, respectively. The mean SUVmax of these metastatic lymph nodes was 4.8 ± 3.9 (range: 1.4 - 13.0) on supine-PET/CT and 5.3 ± 4.4 (range: 2.0 - 14.3). The mean SUVmax ratio of these metastatic lymph nodes showed 1.3 (range: 1.0 - 10.4) in the supine-PET/CT and 1.4 (range: 1.2 - 10.6). There was a no significant difference statistically ($p = 0.25$).

Although no significant differences between supine-PET/CT and mammo-PET/CT were detected in the number of metastatic axillary lymph nodes, the volume of ipsilateral axillary fossa was also significantly wider on mammo-PET/CT than on supine-PET/CT (supine-PET/CT: 21.7 ± 8.7 cm³, mammo-PET/CT: 23.4 ± 10.4 cm³, $p = 0.03$) (Figure 3, Table 1).

No distant metastases were found in any of the patients in this study; therefore, PET/CT including mammo-PET/CT did not influence further therapeutic decisions in any patient.

Discussions

According to the Central Cancer Registry Program 2009, the frequency of breast cancer was 15.1% among women in 2007 and it was reported to be second in cancer occurrence among Korean women, following thyroid cancer.²⁵ In Korea, breast cancer has shown a significant increase every year. Therefore, early detection of breast cancer is associated with attainment of cure through early intervention.²⁶

Initial breast cancer staging has been based on a multimodality approach: X-ray mammography, ultrasonography, MRI, sentinel lymph node biopsy, and bone scintigraphy. However, this multimodality approach is time consuming and uncomfortable for patients. Thus, a noninvasive, single-session approach to breast cancer staging may be desirable.¹¹⁻¹⁶

F-18 FDG PET/CT has been reported to be useful in staging, restaging, and monitoring of treatment response in cancer patients. PET/CT has high sensitivity in detection of the primary tumour and axillary lymph node metastasis, as well as distant metastasis in patients with breast cancer. However, with CT as part of PET/CT, tumour delineation is more difficult to determine than with MRI and PET/CT has been used predominantly for evaluation of distant metastases.¹⁹⁻²³

Because the glandular and fatty tissues of the breast are not uncompressed, prone breast positioning like that used in MR-mammography has a substantial advantage in better differentiation of the primary tumour from its adjacent structures and may improve the assessment of potential infiltration of tumour into the chest wall or skin of the breast. Theoretically, prone positioning may provide more accurate information on the primary tumour and axillary lymph node in PET/CT. In addition, due to enhanced anatomical visualization, the axillary fossa may be evaluated more easily for potential metastatic lymph nodes. MRI

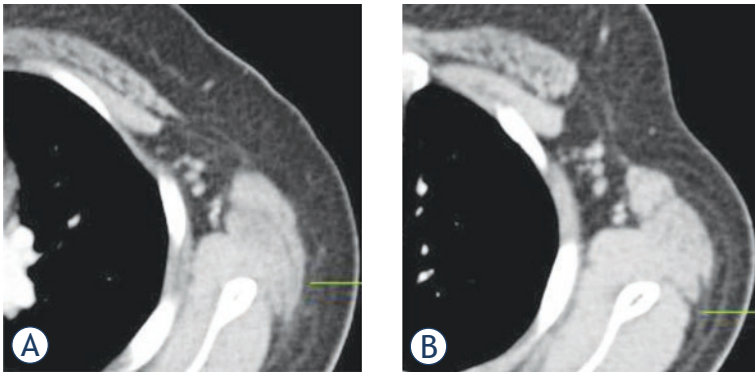


FIGURE 3. Assessment of axillary fossa in the woman with left breast cancer. A The volume of left axillary fossa measured 15 cm³ in the supine-PET/CT. B The volume of axillary fossa measured 24 cm³ in the mammo-PET/CT and the assessment of axillary fossa for the potential of metastatic axillary lymph node can be more clear and easy study group.

has been known to be a sensitive but less specific imaging modality for detection and characterization of breast cancer lesions. Findings from the current study suggest that the protocol for PET/CT-mammography may have similar sensitivity to MR-mammography for detection of intra-mammary lesions.²⁷⁻²⁹ However, the diagnostic accuracy of PET/CT-mammography has not yet been defined. We assessed the diagnostic accuracy of PET/CT-mammography as a single diagnostic modality in preoperative staging of breast cancer patients, compared with conventional PET/CT and MR-mammography.

Orel *et al.*³⁰ reported that MRI showed high sensitivity (91-100%) for staging of invasive breast cancer, and other studies have also reported that the sensitivity of MRI was 93%; however, specificity was relatively low (65%) due to the lack of ability to characterize enhancing lesions as benign or malignant.³¹⁻³³ MRI showed 85% accuracy in breast cancer stage; Heusner *et al.*³⁴ reported that MRI showed 77% accuracy for T stage, and 73% accuracy for focality of the primary tumour.

Antoch *et al.*¹² reported that MRI showed 52% accuracy for T stage and 79% accuracy for N stage; therefore, this result showed lower accuracy than that of another study due to the use of whole body MRI. This study showed that MR-mammography had 70% accuracy for T stage, and 90% for focality of the primary tumour. In comparison with previous studies, MR-mammography showed slightly lower accuracy in T stage and greater accuracy in decision of focality.

In a previous study of FDG PET for staging of breast cancer, Samson *et al.*³⁵ reported that FDG

PET had 89% sensitivity, and Antoch *et al.*¹² reported that FDG PET/CT showed 80% accuracy in T stage, and 93% accuracy in N stage. According to this data, conventional PET/CT (supine-PET/CT) showed 67.5% accuracy in T stage and mammo-PET/CT showed 72.5% accuracy in T stage, and 95% accuracy for focality of the primary lesion. Supine-PET/CT and mammo-PET/CT showed similar accuracy (77.8%) for N stage. This study showed slightly lower accuracy than that of current studies in T and N stage of breast cancer patients; however, appropriate comparison between the results would be difficult because only a few studies of mammo-PET/CT in breast cancer staging have been conducted. However, like the preceding study, the current study suggests that this PET/CT protocol for breast cancer may be similar to MRI for detection of intra-mammary cancer lesions. The accuracy of assessment of the primary tumour was also similar between mammo-PET/CT and MR-mammography in this study.

Heusner *et al.* reported that the area of axillary fossa (cm²) was significantly wider on mammo-PET/CT than on supine-PET/CT and anatomical structures of the axilla may be more easily differentiated from one another.²⁴ Although we assessed the volume of axillary fossa and no significant differences were detected in the number of metastatic axillary lymph nodes, this data also showed that the volume of axillary fossa was wider on mammo-PET/CT than on supine-PET/CT.

None of the patients in this study had distant metastasis; however, Heusner *et al.* reported that PET/CT influenced further therapeutic decisions in 5 patients by detecting the unexpected distant metastasis or synchronous malignancy.³⁴

There are some technical limitations in acquisition of whole body mammo-PET/CT. We acquired the mammo-PET/CT image after conventional supine-PET/CT. A whole body mammo-PET/CT protocol, instead of the combined whole body supine-PET/CT with mammo-PET/CT, should be discussed, as this would reduce the examination time. However, patient tolerance may limit this protocol, because the acquisition time can be up to 90 minutes. Use of state-of-the-art multislice PET/CT systems will further reduce the examination times, compared with PET/CT scanners, with fewer detector rows. In this setting, a whole body mammo-PET/CT may be clinically feasible.

Based on our data, mammo-PET/CT improved the accuracy in initial staging of breast cancer and showed that the evaluation of axillary fossa was more clearly and easily, compared with supine-

PET/CT. Also mammo-PET/CT indicated the similar accuracy with MR-mammography in T stage and was more correct than MR-mammography for defining focality of lesion. Furthermore, PET/CT can acquire whole body image, so has the advantage for detecting the unexpected, distant metastasis and changing the treatment strategy.

Acknowledgement

This study was supported by a grant from the National R&D Program for Cancer Control, Ministry Health, Welfare and Family Affairs, Republic of Korea (0620220 and 0720420).

References

- Jemal A, Siegel R, Ward E, Murray T, Xu J, Smigal C, et al. Cancer statistics, 2006. *CA Cancer J Clin* 2006; **56**: 106-30.
- Kopans DB. The positive predictive value of mammography. *Am J Roentgenol* 1992; **158**: 521-6.
- Bird RE, Wallace TW, Yankaskas BC. Analysis of cancer missed at screening mammography. *Radiology* 1992; **184**: 613-7.
- Adriaenssens N, Belsack D, Buyl R, Ruggiero L, Breucq C, De Mey J, Lievens P, Lamote J. Ultrasound elastography as an objective diagnostic measurement tool for lymphoedema of the treated breast in breast cancer patients following breast conserving surgery and radiotherapy. *Radiol Oncol* 2012; **46**: 284-95.
- Zebic-Sinkovec M, Hertl K, Kadivec M, Cavlek M, Podobnik G, Snoj M. Outcome of MRI-guided vacuum-assisted breast biopsy – initial experience at Institute of Oncology Ljubljana, Slovenia. *Radiol Oncol* 2012; **46**: 97-105.
- Agnese DM. Advances in breast imaging. *Surg Technol Int* 2005; **14**: 51-6.
- Scheidhauer K, Walter C, Seemann MD. FDG PET and other imaging modalities in the primary diagnosis of suspicious breast lesions. *Eur J Nucl Med Mol Imaging* 2004; **31**: 70-9.
- Thurlimann B, Muller A, Senn HJ. Management of primary breast cancer: an update. *Onkologie* 2004; **27**: 175-9.
- Rausch DR, Hendrick RE. How to optimize clinical breast MR imaging practices and techniques on your 1.5-T system. *Radiographics* 2006; **26**: 1469-84.
- Berg WA, Gutierrez L, NessAiver MS, Carter WB, Bhargavan M, Lewis RS, et al. Diagnostic accuracy of mammography, clinical examination, US, and MR imaging in preoperative assessment of breast cancer. *Radiology* 2004; **233**: 830-49.
- Winnekenendonk G, Krug B, Warm M, Gohring UJ, Mallmann P, Lackner K. Diagnostic value of preoperative contrast-enhanced MR imaging of the breast. *Rofo* 2004; **176**: 688-93.
- Antoch G, Vogt FM, Freudenberg LS, Nazaradeh F, Goehde SC, Barkhausen J, et al. Whole-body dual-modality PET/CT and whole-body MRI for tumor staging in oncology. *JAMA* 2003; **290**: 3199-206.
- Czernin J, Allen-Auerbach M, Schelbert HR. Improvements in cancer staging with PET/CT: literature-based evidence as of September 2006. *J Nucl Med* 2007; **48** (Suppl 1): 78S-88S.
- Blodgett TM, Meltzer CC, Townsend DW. PET/CT: form and function. *Radiology* 2007; **242**: 360-85.
- Zangheri B, Messa C, Picchio M, Gianolli L, Landoni C, Fazio F. PET/CT and breast cancer. *Eur J Nucl Med Mol Imaging* 2004; **31** (Suppl 1): 135S-142S.
- Tatsumi M, Cohade C, Mourtzikos KA, Fishman EK, Wahl RL. Initial experience with FDG-PET/CT in the evaluation of breast cancer. *Eur J Nucl Med Mol Imaging* 2006; **33**: 254-62.
- Hodolic M. Role of F-18-choline PET/CT in evaluation of patients with prostate carcinoma. *Radiol Oncol* 2011; **45**: 17-21.
- Kim JS, Jeong YJ, Sohn MH, Jeong HJ, Lim ST, Kim DW, et al. Usefulness of F-18 FDG PET/CT in subcutaneous panniculitis-like T cell lymphoma: disease extent and treatment response evaluation. *Radiol Oncol* 2012; **46**: 279-83.
- Radan L, Ben-Haim S, Bar-Shalom R, Guralnik L, Israel O. The role of FDG-PET/CT in suspected recurrence of breast cancer. *Cancer* 2006; **107**: 2545-51.
- Beresford M, Lyburn I, Sanghera B, Makris A, Wong WL. Serial integrated ¹⁸F-fluorodeoxythymidine PET/CT monitoring neoadjuvant chemotherapeutic response in invasive ductal carcinoma. *Breast J* 2007; **13**: 424-5.
- Li D, Chen JH, Wang J, Ling R, Yao Q, Wang L. Value of fused F-18 FDG PET/CT images in predicting efficacy of neoadjuvant chemotherapy on breast cancer. [in Chinese]. *Ai Zheng* 2007; **26**: 900-4.
- Reddy DH, Mendelson EB. Incorporating new imaging models in breast cancer management. *Curr Treat Options Oncol* 2005; **6**: 135-45.
- Fischer U, Kopka L, Grabbe E. Breast carcinoma: effect of preoperative contrast-enhanced MR imaging on the therapeutic approach. *Radiology* 1999; **213**: 881-8.
- Heusner TA, Freudenberg LS, Kuehl H, Hauth AM, Haibach PV, Forsting M, et al. Whole-body PET/CT-mammography for staging breast cancer: initial results. *Br J Radiol* 2008; **81**: 743-8.
- Ko BS, Noh WC, Kang SS, Park BW, Kang EY, Paik NS, et al. Changing patterns in the clinical characteristics of Korean breast cancer from 1996-2010 using an online nationwide breast cancer database. *J Breast Cancer* 2012; **15**: 393-400.
- Andersson I. Mammographic screening and mortality from breast cancer: mammographic screening trial. *Br J Med* 1998; **297**: 943-8.
- Lehman CD, Blume JD, Weatherall P, Thickman D, Hylton N, Warner E, et al. Screening women at high risk for breast cancer with mammography and magnetic resonance imaging. *Cancer* 2005; **103**: 1898-905.
- Friedrich M. MRI of the breast: state of the art. *Eur Radiol* 1998; **8**: 707-25.
- Bedrosian I, Mick R, Orel SG, Schnall MD, Reynolds C, Spitz F, et al. Changes in the surgical management of patients with breast carcinoma based on preoperative magnetic resonance imaging. *Cancer* 2003; **98**: 468-73.
- Orel SG, Schnall MD. MR imaging of the breast for detection, diagnosis and staging of breast cancer. *Radiology* 2001; **220**: 3-30.
- Schelfout K, Van Goethem M, Kersschot E, Colpaert C, Schelfhout AM, Leyman P, et al. Contrast-enhanced MR imaging of breast lesions and effect on treatment. *Eur J Surg Oncol* 2004; **30**: 501-7.
- Hollingsworth AB, Stough RG, O'Dell CA, Brekke CE. Breast magnetic resonance imaging for preoperative locoregional staging. *Am J Surg* 2008; **196**: 389-97.
- Liberman L, Morris EA, Lee MJ, Kaplan JB, LaTrenta LR, Menell JH, et al. Breast lesions detected on MR imaging: features and positive predictive value. *Am J Roentgenol* 2002; **179**: 171-8.
- Heusner TA, Kuemmel S, Umutlu L, Koeninger A, Freudenberg LS, Hauth AM, et al. Breast cancer staging in a single session: whole-body PET/CT mammography. *J Nucl Med* 2008; **49**: 1215-22.
- Samson DJ, Flamm CR, Pisano ED, Aronson N. Should FDG PET be used to decide whether a patient with an abnormal mammogram or breast finding at physical examination should undergo biopsy? *Acad Radiol* 2002; **9**: 773-83.

Role of contrast-enhanced ultrasound in evaluating the efficiency of ultrasound guided percutaneous microwave ablation in patients with renal cell carcinoma

Xin Li^{1,2}, Ping Liang¹, Jie Yu¹, Xiao-Ling Yu¹, Fang-Yi Liu¹, Zhi-Gang Cheng¹, Zhi-Yu Han¹

¹ Interventional Ultrasound Department of Chinese PLA General Hospital, Beijing, China

² Medical College of Nankai University, Tianjin, China

Radiol Oncol 2013; 47(4): 398-404.

Received 12 January 2013

Accepted 4 April 2013

Correspondence to: Ping Liang, M.D., Interventional Ultrasound Department of Chinese PLA General Hospital, 28 Fuxing Road, Beijing 100853, China. Tel: +86 10 66939530; Fax: +86 10 68161218; Email: liangping301@hotmail.com

Disclosure: No potential conflicts of interests were disclosed.

Background. The aim of the study was to evaluate the efficiency and feasibility of contrast-enhanced ultrasound (CEUS) with Sonovue in assessing of renal cell carcinomas (RCCs) following ultrasound (US)-guided percutaneous microwave ablation (MWA).

Patinets and methods. Seventy-nine patients (60 males and 19 females) with 83 lesions (mean size 3.2±1.6 cm) were treated by US-guided percutaneous MWA. The CEUS results of the third day after the ablation were compared with the synchronous contrast-enhanced computed tomography (CT)/magnetic resonance imaging (MRI) results and biopsy pathological results. The follow-up was performed by CEUS and CT/MRI after 1, 3, 6 months and every 6 months subsequently. The combination of clinical follow-up results and CT/MRI imaging findings was the reference standard of CEUS results for evaluating the therapeutic effect. The identification of residual or recurrence tumour was assessed by two blinded radiologists.

Results. On the third day after MWA, CEUS showed 68 of 83 lesions (68/83, 81.9%) successfully ablated and 15 of 83 (18.1%) with residual tumours. Among residual tumours, 13 (86.7%) were confirmed by contrast-enhanced CT/MRI findings and biopsy results. The sensitivity, specificity, accuracy, positive and negative predictive value of CEUS evaluating the short-term MWA effectiveness were 100%, 97.1%, 97.6%, 86.7% and 100%, respectively. During the six years follow-up (median 26 months), the CEUS showed recurrence in 7 patients, and six of them achieved consistent results on CEUS and CT/MRI imaging. The sensitivity, specificity, accuracy, positive and negative predictive value for CEUS evaluating long-term MWA effectiveness were 85.7%, 98.7%, 97.6%, 85.7% and 98.7%, respectively.

Conclusions. The post-procedural CEUS demonstrated as an effective and feasible method in evaluating a therapeutic effect of RCCs following MWA.

Key words: contrast enhanced ultrasound; microwave ablation; renal cell carcinoma

Introduction

The incidence of renal cell carcinoma (RCC) has been increasing during the last decades of years. It accounts for 2.1% of all malignancies and is responsible for 1.5% of all cancer deaths worldwide.¹ Thermal ablation including radiofrequency ablation (RFA) and cryoablation has rapidly expanded

as an effective treatment option for patients who are sub optimal candidates for surgical and laparoscopic renal surgery.²⁻⁴ Good local tumor control and survival rate have been recently reported for ultrasound (US) -guided percutaneous microwave ablation (MWA) for RCC, especially for small ones.⁵ Thermal ablation has rapidly expanded as an effective treatment option. To obtain a good thera-

TABLE 1. Patients and renal cell carcinomas characteristics

Characteristics	Data
Patients	
Male/Female	61/19
Age (mean±sd [rang]) years	64.5±14.8 (22-82)
Bilateral tumours	4 (4.8%)
Renal cell carcinomas	
Size (cm)	
mean±sd [rang]	3.2±1.6 (0.6-7.8)
≤4	66 (78.6%)
>4	18 (21.4%)
Location(side)	
Right/Left	48/36
Location(type)	
Exophytic*	16 (19.0%)
Intraparenchymal**	46 (54.8%)
Endophytic ***	22 (26.2%)
Histological diagnoses by biopsy	
Renal clear cell carcinoma	76 (90.5%)
Renal papillary cell carcinoma	6 (7.1%)
Chromophobe renal cell carcinoma	2 (2.4%)
Median follow-up (month)	26 (3-74)

* Exophytic lesions were defined as nodules beyond the renal contour with no component extending into the renal sinus.

** Intraparenchymal lesions were defined as nodules confined within the parenchyma without contour bulging or sinus extension.

*** Endophytic lesions were defined as nodules that extended into the renal sinus and were in close proximity to the collecting structures or the ureters.

peutic response, it is extremely important to assess the ablation completeness of the lesions as soon as possible after the treatment. Traditional computed tomography (CT) or magnetic resonance imaging (MRI) are often used to assess the ablation therapeutic efficacy.⁶ On the other hand the advantages of contrast-enhanced ultrasound (CEUS) as a safe, well tolerated, non-ionising imaging method with real-time multiplanar imaging, using nontoxic contrast agent have been well documented.⁷ CEUS has already been widely used in assessing thermal treatment in liver carcinoma with high a diagnostics accuracy.⁸ It has been proposed that CEUS was an alternative to CT and MRI in the follow-up of renal tumour treated with RFA.⁹ MWA results in higher thermal efficiency than RFA¹⁰, so for the rich blood organ (such as kidney) ablation, the tumour necrosis boundary may show a different CEUS pattern. To our knowledge, there is no paper re-

porting the application of CEUS in evaluating the therapeutic effect of MWA for RCC.

The aim of this study is to summarize our experience of the efficacy of CEUS in evaluating the short and long-term therapeutic effect in patients with RCC after MWA, using CT/MRI as reference standard. The ultimate goal is to find a simple, effective, convenient and safe evaluation technology to improve the ablation efficacy.

Patients and methods

Patients

This prospective study was approved by our institutional review board. The written informed consent for the procedure was obtained from each enrolled patient. Between April 2006 and June 2012, 84 RCC lesions in 80 patients were confirmed pathologically by US-guided percutaneous biopsy. Seventy-nine patients with 83 lesions were recruited and one patient with lesion diameter of 9.7 cm was excluded from the study due to the palliative treatment. All patients were treated on an inpatients basis. Patients' characteristics were listed in Table 1. Pre- and post-ablation imaging (conventional US, CEUS and CT/MRI) were implemented to evaluate the characteristics of the tumours and ablation effectiveness. The tumour diagnosis was pathologically confirmed by intra-procedure biopsy.

Ablation procedure

US-guided core needle biopsy (18 G, Bard, Japan) was performed just before the ablation during the same procedure. All ablations were performed using the microwave unit (KY-2000; Kangyou Medical, Nanjing, China) producing microwave energy (maximum power 100 W) through a 15-gauge cooled-shaft needle antenna with the emitting frequency of 2450 MHz. The patients underwent MWA under vein anesthesia, with a percutaneous US-guided and monitored approach using an Acuson Sequoia 512 scanner (Signature 10.2; Siemens Medical Solutions, Mountain View, Calif) with 3.5-5.0 MHz curved-array multi-frequency transducers. For tumours less than 2.0 cm, one antenna was inserted in the centre of the lesion, and for tumours measured 2.0 cm or larger, two antennae were used according to the characters of the lesion. The ablation time was from 300 to 600 seconds based on the tumour size. When the hyperechoic range covered the entire lesion, the microwave emitting was stopped.

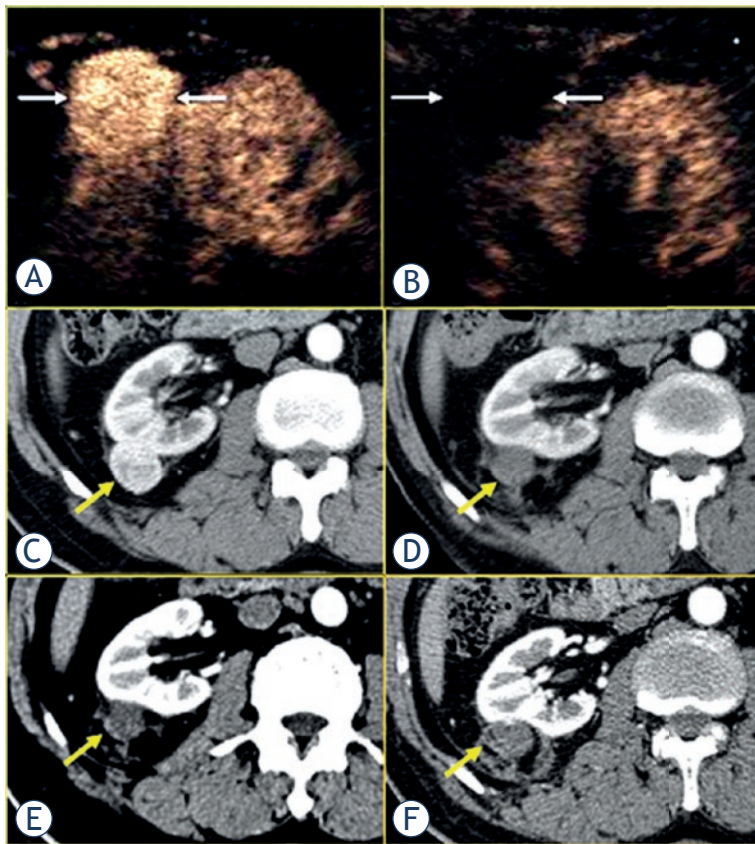


FIGURE 1. Images in 82-year-old female with a 3.9 cm x 3.7 cm renal clear cell carcinoma treated with microwave ablation (MWA). (A) Pre-ablation contrast-enhanced US scan showed one hyper-enhancement lesion exophytically (arrow). (B) Seven days after ablation contrast-enhanced US showed the whole lesion no-enhancement continuously. (C) Transverse contrast-enhanced multidetector-row CT imaging showed one hyper-intense lesion pre-ablation and hypo-intense one in arterial phase 7 days (D), 1 month (E) and 6 months (F) after ablation.

CEUS

The conventional US and CEUS were performed with an Acuson Sequoia 512 scanner and 4V1 transducer with frequencies of 1 - 4MHz. The CEUS imaging technique was contrast pulse sequencing (CPS) soft-ware which permitted real-time depiction of lesion blood perfusion under low mechanical index ($MI < 0.2$) in order to avoid microbubble disruption. A bolus injection of 1.0-1.2 ml of sulphur hexafluoride-filled microbubble contrast agent (Sonovue BR1; Bracco SpA; Milan, Italy) was administrated through a 20-gauge *canula* placed in the antecubital vein. The injection of Sonovue was followed by a flush of 5 ml 0.9% sodium chloride solution. All patients tolerated Sonovue application well. The entire examination was stored as a dynamic digital video file on the hard disk of the US scanner and recorded on a digital video recorder for further analysis.

CT and MRI

Contrast-enhanced CT was performed in 47 patients with multi-detector row CT (Light speed 16; GE Medical Systems, Milwaukee, WI, USA) with a section thickness of 5 mm, a 1.35:1.0 pitch, 120 kV, and 250 mA, and contrast medium (iopromide, Ultravist 300; Schering, Berlin, Germany). Contrast-enhanced MRI was performed in 32 patients using a 1.5-T unit (Signa Echo-Speed; GE Medical Systems) with the sequences: spin-echo T1-weighted (500/15 [repetition time msec/echo time msec], 256 x 192 matrix, and two signals acquired); fat-suppressed T2-weighted respiratory-triggered fast spin-echo (3000-4000/102, 256 x 256 matrix, and three signals acquired); and fat-suppressed spin-echo T1-weighted (500/15, 256 x 192 matrix, and two signals acquired) sequence. Fat-suppressed T1-weighted sequence was performed prior to and three times (scanning delay of 0 seconds for the corticomedullary phase, 70 seconds for the nephrographic phase, and 180 seconds for the excretory phase) after dynamic injection of 0.1 mmol of gadopentetate dimeglumine (Magnevist; Schering, Berlin, Germany) per kilogram of body weight. The subtraction of the postcontrast image from the precontrast image was performed for all time points.

Follow-up

Three days after MWA, contrast-enhanced imagings (CEUS + CT, or CEUS + MRI) were performed to evaluate the ablation effect, then 1, 3, 6 months and every 6 months subsequently. The CEUS results of the third day after the ablation were compared with the synchronous contrast-enhanced CT/MRI results. If CEUS and CT/MRI were both negative, the patient went into the follow-up stage. However, if the results were not consistent or both positive, then US-guided core needle biopsy was performed for the enhanced area and the patient underwent another ablation session for the possible residual area. The combination of clinical follow-up results and CT/MRI imaging results were reference standard of CEUS results for the long-term therapeutic effect. Every imaging was reviewed by two experienced radiologists (P.L., X.L.Y.).

Imaging analysis

The criteria for CEUS imaging were: inflammatory congestion caused by MWA displayed uniformly circular enhancement around the necrosis zone. If irregular peripheral enhancement in scattered,

nodular, or eccentric pattern was noted, this was thought to indicate the presence of residual, incompletely ablated tumor.¹¹ This finding indicated the incomplete local treatment and a further ablation was considered if the patient still met the criteria for MWA. In patients with complete necrosis, a well-defined non-enhancing zone on CEUS and CT/MRI imaging was noted and the lesion shrank gradually over time.

Statistical analysis

Statistics was performed by version SPSS 16.0 for windows statistical package (SPSS, Chicago, Ill). The baseline characteristic of patients and tumours were expressed as mean \pm SD or median. Sensitivity, specificity, accuracy, positive predictive value (PPV) and negative predictive value (NPV) were calculated for CEUS in diagnosing accuracy of MWA effect for RCC.

Results

Seventy-nine patients with 83 solid lesions treated with percutaneous MWA were enrolled in our study with mean age of 64.5 ± 14.8 (22-82) years. There were 75 patients with one lesion and 4 patients with two. The lesions included clear cell carcinoma in 71 patients, papillary carcinoma in 6 patients, and chromophobe carcinoma in 2 patients. The mean size of the tumours was 3.2 ± 1.6 cm. The sixty-eight of 83 (81.9%) lesions were successfully ablated in one session, 15 of 83 (18.1%) in two sessions. No severe procedure-related complications (including haematuria, pneumothorax, sepsis, renal infarction, skin burns, seeding and so on) were observed.

On the third day after MWA, CEUS showed that 68 of 83 lesions (82.9%) were successfully ablated. The results of CEUS were confirmed by contrast-enhanced CT/MRI three days after MWA (Figure 1). Fifteen of 83 (18.3%) lesions appeared residual tumour on CEUS. Among them biopsy results verified 13 residual tumours (Figure 2) and the second CEUS-guided ablations were done. The sensitivity, specificity, accuracy, PPV and NPV of CEUS evaluating instant effect of MWA of RCC were 100%, 97.1%, 97.6%, 86.7% and 100%, respectively (Table 2).

During the median follow-up period of 26 months (rang 3-74 months), seventy-six patients survived and three patients died of heart failure, gastrorrhagia and multiple organs failure at

TABLE 2. Evaluation performance of contrast-enhanced ultrasound (CEUS) on assessment of the therapeutic effects for renal cell carcinomas on the third day after microwave ablation

Follow-u CEUS	Reference standard	
	Residual	No residual
Residual	13	2
No residual	0	68

TABLE 3. Evaluation performance of contrast-enhanced ultrasound (CEUS) on assessment of the therapeutic effects after microwave ablation for renal cell carcinomas during the follow-up

Follow-u CEUS	Reference standard	
	Recurrence	No recurrence
Recurrence	6	1
No recurrence	1	75

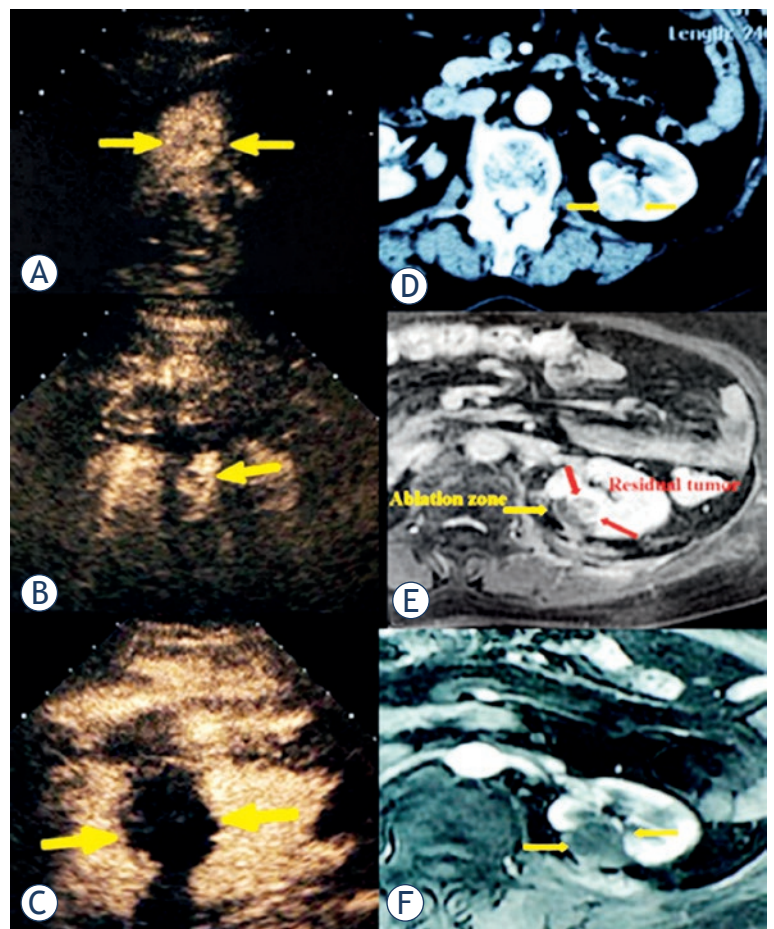


FIGURE 2. 72-year-old female with a 4.5 cm x 3.9 cm renal clear cell carcinoma was treated with microwave ablation (MWA). (A) Pre-ablation contrast-enhanced US scan showed one hyper-enhancement lesion (arrow), (B) and 3 days after ablation showed a very small hyper-enhancement adjacent to the ablation zone. (C) Then the patient received another ablation and reached completed necrosis. Transverse contrast-enhanced MR imaging showed one hyper-intense lesion a little exophytic and adjacent to renal pelvis in arterial phase pre-ablation and showed the same hyper-intense (residual tumour) (red arrow) homochronously (D), then no-intense after another ablation (F).

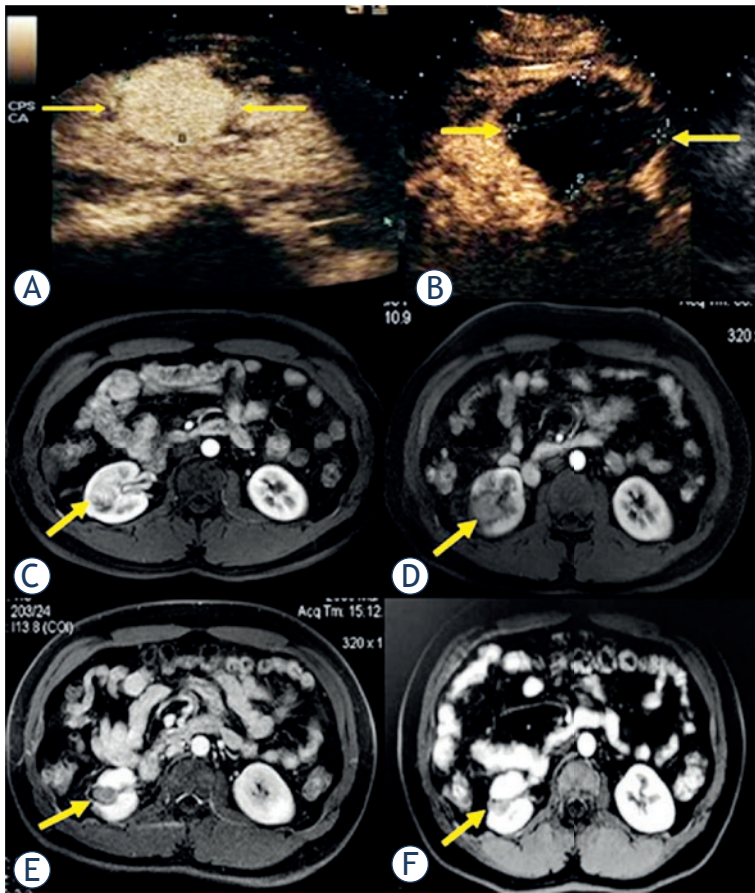


FIGURE 3. Pre-ablation contrast-enhanced US showed a hyper-enhancement 2.4 cm x 1.9 cm renal clear cell carcinoma in renal parenchyma in a 45-year-old man (A, arrow). Transverse contrast-enhanced MR imaging showed one hyper-intense lesion adjacent to renal pelvis pre-ablation (C) and hypo-intense in arterial phase 7 days (D), 1 year (E) and 2 years (F) after ablation, and the lesion shrunk gradually obviously.

37, 39, 61 months after the ablation respectively. Seventy-six (76/83) lesions showed a completed ablation during the follow-up (Figure 3). Seven (7/83) lesions were detected recurrent tumour, confirmed by CEUS and CT/MRI in six patients with consistency. One patient with the lesion (max diameter 4.7 cm, located exophytic and adjacent to intestinal tract) showed a completed ablation at 6 months after the ablation on CEUS, but local tumour progression was detected on MRI and then confirmed by subsequent nephrectomy (Figure 4). At 15 months after the ablation CEUS detected recurrence in one patient with max diameter 5.8 cm lesion located endophytic close to pelvis but the result was denied by MRI, while the CT imaging and biopsy result verified the result of CEUS and the CT and CEUS confirmed complete necrosis during 74 months follow-up. The sensitivity, specificity,

accuracy, PPV and NPV for CEUS detecting residual or recurrence tumour during the follow-up period were 85.7%, 98.7%, 96.7%, 85.7% and 98.7%, respectively (Table 3).

Discussion

The image-guided thermal ablation has been widely used for renal lesions treatment on account of the technology promotion, and obtained a favourable curative effect parallel to nephron-sparing surgery especially for small ones.^{4,12} To achieve radical clinical results after MWA of renal tumours, it is important to select suitable patients. Indications for MWA of RCC including patients with small lesions (size less than 4 cm), patients of advanced age or poor surgical candidates due to significant comorbidities, those with single kidney or multiple tumours in both kidneys; and patients with ablation preference. In addition, the timely and accurate evaluation of the therapeutic effects is also momentous for promoting the ablation effect. The CT/MRI as traditional imaging in evaluating the ablation treatment efficacy has some limitations. CEUS with the second generation contrast agent Sonovue as a useful, convenient, no-hepatotoxicity and no-nephrotoxicity tool has been widely used and provided abundant diagnosis and assessment information, especially suitable for renal function impaired patients. There were several reports on CUES assessment of RFA or cryoablation of renal lesions¹³⁻¹⁵, but in the MWA field, a study on CEUS evaluation was seldom.

To investigate the role of CEUS in evaluating the MWA of kidney, we performed the short-term (three days) and long-term observation by using CEUS as evaluation tool after MWA of RCC with promising results.

Though CEUS confirmed comparable results with CT/MRI in evaluation of RCC ablation effect, CEUS had the advantages in real-time showing the ablation zone, the surrounding renal parenchyma and the renal vessels that may provide potential superiority for detecting local tumour progression. However, just as conventional US, CEUS is subject to unclear lesion display for abdominal gas shielding or relative operator dependence of US. The optimal time of CEUS to evaluate the therapeutic effects after thermal ablation was another important point to promote the diagnosis ability. The timely and accurate detection of the residual tumour was important for choosing a proper treatment as early as possible to improve the tumour-free survival

rate. One week to one month interval after the ablation were preferred by some researchers.¹³⁻¹⁶ In our study the initial evaluation time was chosen as the third day after MWA due to the fact that congestion zone 72 hours after the thermal ablation was less evident than within 24 hours after the ablation, which may decrease the distraction for the CEUS and another session could be provided timely if necessary.

This study has some limitations as well. Firstly, post-ablation biopsy with pathological results was not performed in all lesions due to a bleeding risk. Some authors had pointed out that the use of needle biopsy had some limitation in depicting residual lesions after thermal ablation.¹⁷ Secondly, to some extent, the CEUS imaging evaluation was depended on the experience of the radiologists. Larger series and longer follow-up period are needed to further confirm the results of our study. Also comparative investigation of CEUS evaluation in MWA and RFA of RCC is mandatory.

Conclusions

Ultimately the post-procedural CEUS appearances to be a convenient, repeatable, less-toxically technology with high diagnosis accuracy and plays a promising role in evaluating the therapeutic effect of RCCs following MWA.

References

1. Ferlay J, Shin HR, Bray F, Forman D, Mathers C, Parkin DM. Estimates of worldwide burden of cancer in 2008: GLOBOCAN 2008. *Int J Cancer* 2010; **115**: 2893-917.
2. Liang P, Wang Y, Zhang D, Yu X, Gao Y, Ni X. Ultrasound guided percutaneous microwave ablation for small renal cancer: initial experience. *J Urol* 2008; **180**: 844-8.
3. Schmit GD, Thompson RH, Kurup AN, Weisbrod AJ, Carter RE, Callstrom MR, et al. Percutaneous cryoablation of solitary sporadic renal cell carcinomas. *BJU Int* 2012; **110**: E526-31.
4. Adeyanju OO, Al-Angari HM, Sahakian AV. The optimization of needle electrode number and placement for irreversible electroporation of hepatocellular carcinoma. *Radiol Oncol* 2012; **46**: 126-35.
5. Yu J, Liang P, Yu XL, Cheng ZG, Han ZY, Mu MJ, et al. US-guided percutaneous microwave ablation of renal cell carcinoma: intermediate-term results. *Radiology* 2012; **263**: 900-8.
6. Frieser M, Kiesel J, Lindner A, Bernatik T, Haensler JM, Janka R, et al. Efficacy of contrast-enhanced US versus CT or MRI for the therapeutic control of percutaneous radiofrequency ablation in the case of hepatic malignancies. *Ultraschall Med* 2011; **32**: 148-53.
7. Piscaglia F, Bolondi L. The safety of sonovue in abdominal applications: retrospective analysis of 23188 investigations. *Ultrasound Med Biol* 2006; **32**: 1369-75.
8. Bartolotta TV, Taibbi A, Midiri M, De Maria M. Hepatocellular cancer response to radiofrequency tumor ablation: contrast-enhanced ultrasound. *Abdom Imaging* 2008; **33**: 501-11.

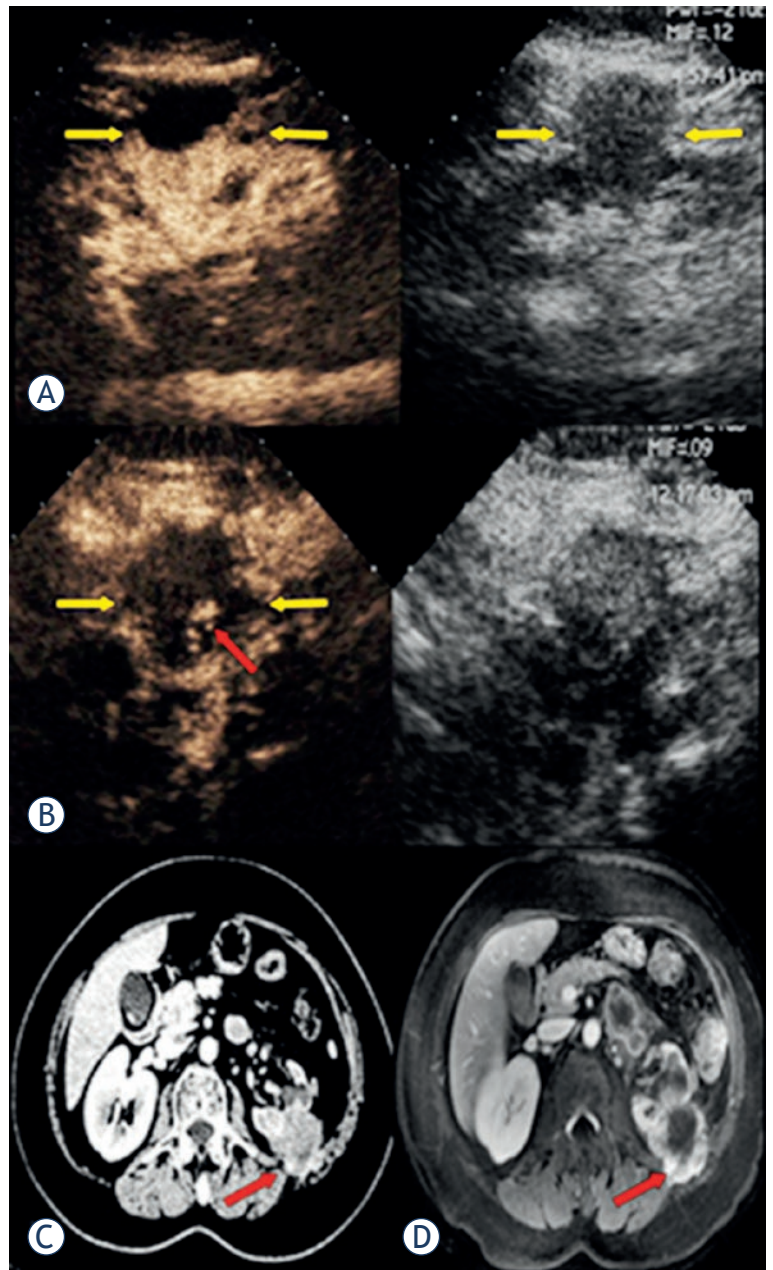


FIGURE 4. Pre-ablation contrast-enhanced US showed a 4.7 cm x 3.9 cm exophytic renal papillary cell carcinoma heterogeneous hyper-enhancement with no-enhancement zone in a 56-year-old woman (A, arrow), and 1 month after ablation contrast-enhancement US showed an hyper-enhancement area in cortical phase which was diagnosed as abnormal perfusion (B, red arrow), while the corresponding period CT and MRI showed the hyper-enhancement in article phase and diagnosed as a recurrence tumour (C, D, red arrow). Then the patient received biopsy and another ablation and verified the recurrence.

9. Meloni MF, Bertolotto M, Alberzoni C, Lazzaroni S, Filice C, Livraghi T, et al. Follow-up after percutaneous radiofrequency ablation of renal cell carcinoma: contrast-enhanced sonography versus contrast-enhanced CT or MRI. *AJR Am J Roentgenol* 2008; **191**: 1233-8.
10. Yu J, Liang P, Yu X, Liu F, Chen L, Wang Y. A comparison of microwave ablation and bipolar radiofrequency ablation both with an internally cooled probe: results in ex vivo and in vivo porcine livers. *Eur J Radiol* 2011; **79**: 124-30.

11. Goldberg SN, Grassi CJ, Cardella JF, Charboneau JW, Dodd GD 3rd, Dupuy DE, et al. Image-guided tumor ablation: standardization of terminology and reporting criteria. *Radiology* 2005; **235**: 728-39.
12. Gervais DA, McGovern FJ, Arellano RS, McDougal WS, Mueller PR. Renal cell carcinoma: clinical experience and technical success with radiofrequency ablation of 42 tumors. *Radiology* 2003; **226**: 417-24.
13. Hoeffel C, Pousset M, Timsit MO, Elie C, Méjean A, Merran S, et al. Radiofrequency ablation of renal tumours: diagnostic accuracy of contrast-enhanced ultrasound for early detection of residual tumour. *Eur Radiol* 2010; **20**: 1812-21.
14. Kong WT, Zhang WW, Guo HQ, Qiu JL, Tang M, Jiang ZM, et al. Application of contrast-enhanced ultrasonography after radiofrequency ablation for renal cell carcinoma: is it sufficient for assessment of therapeutic response? *Abdom Imaging* 2011; **36**: 342-7.
15. Kunkle DA, Uzzo RG. Cryoablation or radiofrequency ablation of the small renal mass: a meta-analysis. *Cancer* 2008; **113**: 2671-80.
16. Barwarik, Wijkstra H, van Delden OM, de la Rosette JJ, Laguna MP. Contrast-enhanced ultrasound for the evaluation of the criolesion after laparoscopic renal cryoablation: An initial report. *J Endourol* 2013; **27**: 402-7.
17. Gervais DA, McGovern FJ, Arellano RS, McDougal WS, Mueller PR. Radiofrequency ablation of renal cell carcinoma: part 1, Indications, results, and role in patient management over a 6-year period and ablation of 100 tumors. *Am J Roentgenol* 2005; **185**: 64-71.

Impact of CD133 positive stem cell proportion on survival in patients with glioblastoma multiforme

Marju Kase¹, Ave Minajeva¹, Kristi Niinepuu¹, Sandra Kase², Markus Vardja³, Toomas Asser^{1,4}, Jana Jaal^{1,3}

¹ Faculty of Medicine, University of Tartu, Estonia

² Riga Stradinš University, Riga, Latvia

³ Hematology and Oncology Clinic, Dept. of Radiotherapy and Oncological Therapy, Tartu University Hospital, Estonia

⁴ Neurology Clinic, Dept. of Neurosurgery, Tartu University Hospital, Estonia

Radiol Oncol 2013; 47(4): 405-410.

Received 14 April 2013

Accepted 17 July 2013

Correspondence to: Jana Jaal, M.D., Ph.D., Department of Radiotherapy and Oncological Therapy, Tartu University Hospital, Vallikraavi str. 10, 51003 Tartu, Estonia. Phone: +372 7319821; Fax: +372 7319804; Email: Jana.Jaal@kliinikum.ee

Disclosure: No potential conflicts of interest were disclosed.

Background. The aim of the study was to assess the impact of CD133-positive (CD133+) cancer stem cell proportions on treatment results of glioblastoma multiforme (GBM) patients.

Patients and methods. Patients with GBM (n = 42) received postoperative radiotherapy (± chemotherapy). Surgically excised GBM tissue sections were immunohistochemically examined for CD133 expression. The proportions of CD133+ GBM cells were determined (%). The proportion of CD133+ GBM stem cells was established by 2 independent researchers whose results were in good accordance (R = 0.8, p < 0.01). Additionally, CD133 expression levels were correlated with patients overall survival.

Results. The proportion of CD133+ cells varied between patients, being from 0.5% to 82%. Mean and median proportions of CD133+ cells of the entire study group were 33% ± 24% (mean ± SD) and 28%, respectively. Clinical data do not support the association between higher proportion of stem cells and the aggressiveness of GBM. Median survival time of the study group was 10.0 months (95% CI 9.0–11.0). The survival time clearly depended on the proportion of CD133+ cells (log rank test, p = 0.02). Median survival times for patients with low (< median) and high (≥ median) proportion of CD133+ cells were 9.0 months (95% CI 7.6–10.5) and 12.0 months (95% CI 9.3–14.7), respectively. In multivariate analysis, the proportion of CD133+ cells emerged as a significant independent predictor for longer overall survival (HR 2.0, 95% CI 1.0–3.8, p = 0.04).

Conclusions. In patients with higher stem cell proportion, significantly longer survival times after postoperative radiotherapy were achieved. Underlying reasons and possible higher sensitivity of GBM stem cells to fractionated radiotherapy should be clarified in further studies.

Key words: glioblastoma multiforme; CD133; stem cells; radiotherapy; survival

Introduction

Central nervous system (CNS) cancers are generally considered rare tumours. However, according to recent epidemiological study, there are about 27700 new CNS tumour cases each year in Europe.¹ Glioblastoma multiforme (GBM) is the most aggressive and rapidly fatal type of a brain tumour in

adults that accounts for approximately 20% of all malignant primary CNS cancers.² In spite of decades of intensive research, the prognosis of patients with GBM is still poor with a median survival time up to 14.6 months.³ Since 1978, local radiotherapy, administered after debulking surgery, has been a mainstay of standard treatment of GBM patients.⁴ Although radiotherapy results in excellent local

TABLE 1. Characteristics of 42 patients with glioblastoma multiforme

Variable	No of patients (n = 42)	Percentage (%)
Gender		
• Male	23	55%
• Female	19	45%
Age, years (range)*	30–77	
Radiotherapy dose (range)	30–60 Gy	
Chemotherapy**		
• No	16	38%
• Yes	26	62%

* Age at the time of operation; ** Used for recurrent disease

control and cure rates in most solid tumours, the efficacy of this treatment modality in GBM is limited. Almost all GBM patients develop fast disease progression and tumour recurrence within or immediately adjacent to the high-dose radiation volumes.⁵ Therefore, GBM is by nature one of the most radioresistant tumours that represents a big challenge in neuro-oncology.

Detailed information about molecular mechanisms of radioresistance of GBM is not known. However, previous studies have shown that radioresistance may involve many tumour cell and surrounding microenvironment processes, including changes in growth factors, receptors, different signalling and apoptotic pathways and DNA repair mechanisms.^{6,7} Additionally, previous *in vitro* and *in vivo* studies have proposed that CD133 positive (CD133+) tumour cells represent the cellular population that confers GBM radioresistance and could therefore be the source of tumour recurrence after radiation.⁸ CD133 is a transmembrane glycoprotein which is expressed in different type of progenitor cells, including hematopoietic stem cells. In GBM, CD133+ cells are considered stem cells because of their ability to self-renew, differentiate and to initiate tumour formation *in vivo*.⁹

Whether higher proportion of CD133+ GBM cells (stem cell population) contributes to worse treatment results after postoperative radiotherapy was tested in the present study.

Material and methods

Between January 2006 and December 2008, 42 patients with GBM were treated with postoperative three-dimensional radiotherapy at Tartu University

Hospital or North Estonian Medical Centre. Characteristics of patients are listed in Table 1.

Radiotherapy treatment planning and treatment parameters

Treatment planning was performed using CT/MRI scans and TPS XiO CMS treatment planning system. The gross tumour volume (GTV) encompassed the resection cavity and any residual tumour. A 2–3 cm margin was added to create clinical target volume (CTV). Critical tissues were spared (brainstem, chiasma). For planned target volume (PTV), 0.5 cm margin was included. Treatments were performed using linear accelerators (30–60 Gy in 2.0 Gy fractions; mean dose 54 Gy). The prescribed dose was normalized to 100% at the isocenter and PTV was covered by 95% isodose surface (ICRU Report 50). None of the patients received concomitant and adjuvant chemotherapy with temozolomide (available in Estonia since 2010). However, for recurrent disease, 26 patients received chemotherapy with lomustine (CCNU).

Immunohistochemistry (IHC)

Haematoxylin and eosin stained sections (4 µm thick) were used for primary diagnosis. The diagnosis of GBM was confirmed by 2 independent pathologists.

Additional sections were cut from archived paraffin blocks and stained according to standard IHC protocol. For immunohistochemistry, a primary antibody against CD133 was applied (Biorbyt Ltd., #orb18124, United Kingdom, dilution 1:50). Diaminobenzidine was used as chromogen.

The evaluation and scoring of slides were carried out in a blinded fashion by 2 independent researchers. The proportion of CD133+ cells was determined in randomly taken microscopic fields at a magnification of 400. For individual values, the mean of 6 microscopic fields was calculated (%). The proportion of CD133+ GBM cells was determined in areas with vital tumour tissue. Additionally to CD133+, the overall proportion of necrosis (%) was determined in haematoxylin-eosin stained tissue sections by an experienced pathologist.

Individual means of CD133+ cell proportions were used to determine group median value. According to the median value of CD133+ proportions, patients were divided into subgroups < median (less than median) and ≥ median (equal and more than median). These groups were used in survival analysis.

Statistical analysis

The SPSS statistical software was used to calculate individual means, group mean, and standard deviation of the mean, as well as median value. Additionally, Pearson correlation analysis was utilized. The proportion of pre-irradiation CD133+ GBM cells was correlated with the overall survival (OS) that was defined as the period from the date of operation to the date of death resulting from GBM or to the date of last analysis. Survival curves were created using the Kaplan-Meier method and differences between the groups were compared using the log-rank test. Multivariate analysis was performed using the Cox proportional hazards model. A p-value < 0.05 was regarded statistically significant.

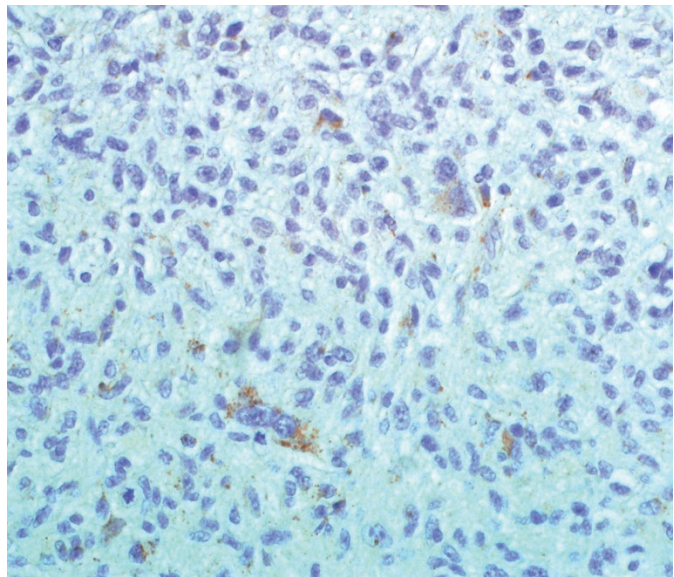
Study was carried out with permission of Research Ethics Committee of the University of Tartu. The study was carried out according to the Declaration of Helsinki.

Results

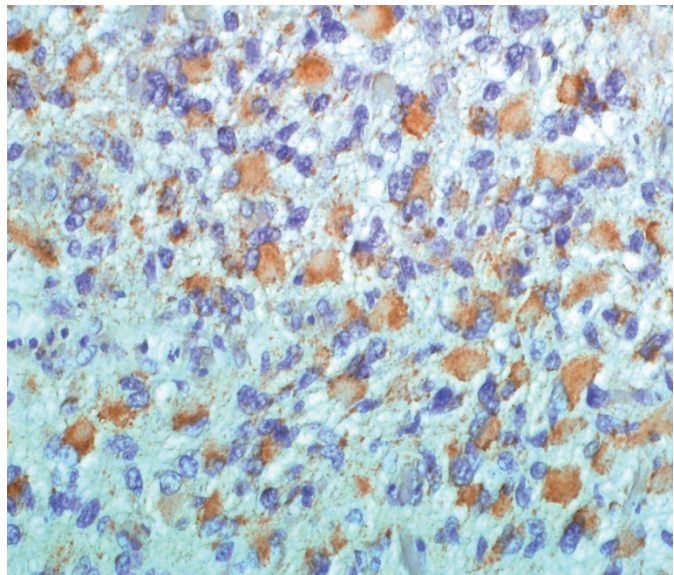
Proportion of CD133+ GBM cells

In GBM tumour samples, the proportion of CD133+ cells varied greatly between patients. Figure 1 illustrates low (< median) and high (\geq median) CD133+ cell proportions in tumour tissue. The proportion of CD133+ GBM stem cells was determined by 2 independent researchers whose results were in good accordance ($R = 0.8$, $p < 0.0001$). Among individual GBM patients ($n = 42$), the proportion of CD133+ stem cells in tumour tissue ranged from 0.5% to 82% (individual means). Mean and median proportions of CD133+ cells of the entire study group were $33\% \pm 24\%$ (mean \pm standard deviation) and 28%, respectively. According to individual values, patients were divided into two groups: patients with low (< median) and high (\geq median) proportion of CD133+ GBM cells. Groups were sufficiently balanced, since there were 20 patients (48%) with low (< median) and 22 patients (52%) with high (\geq median) proportion of CD133+ cells.

Additionally to immunohistochemistry, the overall proportion of necrosis (%) was determined in haematoxylin-eosin stained tissue sections. The mean proportion of necrosis of the entire study group was $38 \pm 31\%$ (mean \pm standard deviation). Correlation analysis, based on individual values, revealed a significant association between the proportion of stem-cells and the percentage of necrosis ($p < 0.01$).



A



B

FIGURE 1. Different proportions of CD133+ stem cells (1A: low, 1B: high) in glioblastoma multiforme.

Correlation of CD133+GBM cell proportion with overall survival

At the time of analysis 40 patients had died. The median OS of the whole study group was 10.0 months (95% CI 9.0–11.0). Figure 2 illustrates the OS among patients with low and high proportion of CD133+ GBM cells. The survival times clearly depended on the proportion of CD133+ cells (log rank test, $p = 0.02$). Median survival times for patients with low (< median) and high (\geq median) proportion of CD133+ cells were 9.0 months (95% CI 7.6–10.5) and 12.0 months (95% CI 9.3–14.7), respectively.

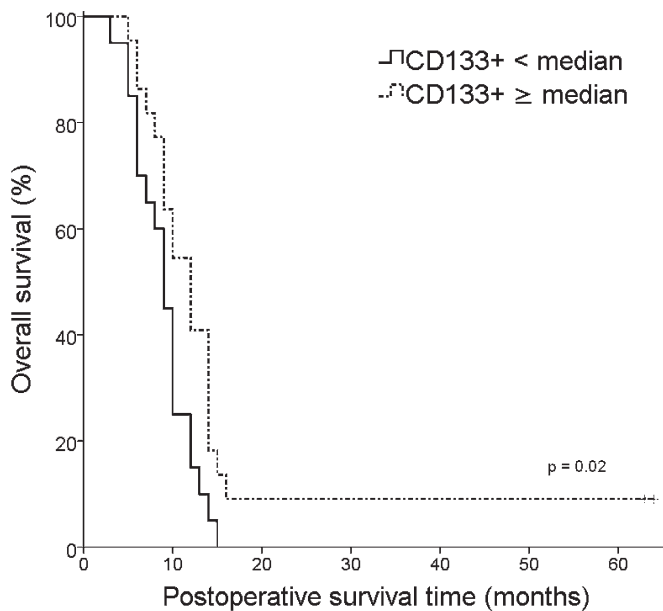


FIGURE 2. Kaplan-Meier analysis of overall survival (OS) according to CD133+ GBM stem cell proportions (< median vs \geq median).

In multivariate analysis (Table 2), the proportion of CD133+ cells (HR 2.0, 95% CI 1.0–3.8, $p = 0.04$) and Karnofsky performance score (HR 2.2, 95% CI 1.0–4.8, $p = 0.04$) emerged as significant independent prognostic factors for OS.

Discussion

The molecular basis of radioresistance of GBM is not known. Therefore, a precise knowledge about underlying mechanisms is essential to develop clinically useful methods to radiosensitize and treat this incurable disease. Previous *in vitro* and *in vivo* studies have proposed that CD133+ tumour cells represent the cellular population that confers GBM radioresistance and could therefore be the source of tumour recurrence after radiation.⁸

According to the brain tumour cancer stem cell model, a subpopulation of cancer cells possesses the capacity of self-renewal, tumour formation and the capability to form progeny with a more restricted fate.¹⁰ In GBM, several stem cell candidate markers have been explored, however, out of these, CD133 is the most studied.^{7,11} CD133+ GBM cells are considered stem cells because of their ability to self-renew, differentiate and to initiate tumour formation *in vivo*.⁹ An injection of as few as 100 CD133+ cells has been shown to produce a tumour that could be serially transplanted and

which was phenotypically resembled the patients original tumor.⁹

In the current study, the presence of CD133+ cells in GBM tissue was detected by immunohistochemical staining method. The proportion of CD133+ GBM stem cells was determined in surgically excised tumour tissue, *i.e.* prior radiotherapy. The study revealed wide variability in the proportion of these cells. Among evaluated GBM samples, there were tumours that contained only 0.5% CD133+ GBM cells but also tissues in which the proportion of CD133+ cells was as high as 82%. The variability in CD133+ GBM stem cell proportions has also been reported in studies of 37 and 44 consecutive GBM patients, where CD133 expression ranged between 0.5% and 10.0%.^{12,13} However, in our study, somewhat higher CD133+ GBM cell proportions were detected (median 28%) that might be related to the use of different primary CD133 antibody clone.¹⁴

Present study revealed the correlation between the proportion of CD133+ stem cells and the overall proportion of tissue necrosis. It is widely accepted that necrosis typically develops in hypoxic (low-oxygen) environments. In GBM, the expression of hypoxia markers (carbonic anhydrase IX [CAIX] hypoxia inducible factor-1 [HIF-1 α]) has been shown to be especially high in tumour regions containing 10% to 45% necrosis of total area.¹⁵ Additionally, it has been reported that tumour-initiating CD133+ GBM stem cells are preferentially expanded in hypoxic conditions.^{15,16} Therefore, hypoxia might have also influenced the proportion of CD133+ GBM cells in the present study.

Additionally to the determination of CD133+ cell proportions, tumour CD133 expression levels were correlated with GBM patients overall survival. The median survival of the entire study group was 10.0 months. This is in a good accordance with previous studies where postoperative radiotherapy has resulted in median survival of 9–11.6 months.^{4,17} However, the survival time clearly depended on the proportion of CD133+ GBM stem cells. Median survival times for patients with low (< median) and high (\geq median) proportion of CD133+ cells were 9.0 months and 12.0 months respectively. In contrast to what was expected, significantly longer survival times after postoperative radiotherapy were achieved in patients with higher stem cell proportion. To the knowledge of authors, there are no other clinical studies that would have evaluated the prognostic significance of CD133 expression after GBM radiotherapy. Nevertheless, clinical series that have used radiochemotherapy (radiotherapy and concomitant plus adjuvant temozolomide),

TABLE 2. Multivariate analysis for overall survival (OS)

Variable		OS	
		p	HR (95% CI)
CD133+	< median vs ≥ median	0.04	1.99 [1.04–3.83]
Radiotherapy dose*	range 30–60 Gy	0.24	0.96 [0.90–1.03]
Chemotherapy	yes vs no	0.75	1.13 [0.54–2.37]
Karnofsky performance score	< 70% vs ≥ 70%	0.04	2.24 [1.04–4.83]

* Continuous variable; HR = hazard ratio; CI = confidence interval

which currently represents standard-of-care treatment for GBM, have shown opposite results. In clinical study of 44 GBM patients, the CD133+ tumour cell proportion of ≥ 2% negatively correlated with overall survival.¹² Additionally, mRNA expression analyses in GBM patients showed that high sample CD133 mRNA expression was a significant prognostic factor for adverse overall survival.^{18,19} These opposite results may be related to other treatment protocol (radiochemotherapy), different primary antibody used for CD133 immunohistochemical detection, as well as to the fact that mRNA expression study samples contained up to 50% of non-tumour tissue, which may also have contained CD133.²⁰

Similarly to our findings, different clinical outcomes were documented in a study that divided GBM patients into 2 groups (CD133-low, CD133-high) according to CD133+ cell ratio either < 3% or ≥ 3%, as detected by the fluorescence activated cell scanning (FACS) analysis of primary tumour cultures. Namely, tumours from CD133-low GBM patients were shown to have tendency to be localized within the deeper structures of the brain, to show more invasive growth patterns and ventricle involvement, as well as relatively higher rate of disease progression after radiotherapy and chemotherapy.²¹ Also, although not in primary GBM, significantly longer survival times were detected in recurrent GBM patients with higher proportion of CD133+ cells.¹³ In addition, the multivariate analysis of the present study revealed that next to the well-established prognostic factor Karnofsky performance status (KPS), CD133+ GBM stem cell proportion emerged as a significant independent predictor for overall survival. This clearly suggests that GBM patients with high proportion of CD133+ tumour cells respond better to radiotherapy and achieve better treatment response that consequently result in longer survival times.

It has been widely accepted that CD133+ GBM stem cells are especially radioresistant.⁸ The find-

ings of our study point toward the possibility that these cells might be, in contrast to what has been believed, radiosensitive. The radioresistant nature of CD133+ GBM stem cells has been mainly documented in studies that compare isolated CD133+ and CD133- GBM cell lines.^{8,22} However, when compared to the traditional glioblastoma established cell lines that contain heterogeneous cell subpopulations, higher radiosensitivity of CD133+ GBM stem cells has been seen. It has been previously reported that CD133+ GBM stem cells have a reduced capacity to repair radiation-induced double strand breaks, which is likely to be a major contributor to the relatively greater degree of radiosensitivity.²³ Therefore, the radiosensitivity of CD133+ GBM stem cells might be greatly underestimated.

As mentioned earlier, a correlation between the proportion of CD133+ GBM stem cells and the overall proportion of tissue necrosis was found. This shows indirectly that also a surrounding microenvironment may contribute to the radiation response of GBM stem cells. Indeed, recent publications have confirmed this relationship. It has been demonstrated that GBM stem cells irradiated *in vivo* within orthotopic xenografts are less susceptible to double strand breaks induction and have greater capacity to repair damage as compared to same tumour cells irradiated under *in vitro* growth conditions.²⁴ Moreover, close correlation between CD133+ GBM cells and hypoxia¹⁵, vascular structures²⁵, extracellular matrix (ECM) components⁷, as well as inflammation and immunoregulatory markers²⁶ have been reported. This all shows that radiation response of CD133+ GBM stem cells are determined by a numerous known and unknown processes that can be collectively named as “micro-environment-stem cell unit”.⁷

The present study has several limitations. These include retrospective data collection and small number of patients. Also, some important variables, such as tumour O6-methylguanine-DNA

methyltransferase (MGMT) methylation status, isocitrate dehydrogenase 1 (IDH1) gene mutation status, recursive partitioning analysis (RPA) and patient's quality of life scores were not recorded. However, this small study showed that there is no association between higher proportion of stem cells and the aggressiveness of GBM. In contrast, in patients with higher stem cell proportion, significantly longer survival times after postoperative radiotherapy were achieved. Since radiotherapy is one of the main treatment modalities in GBM, further studies are needed to clarify these results for better understanding of GBM biology that consequently may result in more effective treatment methods to fight this devastating disease.

Acknowledgments

This work was supported by Estonian Research Council (grant ETF8862, grant IUT2-4).

References

- Crocetti E, Trama A, Stiller C, Caldarella A, Soffietti R, Jaal J, et al. Epidemiology of glial and non-glial brain tumors in Europe. *Eur J Cancer* 2012; **48**: 1532-42.
- Lee CH, Jung KW, Yoo H, Park S, Lee SH. Epidemiology of primary brain and central nervous system tumors in Korea. *J Korean Neurosurg Soc* 2010; **48**: 145-52.
- Stupp R, Mason WP, van den Bent MJ, Weller M, Fisher B, Taphoorn MJ, et al. Radiotherapy plus concomitant and adjuvant temozolomide for glioblastoma. *N Engl J Med* 2005; **352**: 987-96.
- Walker MD, Alexander E Jr, Hunt WE, MacCarty CS, Mahaley MS Jr, Mealey J Jr, et al. Evaluation of BCNU and/or radiotherapy in the treatment of anaplastic gliomas. A cooperative clinical trial. *J Neurosurg* 1978; **49**: 333-43.
- Minniti G, Amelio D, Amichetti M, Salvati M, Muni R, Bozzao A, et al. Patterns of failure and comparison of different target volume delineations in patients with glioblastoma treated with conformal radiotherapy plus concomitant and adjuvant temozolomide. *Radiother Oncol* 2010; **97**: 377-81.
- Kase M, Vardja M, Lipping A, Asser T, Jaal J. Impact of PARP-1 and DNA-PK expression on survival in patients with glioblastoma multiforme. *Radiother Oncol* 2011; **101**: 127-31.
- Mannino M, Chalmers AJ. Radioresistance of glioma stem cells: intrinsic characteristic or property of the 'microenvironment-stem cell unit'? *Mol Oncol* 2011; **5**: 374-86.
- Bao S, Wu Q, McLendon RE, Hao Y, Shi Q, Hjelmeland AB, et al. Glioma stem cells promote radioresistance by preferential activation of the DNA damage response. *Nature* 2006; **444**: 756-60.
- Singh SK, Hawkins C, Clarke ID, Squire JA, Bayani J, Hide T, et al. Identification of human brain tumor initiating cells. *Nature* 2004; **432**: 396-401.
- Laks DR, Visnyei K, Kornblum HI. Brain tumor stem cells as therapeutic targets in models of glioma. *Yonsei Med J* 2010; **51**: 633-40.
- Dell'Albani P. Stem cell markers in gliomas. *Neurochem Res* 2008; **33**: 2407-15.
- Pallini R, Ricci-Vitiani L, Banna GL, Signore M, Lombardi D, Todaro M, et al. Cancer stem cell analysis and clinical outcome in patients with glioblastoma multiforme. *Clin Cancer Res* 2008; **14**: 8205-12.
- Pallini R, Ricci-Vitiani L, Montano N, Mollinari C, Biffoni M, Cenci T, et al. Expression of the stem cell marker CD133 in recurrent glioblastoma and its value for prognosis. *Cancer* 2011; **117**: 162-74.
- Hermansen SK, Christensen KG, Jensen SS, Kristensen BW. Inconsistent immunohistochemical expression patterns of four different CD133 antibody clones in glioblastoma. *J Histochem Cytochem* 2011; **59**: 391-407.
- Pistollato F, Abbadi S, Rampazzo E, Persano L, Della Puppa A, Frasson C, et al. Intratumoral hypoxic gradient drives stem cells distribution and MGMT expression in glioblastoma. *Stem Cells* 2010; **28**: 851-62.
- Sheehan JP, Shaffrey ME, Gupta B, Lerner J, Rich JN, Park DM. Improving the radiosensitivity of radioresistant and hypoxic glioblastoma. *Future Oncol* 2010; **6**: 1591-1601.
- Westphal M, Hilt DC, Bortey E, Delavault P, Olivares R, Warnke PC, et al. A phase 3 trial of local chemotherapy with biodegradable carmustine (BCNU) wafers (Gliadel wafers) in patients with primary malignant glioma. *Neuro Oncol* 2003; **5**: 79-88.
- Metellus P, Nanni-Metellus I, Delfino C, Colin C, Tchogandjian A, Coulibaly B, et al. Prognostic impact of CD133 mRNA expression in 48 glioblastoma patients treated with concomitant radiochemotherapy: a prospective patient cohort at a single institution. *Ann Surg Oncol* 2011; **18**: 2937-45.
- Ardebili SY, Zajc I, Gole B, Campos B, Herold-Mende C, Drmota S, et al. CD133/prominin 1 is prognostic for GBM patients survival, but inversely correlated with cysteine cathepsins expression in glioblastoma derived spheroids. *Radiol Oncol* 2011; **45**: 102-15.
- Zhang M, Song T, Yang L, Chen R, Wu L, Yang Z, et al. Nestin and CD133: valuable stem cell-specific markers for determining clinical outcome of glioma patients. *J Exp Clin Cancer Res* 2008; **27**: 85.
- Joo KM, Kim SY, Jin X, Song SY, Kong DS, Lee JI, et al. Clinical and biological implications of CD133-positive and CD133-negative cells in glioblastomas. *Lab Invest* 2008; **88**: 808-15.
- Jamal M, Rath BH, Tsang PS, Camphausen K, Tofilon PJ. The brain microenvironment preferentially enhances the radioresistance of CD133(+) glioblastoma stem-like cells. *Neoplasia* 2012; **14**: 150-58.
- McCord AM, Jamal M, Williams ES, Camphausen K, Tofilon PJ. CD133+ glioblastoma stem-like cells are radiosensitive with a defective DNA damage response compared with established cell lines. *Clin Cancer Res* 2009; **15**: 5145-53.
- Jamal M, Rath BH, Williams ES, Camphausen K, Tofilon PJ. Microenvironmental regulation of glioblastoma radioresponse. *Clin Cancer Res* 2010; **16**: 6049-59.
- Christensen K, Schroder HD, Kristensen BW. CD133+ niches and single cells in glioblastoma have different phenotypes. *J Neurooncol* 2011; **104**: 129-43.
- Schwartzbaum JA, Huang K, Lawler S, Ding B, Yu J, Chiocca EA. Allergy and inflammatory transcriptome is predominantly negatively correlated with CD133 expression in glioblastoma. *Neuro Oncol* 2010; **12**: 320-27.

Dosimetric evaluation of an ipsilateral intensity modulated radiotherapy beam arrangement for parotid malignancies

Eda Yirmibesoglu^{1,2}, David V. Fried², Mark Kostich², Julian Rosenman^{2,4}, William Shockley^{3,4}, Mark Weissler^{3,4}, Adam Zanation^{3,4}, Bishamjit Chera^{2,4}

¹ Department of Radiation Oncology, Kocaeli University Faculty of Medicine, Kocaeli, Turkey

² Department of Radiation Oncology, University of North Carolina Hospitals, Chapel Hill, NC, USA

³ Department of Otolaryngology/Head & Neck Surgery, University of North Carolina Hospitals, Chapel Hill, NC, USA

⁴ Lineberger Comprehensive Cancer Center, University of North Carolina Hospitals, Chapel Hill, NC, USA

Radiol Oncol 2013; 47(4): 411-418.

Received 27 August 2012

Accepted 25 November 2012

Correspondence to: Bishamjit S. Chera, M.D., 101 Manning Drive CB# 7512 Chapel Hill, NC 27514, USA. Phone: +919-445-5286; Fax: +919-966-7681; E-mail: bchera@med.unc.edu

Disclosure: No potential conflicts of interest were disclosed.

Background. We conducted a dosimetric comparison of an ipsilateral beam arrangement for intensity modulated radiotherapy (IMRT) with off-axis beams.

Patients and methods. Six patients who received post-operative radiotherapy (RT) for parotid malignancies were used in this dosimetric study. Four treatment plans were created for each CT data set (24 plans): 1) ipsilateral 4-field off-axis IMRT (4fld-OA), 2) conventional wedge pair (WP), 3) 7 field co-planar IMRT (7fld), and 4) ipsilateral co-planar 4-field quartet IMRT (4fld-CP). Dose, volume statistics for the planning target volumes (PTVs) and planning risk volumes (PRVs) were compared for the four treatment techniques.

Results. Wedge pair plans inadequately covered the deep aspect of the PTV. The 7-field IMRT plans delivered the largest low dose volumes to normal tissues. Mean dose to the contralateral parotid was highest for 7 field IMRT. Mean dose to the contralateral submandibular gland was highest for 7 field IMRT and WP. 7 field IMRT plans had the highest dose to the oral cavity. The mean doses to the brainstem, spinal cord, ipsilateral temporal lobe, cerebellum and ipsilateral cochlea were similar among the four techniques.

Conclusions. For postoperative treatment of the parotid bed, 4-field ipsilateral IMRT techniques provided excellent coverage while maximally sparing the contralateral parotid gland and submandibular gland.

Key words: intensity modulated radiotherapy; parotid; dosimetry

Introduction

The standard of care treatment of parotid gland malignancies is surgery followed by postoperative radiotherapy (RT) when indicated. Postoperative RT has been shown to improve loco-regional control and is generally recommend for tumors with high-risk features such as high grade, positive or close margins, lymph node metastases, or tumor recurrence.¹ The post-surgical parotid bed and cranial portions of level II are the primary targets and levels I – III of the ipsilateral neck are treated

electively if the neck has not been dissected and adjuvantly if there are ≥ 2 positive nodes or node(s) and/or node(s) with extracapsular extension.

Historically, a wedge pair technique was used to treat the post-surgical parotid bed. If there were indications for treatment of the neck, an isocentrically matched low anterior neck field was added. The ipsilateral wedge pair beam arrangement creates a “pie” shaped dose distribution while sparing the contralateral parotid and submandibular gland. The potential shortcoming of the wedge pair technique is suboptimal coverage of the deep aspects

of the parotid bed (e.g. deep lobe of the parotid). Contemporarily intensity modulated radiotherapy (IMRT) is the most frequently utilized radiation treatment technique for head and neck cancer and is frequently used for the postoperative treatment of parotid and other malignancies.² The potential benefits of IMRT include improved normal tissue sparing and target coverage through highly conformal dose distributions with steep dose gradients. Typically, IMRT is delivered with 7 to 9 axial beams equidistantly spaced along the transverse axis. The use of multiple co-planar beams (as compared to ipsilateral beams) will result increased dose to the contralateral parotid and submandibular glands which may cause significant xerostomia. However, multiple beams from various angles provide more degrees of freedom and thus improve the dose to the deep aspects of the post-surgical parotid bed.

At our institution patients receiving postoperative radiotherapy for parotid malignancies are treated with IMRT using an ipsilateral off-axis quartet beam arrangement. This technique maximally spares the contralateral parotid and submandibular glands and provides excellent coverage of the deep aspects of the parotid bed. Hence it combines the benefits of the wedge pair and the 7 field co-planar IMRT techniques. We here-in describe our 4-field off-axis ipsilateral IMRT technique and present a dosimetric comparison of this technique to conventional wedge pair, 4-field co-planar IMRT, and 7 field co-planar IMRT plans.

Patients and methods

We obtained approval from our institutional IRB for this study (IRB# 09-2146). The current dosimetric study used computed tomography (CT) simulation data sets from 6 patients who were treated with postoperative radiotherapy for parotid malignancies. All of these patients had elective neck dissections and were pathologically node negative. Thus none of these patients received neck irradiation. 5 out of 6 of these patients had already received postoperative radiation treatment using the 4-field off-axis ipsilateral IMRT technique. One patient was treated with a conventional wedge pair technique prior to our institutions adoption of the 4-field ipsilateral IMRT technique.

CT Simulation

Patients were placed in the supine position and the head and neck were immobilized with a custom-

ized AquaPlast mask (WFR/Aquaplast Corp. and Qfix Systems, Avondale, PA). The neck was extended and the shoulders were relaxed downward with gentle traction. CT images were obtained with a Philips Brilliance Big Bore, 16-slice CT scanner (Amsterdam, Netherlands). The image slice thickness was 3 mm, and patients were scanned from the vertex to the below the clavicles. Intravenous contrast was not used.

Volume definition

Target and organ at risk volumes (OARs) were delineated using PLUNC. The clinical and planning target volumes (CTV, PTV) that were delineated at the time of their initial treatment planning were used for this dosimetric study. Typically the CTV encompassed the post-surgical parotid bed, adjacent parapharyngeal space, and course of the facial nerve to the styloid mastoid foramen. None of the 6 patients in this study had a positive proximal facial nerve margin and thus neither the CTV nor the PTV encompassed the course of the facial nerve proximal to the styloid mastoid foramen (*i.e.* inner ear and/or brainstem). The PTV was created by uniformly expanding the CTV by 3 mm. The PTV and CTV were subtracted 4 mm within the skin. The following OARs were contoured: contralateral parotid gland, contralateral submandibular gland, ipsilateral cochlea, contralateral cochlea, ipsilateral temporal lobe, brainstem, cerebellum, and cervical spinal cord. OARs were uniformly expanded 3 mm to create planning risk volumes (PRVs).

Treatment planning and prescription dose

Four treatment plans were created for each CT data set (24 plans): 1) conventional wedge pair, 2) 7-field co-planar IMRT, 3) 4-field off-axis IMRT and 4) 4-field co-planar IMRT. 70 Gy was prescribed to the PTV. 70 Gy was chosen because it represents the maximum dose prescribed for this treatment.

For the conventional wedge pair two oblique fields (approximately with 90° angles) were used. The beam angles for the oblique fields were chosen to exclude the contralateral parotid and submandibular glands and provide adequate coverage of the PTV. Furthermore one of the oblique beams excluded the brainstem and spinal cord. Wedges were used for both oblique fields and weighted to provide acceptable coverage of the PTV. By convention and in accordance with historical standards the wedge pair plans were normalized such

TABLE 1. Dose Volume Statistics for Planning Target Volume (PTV) and Clinical Target Volume (CTV)

	Wedge pair		7 field co-planar IMRT		4-field off-axis		4-field co-planar	
	Mean	SD	Mean	SD	Mean	SD	Mean	SD
PTV								
Mean (Gy)	71.6	0.65	71.8	0.56	71.8	0.61	71.5	0.36
Max dose (Gy)	77.2	0.71	75.5	0.98	75.9	1.3	75.6	0.67
Min dose(Gy)	51.2	5.9	65.2	2.8	57.3	8.9	58.1	6.7
V95 (%)	95.4	0.45	99.9	0.15	99.4	0.49	99.1	0.72
V105 (%)	31.3	10.7	14.3	14.7	16.8	13.6	8.8	5.2
V110 (%)	1.23	2.88	0	0	0.01	0	0	0
CTV								
Mean (Gy)	71.8	0.92	71.9	0.58	71.9	0.60	70.6	0.90
Max dose (Gy)	75.5	0.60	75.5	0.92	75.8	1.2	75.5	0.60
Min dose(Gy)	59.1	8.8	66.5	2.3	59.5	7.1	59.1	8.8
V95 (%)	97.2	3.7	99.9	0.2	99.4	0.5	97.2	3.7
V105 (%)	4.75	4.3	15.3	15.4	17.9	14.3	4.8	4.3
V110 (%)	1.1	2.7	0	0	0	0	0	0

IMRT = Intensity modulated radiation therapy; SD = standard deviation; PTV = planning target volume; Max = maximum dose received by 0.1cc; Min = minimum dose received by 0.1cc; V95(%), V105 (%), V100, V110(%) = percentage of volume receiving 95%, 105%, 100%, and 110% of prescribed dose, respectively

that 95% of the PTV received 95% of the dose. Normalization to 100% would result in excessive heterogeneity ($\geq 120\%$) that would be clinically unacceptable.

For the 7-field co-planar IMRT seven equally spaced beams (approximately every 52°) were isocentrically centered on the PTV. The field and table angles for the 4-field off axis IMRT plan were: A45R-45I, A45R-45S, P45R-45I, P45R-45S (right side) and A45L-45S, A45L-45I, P45L-45S, P45L-45I (left side) (Figure 1). For example A45R-45I translates into a 45 degree right anterior oblique beam with a 45 degree inferior tablekick. These beam angles were selected to exclude the eye, shoulder, and contralateral parotid and submandibular glands from the beams. Depending on a patient's anatomy the beam angles may require minor adjustments to exclude the eye and shoulder. Another 4-field coplanar IMRT plan was created for comparison purposes according to the 4-field class solution published by Nutting *et al.* The 4-field coplanar IMRT plan consisted of paired ipsilateral co-planar anterior and posterior oblique beams with the following angles: 15, 45, 145, and 170° from the anterior plane.³

The IMRT treatment planning process was similar for both the 7-field and 4-field IMRT plans.⁴ Dose objectives were iteratively selected for the PTV and PRVs to meet pre-defined dose constraints. Ghost structures were also used to improve dose con-

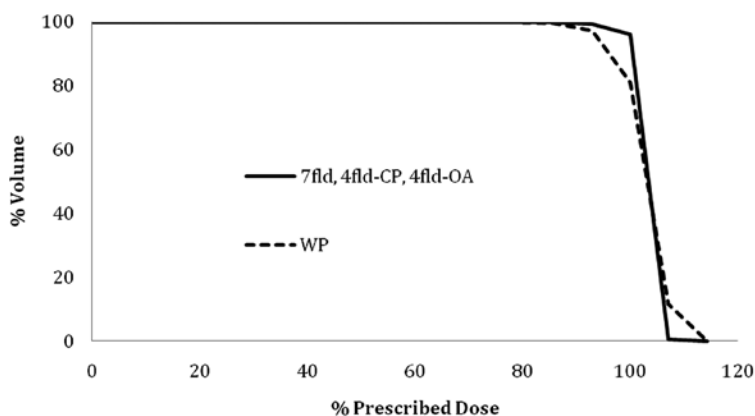


FIGURE 1. Three-dimensional representation of the orientation of the 4 beams used in the 4-field off-axis IMRT plans for a target on the right side of a patient. A45R-45I = 45 degree right anterior oblique beam with a 45 degree inferior Table kick; A45R-45S = 45 degree right anterior oblique beam with a 45 degree superior Table kick; P45R-45I = 45 degree right posterior oblique beam with a 45 degree inferior Table kick; P45R-45S = 45 degree right posterior oblique beam with a 45 degree superior Table kick.

formity around the PTV and avoidance of PRVs. 70 Gy was prescribed to the PTV. The PTV dose constraints were: 95% of the PTV receives 100% of the prescription dose, 99% of the PTV receives 93% of the prescription dose, and $<20\%$ of the PTV receives 110% of the prescription dose. Because the contralateral parotid and submandibular glands are in the beam path of several beams in the 7-field IMRT, these PRVs were included in the IMRT opti-

TABLE 2. Conformality of the high dose region and the integral dose

Isodose Volume	Wedge pair			7 field co-planar IMRT			4-field off-axis IMRT			4-field co-planar IMRT		
	Mean (cc)	% PTV	SD	Mean (cc)	% PTV	SD	Mean (cc)	% PTV	SD	Mean (cc)	% PTV	SD
70 Gy to PTV	157	81	42	188	97	52	189	97	52	191	98	53
70 Gy to NT	71	-	15	73	-	22	101	-	33	116	-	19
66.5 Gy to PTV	185	95	52	193	100	53	193	100	53	192	100	53
66.5 Gy to NT	127	-	16	129	-	23	144	-	30	153	-	19
50 Gy to NT*	243	-	43	292	-	47	276	-	41	360	-	46
35 Gy to NT*	342	-	48	597	-	84	424	-	69	484	-	59
14 Gy to NT*	1647	-	281	1724	-	320	1205	-	159	1070	-	104

Volume of Normal Tissue (NT) and Planning Target Volume (PTV) receiving various doses. Normal tissue represents all of normal tissue outside of the PTV (i.e. Skin minus PTV). The integral dose (14 to 50 Gy) was higher in the 7 field IMRT plan. However, the volume of NT receiving 95% of the prescription dose (i.e. 66.5 Gy) was smallest for the 7 field IMRT plan. IMRT = intensity modulated radiotherapy. *Since plans were prescribed 70 Gy at the 95%-100% isodose line, all PTV's received 100% coverage of the 50 Gy, 24 Gy, and 14Gy.

mization for the 7-field treatment plans. The dose to the contralateral parotid and submandibular gland was minimized as much as allowable while meeting the dose constraints for the PTV. It was unnecessary to optimize the 4-field IMRT plan for the contralateral parotid and submandibular gland, because the beams excluded the contralateral parotid and submandibular gland.

Plan evaluation and comparison

Dose, volume statistics were collected for PTV, CTV, and PRVs for all 24 plans. The maximum dose and the minimum dose were defined as the dose received by 0.1cc of the defined structure. Volume of PTV and non-specified normal tissues outside of the PTV receiving 70Gy, 66.5Gy (i.e. 95% of prescription dose), 50Gy, 35Gy and 14Gy were recorded to assess the conformality of each plan. The mean values and standard deviations were calculated for reported dose, volume statistics. Dose volume histograms (DVH) were created for PTV, and PRVs.

Results

Dose to CTV and PTV

Dose volume data for the PTV are listed in Table 1 and related dose volume histograms in Figure 2. Representative isodose distributions for the four treatment plans are depicted in Figure 3. The PTV coverage was similar for both the 7 field and 4 field IMRT plans. As expected, the medial aspect of the PTV (i.e. deep aspect of the post-surgical parotid bed) was inadequately covered with the wedge pair plans (Figure 3, A & E). Dose statistics regard-

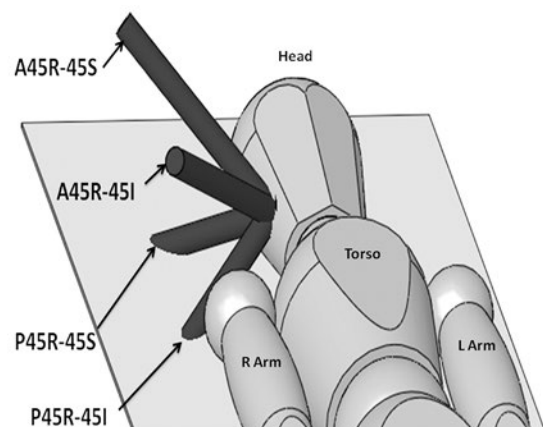


FIGURE 2. Dose volume histogram of the Planning Target Volume (PTV) for wedge pair (WP), 7-field IMRT (7fld), 4-field co-planar (4fld-CP), and 4-field off-axis (4fld-OA) IMRT plans.

ing the conformality of the high dose (i.e. 100% and 95% of the prescription dose) and the integral dose are shown in Table 2. The wedge pair had the worst coverage of the PTV in terms of dose covered by 100% and 95% of the prescription. The wedge pair and 7-field IMRT plans had the least high dose delivered to normal tissues, and the four field plans had much less low dose (i.e. integral dose) delivered to normal tissues.

Dose to PRVs

Dose volume data for the PRVs can be found in Table 3 and Figure 4 and 5. Due to the ipsilateral beam arrangement, the mean doses for the contralateral parotid gland, submandibular gland and cochleare lower in the wedge pair plan and 4-field IMRT plans. The mean dose and maximum dose to

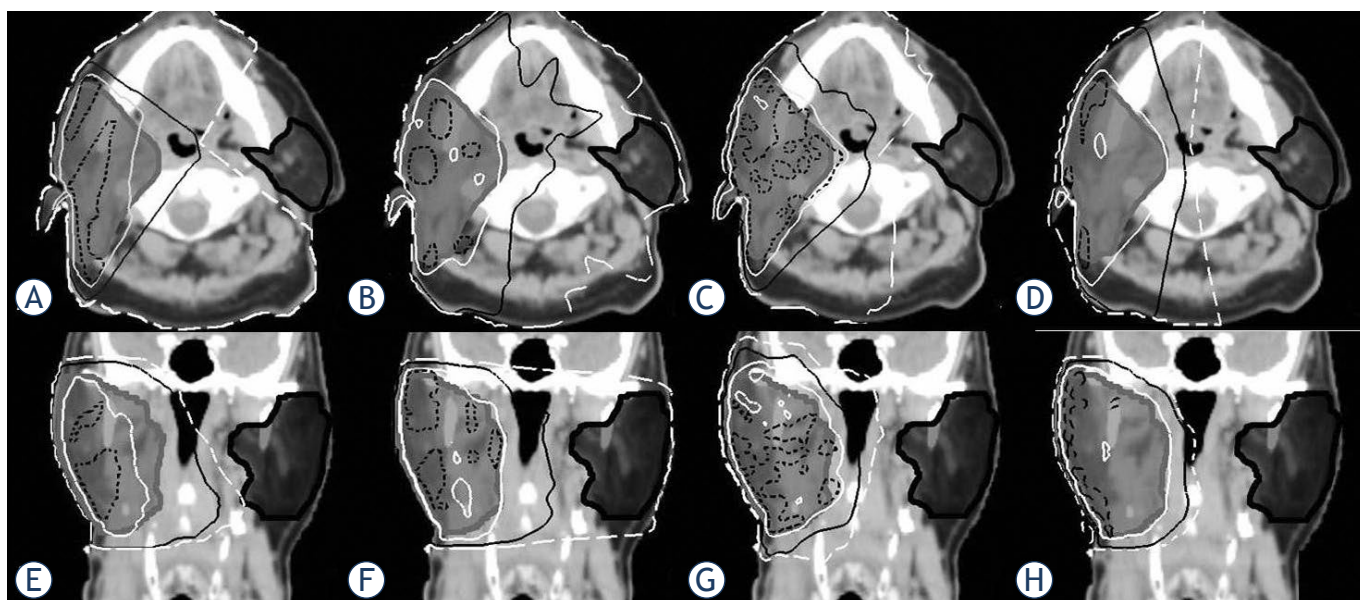


FIGURE 3. Transverse and coronal view of computed tomography images with isodose distributions at the isocenter level in a representative patient with left sided disease. (A, E) wedge pair; (B, F) 7-field IMRT; (C, G) 4-field IMRT off-axis; (D, H) 4-field IMRT co-planar. The isodoses are 105% (dashed black), 100% (white), 50% (black) and 25% (dashed white) of the prescribed dose (70Gy).

the ipsilateral cochlea are similar for all four plans. There is no clinically significant difference in the maximum dose and the volume receiving ≥ 60 Gy to the brain, ipsilateral temporal lobe, and cerebellum. The maximum dose to the brainstem and cervical spinal cord were similar in all techniques. The mean dose to the oral cavity was highest for the 7 field IMRT plan and least for the 4 field IMRT plans.

Discussion

We performed a dosimetric study comparing our institutional specific ipsilateral 4-field off-axis IMRT treatment technique with conventional wedge pair, 7-field co-planar IMRT, and 4-field co-planar IMRT plans for the postoperative treatment of parotid gland malignancies. As expected the ipsilateral 4-Field IMRT techniques spared the contralateral parotid gland and submandibular gland as well as the wedge pair technique and provided PTV coverage similar to the co-planar 7-field IMRT technique. Furthermore, the deep/medial aspects of the PTV and CTV were underdosed with the wedge pair technique. Thus the ipsilateral 4-field IMRT techniques combine the benefits of the wedge pair and co-planar 7 field IMRT plans. Thus, the ipsilateral 4-field IMRT technique may be the preferred method for irradiating the post-sur-

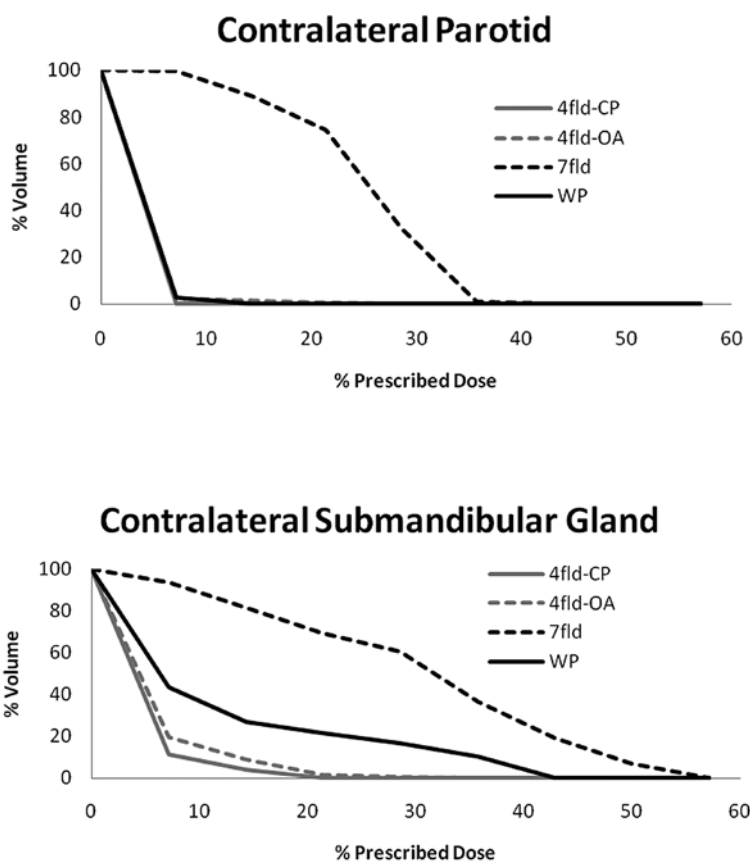


FIGURE 4. Dose volume histograms of the contralateral parotid gland and contralateral submandibular gland for wedge pair (WP), 7-field IMRT (7fld), 4-field co-planar (4fld-CP), and 4-field off-axis (4fld-OA) IMRT plans.

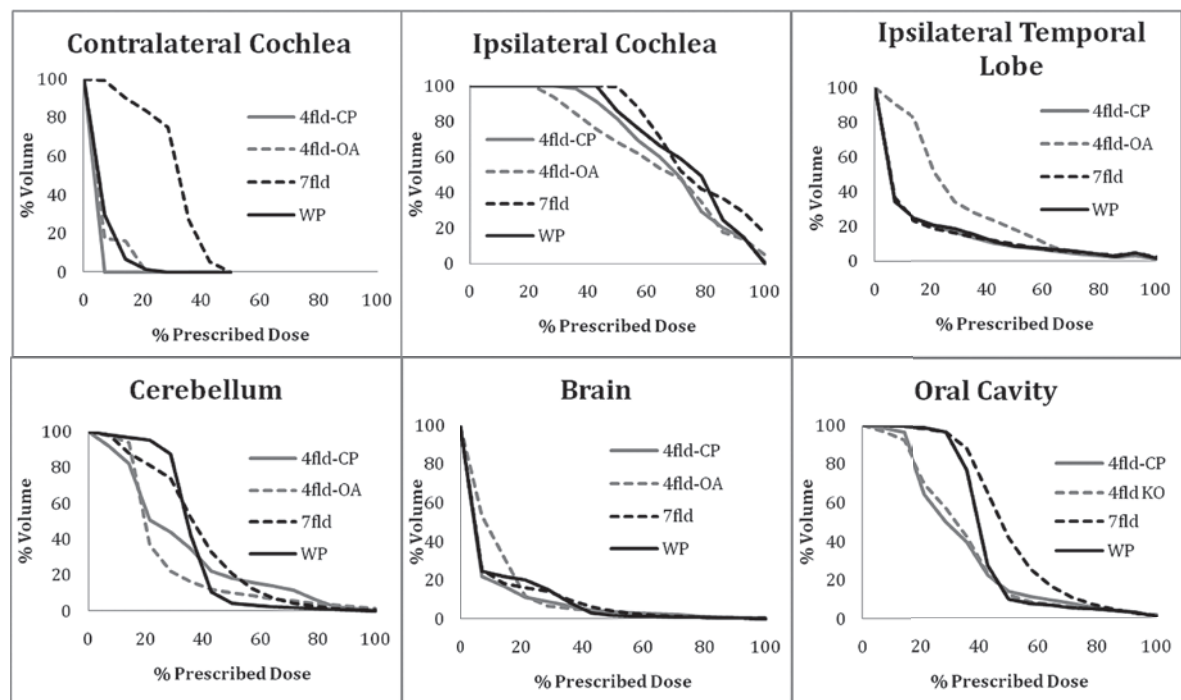


FIGURE 5. Dose volume histograms of the ipsilateral cochlea, contralateral cochlea, ipsilateral temporal lobe and cerebellum for wedge pair (WP), 7-field IMRT (7fld), 4-field co-planar (4fld-CP), and 4-field off-axis (4fld-OA) IMRT plans.

gical parotid bed. The two 4-field IMRT techniques were very similar to one another. However there is an increase in low dose (*i.e.* <10Gy IDL) to the brain and neck and increased complexity because of the use of table kicks with our institution specific 4-field off-axis IMRT plan.

Historically, the conventional wedge pair technique has been predominantly used for the post-operative treatment of parotid malignancies.¹ Other ipsilateral techniques, such as mixed photon electron beams, have been used and evaluated. Yaparalvi *et al.* conducted a study concerning comparison of unilateral radiotherapy techniques for postoperative parotid gland tumors based on dose distribution and DVHs, they concluded that the ipsilateral wedge pair technique was the optimal unilateral treatment techniques.⁵

IMRT treatment planning is extensively used for the treatment of head and neck cancers. IMRT produces highly conformal dose distribution that can reduce the dose to normal tissue structures. Specifically, IMRT has been observed to improve reduce the severity of xerostomia through the sparing of the contralateral parotid gland.⁶ The most common beam arrangement used for IMRT planning is 7 to 9 equally spaced co-planar beams. When ipsilateral RT is possible (*e.g.* parotid malignancies) the 7 to 9 equidistant beam arrangement is

not optimal. More beams increase the conformity of the high dose distribution at the cost of increasing the dose to contralateral normal tissues. In addition to the presented data, others have conducted dosimetric studies of IMRT for parotid malignancies. Nutting *et al.* and Rowbottom *et al.* reported that IMRT with seven to nine fields reduced the dose to most normal tissues compared to conventional wedge pair, but the dose to contralateral OARs was increased.^{3,7} Furthermore Nutting *et al.* also evaluated 3- and 4-field off-axis IMRT beam arrangements but these plans increased the PTV dose inhomogeneity, and increased the dose to the brain.³ They observed 17.6 cc of brain received > 54 Gy in their 4-field off-axis plan *vs.* 1.9 cc in their coplanar 4-field IMRT class solution plan and 2 cc in their 7-field co-planar IMRT plan. They did not detail the beam arrangements for these off-axis IMRT plans.³ In comparison we did not observe a significant increase PTV dose heterogeneity in our 4-field off-axis IMRT technique. We did observe an increase in low dose to the brain (Figure 5) for the 4-field off-axis technique, however, the volume of brain, ipsilateral temporal lobe, and cerebellum receiving > 60 Gy was similar for the 7-field co-planar IMRT, 4-field off-axis, and 4-field coplanar IMRT plans.

TABLE 3. Dose volume statistics for planning risk volumes

	Wedge pair		7 field co-planar IMRT		4-field off-axis IMRT		4-field co-planar IMRT	
	Mean	SD	Mean	SD	Mean	SD	Mean	SD
Mean Dose Contralateral Parotid (Gy)	2.6	0.54	17.4	2.0	1.3	0.84	0.91	0.12
Mean Dose Contralateral Submandibular (Gy)	8.5	4.5	20.5	6.8	3.6	1.5	2.6	0.86
IpsilateralCochlea								
Mean (Gy)	50.8	9.0	54	12.2	44.9	14.6	47.7	9.7
Max dose (Gy)	60.6	8.6	59.8	11.8	56.7	11.5	58.4	9.2
Contralateral Cochlea								
Mean (Gy)	4.8	1.7	21	6.2	3.5	4.6	1.6	0.2
Max dose (Gy)	7.4	3.9	24.5	5.4	4.6	4.9	2.3	0.3
Brain								
Max dose (Gy)	71.7	3.0	71.4	2.6	72.6	1.9	71.6	2.0
Volume ≥ 60 Gy (cc)	8.1	6.3	10.5	14.0	11.5	13.0	10.6	10.3
IpsilateralTemporal Lobe								
Max dose (Gy)	68.3	3.4	69.8	3.7	67.7	5.4	68.7	4.7
Volume ≥ 60 Gy (cc)	4.6	4.7	4.8	8.6	3.4	5.3	3.0	4.0
Cerebellum								
Max dose (Gy)	68.5	4.2	68.4	4.8	68.8	7.8	69.6	3.4
Volume ≥ 60 Gy (cc)	1.5	1.5	2.7	2.8	5.5	5.4	4.2	3.7
Max Dose Brain Stem(Gy)	38.6	8.3	45.1	8.7	32.8	7.8	36.3	5.7
Max Dose Spinal Cord(Gy)	40.3	6.5	45.9	7.0	39.8	4.9	43.0	5.6
Oral Cavity (Gy)	30.1	2.8	35.8	4.5	24.1	4.8	23.6	2.7

PRVs= planning risk volumes; IMRT= Intensity modulated radiation therapy; SD= standard deviation; Max= maximum (dose received by 0.1 cc); Volume ≥ 60 Gy= volume receiving ≥ 60 Gy.

The contralateral lymphatics are rarely at risk in parotid malignancies; the possible exception being large volume ipsilateral nodal disease potentially causing aberrant lymphatic flow to the contralateral neck. Thus, the contralateral side may be completely spared from RT. The most efficient method for minimizing radiation dose to the contralateral side is careful beam selection. "Beam optimization" is a primary first step in IMRT treatment planning and must be done by the dosimetrist/physician/physicist. When using IMRT, the standard 7 to 9 field equidistant field arrangement used for the majority of head and neck cancer IMRT is not the optimal beam arrangement for post-operative RT of parotid malignancies. This beam arrangement substantially increases the dose delivered to the contralateral normal tissues, especially the major salivary glands. Bragg *et al.* reported that a five field beam arrangement was optimal; however the resultant mean dose the contralateral parotid was 10 to 11 Gy.⁸ We observed the contralateral parotid and submandibular gland radiation dose in the

7-field IMRT plan to be below the commonly accepted tolerance dose (*i.e.* mean dose < 26 Gy and mean dose < 35 Gy), however the dose to these structures was substantially lower for the 4-field IMRT plans (Table 3, 17 to 21 Gy *vs.* 1 to 2 Gy). In fact, the dose to the contralateral major salivary glands was similar for the wedge pair and 4-field IMRT plans (Table 3). It is reasonable to rationalize that 17 to 20 Gy to the contralateral salivary glands will impair salivary production. Previous studies have reported that mean doses < 10-15 Gy to the salivary gland resulted in minimal reduction in function and impairment in salivary function gradually increased at radiation doses of 20-40 Gy.^{9,10} Furthermore, the recent QUANTEC review, noted that mean doses < 10 Gy to the parotid gland resulted in better function.¹¹

The 4-field off-axis and co-planar IMRT plans both provide adequate coverage of the PTV/CTV, have a similar conformality of the high dose region, and maximally spare the contralateral major salivary glands. However, the integral brain dose

is higher in the 4-field off-axis planar plan. The 4-field off-axis plan is also more complicated because “Table kicks” are required. Furthermore if the ipsilateral neck requires RT, it would be difficult to match a low anterior neck field to the 4-field off-axis plan. Thus the 4-field co-planar IMRT technique published by Nutting *et al.* is the better 4-field technique. Since conduction of this dosimetric study, we at UNC-CH have transitioned from the 4-field off-axis technique to using the 4-field co-planar technique.

Conclusions

For postoperative treatment of the parotid bed, the ipsilateral 4-field off-axis or co-planar IMRT techniques provide excellent target coverage (specifically the deep/medial aspect of the parotid bed) while maximally sparing the contralateral parotid and submandibular glands. Should cervical nodes require treatment, it may be difficult to match a low anterior neck field to the 4-field off-axis technique. Furthermore the 4-field off-axis technique is more complex because of the use of table kicks. The 4-field co-planar IMRT technique is preferable for the postoperative treatment of the parotid bed.

References

1. Garden AS, el-Naggar AK, Morrison WH, Callender DL, Ang KK, Peters LJ. Postoperative radiotherapy for malignant tumors of the parotid gland. *Int J Radiat Oncol Biol Phys* 1997; **37**: 79-85.
2. Bailey DW, Kumaraswamy L, Podgorsak MB. A fully electronic intensity-modulated radiation therapy quality assurance (IMRT QA) process implemented in a network comprised of independent treatment planning, record and verify, and delivery systems. *Radiol Oncol* 2010; **44**: 124-30.
3. Nutting CM, Rowbottom CG, Cosgrove VP, Henk JM, Dearnaley DP, Robinson MH et al. Optimisation of radiotherapy for carcinoma of the parotid gland: a comparison of conventional, three-dimensional conformal, and intensity-modulated techniques. *Radiother Oncol* 2001; **60**: 163-72.
4. Chang SX, Cullip TJ, Rosenman JG, Halvorsen PH, Tepper JE. Dose optimization via index-dose gradient minimization. *Med Phys* 2002; **29**: 1130-46.
5. Yaparpalvi R, Fontenla DP, Tyerech SK, Boselli LR, Beitler JJ. Parotid gland tumors: a comparison of postoperative radiotherapy techniques using three dimensional (3D) dose distributions and dose-volume histograms (DVHS). *Int J Radiat Oncol Biol Phys* 1998; **40**: 43-9.
6. Nutting CM, Morden JP, Harrington KJ, Urbano TG, Bhide SA, Clark C et al. Parotid-sparing intensity modulated versus conventional radiotherapy in head and neck cancer (PARSPORT): a phase 3 multicentre randomised controlled trial. *Lancet Oncol* 2011; **12**: 127-36.
7. Rowbottom CG, Nutting CM, Webb S. Beam-orientation optimization of intensity-modulated radiotherapy: clinical application to parotid gland tumours. *Radiother Oncol* 2001; **59**: 169-77.
8. Bragg CM, Conway J, Robinson MH. The role of intensity-modulated radiotherapy in the treatment of parotid tumors. *Int J Radiat Oncol Biol Phys* 2002; **52**: 729-38.
9. Chao KS, Deasy JO, Markman J, Haynie J, Perez CA, Purdy JA, et al. A prospective study of salivary function sparing in patients with head-and-neck cancers receiving intensity-modulated or three-dimensional radiation therapy: initial results. *Int J Radiat Oncol Biol Phys* 2001; **49**: 907-16.
10. Blanco AI, Chao KS, El Naqa I, Franklin GE, Zakarian K, Vivic M, et al. Dose-volume modeling of salivary function in patients with head-and-neck cancer receiving radiotherapy. *Int J Radiat Oncol Biol Phys* 2005; **62**: 1055-69.
11. Deasy JO, Moiseenko V, Marks L, Chao KS, Nam J, Eisbruch A. Radiotherapy dose-volume effects on salivary gland function. *Int J Radiat Oncol Biol Phys* 2010; **76**: S58-63.

Radiol Oncol 2013; 47(4): 311-318.
doi:10.2478/raon-2013-0062

Mikro RNA in dolge nekodirajoče RNA: možnosti v diagnostiki in terapiji raka

Hauptman N in Glavač D

Izhodišča. Nekodirajoče RNA (ncRNAs) so ključne molekule, ki regulirajo celične procese, in so potencialni biološki označevalci v mnogih boleznih. Mikro RNA in dolge nekodirajoče RNA raziskujejo pri diagnosticiranju raka, pa tudi kot napovedne tumorske označevalce za izhod bolezni in kot terapevtska orodja pri bolnikih z rakom. Z njihovim profilom izražanja razlikujejo različne vrste in podvrste raka.

Zaključki. Številne raziskave potrjujejo vključitev nekodirajočih RNA v začetek, razvoj in napredovanje raka, vendar so bile šele pred kratkim opredeljene kot nova diagnostična in napovedna orodja. To je lahko koristno pri zdravljenju raka v prihodnosti, saj so nekodirajoče RNA naravne protismerne interakcijske molekule vključene v regulacijo številnih genov povezanih s preživetjem in proliferacijo. Raziskave so usmerjene v razvoj uporabnih označevalcev za diagnozo in napoved poteka raka ter v razvijanje novih terapij na osnovi RNA, od katerih so nekatere že v kliničnih preskušanjih.

Radiol Oncol 2013; 47(4): 319-329.
doi:10.2478/raon-2013-0053

Pomen kalikreinskih peptidaz kot biomarkerjev pri malignomih ženskih in moških spolnih organov

Schmitt M, Magdolen V, Yang F, Kiechle M, Bayani J, M. Yousef GM, Scorilas A, Diamandis EP, Dorn J

Izhodišča. Kalikreinske (KLK) peptidaze, ki se izražajo v tumorskem tkivu, so klinično pomembni biološki označevalci, ki so lahko napovedni dejavniki preživetja ali pa napovedni dejavniki odgovora na zdravljenje s tarčnimi zdravili. V spolnih organih žensk in moških se izraža vseh 15 KLK peptidaz: v normalni prostati, dojki, materničnem vratu in modih, vendar se v maternici/endometriju in ovarijih izražajo samo nekateri.

Zaključki. Ugotavljamo veliko podatkov o povišanih koncentracijah kalikreinskih peptidaz pri rakah ovarija, kjer predstavljajo pomemben biološki označevalec za določanje fenotipa raka. Nasprotno so pri raku dojke nekatere kalikreinske peptidaze znižane, vendar je povišana kalikreinska peptidaza 4, tako kot tudi pri raku ovarija in prostate. V takih primerih lahko sintetični zaviralci kalikreinske peptidaze predstavljajo blokatorje nekaterih proteolitičnih aktivnosti določenih kalikreinskih peptidaz. Lahko bi jih uporabili za tarčna zdravila, ki bi vplivala na rast tumorjev in njihovo zasevanje.

Radiol Oncol 2013; 47(4): 330-337.

doi:10.2478/raon-2013-0063

Razmnoževanje dveh linij glioblastomskih matičnih celic posreduje rastni dejavnik bFGF in ne EGF

Podergajs N, Brekka N, Radlwimmer B, Herold-Mende C, Talasila KM, Tiemann K, Rajčević U, Lah TT, Bjerkgvig R, Miletić H

Izhodišča. Glioblastomske matične celice, pridobljene iz glioblastomov bolnikov, so dragocen model za osnovne in klinične raziskave zdravljenja. Glioblastomske matične celice običajno gojijo v gojišču brez seruma, v t.i. mediju Neural Basal z dodanima rastnima dejavnikoma - bazičnim fibroblastnim rastnim dejavnikom (bFGF) in epidermalnim rastnim dejavnikom (EGF). Vpliva teh dveh rastnih dejavnikov na obnašanje glioblastomskih matičnih celic pa ne poznamo dovolj dobro. Pred kratkim so predlagali, da bi glioblastomske matične celice, ki izražajo pomnožen receptor epidermalnega rastnega dejavnika (EGFR), gojili v mediju brez EGF, saj je ta povzročil hitro izgubo izražanja EGFR. Ker bolnikov bioptični material navadno prenesemo v gojišča še preden je znan njegov genomski profil, se sprašujemo, ali naj primarne celice glioblastomov brez pomnoženega EGFR gojimo v odsotnosti EGF.

Materiali in metode. Da bi odgovorili na gornje vprašanje, smo uporabili dve heterogeni celični liniji glioblastomskih matičnih celic (NCH421k in NCH644), ki ne izražata pomnoženega EGFR.

Rezultati. Ugotovili smo, da čeprav obe celični liniji izražata nizke vrednosti EGFR pri standardnih pogojih gojenja, je prisotnost samega bazičnega fibroblastnega rastnega dejavnika močno povečala izražanje EGFR v NCH644. Izražanje označevalcev matičnih celic, nestina in CD133, je bilo višje v prisotnosti samega bFGF v primerjavi z EGF v obeh celičnih linijah. Pomembno je tudi, da je bFGF dejavnik spodbudil rast obeh celičnih linij: preko stimulatornega delovanja na proliferacijo v celicah NCH421k in preko povečanja odpornosti na apoptozo v celicah NCH644. Epidermalni rastni dejavnik ni imel takšnega učinka.

Zaključki. Pokazali smo, da je glioblastomske matične celice brez pomnoženega EGFR prav tako mogoče uspešno gojiti le v mediju z bFGF, medtem ko EGF nima pomembnega vpliva na gojenje teh celic in ga lahko opustimo.

Radiol Oncol 2013; 47(4): 338-345.

doi:10.2478/raon-2013-0052

Heterogenost lokalizacije uroplakinov v humanem normalnem uroteliju, papilomih in papilarnih karcinomih

Zupančič D in Romih R

Izhodišča. Uroplakini so z diferenciacijo povezani membranski proteini urotelija. Primerjali smo izražanje uroplakinov in njihovo ultrastrukturno lokalizacijo v humanem normalnem uroteliju, v papilomih in papilarnih karcinomih. Zaradi visoke stopnje ponovnega pojavljanja teh tumorjev, ki se zdravijo s transuretralno resekcijo, smo poleg tumorja proučili tudi mejo resekcije in nevpleten urotelj.

Bolniki in metode. Vzorce sečnega mehurja smo odvzeli kontrolnim osebam brez tumorjev in bolnikom s papilom in papilarnimi karcinomi. Naredili smo imunohistokemično in imunoelektronsko označevanje uroplakinov.

Rezultati. V normalnem humanem uroteliju z neprekinjeno plastjo uroplakin pozitivnih površinskih celic so bili uroplakini lokalizirani v ploščatih fuziformnih veziklih in v apikalni plazmalemi dežnikastih celic. Izražanje uroplakinov v papilomih in papilarnih karcinomih je bilo raznoliko. V tumorjih smo opazili tri nenavadne diferenciacijske stopnje, ki jih v normalnem uroteliju ni. Raznoliko izražanje uroplakinov in nenavadno diferenciacijo smo občasno našli tudi v uroteliju z meje resekcije in v nevpletenem uroteliju.

Zaključki. Pokazali smo, da pride v urotelijskih tumorjih do spremenjene ultrastrukturne lokalizacije uroplakinov v primerjavi z normalnim urotelijem. Imunooznačevanje na ultrastrukturnem nivoju nam pri bolnikih s papilomi in papilarnimi karcinomi pokaže nenavadno urotelijsko diferenciacijo. Možno je, da nenavadne diferenciacijske stopnje urotelijskih celic, ki smo jih našli v meji resekcije in v nevpletenem uroteliju, prispevajo k visoki stopnji ponovnega pojavljanja.

Radiol Oncol 2013; 47(4): 346-357.
doi:10.2478/raon-2013-0050

Biološki učinki kompleksov *trans*-dichloridoplatinum(II) z 3- in 4-acetilpiridinom v primerjavi s cisplatinom

Filipović L, Arandžević S, Gligorijević N, Krivokuća A, Janković R, Srdić-Rajić T, Rakić G, Tešić Z, Radulović S

Izhodišča. V prešnji raziskavi smo poročali o sintezi in citotoksičnosti dveh kompleksov *trans*-platinum(II): *trans*-[PtCl₂(3-acetilpiridin)₂] (**1**) in *trans*-[PtCl₂(4-acetilpiridin)₂] (**2**), med katerima je bila substanca **2** zelo citotoksična. Namen pričujoče raziskave je bil proučevanje bioloških mehanizmov in aktivnosti teh dveh substanc v primerjavi s cisplatinom na celicah HeLa, MRC-5 in MS1.

Materiali in metode. S pomočjo testa sulforodamin B (SRB) smo določali citotoksičnost substanc. Kolagenolitično aktivnost smo določali s testom želatinske cimo grafije, medtem ko smo učinek substanc na matrične metaloproteineze 2 in 9 določali s kvantifikacijo izražanja mRNA s pomočjo kvantitativne polimerazne verižne reakcije (PCR) v realnem času. Apoptotični potencial celic in spremembe v celičnem ciklusu smo določali z analizo fluorescenčno aktiviranih razvrčenih celic (FACS). Z analizo Western smo določali učinek na izražanje DNA popravljalnega encima ERCC1, in kvantitativni PCR v realnem času za izražanje mRNA tega gena. Antiangiogeni potencial smo določali *in vitro* s testom tvorjenja kapilaram podobnih struktur. Intracelularno količino platine smo določali z induktivno sklopljeno plazemsko emisijsko spektrometrijo.

Rezultati. Določili smo selektiven citotoksičen učinek substance **2** in s pretočno citometrijo na celicah HeLa apoptotično aktivnost substance **2**, medtem ko je imela substanca **1** tako citotoksično kot apoptotično aktivnost. Obe substanci, **1** in **2**, sta zavirali izražanje encima ERCC1, kot sta tudi zavirali MMP-9 mRNA izražanje v celicah HeLa, poleg tega je substance **2** zmanjšala tvorjenja kapilaram podobnih struktur na MS1 celicah.

Zaključki. Sposobnost substance **2** za različne in specifične aktivnosti *in vitro*, kot je citotoksičnost, nakazuje na potencialno vrednost *trans*-platinum(II) kompleksov z nadomeščenim pirimidinom.

Radiol Oncol 2013; 47(4): 358-365.
10.2478/raon-2013-0054

Vloga pozitronske emisijske tomografije s fluorodeoksiglukozo (^{18}F) za določanje odgovora na zdravljenje z elektrokemoterapijo lokoregionalnih recidivov raka dojke

Wichmann Matthiessen L, Hjorth Johannesen H, Skougaard K, Gehl J, Westergren Hendel H

Izhodišča. Elektrokemoterapija je zelo učinkovita pri zdravljenju malih kožnih zasevkov. Metodo preizkušajo tudi na velikih kožnih recidivih raka dojke, ki jih pogosto vidimo kot konfluentne mase z vnetnimi področji. Za ugotavljanje stopnje odgovora na elektrokemoterapijo lahko uporabljamo pozitronsko emisijsko tomografijo s fluorodeoksiglukozo (^{18}F) in računalniško tomografijo (FDG-PET/CT). Vendar standardna preiskava FDG-PET/CT ne more ločiti vnetno in tumorsko tkivo. Z dvostopenjskim časovnim slikanjem (*dual time point imaging – DTPI*) pa lahko oboje ločimo. Namen raziskave je bil določiti uporabnost dvostopenjskega časovnega slikanja FDG-PET/CT pri oceni odgovora na zdravljenje po elektrokemoterapiji.

Bolniki in metode. V klinični raziskavi II. faze smo 11 bolnic ovrednotili s FDG-PET/CT v treh časovnih točkah: 60, 120 in 180 minut po injiciranju FDG. Slikanje smo izvedli pred elektrokemoterapijo in 3 tedne po njej.

Rezultati. Po zdravljenju z elektrokemoterapijo smo zaznali značilno znižanje največjega standardnega privzema 60 minut po injiciranju FDG. Kopičenje se je nadaljevalo do 120 minut po injiciranju in stabiliziralo pri 180 minutah. S takšnim pristopom smo lahko zaznali zmanjšanje v kopičenju pri treh lezijah zdravljenih z elektrokemoterapijo, pri dveh lezijah smo ugotovili spremembo iz stabilnega metabolnega stanja v delno in pri eni leziji iz delnega v stabilno metabolično stanje. Za sledenje učinka elektrokemoterapije se je pokazalo najprimernejše slikanje pri časih 60 in 180 minut po injiciranju FDG.

Zaključki. Raziskava nakazuje uporabnost FDG-PET/CT s slikanjem 60 in 180 minut po injiciranju FDG pri vrednotenju odgovora na zdravljenje kožnih recidivov raka dojke z elektrokemoterapijo.

Radiol Oncol 2013; 47(4): 366-369.
doi:10.2478/raon-2013-0059

Elektrokemoterapija kot nova terapevtska možnost za zdravljenje raka Merkelovih celic v predelu glave in vratu. Prikaz primera

Scelsi D, Mevio N, Bertino G, Occhini A, Brazzelli V, Morbini P, Benazzo M

Izhodišča. Rak Merkelovih celic je redek, a agresiven tumor s slabo napovedjo poteka bolezni. Izhaja iz kožnih mehano-receptorjev, ki so v bazalni plasti epidermisa. Zdravljenje zgodnjih stadijev tumorjev je kirurško in/ali radioterapevtsko, medtem ko je zdravljenje ob ponovitvi bolezni še nedorečeno.

Prikaz primera. Opisujemo 84 let staro bolnico, pri kateri se je ponovil rak Merkelovih celic in smo jo zdravili s štirimi ponovljenimi elektrokemoterapijami v času 20 mesecev. Ugotovili smo objektivni odgovor na zdravljenje in dobro kakovost preostanka življenja.

Zaključki. Primer kaže na učinkovitost elektrokemoterapije pri lokalno napredovalem raku Merkelovih celic v področju glave in vratu pri bolnikih, ki niso primerni za standardno zdravljenje.

Radiol Oncol 2013; 47(4): 370-375.
doi:10.2478/raon-2013-0051

Minimalno invazivno zdravljenje peristomalnega zasevka raka želodca ob iliostomi z elektrokemoterapijo

Campana LC, Scarpa M, Sommariva A, Bonandini E, Valpione S, Sartore L, Rossi CR

Izhodišča. Peristomalni zasevki so redkost, vendar povzročajo veliko morbiditeto. Kirurška resekcija s prestavitvijo stome je standardni način zdravljenja. Predstavljamo alternativno minimalno invazivno metodo, elektrokemoterapijo, kjer z lokalno aplikacijo električnih pulzov povečamo učinkovitost citostatikov.

Bolnik in metode. Pri 49-letnem moškem z napredovalim rakom želodca smo ugotovili kožni zasevek okoli ileostome. Ulceriran in cedeč tumor mu je poslabšal kakovost življenja. Bolnik je imel stalne težave z nameščanjem stome, ki jo je težko pritrtil na kožo, blato se je izlivalo. Elektrokemoterapijo smo izvajali 20 minut v blagi splošni sedaciji. Po intravenski aplikaciji bleomicina (15.000 IU/m²) smo z igelnimi elektrodami dovajali električne pulze na tumor.

Rezultati. Elektrokemoterapija ni imela stranskih učinkov in bolnik je bil odpuščen iz bolnišnice isti dan. Po enem tednu se je zasevek sploščil in v enem mesecu značilno zmanjšal. Najvažnejše pa je, da se je koža okoli peristome zacelila, bolnik si je lahko brez težav namestil stomo, ki mu je dobro služila v nadaljnjih mesecih do smrti.

Zaključki. Primer nakazuje na izvedljivost in uporabnost elektrokemoterapije kot minimalnega invazivnega posega za zdravljenje peristomalnih tumorjev. Na izbranih primerih lahko elektrokemoterapija izboljša kakovost življenja bolnikov, hitro kontrolira rast tumorja in omogoča ponovno nameščanje stome.

Radiol Oncol 2013; 47(4): 376-381.
doi:10.2478/raon-2013-0058

Učinki ionizirajočega sevanja na človeške mioblaste - prekurzorje skeletne mišičnine

Jurdana M, Čemažar M, Pegan K, Marš T

Izhodišča. Namen raziskave je bil proučiti učinek različnih odmerkov ionizirajočega sevanja na človeške mioblaste, prekurzorje skeletne mišičnine v kulturah *in vitro*.

Materiali in metode. Celične kulture *in vitro* človeških mioblastov pridobljenih iz koščkov mišičnega tkiva smo obsevali z aparatom Darpac 200 X-ray z različnimi odmerki (4–8 Gy) ionizirajočega sevanja. Akutne učinke sevanja smo spremljali z ugotavljanjem sproščanja citokina IL-6 ter z ugotavljanjem stresnega odziva celic. Stresni odziv smo določali z ravno beljakovin toplotnega šoka (HSP). Dolgotrajne učinke ionizirajočega sevanja smo sledili z določljivijo sposobnosti proliferacije in določitvijo celične smrti.

Rezultati. V primerjavi s celičnimi kulturami mioblastov, ki niso bile izpostavljene sevanju, ter celičnimi kulturami, ki smo jim rast zavirali z inhibitorjem ARA C, se je proliferacija obsevanih mioblastov zmanjšala 72 ur po izpostavitvi sevanju. Ta učinek je bil odvisen od doze sevanja in je bil pri višjih odmerkih izrazitejši. Neposreden učinek sevanja na smrt celic smo določili z merjenjem aktivnosti encima LDH. Aktivnost LDH se je po sevanju povečala. Po obsevanju z nižjimi odmerki so se človeški mioblasi odzvali tudi z zmanjšanim izločanje citokina IL-6. Večji odmerki sevanja so sprožili stresni odziv s povišano ravno stresnih označevalcev, kot sta HSP 27 in 70.

Zaključki. Glede na pridobljene rezultate lahko sklepamo, da je občutljivost človeških mioblastov na sevanje odvisna od odmerka sevanja. Ob večjih odmerkih sevanja je zmanjšana sposobnost proliferacije in izločanja citokina IL-6. Ker so mioblasi ključne celice, udeležene v procesu mišične regeneracije, bi ti učinki lahko vplivali na regeneracijsko sposobnost skeletne mišice po obsevanju.

Radiol Oncol 2013; 47(4): 382-389.

doi:10.2478/raon-2013-0056

Rekombinantni humani eritropoetin spremeni izražanje genov in pospeši proliferacijo celic MCF-7 raka dojke

Trošt N, Stepišnik T, Berne S, Pucer A, Petan T, Komel R, Debeljak N

Izhodišča. Signalizacija preko eritropoetina (EPO) ni značilna le za eritopoetski sistem, ampak je bila potrjena tudi v tumorskem tkivu, med drugim pri raku dojke. Eritropoetinski receptor (EPOR) je izražen v treh različnih izooblikah. Topni (EPOR-S) in skrajšani (EPOR-T) receptor tekmujeta s funkcionalnim EPOR za vezavo liganda (EPO), torej je njuno delovanje antagonistično. Namen raziskave je bil določiti vlogo rekombinantnega humanega EPO (rHuEPO) na proliferacijo celic raka dojke ter opredeliti njegovo vlogo na izražanje EPOR ter genov zgodnjega odziva.

Materiali in metode. Celično linijo MCF-7 smo izpostavili rHuEPO za 72 ur in 10 tednov, pri čemer smo analizirali vpliv rHuEPO na proliferacijski potencial celic, izražanje genov zgodnjega odziva ter na izražanje različnih izooblik receptorja EPOR. V naboru celičnih linij raka dojke smo primerjali izražanje funkcionalnega EPOR in EPOR-T ter določili korelacijo med izražanjem obeh izooblik in invazivnostjo celic.

Rezultati. Visoke koncentracije rHuEPO (40 U/ml) povečajo proliferacijo MCF-7 celic neodvisno od časa predhodne izpostavitve, medtem ko pri nižjih koncentracijah (5 U/ml) povečano proliferacijo opazimo le po predhodni 10 tedenski izpostavitvi. Funkcionalnost EPO-EPOR signalizacije smo pokazali tudi na nivoju aktivacije genov *EGR1* in *FOS* ter regulacije izražanja EPOR; izpostavitve MCF-7 celic rHuEPO je namreč povišala izražanje funkcionalnega EPOR, medtem ko na EPOR-T ni imela vpliva. Povišano izražanje EPOR smo pokazali tudi po 10 tedenski izpostavitvi rHuEPO. Korelacije med izražanjem EPOR in invazivnostjo celičnih linij MCF-7, MDA-MB-231, Hs578T, Hs578Bst, SKBR3, T-47D in MCF-10A nismo uspeli potrditi.

Zaključki. Vpliv rHuEPO na proliferacijo MCF-7 celic je odvisen od uporabljene koncentracije in časa izpostavitve in regulira prepisovanje genov *EGR1*, *FOS* in EPOR. Korelacije med izražanjem izooblik EPOR in invazivnostjo celičnih linij raka dojke nismo uspeli pokazati.

Radiol Oncol 2013; 47(4): 390-397.
doi: 10.2478/raon-2013-0031

Uporabnost F-18 PET/CT mamografije pri preoperativnem določanju stadija raka dojke. Primerjava s konvencionalnim PET/CT in MR mamografijo

Moon EH, Lim ST, Han YH, Jeong YJ, Kang YH, Jeong HJ, Sohn MH

Izhodišča. Cilj raziskave je bil primerjati diagnostično učinkovitost PET/CT mamografije s pomočjo fluorine-18 fluoro-deoxyglukose (m-PET/CT) pri odkrivanju bolnikov s karcinomom dojke in primerjava le-te z učinkovitostjo konvencionalnega PET/CT prsnega koša (s-PET/CT) ter MR mamografije

Bolniki in metode. V raziskavo smo vključili 40 bolnic ($52,0 \pm 12,0$ let) z rakom dojke, pri katerih smo naredili s-PET/CT, m-PET/CT in MR mamografijo med aprilom in avgustom leta 2009. Z obema načinoma PET/CT-ja smo primerjali velikost tumorja, razdaljo od tumorja do stene prsnega koša, razdaljo tumorja do kože, volumen pazdušne lože ter število metastatskih pazdušnih bezgavk. Z m-PET/CT in MR mamografijo pa smo ocenjevali fokalnost primarnega tumorja dojke ter velikost tumorja. Histološki izvid je bil referenčni standard.

Rezultati. Primerjava med s-PET/CT in m-PET/CT je pokazala statistično značilne razlike v velikosti tumorja (s-PET/CT: $1,3 \pm 0,6$ cm, m-PET/CT: $1,5 \pm 0,6$ cm; $p < 0,001$), razdalji od tumorja do stene prsnega koša ($1,8 \pm 0,9$ cm, $2,2 \pm 2,1$ cm; $p < 0,001$) in razdalje od tumorja do kože ($1,5 \pm 0,8$ cm, $2,1 \pm 1,4$ cm; $p < 0,001$). Z m-PET/CT smo ugotovili značilno večji volumen pazdušne lože v primerjavi s s-PET/CT ($21,7 \pm 8,7$ cm³ vs. $23,4 \pm 10,4$ cm³; $p = 0,03$) ter pravilneje določen stadij T primarnega tumorja (72,5 % vs. 67,5 %). Razlike v številu metastatskih pazdušnih bezgavk ugotovljene z obema metodama niso bile statistično značilne. V primerjavi z MR mamografijo je m-PET/CT omogočil boljše določanje fokalnosti tumorja (95% vs. 90%). Glede na stadij bolezni T je bilo z m-PET/CT ugotovljeno 72,5 % ujemanje s patološkim izvidom, z MR mamografijo pa 70%.

Zaključek. M-PET/CT omogoča pravilnejšo opredelitev stadija T raka dojke ter jasnejšo razmejitev pazdušne lože kot s-PET/CT. Poleg tega je mPET/CT uporabnejši kot MR mamografija saj enako natančno opredelivši stadija T raka dojke, omogoča pa natančnejšo opredelitev fokalnosti lezije.

Radiol Oncol 2013; 47(4): 398-404.

doi:10.2478/raon-2013-0038

Pomen ultrazvoka ob uporabi kontrastnega sredstva za oceno učinkovitosti ultrazvočno vodene perkutane mikrovalovne ablacije raka ledvic

Li X, Liang P, Yu J, Yu XL1, Liu FY, Cheng ZG, Han ZY

Izhodišča. Namen raziskave je bil ovrednotiti učinkovitost in uporabnost ultrazvoka (UZ) ob uporabi kontrastnega sredstva Sonovue za oceno zdravljenja raka ledvic z ultrazvočno vodeno perkutano mikrovalovno ablacijo.

Bolniki in metode. Pri 79 bolnikih (60 moških in 19 žensk) smo z ultrazvočno vodeno perkutano mikrovalovno ablacijo zdravili 83 tumorskih sprememb (povprečna velikost $3,2 \pm 1,6$ cm). Tretji dan po posegu smo ovrednotili učinkovitost posega z UZ ob uporabi kontrastnega sredstva. Rezultate smo primerjali z izvidi računalniške tomografije (CT) in magnetne resonance (MRI) ter s histološkimi izvidi biopsije. Ponovno oceno smo opravili z UZ ob uporabi kontrastnega sredstva in s CT/MRI po 1, 3, 6 mesecih in nato vsakih naslednjih 6 mesecev. Kot referenčni standard za oceno učinkovitosti zdravljenja, s katerim smo primerjali rezultate UZ ob uporabi kontrastnega sredstva, smo uporabili kombinacijo kliničnega pregleda in izvide preiskav CT/MRI. Vse slikovne preiskave sta neodvisno interpretirala dva radiologa.

Rezultati. Tretji dan po mikrovalovni ablaciji je bil glede na UZ s kontrastnim sredstvom pri 68 od 83 tumorskih sprememb (81,9%) prisoten popoln odgovor na zdravljenje, pri 15 od 83 tumorskih sprememb (18,1%) pa so videli njegov ostanek. Z biopsijo smo pri 13 od 15 spremembah (86,7%) potrdili raka. Senzitivnost, specifičnost, natančnost, pozitivne in negativne napovedne vrednosti UZ ob uporabi kontrastnega sredstva za oceno kratkoročne učinkovitosti mikrovalovne ablacije so bile 100 %, 97,1 %, 97,6%, 86,7 % in 100 %. Obdobje sledenja je trajalo 6 let (povprečno 26 mesecev). V tem času smo z UZ ob uporabi kontrastnega sredstva zaznali ponovitev bolezni pri 7 bolnikih, s CT/MRI pa pri 6 bolnikih. Senzitivnost, specifičnost, natančnost, pozitivne in negativne napovedne vrednosti UZ ob uporabi kontrastnega sredstva za oceno dolgoročne učinkovitosti mikrovalovne ablacije so bile 85,7 %, 98,7 %, 97,6 %, 85,7 % in 98,7 %.

Zaključki. Ultrazvok ob uporabi kontrastnega sredstva je bil pričujoči raziskavi učinkovita in uporabna metoda za oceno terapevtskega efekta mikrovalovne ablacije pri bolnikih z rakom ledvic.

Radiol Oncol 2013; 47(4): 405-410.

doi:10.2478/raon-2013-0055

Vpliv deleža CD133 pozitivnih matičnih celic na preživetje bolnikov z glioblastomom multiforme

Kase M, Minajeva A, Niinepuu K, Kase S, Vardja M, Asser T, Jaal J

Izhodišča. Namen raziskave je bil ugotoviti pomen deleža CD133 pozitivnih (CD133+) karcinomskih matičnih celic na rezultate zdravljenja bolnikov z glioblastomom multiforme (GBM).

Bolniki in metode. Bolniki z GBM ($n = 42$) so prejeli pooperativno radioterapijo (\pm kemoterapijo). V tkivnih rezinah kirurško odstranjenih GBM smo imunohistokemično določili izražanje CD133. Delež CD133+ celic GBM sta ugotavljala neodvisno dva raziskovalca. Njunji rezultati so se ujemale ($R = 0,8$, $p < 0,01$). Poleg tega smo analizirali povezavo med nivojem izražanja CD133 in preživetjem bolnikov.

Rezultati. Med bolniki se je delež CD133+ celic razlikoval in je znašal med 0,5 % in 82 %. Povprečen odstotek CD133+ celic je bil $33 \% \pm 24 \%$, srednja vrednost pa 28 %. Klinični podatki niso pokazali povezave med visokimi deleži matičnih celic in agresivnostjo GBM. Srednji čas preživetja je bil 10,0 mesecev (95 %, interval zaupanja [CI] 9,0 – 11,0). Čas preživetja je bil odvisen od deleža CD133+ celic (log rank test, $p = 0,02$). Srednji čas preživetja v skupini z nizkim (< srednja vrednost) in visokim deležem CD133 celic (> srednja vrednost) je bil 9,0 mesecev (95 % CI 7,6 – 10,5) in 12,0 mesecev (95 % CI 9,3 – 14,7). Multivariatna analiza je pokazala, da je delež CD133+ celic statistično značilno neodvisen napovedni dejavnik preživetja bolnikov z GBM (razmerje ogroženosti [HR] 2,0; 95 % CI 1,0 – 3,8; $p = 0,04$).

Zaključki. Bolniki z visokim deležem CD133+ celic imajo značilno daljši čas preživetja po pooperativni radioterapiji. V nadaljnjih raziskavah bi bilo potrebno proučiti vzrok za to in morebitno višjo občutljivost karcinomskih matičnih celic GBM na frakcionirano radioterapijo.

Radiol Oncol 2013; 47(4): 1-IX.

Radiol Oncol 2013; 47(4): 411-418.
doi:10.2478/raon-2013-0010

Dozimetrično ovrednotenje intenzitetnomodulirane radioterapije obušesnih slinavk v primeru istostranske razporeditve obsevalnih polj

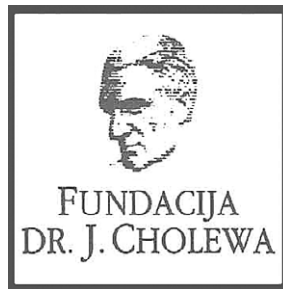
Yirmibesoglu E, Fried DV, Kostich M, Rosenman J, Shockley W, Weissler M, Zanation A, Chera B

Izhodišča. Izvedli smo dozimetrično primerjavo intenzitetnomodulirane radioterapije (IMRT) pri istostranski razporeditvi obsevalnih polj izven centralne osi.

Bolniki in metode. V dozimetrično klinično raziskavo smo vključili 6 bolnikov z malignim obolenjem obušesnih slinavk, ki smo jih pooperativno obsevali. Za vsak set računalniškotomografskih slik smo izdelali štiri obsevalne načrte (24 načrtov): 1) IMRT s štirimi istostranskimi obsevalnimi polji izven centralne osi, 2) običajni obsevalni načrt s parom klinastih obsevalnih polj (WP), 3) IMRT s 7 nekoplanarnimi obsevalnimi polji (7P), 4) IMRT s štirimi koplanarnimi istostranskimi obsevalnimi polji (4PCP). Pri vseh štirih obsevalnih tehnikah smo primerjali doze in dozno-volumske histograme za načrtovalne tarčne volumne (PTVs) in za rizične tarčne volumne (PRVs).

Rezultati. Običajni obsevalni načrti z dvema klinastima obsevalnima poljema ne pokrivajo primerno globljih pordočij PTV. Največji volumni z nizkimi dozami na normalna tkiva se pojavijo pri uporabi IMRT tehnike s sedmimi nekoplanarnimi obsevalnimi polji. Povprečna doza na drugo obušesno slinavko je bila najvišja pri 7P in WP. Najvišjo dozo v ustni votlini dobimo pri uporabi IMRT tehnike s sedmimi nekoplanarnimi polji. Povprečne doze na možgansko deblo, hrbtenico, istostransko prednjo ložo, možganovino in istostransko kohlelo so bile podobne za vse štiri obsevalne tehnike.

Zaključki. Pri 4PCP pooperativnem obsevanju obušesne slinavke lahko dosežemo odlično pokritje tarčnega volumna, obenem pa so doze na drugo obušesno in na podčeljustno slinavko minimalne.



FUNDACIJA "DOCENT DR. J. CHOLEWA"
JE NEPROFITNO, NEINSTITUCIONALNO IN NESTRANKARSKO
ZDRUŽENJE POSAMEZNIKOV, USTANOV IN ORGANIZACIJ, KI ŽELIJO
MATERIALNO SPODBUJATI IN POGLABLJATI RAZISKOVALNO
DEJAVNOST V ONKOLOGIJI.

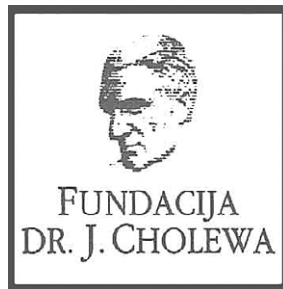
OB JUBILEJNI, 20. OBLETNICI DELOVANJA
FUNDACIJA »DOCENT DR. JOSIP CHOLEWA« V SODELOVANJU Z
MEDICINSKO FAKULTETO LJUBLJANA, UNIVERZITETNIM KLINIČNIM CENTROM
LJUBLJANA IN ONKOLOŠKIM INŠTITUTOM LJUBLJANA
PRIREJA STROKOVNI SIMPOZIJ Z NASLOVOM:

»NOVOSTI V DIAGNOSTIKI IN ZDRAVLJENJU RAKA«

SIMPOZIJ BO POTEKAL V LJUBLJANI, DNE 13. DECEMBRA 2013
V MODRI DVORANI DOMUS MEDICA, DUNAJSKA CESTA 162.

DUNAJSKA 106
1000 LJUBLJANA

ŽR: 02033-0017879431



Activity of "Dr. J. Cholewa" Foundation for Cancer Research and Education - a report for the third quarter of 2013

The Dr. J. Cholewa Foundation for Cancer Research and Education is a non-profit, non-political and non-government organisation that unites individuals, professionals, institutions and other organisations in their effort to achieve optimal results in cancer research, education, treatment and prevention. It provides financial support for physicians and other experts interested in all the subjects associated with cancer, resulting in a number of successful initiatives and projects.

The Foundation continues to provide regular financial support to "Radiology and Oncology", an international scientific journal that is edited, published and printed in Ljubljana, Slovenia.

"Radiology and Oncology" publishes scientific research articles, reviews, case reports, short reports and letters to the editor about research and studies in experimental and clinical oncology, supportive therapy, experimental and clinical research in radiology, radiophysics, prevention and early diagnostics of different types of cancer. It is an open access journal available in pdf format and with an important Science Citation Index Impact factor. All the abstracts in "Radiology and Oncology" are translated in Slovenian and the journal can thus provide sufficient scientific information from various fields of high quality cancer research to interested lay public in Slovenia.

The Foundation also continues to provide financial support for the publication of a number of information materials and brochures published by Slovenian Cancer Association, a member of European Cancer Leagues and UICC and most important lay association and organization involved in cancer education of lay and professional public in Slovenia. As such, the Foundation is preparing and organizing a scientific and educational conference with a purpose to transfer the information about latest developments in the diagnostics and treatment of various types of cancer to general practitioners, other medical experts in primary health care and to anyone else interested in the aforementioned topic. It is planned the conference will take place in the middle of December 2013 in Ljubljana.

The Dr. J. Cholewa Foundation for Cancer Research and Education continues to provide financial and other means of support to all in Slovenia interested in the fight against cancer to organise scientific and other meetings of specific interest in different fields of cancer research and education.

Borut Štabuc, M.D., Ph.D.
Andrej Plesničar, M.D., M.Sc.
Viljem Kovač, M.D., Ph.D.
Tomaž Benulič, M.D.

TANTUM VERDE®



Lajšanje bolečine in oteklin pri vnetju v ustni votlini in žrelu, ki nastanejo zaradi okužb in stanj po operaciji in kot posledica radioterapije (t.i. radiomukozitis).



Imetnik dovoljenja za promet
CSC Pharma d.o.o.
Jana Husa 1a
1000 Ljubljana



www.tantum-verde.si

Tantum Verde 1,5 mg/ml oralno pršilo, raztopina

Kakovostna in količinska sestava

1 ml raztopine vsebuje 1,5 mg benzidaminijevega klorida, kar ustreza 1,34 mg benzidamina. V enem razpršku je 0,17 ml raztopine. En razpršek vsebuje 0,255 mg benzidaminijevega klorida, kar ustreza 0,2278 mg benzidamina. En razpršek vsebuje 13,6 mg 96 odstotnega etanola, kar ustreza 12,728 mg 100 odstotnega etanola, in 0,17 mg metilparahidroksibenzoata (E218).

Terapevtske indikacije

Samozdravljenje: lajšanje bolečine in oteklin pri vnetju v ustni votlini in žrelu, ki so lahko posledica okužb in stanj po operaciji. Po nasvetu in navodilu zdravnika: lajšanje bolečine in oteklin v ustni votlini in žrelu, ki so posledica radiomukozitisa.

Odmerjanje in način uporabe

Uporaba 2- do 6-krat na dan (vsake 1,5 do 3 ure). Odrasli: 4 do 8 razprškov 2- do 6-krat na dan. Otroci od 6 do 12 let: 4 razprški 2- do 6-krat na dan. Otroci, mlajši od 6 let: 1 razpršek na 4 kg telesne mase; do največ 4 razprške 2 do 6-krat na dan.

Kontraindikacije

Znana preobčutljivost za zdravilno učinkovino ali katerokoli pomožno snov.

Posebna opozorila in previdnostni ukrepi

Pri manjšini bolnikov lahko resne bolezni povzročijo ustne/žrelne ulceracije. Če se simptomi v treh dneh ne izboljšajo, se mora bolnik posvetovati z zdravnikom ali zobozdravnikom, kot je primerno. Zdravilo vsebuje aspartam (E951) (vir fenilalanina), ki je lahko škodljiv za bolnike s fenilketonurijo. Zdravilo vsebuje izomalt (E953) (sinonim: izomaltitol (E953)). Bolniki z redko dedno intoleranco za fruktozo ne smejo jemati tega zdravila. Uporaba benzidamina ni priporočljiva za bolnike s preobčutljivostjo za salicilno kislino ali druga nesteroidna protivnetna zdravila. Pri bolnikih, ki imajo ali so imeli bronhialno astmo, lahko pride do bronhospazma. Pri takih bolnikih je potrebna previdnost.

Medsebojno delovanje z drugimi zdravili in druge oblike interakcij

Pri ljudeh raziskav o interakcijah niso opravljali.

Nosečnost in dojenje

Tantum Verde z okusom mentola 3 mg pastile se med nosečnostjo in dojenjem ne smejo uporabljati.

Vpliv na sposobnost vožnje in upravljanja s stroji

Uporaba benzidamina lokalno v priporočenem odmerku ne vpliva na sposobnost vožnje in upravljanja s stroji.

Neželeni učinki

Bolezni prebavil Redki: pekoč občutek v ustih, suha usta.

Bolezni imunskega sistema Redki: preobčutljivostna reakcija.

Bolezni dihal, prsnega koša in mediastinalnega prostora Zelo redki: laringospazem.

Bolezni kože in podkožja Občasni: fotosenzitivnost. Zelo redki: angioedem.

Rok uporabnosti

4 leta. Zdravila ne smejo uporabljati po datumu izteka roka uporabnosti, ki je naveden na ovojnjini. Posebna navodila za shranjevanje Za shranjevanje pastil niso potrebna posebna navodila. Platenko z raztopino shranjujte v zunanji ovojnjini za zagotovitev zaščite pred svetlobo. Shranjujte pri temperaturi do 25°C. Shranjujte v originalni ovojnjini in nedosegljivo otrokom.

Za bolnike z napredovalim neploščatoceličnim* NSCLC

OMOGOČI PREŽIVETJE.



OHRANJA BOLEZEN
POD NADZOROM.

ALIMTA®
pemetreksed

*Žlezni, velikocelični rak pljuč in druge histologije.
NSCLC - Nedrobnoocelični rak pljuč

SKRAJŠAN POVZETEK GLAVNIH ZNAČILNOSTI ZDRAVILA

Ime zdravila ALIMTA 100 mg prašek za raztopino za infundiranje in ALIMTA 500 mg prašek za raztopino za infundiranje **Kakovostna in količinska sestava** ALIMTA 100 mg: vsaka viala vsebuje 100 mg pemetrekseda (v obliki dinatrijevega pemetrekseda). Po pripravi vsebuje vsaka viala 25 mg/ml pemetrekseda. Pomožne snovi: Vsaka viala vsebuje približno 11 mg natrija, manitol, klorovodikova kislina, natrijev hidroksoid. ALIMTA 500 mg: vsaka viala vsebuje 500 mg pemetrekseda (v obliki dinatrijevega pemetrekseda). Po pripravi vsebuje vsaka viala 25 mg/ml pemetrekseda. Pomožne snovi: Vsaka viala vsebuje približno 54 mg natrija, manitol, klorovodikova kislina, natrijev hidroksoid. **Terapevtske indikacije:** ALIMTA je v kombinaciji s cisplatinom indicirana za zdravljenje bolnikov z neresekabilnim malignim pleuralnim mezoteliomom, ki jih še nismo zdravili s kemoterapijo. ALIMTA je v kombinaciji s cisplatinom indicirana kot zdravljenje prvega izbora za bolnike z lokalno napredovalim ali metastatskim nedrobnooceličnim rakom pljuč, ki nima pretežno ploščatocelične histologije. ALIMTA je indicirana kot monoterapija za zdravljenje drugega izbora bolnikov z lokalno napredovalim ali metastatskim nedrobnooceličnim pljučnim rakom, ki nima pretežno ploščatocelične histologije. **Odrmerjanje in način uporabe:** Odrmerjanje: ALIMTA smejo dajati le pod nadzorom zdravnika, usposobljenega za uporabo kemoterapije za zdravljenje raka. ALIMTA v kombinaciji s cisplatinom: Priporočeni odmerek ALIMTE je 500 mg/m² telesne površine (TP), dan kot intravenska infuzija v 10 minutah prvi dan vsakega 21-dnevnega ciklusa. Priporočeni odmerek cisplatina je 75 mg/m² TP, infundiran v dveh urah približno 30 minut po zaključku infuzije pemetrekseda prvi dan vsakega 21-dnevnega ciklusa. Bolniki morajo prejeti zadostno antiemetično zdravljenje, pred in/ali po prejemanju cisplatina jih moramo tudi ustrezno hidrirati. ALIMTA kot samostojno zdravilo: Priporočeni odmerek ALIMTE je 500 mg/m² TP, dan kot intravenska infuzija v 10 minutah prvi dan vsakega 21-dnevnega ciklusa. **Režim premedikacije:** Da zmanjšamo incidenco in resnost kožnih reakcij, dajemo kortikosteroid dan pred dajanjem pemetrekseda, na dan dajanja pemetrekseda in naslednji dan. Kortikosteroid naj ustreza 4 mg dexametazona, danega peroralno dvakrat dnevno. Za zmanjšanje toksičnosti morajo bolniki dnevno jemati tudi peroralno folno kislino ali multivitaminski pripravek, ki jo vsebuje (350 do 1000 mikrogramov). V sedmih dneh pred prvim odmerkom pemetrekseda morajo vzeti vsaj pet odmerkov folne kisline, odmerjanje pa morajo nadaljevati ves čas zdravljenja in še 21 dni po zadnjem odmerku pemetrekseda. Bolniki morajo prejeti tudi intamskularno injekcijo vitamina B12 (1000 mikrogramov) v tednu pred prvim odmerkom pemetrekseda in enkrat vsake tri cikluse zatem. Kasnejše injekcije vitamina B12 lahko dajemo isti dan kot pemetreksed. **Kontraindikacije:** Preobčutljivost za zdravilo učinkovino ali katerokoli pomožno snov. Dojenje. Sočasno cepljenje proti rumeni mrzlici. **Posebna opozorila in previdnostni ukrepi:** Pemetreksed lahko zavre delovanje kostnega mozga, kar se kaže kot nevropenija, trombocitopenija in anemija (ali pancitopenija). Mielosupresija običajno predstavlja toksičnost za omejitve odmerka. Pri bolnikih, ki pred zdravljenjem niso prejeli kortikosteroidov, so poročali o kožnih reakcijah. Uporabe pemetrekseda pri bolnikih z očistkom kreatinina < 45 ml/min ne priporočamo. Bolniki z blagim do zmernim popuščanjem delovanja ledvic naj se izogibajo jemanju NSAID-ov z dolgimi razpolovnimi časi izločanja vsaj 5 dni pred dajanjem pemetrekseda, na dan dajanja in še vsaj 2 dni po dajanju pemetrekseda. Poročali so o resnih ledvičnih primerih, vključno z akutno ledvično odpovedjo, s pemetreksedom samim ali v povezavi z drugimi kemoterapevtiki. Pri bolnikih s klinično pomembno taksico znižanje prostora moramo razmisliti o drenaži izliva pred dajanjem pemetrekseda. Kot posledico toksičnosti pemetrekseda v kombinaciji s cisplatinom za prebavila so opažali hudo dehidracijo, zato moramo bolnike pred prejetjem terapije in/ali po njej ustrezno hidrirati, prejeti morajo zadostno antiemetično zdravljenje. Občasno so v kliničnih študijah pemetrekseda, običajno ob sočasnem dajanju z drugo citotoksično učinkovino, poročali o resnih srčnožilnih dogodkih, vključno z miokardnim infarktom in možganskožilnimi dogodki. Odsvetujemo uporabo živih oslabljenih cepiv. Spolno zrelim moškim odsvetujemo zaploditev otroka v času zdravljenja in še 6 mesecev zatem. Priporočamo ukrepe proti zanositvi ali vzdržnosti. Zaradi možnosti, da zdravljenje s pemetreksedom povzroči trajno neplodnost, naj se moški pred začetkom zdravljenja posvetujejo o shranjevanju semen. Ženske v rodni dobi morajo v času zdravljenja s pemetreksedom uporabljati učinkovito kontracepcijo. Poročali so o primerih radijskega pljučnice pri bolnikih, ki so jih zdravili z radiacijo pred, med ali po zdravljenju s pemetreksedom. Poročali so o radijskem izpuščaju pri bolnikih, ki so se zdravili z radioterapijo pred tedni ali leti. **Medsebojno delovanje z drugimi zdravili in druge oblike interakcij:** Sočasno dajanje nefrotoksičnih zdravil (denimo, aminoglikozidov, diuretikov zanke, spojin platine, ciklosporina) lahko potencialno povzroči zakasneli odtsek pemetrekseda. Sočasno dajanje snovi, ki se tudi izločajo s tubulno sekrecijo (denimo, probenecid, penicilin), lahko potencialno povzroči zakasneli odtsek pemetrekseda. Pri bolnikih z normalnim delovanjem ledvic lahko visoki odmerki nesteroidnih protivnetnih zdravil (NSAID-ov, denimo, ibuprofen) in aceticilicilne kisline v visokih odmerkih zmanjšajo eliminacijo pemetrekseda in tako lahko povečajo pojavnost neželenih učinkov pemetrekseda. Pri bolnikih z blagim do zmernim popuščanjem delovanja ledvic se moramo izogibati sočasnemu dajanju pemetrekseda z NSAID-om (denimo, ibuprofen) ali aceticilicilne kisline v visokih odmerkih 2 dni pred dajanjem pemetrekseda, na dan dajanja in še 2 dni po dajanju pemetrekseda. Sočasnemu dajanju NSAID-ov z daljšimi razpolovnimi časi s pemetreksedom se moramo izogibati vsaj 5 dni pred dajanjem pemetrekseda, na dan dajanja in še vsaj 2 dni po dajanju pemetrekseda. Velika različnost med posamezniki v koagulacijskem statusu v času bolezni ter možnost medsebojnega delovanja med peroralnimi antikoagulacijskimi učinkovinami ter kemoterapijo proti raku zahtevata povečano pogostost spremljanja INR. **Kontraindicirana sočasna uporaba:** Zelo pogosti: tveganje za smrtno generalizirano bolezen po cepilju. **Odsvetovana sočasna uporaba:** Živa oslabljena cepiva (razen proti rumeni mrzlici): tveganje za sistemske, potencialno smrtno bolezni. **Neželeni učinki** Klinične študije malignega pleuralnega mezotelioma Zelo pogosti: znižani nevtrofilci/granulociti, znižani levkociti, znižani hemoglobin, znižani trombociti, nevropatija-senzorna, diareja, bruhanje, stomatitis/faringitis, slabost, anoreksija, zaprtje, izpuščaji, alopecija, povišan kreatinin, znižan odtsek kreatinina, utrujenost. Pogosti: dehidracija, motnje okusa, konjunktivitis, dispneja. Klinične študije nedrobnooceličnega pljučnega raka ALIMTA monoterapija, zdravljenje 2. izbora. Zelo pogosti: znižani nevtrofilci/granulociti, znižani levkociti, znižani hemoglobin, diareja, bruhanje, stomatitis/faringitis, slabost, anoreksija, izpuščaji/luščenje, utrujenost. Pogosti: znižani trombociti, zaprtje, povišanje SGPT (ALT), povišanje SGOT (AST), srbenje, alopecija, povišana telesna temperatura. Klinične študije nedrobnooceličnega pljučnega raka ALIMTA v kombinaciji s cisplatinom, zdravljenje 1. izbora. Zelo pogosti: znižani hemoglobin, znižani levkociti, znižani trombociti, slabost, bruhanje, anoreksija, zaprtje, stomatitis/faringitis, diareja brez kolostomije, alopecija, izpuščaji/luščenje, povišan kreatinin, utrujenost. Pogosti: nevropatija-senzorna, motnje okusa, dispneja/zgaga. Klinične študije nedrobnooceličnega pljučnega raka ALIMTA monoterapija, vzdrževalno in nadaljevalno zdravljenje. Zelo pogosti: znižani hemoglobin, slabost, anoreksija, utrujenost. Pogosti: znižani levkociti, znižani nevtrofilci, nevropatija-senzorna, bruhanje, mukozitis/stomatitis, povišanje ALT (SGPT), povišanje AST (SGOT), izpuščaji/luščenje, bolečina. Občasno so v kliničnih študijah pemetrekseda poročali o primerih resnih srčnožilnih in možganskožilnih dogodkov, vključno z miokardnim infarktom, angino pectoris, cerebrovaskularnim insultom in prehodnimi ishemičnimi atakami; primerih kolitisa ter o primerih intersticijske pljučnice z respiratorno insuficienco, primerih edema, o ezofagusni/radijskem ezofagitisu in o primerih sepse. Redkeje pa o primerih potencialno resnega hepatitisa in pancitopenije. Po uvedbi zdravila na trg so poročali o primerih akutne odpovedi ledvic s pemetreksedom samim ali v povezavi z drugimi kemoterapevtiki, primerih radijskega pljučnice pri bolnikih, ki so jih zdravili z radiacijo pred, med ali po njihovem zdravljenju s pemetreksedom, primerih radijskega izpuščaja pri bolnikih, ki so se v preteklosti zdravili z radioterapijo, o primerih periferne ishemije, ki je večših vodila v nekrozo okončin, redkih primerih buloznih stanj, kot sta Stevens-Johnsonov sindrom in toksična epidermalna nekroliza, ki so bila v nekaterih primerih usodna in o redkih primerih hemolitične anemije. Poročali so o redkih primerih anafilaktičnega šoka. **Imetnik dovoljenja za promet** Eli Lilly Nederland BV, Grootslag 1 S, NL 3991 RA, Houten, Nizozemska. Datum zadnje revizije besedila 12.11.2012. **Način izdaje zdravila:** H. SAMO ZA STROKOVNO JAVNOST.

Podrobnejše informacije o zdravilu Alimta, so dostopne na spletni strani Evropske agencije za zdravila EMA <http://www.ema.europa.eu> in na lokalnem predstavništvu.

SIALM00067

Eli Lilly Farmaceutvska družba, d.o.o.
Brničeva 41G, 1231 Ljubljana - Črnuče, Slovenija
Telefon: +386 (0)1 5800 010
Faks: +386 (0)1 5691 705

Lilly

Skrajšan povzetek glavnih značilnosti zdravila ZELBORAF

Samo za strokovno javnost.

Ime zdravila: Zelboraf 240 mg filmsko obložene tablete

Kakovostna in količinska sestava: Ena tableta vsebuje 240 mg vemurafeniba (v obliki precipitata vemurafeniba in hipromeloze acetat sukcinata). **Terapevtske indikacije:** Vemurafenib je indiciran za samostojno zdravljenje odraslih bolnikov z neresektabilnim ali metastatskim melanomom, s pozitivno mutacijo BRAF V600. **Odmerjanje in način uporabe:** Zdravljenje z vemurafenibom mora uvesti in nadzorovati usposobljen zdravnik, ki ima izkušnje z uporabo zdravil za zdravljenje raka. **Odmerjanje:** Priporočeni odmerek vemurafeniba je 960 mg (4 tablete po 240 mg) dvakrat na dan (to ustreza celotnemu dnevnemu odmerku 1920 mg). Vemurafenib lahko vzamemo s hrano ali brez nje, izogibati pa se moramo stalnemu jemanju obeh dnevnih odmerkov na prazen želodec. Zdravljenje z vemurafenibom moramo nadaljevati do napredovanja bolezni ali pojava nesprejemljive toksičnosti. Če bolnik izpusti odmerek, ga lahko vzame do 4 ure pred naslednjim odmerkom za ohranitev sheme dvakrat na dan. Obeh odmerkov pa ne sme vzeti hkrati. Če bolnik po zaužitju vemurafeniba bruha, ne sme vzeti dodatnega odmerka zdravila, ampak mora z zdravljenjem normalno nadaljevati. **Prilagoditve odmerjanja:** Za obvladovanje neželenih učinkov ali ob podaljšanju intervala QTc je potrebno zmanjšanje odmerka, začasna prekinitve in/ali dokončno prenehanje zdravljenja (za podrobnosti o prilagoditvi odmerka, prosimo glejte SmPC zdravila). Zmanjšanje odmerka pod 480 mg dvakrat na dan ni priporočljivo. Če se pri bolniku pojavi ploščatocelični karcinom kože, priporočamo nadaljevanje zdravljenja brez zmanjšanja odmerka vemurafeniba. **Posebne populacije:** Za bolnike, starejše od 65 let, prilagajanje odmerka ni potrebno. O bolnikih z okvaro ledvic ali jeter je na voljo malo podatkov. Bolnike s hudo okvaro ledvic ali z zmerno do hudo okvaro jeter je treba pazljivo spremljati. Varnost in učinkovitost vemurafeniba pri otrocih in mladostnikih, mlajših od 18 let, še nista bili dokazani. Podatkov ni na voljo. **Način uporabe:** Tablete vemurafeniba je treba zaužiti cele, z vodo. Ne sme se jih žvečiti ali zdrobiti. **Kontraindikacije:** Preobčutljivost na zdravilno učinkovino ali katerokoli pomožno snov. **Posebna opozorila in previdnostni ukrepi:** Pred uporabo vemurafeniba je treba z validirano preiskavo potrditi, da ima bolnik tumor s pozitivno mutacijo BRAF V600. Dokazi o učinkovitosti in varnosti vemurafeniba pri bolnikih s tumorji z izraženo redko BRAF V600 mutacijo, ki ni V600E ali V600K, niso prepričljivi. Vemurafeniba se ne sme uporabljati pri bolnikih z malignim melanomom, ki ima divji tip BRAF. **Preobčutljivostne reakcije:** V povezavi z vemurafenibom so bile opisane resne preobčutljivostne reakcije, vključno z anafilaksijo. Hude preobčutljivostne reakcije lahko vključujejo Stevens-Johnsonov sindrom, generaliziran izpuščaj, eritem ali hipotenzijo. Pri bolnikih, pri katerih se pojavijo resne preobčutljivostne reakcije, je treba zdravljenje z vemurafenibom dokončno opustiti. **Kožne reakcije:** Pri bolnikih, ki so prejeli vemurafenib, so v ključnem kliničnem preskušanju poročali o hudih kožnih reakcijah, vključno z redkim Stevens-Johnsonovim sindromom in toksično epidermalno nekrozo. Pri bolnikih, pri katerih se pojavi huda kožna reakcija, je treba zdravljenje z vemurafenibom dokončno opustiti. **Podaljšanje intervala QT:** V nekotrolirani, odprti študiji faze II pri predhodno zdravljenih bolnikih z metastatskim melanomom, so opazili podaljšanje intervala QT, odvisnega od izpostavljenosti vemurafenibu. Podaljšanje intervala QT lahko poveča tveganje za ventrikularne aritmije, vključno s t. i. *Torsade de Pointes*. Z vemurafenibom ni priporočljivo zdraviti bolnikov z elektrolitskimi motnjami (vključno z magnezijem), ki jih ni mogoče odpraviti, bolnikov s sindromom dolgega intervala QT in bolnikov, zdravljenih z zdravili, ki podaljšajo interval QT. Pred zdravljenjem z vemurafenibom, en mesec po zdravljenju in po spremembi odmerka je treba pri vseh bolnikih posneti elektrokardiogram (EKG) in kontrolirati elektrolite (vključno z magnezijem). Nadaljnje kontrole so priporočljive predvsem pri bolnikih z zmerno do hudo jetrno okvaro, in sicer mesečno prve 3 mesece zdravljenja, potem pa na 3 mesece oziroma pogosteje, če je to klinično indicirano. Zdravljenja z vemurafenibom ni priporočljivo uvesti pri bolnikih, ki imajo interval QTc > 500 milisekund (ms). **Bolezni oči:** Poročali so o resnih neželenih učinkih na obeh, vključno z uveitisom, iritisom in zaporo mrežnične vene. Bolnikom je treba oči redno kontrolirati glede morebitnih neželenih učinkov na obeh. **Ploščatocelični karcinom kože:** Pri bolnikih, zdravljenih z vemurafenibom, so bili opisani primeri ploščatoceličnega karcinoma kože, vključno s ploščatoceličnim karcinomom, opredeljenim kot keratoakantom ali mešani keratoakantom. Priporočljivo je, da vsi bolniki pred uvedbo zdravljenja opravijo dermatološki pregled in da so med zdravljenjem deležni rednih kontrol. Vsako sumljivo spremembo je treba izrezati, poslati na histopatološko oceno in jo zdraviti v skladu z lokalnimi smernicami. Med zdravljenjem in do šest mesecev po zdravljenju ploščatoceličnega karcinoma mora zdravnik enkrat mesečno pregledati bolnika. Pri bolnikih, ki se jim pojavi ploščatocelični karcinom kože, je priporočljivo nadaljevati zdravljenje brez zmanjšanja odmerka. Nadzor se mora nadaljevati še 6 mesecev po prenehanju zdravljenja z vemurafenibom ali do uvedbe drugega antineoplastičnega zdravljenja. Bolnikom je treba naročiti, naj svojega zdravnika obvestijo o pojavu kakršnih koli sprememb na koži. **Ploščatocelični karcinom kože, ki se ne nahaja na koži:** Pri bolnikih, ki so prejeli vemurafenib v kliničnih preskušanjih, so poročali o primerih ploščatoceličnega karcinoma, ki se ne nahaja na koži. Bolnikom je treba pred uvedbo zdravljenja in na 3 mesece med zdravljenjem pregledati glavo in vrat (pregled mora obsegati vsaj oglede ustne sluznice in palpacijo bezgavk). Poleg tega morajo bolniki pred zdravljenjem in na 6 mesecev med zdravljenjem opraviti računalniško tomografijo (CT) prsnega koša. Pred in po končanem zdravljenju ali kadar je klinično indicirano, je priporočljivo opraviti pregled zadnjika in ginekološki pregled (pri ženskah). Po prenehanju zdravljenja z vemurafenibom se mora nadzor glede ploščatoceličnega karcinoma, ki se ne nahaja na koži, nadaljevati še 6 mesecev ali do uvedbe drugega antineoplastičnega zdravljenja. Nenormalne spremembe je treba obravnavati v skladu s klinično prakso. **Novi primarni melanom:** V kliničnih preskušanjih so poročali o novih primarnih melanomih. Bolnike s takšnimi primeri so zdravili z ekscizijo, bolniki pa so nadaljevali z zdravljenjem brez prilagoditve odmerka. Nadzor nad pojavom kožnih lezij je treba izvajati, kot je navedeno zgoraj pri ploščatoceličnem karcinomu kože. **Poškodbe jeter:** Med uporabo vemurafeniba se lahko pojavijo jetrne laboratorijske nepravilnosti (zvišanje GGt, ALT, alkalne fosfataze, bilirubina, AST). Pred uvedbo zdravljenja in mesečno med zdravljenjem oz. kot je klinično indicirano, je treba kontrolirati jetrne encime (transaminaze in alkalno fosfatazo) ter bilirubin. Laboratorijske nepravilnosti je treba obvladati z zmanjšanjem odmerka, prekinitvijo zdravljenja ali prenehanjem zdravljenja (za podrobnosti o prilagoditvi

odmerka, prosimo glejte SmPC zdravila). **Jetrna okvara:** Bolnikom z jetrno okvaro začetnih odmerkov ni treba prilagajati. Bolnike, ki imajo zaradi metastaz v jetrih blago jetrno okvaro in nimajo hiperbilirubinemije, se lahko nadzoruje v skladu s splošnimi priporočili. Podatkov o bolnikih z zmerno do hudo jetrno okvaro je le malo; pri takih bolnikih je izpostavljenost lahko večja. Tako je posebej po prvih tednih zdravljenja potreben skrben nadzor, saj lahko po daljšem obdobju (več tednih) pride do kopičenja. **Ledvična okvara:** Bolnikom z blago ali zmerno ledvično okvaro začetnih odmerkov ni treba prilagajati. Pri bolnikih z hudo ledvično okvaro je treba vemurafenib uporabljati previdno ter jih pazljivo spremljati. **Fotosenzibilnost:** Pri bolnikih, ki so v kliničnih študijah prejeli vemurafenib, je bila opisana blaga do huda fotosenzibilnost. Vsem bolnikom je treba naročiti, naj se med jemanjem vemurafeniba ne izpostavljajo soncu. V primeru fotosenzibilnosti stopnje 2 (neprenosljivo) ali več so priporočljive prilagoditve odmerka. **Ženske v rodni dobi** morajo med zdravljenjem in vsaj še 6 mesecev po zdravljenju uporabljati učinkovito kontracepcijsko zaščito. Vemurafenib lahko zmanjša učinkovitost hormonskih kontraceptivov. **Sočasno dajanje ipilimumaba** Pri sočasni uporabi ipilimumaba in vemurafeniba so v preskušanju faze I poročali o asimptomatskih zvišanih transaminazi in bilirubina stopnje 3. Glede na te preliminarnе podatke sočasna uporaba ipilimumaba in vemurafeniba ni priporočljiva. **Medsebojno delovanje z drugimi zdravili in druge oblike interakcij:** **Vplivi vemurafeniba na substrate CYP** Vemurafenib lahko poveča izpostavljenost v plazmi tistih snovi, ki se presnavljajo pretežno s CYP1A2; v takem primeru je treba razmisliti o prilagoditvi odmerka. Vemurafenib lahko zmanjša plazemsko izpostavljenost zdravilom, ki se presnavljajo pretežno s CYP3A4. Tako je lahko učinkovitost kontracepcijskih tablet, ki se presnavljajo s CYP3A4 in se uporabljajo sočasno z vemurafenibom, zmanjšana. Pri substratih CYP3A4, ki imajo ozko terapevtsko okno, je treba razmisliti o prilagoditvi odmerka. Zaužitje še ni znano ali lahko vemurafenib pri 100 µM koncentraciji v plazmi, ki je bila opažena pri bolnikih v stanju dinamičnega ravnovesja (približno 50 µg/ml), zmanjša plazemsko koncentracijo sočasno danih substratov CYP2B6, kot je bupropion. Kadar se vemurafenib pri bolnikih z melanomom uporabi hkrati z varfarinom (CYP2C9), je potrebna previdnost.

Tveganja za klinično pomemben učinek na sočasno uporabljene učinkovine, ki so substrati CYP2C8, pa ni mogoče izključiti. Zaradi dolge razpolovne dobe vemurafeniba je mogoče, da popolnega inhibitornega učinka vemurafeniba na sočasno dajano zdravilo ne opazimo, dokler ne mine 8 dni zdravljenja z vemurafenibom. Po končanem zdravljenju z vemurafenibom bo morda potreben 8-dnevni premor, da se izognemo interakcijam z nadaljnjim zdravljenjem. **Vpliv vemurafeniba na transportne sisteme zdravil** Možnosti, da vemurafenib morda poveča izpostavljenost drugih zdravil, ki se prenašajo s P-gp, ni mogoče izključiti. Možen vpliv vemurafeniba na druge prenašalce trenutno ni znan. **Vplivi sočasno uporabljenih zdravil na vemurafenib** Študije *in vitro* kažejo, da sta presnova s CYP3A4 in glukuronidacija odgovorni za presnovo vemurafeniba. Zdi se, da je tudi izločanje z žolčem pomembna pot izločanja. Vemurafenib je treba uporabljati previdno v kombinaciji z močnimi inhibitorji CYP3A4, glukuronidacije in/ali prenašalnih beljakovin (npr. ritonavirjem, sakvinavirjem, telitromicinom, ketokonazolom, itraconazolom, vorikonazolom, posakonazolom, nefazodonom, atazanavirjem). Sočasna uporaba močnih induktorjev P-gp, glukuronidacije, in/ali CYP3A4 (npr. rifampicina, rifabutina, karbamazepina, fenitoina ali šentjanževke [*hypericum perforatum*]) lahko vodi v suboptimalno izpostavljenost vemurafenibu in se ji je treba izogibati. Študije *in vitro* so pokazale, da je vemurafenib substrat sekretornih prenašalcev, P-gp in BCRP. Vplivi induktorjev in inhibitorjev P-gp in BCRP na izpostavljenost vemurafenibu niso znani. Ni mogoče izključiti možnosti, da imajo lahko zdravila, ki vplivajo na P-gp (npr. verapamil, ciklosporin, ritonavir, kinidin, itraconazol) ali BCRP (npr. ciklosporin, gefitinib), vpliv na farmakokinetiko vemurafeniba. Za zdaj ni znano, ali je vemurafenib substrat tudi za druge beljakovinske prenašalce.

Neželeni učinki: Med najpogostejšimi neželenimi učinki (> 30 %), o katerih so poročali v zvezi z vemurafenibom, so artralgija, utrujenost, kožni izpuščaj, fotosenzibilnostna reakcija, navzea, alopecija in srbenje. Zelo pogosto je bil opisan ploščatocelični karcinom kože. Sledijo najpogostejši neželeni učinki, ki so se pojavili pri bolnikih, zdravljenih z vemurafenibom v študiji faze II in III in dogodki iz varnostnih poročil vseh preskušanj. **Zelo pogosti:** ploščatocelični karcinom kože, seboroična keratoza, kožni papilom, zmanjšanje teka, glavobol, disgevizija, kašelj, driska, bruhanje, slabost, zaprtost, fotosenzibilna reakcija, aktinična keratoza, kožni izpuščaj, makulo-papulozen izpuščaj, papulozen izpuščaj, srbenje, hiperkeratoza, eritem, alopecija, suha koža, sončne opekline, artralgija, mialgija, bolečina v okončini, mišično-skeletne bolečine, bolečine v hrbtu, utrujenost, pireksija, periferni edem, astenija, zvišanje GGt. **Pogosti:** folikulitis, bazalnocelični karcinom, novi primarni melanom, ohromelost sedmega živca, omotica, uveitis, sindrom palmarno-plantarne eritrodisestezije, nodozni eritem, pilarna keratoza, artritis, zvišanje ALT, alkalne fosfataze, bilirubina in izguba telesne mase, podaljšanje QT. **Posebne populacije:** Pri starejših bolnikih (≥ 65 let) je možna večja verjetnost neželenih učinkov, vključno s ploščatoceličnim karcinomom kože, zmanjšanjem teka in motnjami srčnega ritma. Med neželene učinke stopnje 3, ki so bili med kliničnimi preskušaji vemurafeniba pri ženskah opisani pogosteje kot pri moških, spadajo kožni izpuščaj, artralgija in fotosenzibilnost. **Režim izdaje zdravila:** Rp/Spec **Imetnik dovoljenja za promet:** Roche Registration Limited, 6 Falcon Way, Shire Park, Welwyn Garden City, AL7 1TW, Velika Britanija **Verzija:** 4.0/13 **Informacija pripravljena:** september 2013

DODATNE INFORMACIJE SO NA VOLJO PRI:
Roche farmacevtska družba d.o.o., Vodovodna cesta 109, 1000 Ljubljana
Povzetek glavnih značilnosti zdravila je dosegljiv na www.roche.si

Zelboraf[®]
vemurafenib

**Posamezniku
prilagojeno zdravljenje
metastatskega melanoma**



Vsak bolnik z metastatskim melanomom je drugačen.

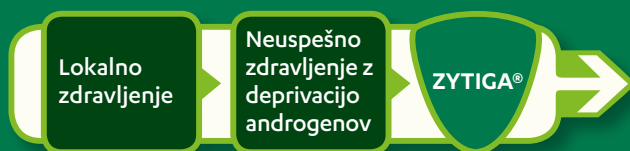
S pravilnim izborom bolnikov in tarčnim zdravljenjem bolnikov z neresektabilnim ali metastatskim melanomom s potrjeno mutacijo BRAF^{V600} z zdravilom ZELBORAF[®], se lahko bistveno izboljša odziv na zdravljenje in celokupno preživetje v primerjavi z dakarbazinom. Neželjeni učinki zdravljenja z zdravilom ZELBORAF[®] so obvladljivi.¹

¹ Povzetek glavnih značilnosti zdravila Zelboraf[®] 27.6.2013.
Dosegljiv na www.ema.europa.eu; dostopano: september 2013.

Nova indikacija

Pravočasno je vse

Za bolnike z metastatskim, na kastracijo odpornim rakom prostate, ki nimajo simptomov ali imajo blage simptome po neuspešnem zdravljenju z deprivacijo androgenov in pri katerih kemoterapija še ni indicirana.¹



- za **47 %** zmanjša tveganje za radiografsko potrjeno napredovanje bolezni ($p < 0,001$),²
- za **8,4 mesece** podaljša čas do uvedbe citotoksične kemoterapije ($p < 0,001$).²

Zdravilo ZYTIGA je v obliki tablet, bolnik jih jemlje enkrat na dan.¹

Čas je vse



SKRAJŠANO NAVODILO ZA PREDPISOVANJE ZDRAVILA:

Ime zdravila: ZYTIGA 250 mg tablete **Kakovostna in količinska sestava:** 250 mg abirateronacetata; pomožne snovi: mikrokristalna celuloza, premreženi natrijev karmeloizat, laktoza monohidrat, magnezijev stearat, povidon, brezvodni koloidni silicijev dioksid, natrijev lavrilsulfat. **Indikacije:** uporaba skupaj s prednizonom ali prednizolonom za zdravljenje na kastracijo odpornega metastatskega raka prostate pri odraslih bolnikih, ki nimajo ali imajo blage simptome po neuspešnem zdravljenju z deprivacijo androgenov in pri katerih kemoterapija še ni klinično indicirana; ter pri odraslih bolnikih, pri katerih je bolezen napredovala med ali po zdravljenju s kemoterapijo z docetakselom. **Odmerjanje:** priporočeni odmerek: 1.000 mg (štiri 250 mg tablete v enem odmerku), 10 mg prednizona ali prednizolona/dan, najmanj dve uri po obroku. Pri bolnikih s hudo okvaro jeter ali ledvic je potrebna previdnost. **Kontraindikacije:** preobčutljivost na zdravilno učinkovino ali katero koli pomožno snov, uporaba zdravila pri ženskah, huda okvara jeter. **Posebna opozorila:** Pri uporabi zdravila pri bolnikih z anamnezo kardiovaskularne bolezni je potrebna previdnost. Pri bolnikih z iztisnim deležem levega prekata < 50% ali s srčnim popuščanjem razreda III ali IV po NYHA varnost uporabe zdravila ni dokazana. Pred začetkom zdravljenja je treba urediti hipertenzijo, zastajanje tekočin in odpraviti hipokaliemijo. Če kadarkoli med zdravljenjem pride do pojava hude hepatotoksičnosti je treba z zdravljenjem prenehati in se ga ne sme ponovno uvesti. Pri bolnikih, ki prejemajo prednizon ali prednizolon in so v stresni situaciji, je lahko pred in med stresno situacijo ter po njej indiciran zvečan odmerek kortikosteroidov. Pri bolnikih z napredovanim metastatskim rakom prostate (rezistentnim na kastracijo) lahko pride do zmanjšanja kostne gostote. Jemanje zdravila v kombinaciji z glukokortikoidi lahko ta učinek poveča. Pri bolnikih z rakom prostate, zdravljenih s ketokonazolom, lahko pričakujemo nižjo stopnjo odziva na zdravljenje. Uporaba glukokortikoidov lahko poslabša hiperglikemijo. Varnost in učinkovitost sočasne uporabe zdravila ZYTIGA in citotoksične kemoterapije ni bila ugotovljena. Bolniki z redko dedno intoleranco za galaktozo, laponsko obliko zmanjšane aktivnosti laktaze ali malabsorpcijo glukoze/galaktoze ne smejo jemati tega zdravila. Zdravilo vsebuje tudi več kot 1 mmol (oziroma 27,2 mg) natrija na odmerek (v štirih tabletah), kar je treba upoštevati pri bolnikih na dieti z nadzorovanim vnosom natrija. Pri bolnikih, ki se zdravijo z zdravilom ZYTIGA se lahko pojavita anemija in spolna disfunkcija. **Interakcije:** zdravila se ne sme jemati s hrano, ker se bistveno poveča absorpcija abirateronacetata. Pri sočasni uporabi z zdravili, ki jih aktivira ali presnavlja CYP2D6, zlasti tistih z majhno terapevtsko širino je potrebna previdnost. In vitro podatki kažejo, da je zdravilo substrat CYP3A4. Med zdravljenjem se uporabi močnih zaviralcev in induktorjev CYP3A4 izogibajte ali bodite še posebej previdni. **Nosečnost in dojenje:** Ženske, ki so noseče in ženske, ki bi lahko bile noseče, morajo v primeru stika ali rokovanja z zdravilom, nositi zaščitne rokavice. V študijah na živalih so ugotovili toksične učinke na sposobnost razmnoževanja. **Neželeni učinki:** okužba sečil, periferni edemi, hipokaliemija, hipertenzija, hipertrigliceridemija, hepatotoksičnost z zvišanimi vrednostmi ALT, AST in celokupnega bilirubina, srčno popuščanje, angina pectoris, aritmija, atrijska fi brilacija, tahikardija, zlomi, dispepsija, izpuščaji, hematurija, adrenalna insuficija. **Imetnik dovoljenja za promet:** Janssen-Cilag International NV, Turnhoutseweg 30, 2340 Beerse, Belgija, Predstavniki v Sloveniji: Johnson & Johnson d.o.o., Šmartinska 53, Ljubljana **Režim izdajanja zdravila:** Rp/Spec. **Datum zadnje revizije besedila:** 18. 12. 2012

Literatura:

- Povzetek glavnih značilnosti zdravila Zytiga, 18. 12. 2012
- Ryan CJ et al. N Engl J Med 2013; 368: 138 - 148

ZYT-SLO-A-051-040313



ERBITUX[®]
CETUXIMAB

See the difference

This is what
tumor shrinkage
looks like



Merck Serono Oncology | *Combination is key*[™]

Erbix 5 mg/ml raztopina za infundiranje
Skrajšan povzetek glavnih značilnosti zdravila

Sestava: En ml raztopine za infundiranje vsebuje 5 mg cetuximaba in pomožne snovi. Cetuximab je himerno monoklonsko IgG1 protitelo. **Terapevtske indikacije:** Zdravilo Erbitux je indicirano za zdravljenje bolnikov z metastatskim kolorektalnim rakom z ekspresijo receptorjev EGFR in nemutiranim tipom KRAS v kombinaciji s kemoterapijo na osnovi irinotekana, kot primarno zdravljenje v kombinaciji s FOLFOX in kot samostojno zdravilo pri bolnikih, pri katerih zdravljenje z oksaliplatinom in irinotekanom ni bilo uspešno ter pri bolnikih, ki ne prenašajo irinotekana. Zdravilo Erbitux je indicirano za zdravljenje bolnikov z rakom skvamoznih celic glave in vratu v kombinaciji z radioterapijo za lokalno napredovalo bolezen in v kombinaciji s kemoterapijo na osnovi platine za ponavljajočo se in/ali metastatsko bolezen. **Odmerjanje in način uporabe:** Zdravilo Erbitux pri vseh indikacijah infundirajte enkrat na teden. Pred prvo infuzijo mora bolnik prejeti premedikacijo z antihistaminikom in kortikosteroidom. Začetni odmerek je 400 mg cetuximaba na m² telesne površine. Vsi naslednji tedenski odmerki so vsak po 250 mg/m². **Kontraindikacije:** Zdravilo Erbitux je kontraindicirano pri bolnikih z znano hudo preobčutljivostno reakcijo (3. ali 4. stopnje) na cetuximab. Kombinacija zdravila Erbitux s kemoterapijo, ki vsebuje oksaliplatin, je kontraindicirana pri bolnikih z metastatskim kolorektalnim rakom z mutiranim tipom KRAS ali kadar status KRAS ni znan. **Posebna opozorila in previdnostni ukrepi:** Če pri bolniku nastopi blaga ali zmerne reakcija, povezana z infundiranjem, lahko zmanjšate hitrost infundiranja. Priporočljivo je, da ostane hitrost infundiranja na nižji vrednosti tudi pri vseh naslednjih infuzijah. Če se pri bolniku pojavi kožna reakcija, ki je ne more prenašati, ali huda kožna reakcija (≥ 3. stopnje po kriterijih CTCAE), morate prekiniti terapijo s cetuximabom. Z zdravljenjem smete nadaljevati le, če se je reakcija izboljšala do 2. stopnje. Če ugotovite intersticijsko bolezen pljuč, morate zdravljenje s cetuximabom prekiniti,

in bolnika ustrezno zdraviti. Zaradi možnosti pojava znižanja nivoja magnezija v serumu se pred in periodično med zdravljenjem priporoča določanje koncentracije elektrolitov. Če se pojavi sum na nevtropenijo, je potrebno bolnika skrbno nadzorovati. Potrebno je upoštevati kardiovaskularno stanje bolnika in sočasno dajanje kardiotoksičnih učinkovin kot so fluoropirimidini. Cetuximab je treba uporabljati previdno pri bolnikih z anamnezo keratitisa, ulcerativnega keratitisa ali zelo suhih oči. **Interakcije:** Pri kombinaciji s fluoropirimidini se je povečala pogostnost srčne ishemije, vključno z miokardnim infarktom in kongestivno srčno odpovedjo ter pogostnost sindroma dlani in stopal. V kombinaciji s kemoterapijo na osnovi platine se lahko poveča pogostnost hude levkopenije ali hude nevtropenije. V kombinaciji s kapecitabinom in oksaliplatinom (XELOX) se lahko poveča pogostnost hude driske. **Neželeni učinki:** Zelo pogosti (≥ 1/10): hipomagneziemija, povečanje ravnih jetrnih encimov, kožne reakcije, blage ali zmerne reakcije povezane z infundiranjem, mukozitis, v nekaterih primerih resen. Pogosti (≥ 1/100, < 1/10): dehidracija, hipokalcemija, anoreksija, glavobol, konjunktivitis, driska, navzeja, bruhanje, hude reakcije povezane z infundiranjem, utrujenost. **Posebna navodila za shranjevanje:** Shranjujte v hladilniku (2 °C - 8 °C). **Pakiranje:** 1 viala z 20 ml ali 100 ml raztopine. **Način in režim izdaje:** H. **Imetnik dovoljenja za promet:** Merck KGaA, 64271 Darmstadt, Nemčija. **Datum zadnje revizije besedila:** Februar 2013. **Pred predpisovanjem zdravila natančno preberite celoten Povzetek glavnih značilnosti zdravila. Podrobnejše informacije so na voljo pri predstavniku imetnika dovoljenja za promet z zdravilom:** Merck d.o.o., Ameriška ulica 8, 1000 Ljubljana, tel.: 01 560 3810, faks: 01 560 3830, el. pošta: info@merck.si

www.merckserono.net
www.Erbitux-international.com



Instructions for authors

The editorial policy

Radiology and Oncology is a multidisciplinary journal devoted to the publishing original and high quality scientific papers, review articles, case reports and varia (editorials, short communications, professional information, book reviews, letters, etc.) pertinent to diagnostic and interventional radiology, computerized tomography, magnetic resonance, ultrasound, nuclear medicine, radiotherapy, clinical and experimental oncology, radiobiology, radiophysics and radiation protection. Therefore, the scope of the journal is to cover beside radiology the diagnostic and therapeutic aspects in oncology, which distinguishes it from other journals in the field.

The Editorial Board requires that the paper has not been published or submitted for publication elsewhere; the authors are responsible for all statements in their papers. Accepted articles become the property of the journal and, therefore cannot be published elsewhere without the written permission of the editors.

Submission of the manuscript

The manuscript written in English should be submitted to the journal via online submission system Editorial Manager available for this journal at: www.radioloncol.com.

In case of problems, please contact Sašo Trupej at saso.trupej@computing.si or the Editor of this journal at gsera@onko-i.si

All articles are subjected to the editorial review and when the articles are appropriated they are reviewed by independent referees. In the cover letter, which must accompany the article, the authors are requested to suggest 3-4 researchers, competent to review their manuscript. However, please note that this will be treated only as a suggestion; the final selection of reviewers is exclusively the Editor's decision. The authors' names are revealed to the referees, but not vice versa.

Manuscripts which do not comply with the technical requirements stated herein will be returned to the authors for the correction before peer-review. The editorial board reserves the right to ask authors to make appropriate changes of the contents as well as grammatical and stylistic corrections when necessary. Page charges will be charged for manuscripts exceeding the recommended length, as well as additional editorial work and requests for printed reprints.

Articles are published printed and on-line as the open access (www.degruyter.com/view/j/raon).

All articles are subject to 500 EUR + VAT publication fee. Exceptionally, waiver of payment may be negotiated with editorial office, upon lack of funds.

Manuscripts submitted under multiple authorship are reviewed on the assumption that all listed authors concur in the submission and are responsible for its content; they must have agreed to its publication and have given the corresponding author the authority to act on their behalf in all matters pertaining to publication. The corresponding author is responsible for informing the coauthors of the manuscript status throughout the submission, review, and production process.

Preparation of manuscripts

Radiology and Oncology will consider manuscripts prepared according to the Uniform Requirements for Manuscripts Submitted to Biomedical Journals by International Committee of Medical Journal Editors (www.icmje.org). The manuscript should be written in grammatically and stylistically correct language. Abbreviations should be avoided. If their use is necessary, they should be explained at the first time mentioned. The technical data should conform to the SI system. The manuscript, excluding the references, tables, figures and figure legends, must not exceed 4000 words, and the number of figures and tables is limited to 8. Organize the text so that it includes: Introduction, Materials and methods, Results and Discussion. Exceptionally, the results and discussion can be combined in a single section. Start each section on a new page, and number each page consecutively with Arabic numerals.

The Title page should include a concise and informative title, followed by the full name(s) of the author(s); the institutional affiliation of each author; the name and address of the corresponding author (including telephone, fax and E-mail), and an abbreviated title (not exceeding 60 characters). This should be followed by the abstract page, summarizing in less than 250 words the reasons for the study, experimental approach, the major findings (with specific data if possible), and the principal conclusions, and providing 3-6 key words for indexing purposes. Structured abstracts are preferred. Slovene authors are requested to provide title and the abstract in Slovene language in a separate file. The text of the research article should then proceed as follows:

Introduction should summarize the rationale for the study or observation, citing only the essential references and stating the aim of the study.

Materials and methods should provide enough information to enable experiments to be repeated. New methods should be described in details.

Results should be presented clearly and concisely without repeating the data in the figures and tables. Emphasis should be on clear and precise presentation of results and their significance in relation to the aim of the investigation.

Discussion should explain the results rather than simply repeating them and interpret their significance and draw conclusions. It should discuss the results of the study in the light of previously published work.

Charts, Illustrations, Images and Tables

Charts, Illustrations, Images and Tables must be numbered and referred to in the text, with the appropriate location indicated. Charts, Illustrations and Images, provided electronically, should be of appropriate quality for good reproduction.

Instructions

Illustrations and charts must be vector image, created in CMYK color space, preferred font "Century Gothic", and saved as .AI, .EPS or .PDF format. Color charts, illustrations and Images are encouraged, and are published without additional charge. Image size must be 2.000 pixels on the longer side and saved as .JPG (maximum quality) format. In Images, mask the identities of the patients. Tables should be typed double-spaced, with a descriptive title and, if appropriate, units of numerical measurements included in the column heading. The files with the figures and tables can be uploaded as separate files.

References

References must be numbered in the order in which they appear in the text and their corresponding numbers quoted in the text. Authors are responsible for the accuracy of their references. References to the Abstracts and Letters to the Editor must be identified as such. Citation of papers in preparation or submitted for publication, unpublished observations, and personal communications should not be included in the reference list. If essential, such material may be incorporated in the appropriate place in the text. References follow the style of Index Medicus. All authors should be listed when their number does not exceed six; when there are seven or more authors, the first six listed are followed by "et al.". The following are some examples of references from articles, books and book chapters:

Dent RAG, Cole P. In vitro maturation of monocytes in squamous carcinoma of the lung. *Br J Cancer* 1981; **43**: 486-95.

Chapman S, Nakielny R. *A guide to radiological procedures*. London: Bailliere Tindall; 1986.

Evans R, Alexander P. Mechanisms of extracellular killing of nucleated mammalian cells by macrophages. In: Nelson DS, editor. *Immunobiology of macrophage*. New York: Academic Press; 1976. p. 45-74.

Authorization for the use of human subjects or experimental animals

When reporting experiments on human subjects, authors should state whether the procedures followed the Helsinki Declaration. Patients have the right to privacy; therefore the identifying information (patient's names, hospital unit numbers) should not be published unless it is essential. In such cases the patient's informed consent for publication is needed, and should appear as an appropriate statement in the article. Institutional approval and Clinical Trial registration number is required.

The research using animal subjects should be conducted according to the EU Directive 2010/63/EU and following the Guidelines for the welfare and use of animals in cancer research (*Br J Cancer* 2010; 102: 1555 – 77). Authors must state the committee approving the experiments, and must confirm that all experiments were performed in accordance with relevant regulations.

These statements should appear in the Materials and methods section (or for contributions without this section, within the main text or in the captions of relevant figures or tables).

Transfer of copyright agreement

For the publication of accepted articles, authors are required to send the License to Publish to the publisher on the address of the editorial office. A properly completed License to Publish, signed by the Corresponding Author on behalf of all the authors, must be provided for each submitted manuscript.

The non-commercial use of each article will be governed by the Creative Commons Attribution-NonCommercial-NoDerivs license.

Conflict of interest

When the manuscript is submitted for publication, the authors are expected to disclose any relationship that might pose real, apparent or potential conflict of interest with respect to the results reported in that manuscript. Potential conflicts of interest include not only financial relationships but also other, non-financial relationships. In the Acknowledgement section the source of funding support should be mentioned. The Editors will make effort to ensure that conflicts of interest will not compromise the evaluation process of the submitted manuscripts; potential editors and reviewers will exempt themselves from review process when such conflict of interest exists. The statement of disclosure must be in the Cover letter accompanying the manuscript or submitted on the form available on www.icmje.org/coi_disclosure.pdf

Page proofs

Page proofs will be sent by E-mail to the corresponding author. It is their responsibility to check the proofs carefully and return a list of essential corrections to the editorial office within three days of receipt. Only grammatical corrections are acceptable at that time.

Open access

Papers are published electronically as open access on www.degruyter.com/view/j/raon, also papers accepted for publication as E-ahead of print.

Za zdravljenje odraslih bolnikov s predhodno zdravljenim, napredovalim nedrobnoceličnim pljučnim rakom, ki je ALK* pozitiven.



Drugačen gen Drugačna terapija

XALKORI
KRIZOTINIB

*anaplastična limfomska kinaza

BISTVENI PODATKI IZ POVZETKA GLAVNIH ZNAČILNOSTI ZDRAVILA

XALKORI 200 mg, 250 mg trde kapsule

▼ Za to zdravilo se izvaja dodatno spremljanje varnosti. Tako bodo hitreje na voljo nove informacije o njegovi varnosti. Zdravstvene delavce naprošamo, da poročajo o kateremkoli domnevnem neželenem učinku zdravila. Glejte poglavje 4.8 povzetka glavnih značilnosti zdravila, kako poročati o neželenih učinkih.

Sestava in oblika zdravila: Ena kapsula vsebuje 200 mg ali 250 mg krizotiniba. **Indikacije:** Zdravljenje odraslih bolnikov s predhodno zdravljenim, napredovalim nedrobnoceličnim pljučnim rakom (NSCLC - non-small cell lung cancer), ki je ALK (anaplastična limfomska kinaza) pozitiven. **Odmerjanje in način uporabe:** Zdravljenje mora uvesti in nadzorovati zdravnik z izkušnjami z uporabo zdravil za zdravljenje rakavih bolezni. **Preverjanje prisotnosti ALK:** Pri izbiri bolnikov za zdravljenje z zdravilom XALKORI je treba opraviti točno in validirano preverjanje prisotnosti ALK. **Odmerjanje:** Priporočeni odmerek je 250 mg dvakrat na dan (500 mg na dan), bolniki pa morajo zdravilo jemati brez prekinitev, in sicer tako dolgo, dokler je mogoče opaziti klinično korist oziroma dokler se ne pojavi nesprejemljiva toksičnost. Če bolnik pozabi vzeti odmerek, ga mora vzeti takoj, ko se spomni, razen če do naslednjega odmerka manjka manj kot 6 ur. V tem primeru bolnik pozabljenega odmerka ne sme vzeti. **Prilagajanja odmerkov:** Glede na varnost uporabe zdravila pri posameznem bolniku in kako bolnik zdravljenje prenaša, utegne biti potrebna prekinitev in/ali zmanjšanje odmerka zdravila na 200 mg dvakrat na dan; če je potrebno še nadaljnje zmanjšanje, pa znaša odmerek 250 mg enkrat na dan. **Prilagajanje odmerkov pri hematološki in nehematološki (povečanje vrednosti AST, ALT, bilirubina; pnevmonitis; podaljšanje intervala QTc) toksičnosti:** glejte preglednici 1 in 2 v povzetku glavnih značilnosti zdravila. **Okvara jeter:** Pri blagi in zmerni okvari je zdravljenje treba izvajati previdno, pri hudi okvari se zdravila ne sme uporabljati. **Okvara ledvic:** Pri blagi in zmerni okvari prilagajanje začetnega odmerka ni priporočeno. Pri hudi bolezni ledvic in končni ledvični odpovedi podatkov ni na voljo, zato ni mogoče dati priporočil o odmerjanju. **Starejši bolniki (≥ 65 let):** Na voljo le omejeni podatki, zato ni mogoče dati priporočil o odmerjanju. **Pediatrična populacija:** Varnost in učinkovitost nista bili dokazani.

Način uporabe: Kapsule je treba pogoltniti cele, z nekaj vode, s hrano ali brez nje. Ne sme se jih zdrobiti, raztopiti ali odpreti. Izogibati se je treba uživanju grenivk, grenivkega soka ter uporabi šentjanževke. **Kontraindikacije:** Preobčutljivost na krizotinib ali katerokoli pomožno snov. Huda okvara jeter. **Posebna opozorila in previdnostni ukrepi:** **Hepatotoksičnost:** Zaradi jemanja zdravila je prišlo do hepatotoksičnosti s smrtnim izidom. Delovanje jeter, vključno z ALT, AST in skupnim bilirubinom, je treba preveriti dvakrat na mesec v prvih 2 mesecih zdravljenja, nato pa enkrat na mesec in kot je klinično indicirano. Ponovitve preverjanj morajo biti pogostejše pri povečanih vrednosti stopnje 2, 3 ali 4. **Pnevmonitis:** Jemanje zdravila je bilo povezano z življenjsko ogrožajočim ali smrtnim pnevmonitisom. Bolnike s simptomi, ki nakazujejo na pnevmonitis, je treba spremljati, zdravljenje pa prekiniti ob sumu na pnevmonitis. **Podaljšanje intervala QT:** Opažali so podaljšanje intervala QTc. Potrebna je pazljiva uporaba pri bolnikih, pri katerih je v preteklosti prišlo do podaljšanja intervala QTc oziroma so k podaljšanju nagnjeni, ter pri tistih, ki jemljejo zdravila, ki podaljšujejo interval QT. **Vplivi na vid:** Opažali so motnje vida; če so trdovratne ali postajajo vedno izrazitejše, je treba razmisliti o oftalmološkem pregledu. **Histološka preiskava, ki ne nakazuje adenokarcinoma:** Na voljo le omejeni podatki pri NSCLC, ki je ALK pozitiven in ima histološke značilnosti, ki ne nakazujejo adenokarcinoma; klinična korist je lahko pri tej podskupini manjša. **Medsebojno delovanje z drugimi zdravili in druge oblike interakcij:** Zdravila, ki lahko povečajo koncentracije krizotiniba v plazmi (atazanavir, indinavir, neflnavir, ritonavir, sakvinavir, itrakonazol, ketokonazol, vorikonazol, klaritromicin, telitromicin, troleandomicin), tudi grenivke in grenivkin sok. Zdravila, ki lahko zmanjšajo koncentracije krizotiniba v plazmi (karbamazepin, fenobarbital, fenitoin, rifabutin, rifampicin, šentjanževka). Zdravila, katerih koncentracije v plazmi lahko krizotinib spremeni (midazolam, alfentanil, cisaprid, ciklosporin, derivati ergot alkaloidov, fentanil, pimozid, kinidin, sirolimus, takrolimus, bupropion, efavirenz, peroralni kontraceptivi, paracetamol, morfin, irinotekan, digoksin, dabigatran, kolhicin, pravastatin). Zdravila, ki podaljšujejo interval QT ali ki lahko povzročijo Torsades de pointes (kinidin, disopiramid, amidaron, sotalol, dofetilid, ibutilid, metadon, cisaprid, moksifloksacin, antipsihotiki). Zdravila, ki povzročajo bradikardijo (verapamil, diltiazem, antagonisti adrenergičnih receptorjev beta, klonidin, guanfacin, digoksin, meflokin, antiholinesteraze, pilokarpin). **Plodnost, nosečnost in dojenje:** Ženske v rodni dobi se morajo izogibati zanositvi. Med zdravljenjem in najmanj 90 dni po njem je treba uporabljati ustrezno kontracepcijo (velja tudi za moške). Zdravilo lahko škoduje plodu in se ga med nosečnostjo ne sme uporabljati, razen če klinično stanje matere ne zahteva takega zdravljenja. Matere naj se med jemanjem zdravila dojenju izogibajo. Zdravilo lahko zmanjša plodnost moških in žensk.

Vpliv na sposobnost vožnje in upravljanja s stroji: Zdravilo ima blag vpliv na sposobnost vožnje in upravljanja s stroji; lahko se pojavijo motnje vida, omotica ali utrujenost. **Neželeni učinki:** Najpogostejši (> 20 %) neželeni učinki katerekoli stopnje v študijah so bili motnje vida, navzea, driska, bruhanje, edemi, zaprtje in utrujenost. Najpogostejša (≥ 3 %) neželena učinka stopnje 3 ali 4 sta bila povečana vrednost ALT in nevropenija. Potencialno resna neželena učinka sta pnevmonitis in podaljšanje intervala QT. Ostali zelo pogosti (≥ 1/10) neželeni učinki so: zmanjšan apetit, nevropenija, omotica, spremenjeno zaznavanje okusa. **Način in režim izdaje:** Predpisovanje in izdaja zdravila je le na recept, zdravilo pa se uporablja samo v bolnišnicah. Izjemoma se lahko uporablja pri nadaljevanju zdravljenja na domu ob odpustu iz bolnišnice in nadaljnjem zdravljenju. **Imetnik dovoljenja za promet:** Pfizer Limited, Ramsgate Road, Sandwich, Kent, CT13 9NJ, Velika Britanija. **Datum zadnje revizije besedila:** 25.4.2013

Pred predpisovanjem se seznanite s celotnim povzetkom glavnih značilnosti zdravila.



Pfizer Luxembourg SARL, GRAND DUCHY OF LUXEMBOURG, 51, Avenue J.F. Kennedy, L – 1855,
Pfizer, podružnica Ljubljana, Letališka cesta 3c, 1000 Ljubljana

